A thesis entitled

SAMPLE INTRODUCTION AND INSTRUMENTATION IN PLASMA SPECTROMETRY

Presented by

James Henry Dean Hartley, Bsc

in part fulfilment of the requirements for the degree of

Doctor of Philosophy

Department of Environmental Sciences,
University of Plymouth,
Drakes Circus,
PLYMOUTH PL4 8AA

Collaborating Establishment:
Johnson Matthey Technology Centre,
Blounts Court,
Sonning Common,
Reading RG4 9NH

October 1992

SAMPLE INTRODUCTION AND INSTRUMENTATION IN PLASMA SPECTROMETRY

ABSTRACT

James H.D. Hartley

Plasma spectrometry is now a widely accepted technique for the determination of the elemental composition of a wide range of sample types. The successful introduction of volatile organic solvents has however been limited,due to the resulting high solvent loading of the plasma and subsequent plasma instability. The design, function and application of a number of novel desolvation systems have been investigated in this study to decrease this loading and facilitate operation with volatile organic solvents.

A desolvation system utilising Peltier coolers to cool the condenser was designed to improve the sample introduction of volatile organic solvents, such as diethyl ether. This system was optimised by the variable step sized simplex procedure. A six fold improvement in the detection limits for elements such as copper and silicon was obtained when compared with a conventionally cooled spray chamber. Further improvements in the detection limits were also obtained by the use of novel flow injection techniques,such as the introduction of a plug of the volatile solvent into a carrier stream of a less volatile solvent, or aqueous medium. The improvements obtained using such desolvation systems were partly due to the facility to increase the sample uptake rates. The introduction of a membrane drying tube between the spray chamber and the plasma torch further enabled the sample volume to be increased and detection limits at sub ng ml^{-1} levels were obtained. The application of these techniques was demonstrated for the analysis of reactive organometallic compounds, such as trimethylgallium for trace metal impurities.

The effect of desolvating slurries before entry into the plasma not only enabled an increase in the transport efficiency but also the atomisation efficiency. It was found that larger particles (up to 8μm c.f 5μm) could be transported to the plasma and subsequently atomised.

The introduction of dry plasmas after desolvation has a profound effect on the plasma. The ionisation temperature and consequently the electron number density, were found to be decreased. This was found to be due to the effect of hydrogen on the thermal conductivity of the plasma. The introduction of molecular hydrogen into the nebulising gas at low levels (1-2% v/v) improved the thermal conductivity and therefore increased the ionisation temperature. The introduction of oxygen caused a decrease in ionisation temperature. The introduction of organic samples was found to have a detrimental effect on the ionisation temperature, caused by the effect of the carbon in the plasma and the oxygen addition required to prevent cone blockage. Desolvation of organic samples was found to increase the ionisation temperature, and provides a reliable method for the routine analysis of such samples.

Finally, the analysis of solid samples by laser ablation, was investigated, particularly for the analysis of samples which may be difficult to digest using conventional methodology. The choice of internal standard and whether the laser was in Q-swich or free running mode were shown to be the most important parameters.

ACKNOWLEDGEMENTS

I would like to thank Dr S.J. Hill for his support through out this study in his role as Director of studies. I equally like to thank the rest of my supervision team of Prof L. Ebdon and Dr P. Ash.

I would also like to thank the Science and Engineering Research Council and Johnson Matthey Technology Centre for there financial support during this project.

The most difficult job on this project was probably turning my illiterate scroll into readable typing for which I would like to thank Bev Hill.

I would also like to thank the gang in the Department for there help and fellowship and can only say "A wreugh-why eva coref ?"

Finally I would like to thank my parents for sticking with me through thick, thin and anorexic

DALLETHENS-EF DYSKY

TABLE OF CONTENTS

LIST OF FIGURES

LIST OF TABLES

CHAPTER 1

1.1 General Introduction

The use of the inductively coupled plasma (ICP) as an atom cell for atomic emission spectrometry and as an ion source for mass spectrometry has found wide acceptance since it was first introduced in 1964 by Greenfield et al. (1) in the UK and Wendt and Fassel (2) in the USA. It is now one of the major tools for trace and ultra-trace analysis of a wide range of sample types.

The unique properties of the ICP derive from the excitation source which is generated by the coupling of the energy from a radiofrequency generator to a gas, normally argon, travelling tangentially in a torch. An induction coil, consisting of a two or three turn water cooled copper coil encompasses the plasma torch. The gas is partially ionised, normally by means of a spark. The electrons are accelerated in the magnetic field and reach energies which are sufficient to ionise gaseous atoms, leading to further ionisation and a self sustaining plasma. The radiofrequency generator normally operates at 27.12 MHz delivering a forward power of between 1 - 3 kW. The magnetic field causes the ions and electrons to flow in the horizontal plane of the coil, which enables the heating of the neutral argon by collisional energy exchange and a very hot fire ball is produced. This enables high temperatures to be produced. In the hottest

part of the plasma temperatures of between 8000 - 10000 K can be obtained.

The geometry of the torch, Figure 1.1.1, enables the punching of a hole in the base of the plasma and consequently a flow of argon into the hottest part of the plasma. This produces a corridor through which the analytical sample is introduced. This lowers the effective temperature to between 6000 - 8000 K. The plasma is not, however, in local thermal equilibrium consequently the gas temperature, excitation temperature and ionisation temperature have different values. At these temperatures atomisation is nearly total and the samples become partially ionised. For atomic emission spectrometry the emission is observed just above the very bright core continuum of the plasma, so a low background is obtained (3).

Samples are normally introduced into the plasma by means of a fine aerosol. A liquid sample is pumped into a nebuliser where the aerosol is produced. A spray chamber is normally employed to prevent large droplets entering the plasma and causing signal fluctuations. Other introduction methods include; the introduction of gases by hydride generation (4), vapours of complexes or direct analysis of the gases (5); solids by direct insertion (6), electrothermal vaporisation (7), slurries (8,9) and laser ablation (10, 11). Liquids have also been analysed by electrothermal vaporisation (12). The ICP has also been

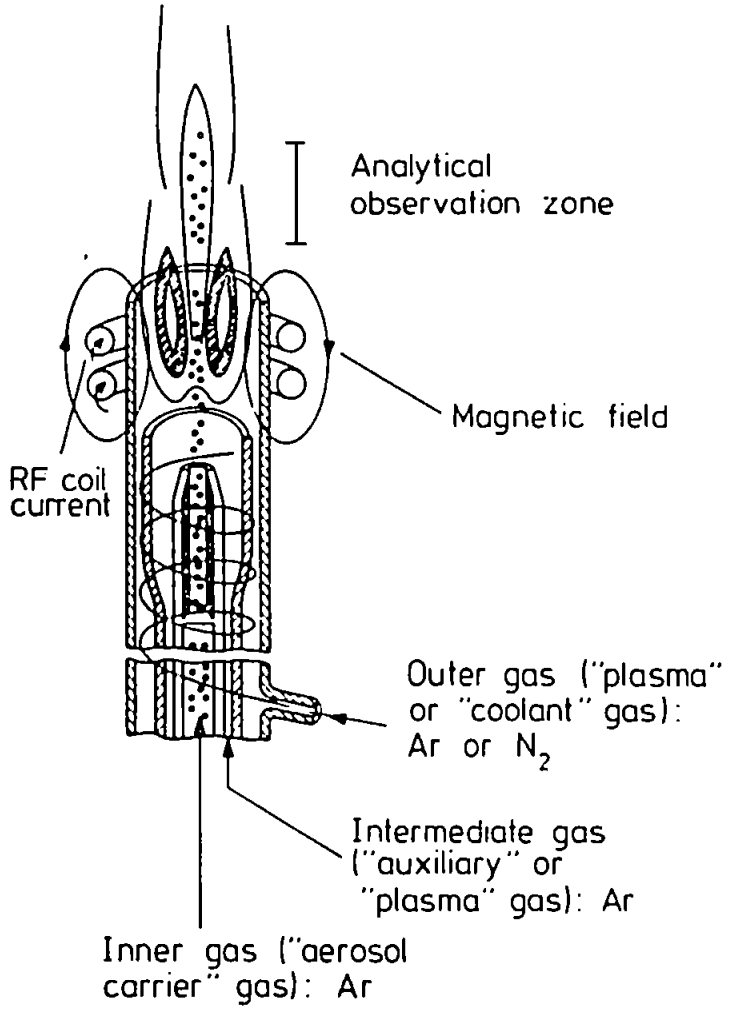

FIG 1.1.1 SCHEMATIC DIAGRAM OF AN ICP

used as a chromatographic detector (13).

The use of an ICP has a number of advantages over the conventional flame source; increased excitation temperature which improves the sensitivity of the technique, long linear range up to four or five orders of magnitude, fewer chemical interferences due to the increased temperature and improved reproducibility.

The majority of ICP's are used as sources for atomic emission spectrometry. Such atomic emission spectrometers are generally one of two types employing either a polychromator or monochromator. The polychromators are equipped with an array of exit slits and photomultiplier tubes (PMT's) for simultaneous multielement analysis. The monochromators have a single exit slit and PMT for sequential multielement analysis. They both work by dispersion of the radiation received into different wavelengths so that the photons of different frequencies appear in the focal plane of a spectroscopic source as an array of monochromatic images of the entrance slit. These images are characterised by their wavelength and called spectral lines. In the atomic spectrum they are discrete. The wavelength of a line is related to the energies (E_p and E_q), of the atomic levels (p, q) between which the transition takes place, and the frequencies by;

$$h\nu_{qp} = \frac{hc}{\gamma_{qp}} = E_q - E_p$$

where c is the speed of light

h is the Planck constant

y is the wavelength

v is the frequency.

Inductively coupled plasmas have also been used as an atom cell for atomic fluorescence spectrometry (AFS) (14) and an ion source for mass spectrometry (MS) (15).

Date and Gray (16) and Houk et al. (17), were the first group to explore the feasibility of using the ICP as an ion source for mass spectrometry. A small fraction of the plasma was extracted through a pinhole sampling orifice into a differentially pumped vacuum system containing an electrostatic ion lens and into a quadrupole mass filter. The major problem associated with this technique is caused by the sampling probe and the method of ion extraction. The two ion extraction methods investigated were boundary layer and continuum. Houk et al., extracted the ions, not directly from the bulk of the plasma but from the cool boundary layer. The ions from the boundary layer may be modified by the ion-molecular reactions and recombinations. In the continuum sampling method a larger extract of the bulk plasma is taken, by the use of a larger extraction aperture which is used to induce continuum flow. This results in a "pinch" discharge in the aperture which leads to photon background interference and raises ion energy, leading to degradation in the resolution of the mass spectrometer. The latter method is the most widely used and involves the plasma playing upon a water cooled nickel core with a 1 mm diameter hole at

the peak, the ions and part of the plasma are drawn through this aperture into the pumped expansion stage. The ions are directed through a secondary, skimmer, cone into the mass spectrometer proper (Fig. 1.1.2). The mass spectrometer is normally a quadrupole type, the ions are focussed using ion lenses and the quadrupole which separates the ions according to their mass to charge ratios (m/z) onto a multi channel analyser.

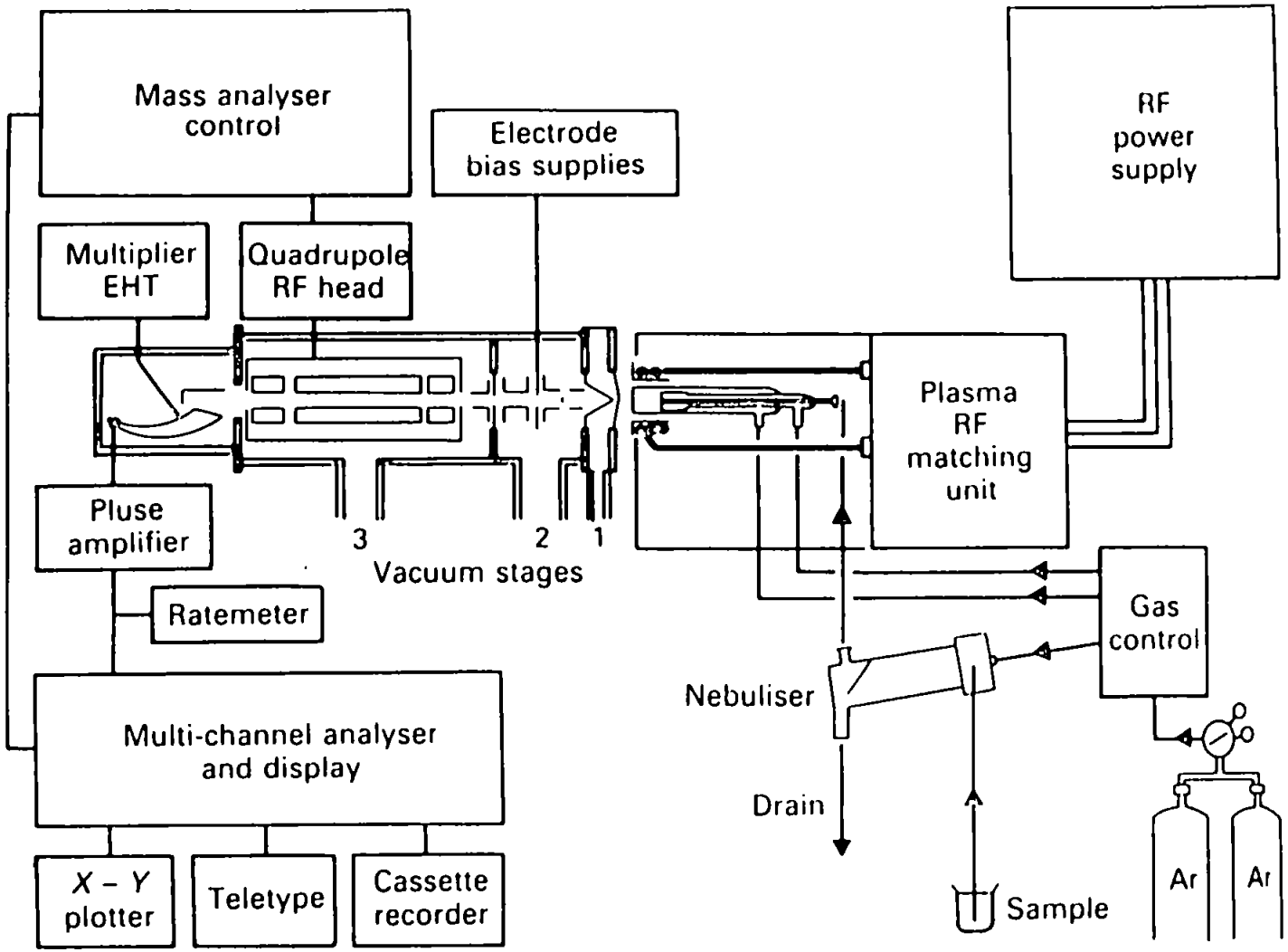

FIG 1.1.2: SCHEMATIC DIAGRAM OF AN ICP-MS

1.2 Analysis of organics by ICP-AES and ICP-MS

The majority of sample types analysed using either an ICP-AES or an ICP-MS, have traditionally been in the form of aqueous solutions. Both techniques are however, being increasingly utilised for the determination of trace and ultratrace levels of metals in organic solvents. This is because although many organic samples (e.g. foods and agrochemicals) can be either ashed or digested prior to dissolution into an aqueous medium, in many cases these processes are either difficult or impossible. The direct introduction of an organic solvent may be of particular interest in circumstances where solvent extraction has been used in sample preparation to remove an analyte from a complex matrix, or where it has been used for sample preconcentration (18-21). In addition, organic solvents are often used in the determination of trace metals in lubricating oils (22-24), crude oils (25); and in metal speciation work, where various solvents may be used in HPLC (26). Thus the direct introduction of a wide range of organic solvents may be beneficial (26-34) . However, these techniques as previously reported in the literature also give rise to a number of operating difficulties which include an increase in background emission, deposition of carbon on cones or torches and a decrease in plasma stability, particularly for the more volatile solvents.

Boorn and Browner (26) analysed thirty common solvents by ICP-AES and discussed their results in terms of aspiration

rates. They found good correlation between aspiration rates and the evaporation factors for most of the solvents, implying that the solvent vapour loading was a major factor influencing plasma stability. For several elements, copper, chromium and iron, the signal intensities were compared using both organic and aqueous solutions. It was found that an enhancement for copper was obtained in many organic solvents. However, in volatile organics chromium and iron were suppressed. The removal of some of the solvent by condensation was found to enhance the signals in line with that expected from transport efficiency predictions. For solvents with a volatility greater than water it was found necessary to increase the forward power, and to prevent torch damage, increase the gas flows. For highly volatile solvents a cooled spray chamber or condenser were required to remove excess vapour from the aerosol stream. Barrett and Pruszkowska (27) investigated a number of plasma parameters including forward power, nebuliser gas flow, and injector diameter, on the background, C line, C_2 and CN bands and a number of atom and ion lines. They found that the excitation potential of a line, diameter of the injector tube, nebuliser gas flow, and solvent used had the greatest effect on the net intensity of a particular line. The injector tube diameter depended on the solvent used. If lines were chosen with similar excitation potentials, it was easier to find common parameters.

The effect of thermostatically controlling the aerosol at

low temperatures has also been investigated (28-30). The temperature region, within which aerosol cooling can be applied advantageously, was found to lie between the maximum tolerable aerosol temperature and the optimum aerosol cooling temperature, the range between these temperatures depending on the solvent. For most solvents the optimum signal to background ratio has been found to be close to the optimum aerosol cooling temperature, with the background increasing and the analyte intensity decreasing to the point where the plasma is unstable. Below this optimum point the analyte tends to become trapped in the condenser. Maessen et al. (28-30) found that the volatility of the organic solvents had a two fold effect on the plasma. Firstly the evaporation rate affected, through a shift in droplet size distribution, the rate at which the analyte was delivered to the plasma. There was also an effect on excitation conditions in the plasma as a result of the saturation vapour pressure.

The use of an ultrasonic nebuliser without a desolvation system has been utilised for the analysis of trace metals in xylene (31). The results obtained showed an increase in nebulisation efficiency of greater than 20%, but with only a few elements exhibiting an improvement in detection limit. This was presumed to be as a result of an increase in the background signal and the use of desolvation could be expected to yield an improvement.

The problem of the slow uptake rates required for the

introduction of volatile organics, resulting in large scale pump noise from the use of peristaltic pumps has been addressed by Nygaard and Sotera (32). They introduced the solvents using a syringe pump system and achieved an improvement of about four in the analyte emission peaks and a subsequent improvement in the detection limits compared with aqueous solutions. However, no directly comparable results from the use of a peristaltic pump were presented.

Hauser and Blades (33), analysed non-metallic inorganics dissolve in xylene using Abel inversion i.e. a mathematical transformation which enables the gradients of temperatures and species densities within the discharge, which are only measured as an average value of the intensity, to be transformed into a single point (radial value). This is possible because of the circular symmetry of the discharge. This study showed that molecular emissions, caused by the organic species was restricted to the lower aerosol channel. Non-metallic emission was found both in the toroidal region and higher up the aerosol channel. The non-metallic intensities proved to be independent of the compounds structure and no matrix effects, caused by incomplete atomisation were observed.

Xu et al. (34) looked at the CN band emission which causes spectral interferences on some of the rare earth elements and yttrium. They found that the emission varies with the organic solvent employed as well as the plasma operating

parameters. The nebuliser gas flow and the forward power were particularly important. The analyte intensities of the spectral lies investigated were enhanced when ethanol or acetone were used due to the enhanced transport efficiency.

Fassel et al. (22) analysed a number of different wear metals using a solution of the wear metals in 4-methyl-2-pentane. The viscosity of the oils studied had little effect on the analytical results. Aleges et al. (23), used undiluted oils, and employed a modified Babington nebuliser, equipped with a sample heater. The heating of the samples, immediately prior to nebulisation greatly increased the output of aerosol and decreased any variations in emission intensity. The type of organometallic standard used in the preparation of standards has also been shown to be unimportant, if the observation height is carefully chosen. This method also offers greater sampling speed and less opportunities for errors.

The introduction of organics into an ICP-MS has been less commonly performed than for ICP-AES. Hutton (35), overcame the problem of carbon deposition on the cones by the addition of a low flow of oxygen into the nebuliser gas. This ensured that the ion extraction was as efficient for organic samples as it was for aqueous samples. He also found that it was necessary to increase the forward power, by about 500 W when compared with the

power typically used for aqueous solution, to sustain a stable plasma and obtain maximum ion response. The background spectra obtained contained a number of molecular mass interferences particularly of low mass, and degraded the detection limits for a number of elements. For the rest of the elements investigated, the detection limits were found to be comparable to those obtained using an aqueous system and were only limited by contamination in the solvents used.

Hausler (36) used a 2% oxygen in argon mixture to destroy the graphite carbon associated with the analysis of organic solvents. The detection limits for a number of elements (below mass 82) in xylene were degraded because of transitory species created in the plasma, which interfered with the analysis. Typical analysis of a fuel oil produced an average error of 18%, although the author concluded that the analysis of petroleum products diluted in xylene could be accomplished without the need for digestion in mineral acids.

In further studies Allain et al. (37) and Longrich (38), introduced organics dissolved in water into an ICP-MS. They found that there were significant signal enhancements. This was not just because of improvements in transport efficiency but also due to the formation of the CO^+ ion from the metal oxide, MO^+, ion, which enabled enhancements of up to six hundred per cent (37) for the introduction of trace metals in a glycerol water mixture.

For the analysis of ethanol in water (38), the effects of the nebuliser gas flow proved to be critical with a decrease from 1.3 l min^{-1} to 0.9 l min^{-1} required to enhance the sensitivity. Ebdon et al. (39), used a variable step size simplex procedure to optimise a number of the operating parameters, for five different organic solvents and water, for the analysis of trace metals in the solvent by ICP-AES. They found that there was no direct relationship between the solvents studied and the optimum operating conditions. They did however make some general conclusions: that for solvents of higher volatility a lower nebuliser gas flow and spray chamber temperature are preferable; and that the maximum signal to background ratio was obtained with lower forward powers compared with aqueous solutions. The detection limits were found to be better with the organic solvents than the aqueous solutions.

1.2.1 **Analysis of Reactive Species**

Alkyl compounds of a variety of elements, primarily from groups II and III, are employed in the preparation of complex semiconductors by the process of metal organic chemical vapour deposition (MOCVD) (40, 41). Many of these organometallics are pyrophoric and react with air and water, the reactions often being vigorous and producing a range of toxic products (42). Although the samples can be stabilised in organic solvents, typically diethyl ether, contamination is a major problem. Contamination of the order of 1μg g^{-1} can completely alter the physical, chemical and optical properties of the resultant semiconductor chips. Consequently sophisticated analytical techniques are required for their analysis.

The literature contains few reports of methodology for the analysis of trace contaminants in such organometallics and most have been primarily concerned with the analysis of trimethylgallium, normally involving the decomposition of the sample. Barnes et al., (43-45) analysed trimethylgallium by two separate methods. In the first the non-volatile impurities were analysed after decomposition in 0.5M hydrochloric acid at temperatures of -78^{o}C, followed by direct nebulisation into an inductively coupled plasma - atomic emission spectrometer (ICP-AES). Inorganic compounds in an aqueous medium were used as standards. The second method involved the direct analysis of the trimethylgallium by the exponential dilution

technique which enables the volatile impurities, such as silicon and zinc to be analysed. Barnes et al., (41) also analysed trimethylaluminium using a decomposition method. In this case the use of acids caused a very vigorous reaction so the sample was decomposed in 95% ethanol, before direct analysis by ICP-AES again using inorganic compounds in an aqueous medium as standards. Jones et al., (47) used an unspecified decomposition procedure for the analysis of volatile impurities in trimethylgallium, trimethylaluminium and trimethylindium by ICP-AES. Direct analysis of electronic grade gas has been reported using an inductively coupled plasma - mass spectrometer (ICP-MS) (48). Other reports include the decomposition of organometallics prior to analysis e.g. trimethylgallium by graphite furnace atomic absorption spectrometry (49), dimethylzinc by gas chromatography (50) and dimethylcadmium by gas chromatography and mass spectrometry (51).

1.3 Desolvation

The most important component affecting the analytical performance of an ICP is the sample introduction system. the normal method for the introduction of liquid samples involves the creation of a fine aerosol of the sample by a nebuliser, which is then carried to the plasma by the nebuliser gas. Pneumatic nebulisers have a typical efficiency of about 1 - 2%. The features required by a nebuliser are good transport efficiency, small droplet size combined with a narrow droplet size distribution, independent variation of the sample aerosol production rate and nebuliser gas flow rate and loading of the plasma with high aerosol content (52, 53).

None of the nebulisers currently in production meet all these criterion, particularly the last factor i.e. loading of the plasma which is ambiguous. The introduction of a high sample loading into the plasma has a detrimental effect on the plasma excitation conditions and hence the analytical performance. This is mostly due to the high energy required to desolvate the droplets, leaving less energy for excitation. An obvious remedy to this problem is the removal of some or most of the aerosol prior to its entering the plasma, using some means of desolvation.

A variety of methods have been used to cool the condenser part of the desolvation system including pumped ice cold

water (54, 55), pumped cooled ethylene glycol and water (56), membrane gas-liquid separators (57-58) and thermoelectric devices (59).

Uchida et al. (54), reported improvements in sensitivity of up to sixteen times, although a decrease in stability was observed caused by larger aerosol size distribution, and thus the detection limits improved by only a factor of ten. These workers found approximately 50% of the analyte in the drain, due to recombination of the large aerosol droplets with condensed water. They suggested the use of ultrasonic-nebulisation or a large nebulisation chamber, to remove the large droplets from the system.

Tsukahama and Kibuta (56), investigated the influence of solvent loading on the signals of ions, varying the amount of water vapour entering the plasma by variation in the condenser temperature. They found that the formation of oxides and doubly charged species decreased with decreasing amounts of water vapour. A decrease of an order of magnitude was noted when the condenser was at $0^{o}C$, compared with those obtained using a conventional sample introduction system. It was also found that the ion kinetic energies decreased with decreasing water vapour.

The effect of introducing organics into the plasma, using desolvation has been widely studied. Huang et al. (60), introduced rare earth elements into a plasma, in 95%

ethanol. Using desolvation, they found between a five and ten fold improvement in the detection limits, caused by a higher transport efficiency. The amount of analyte reaching the plasma was found to depend on the ethanol concentration and the desolvation temperature. Wiederin et al. (61), employed a cryogenic desolvation system, which cooled the condenser down to -80°C, for the analysis of organics after ultrasonic nebulisation. The detection limits obtained for analytes in methanol, acetone, acetonitrile and ethanol, were comparable with those obtained following ultrasonic nebulisation of aqueous solutions. The detection limits were approximately the same, regardless of the solvent used. The use of cooled mini spray chambers and desolvation has also been compared (62), and in this case the analytical performance of the two approaches for the introduction of methanol was found to be comparable. Another comparison of the effects of desolvation with aqueous and organic sample introduction into an ICP (55), found that unlike aqueous sample introduction the excitation characteristics were strongly affected by the interaction of solvent loading with the plasma. The decrease in the amount of solvent entering the plasma, by desolvation, substantially decreases the organic band emission. Desolvation also prevents the plasma energy being used to dissociate the pyrolysis products of the solvent, and there is also a great variation in the emission height profiles, with a large upward shift when there is an increase in the solvent loading.

Gervais and Salin (63), desolvated slurries prior to analysis by ICP-AES. They found an increase in signal intensity although the increase was significantly less for the slurries than for the aqueous standards. There was also only a marginal improvement in the detection limits, due to a comparable increase in noise.

1.4 Analysis of Solid Samples

Most samples analysed by ICP, are in liquid form, normally in aqueous solution, which may be nebulised into a fine aerosol before entry into the plasma. However, many samples are not solutions but solids, which may require extensive pretreatment to bring into solution. This often requires using hazardous and time-consuming procedures, with the possibility of introducing contaminants, the loss of volatile analytes and also the risk of incomplete dissolution. Consequently there has been much interest in the possibility of direct solids analysis.

A paper by Broekaert et al. (64) has discussed some of the solid sampling methods available, including electroerosion, direct insertion and slurry atomisation. Other techniques however include electrothermal vaporisation, laser ablation and glow discharge. Electroerosion, is an arc discharge technique used with conducting solids. Good detection limits have been reported for the technique, but the linear calibration range is short. The problem of matrix matching the standards, and the small number of samples which can be analysed by this technique have limited its usefulness.

Direct insertion of solid samples, involves the placing of the sample in a cup which is inserted into the base of the plasma. Normally the cups are constructed of graphite but for elements which form refractory carbides, molybdenum,

thallium or tungsten cups have been used. This technique provides a very high analyte transportation and enables the determination of low levels of analytes in electrically non-conducting powders (64).

Electrothermal vaporisation (ETV), enables micro-samples to be vaporised to form a vapour or particulate aerosol suitable for transport to the ICP (65). The technique, normally employs a graphite rod which is resistively heated to vaporise the sample, which is then transported in an argon flow to the plasma. The technique enables very high transport efficiencies, but the short transient nature of the signal may cause problems. There are also difficulties associated with, variable vaporisation, the matrix, and the necessity to have samples which are capable of vaporisation.

1.4.1 **Analysis of Slurries**

Slurries are finely ground particles suspended in an aqueous or non-aqueous medium, which act both in terms of transport and atomisation as simple solutions. Under optimal conditions the slurry can be calibrated by using simple aqueous standards.

The technique for first investigated, in ICP-AES, for the nebulisation of alumina slurries (1), although this was a purely qualitative study. The major interest in the technique came in the early 1980's. The analysis of

geological materials, was reported by Fuller et al. (65), who produced slurries by the dispersion of the milled material in a sodium hexametaphosphate solution, and a gelling agent, to stabilise the slurry. The results showed poor recoveries (20 - 50%), compared with aqueous calibration, even when the particles produced were less than 6 μm. The influence of the gelling agents on the transportation and atomisation was not investigated, although the use of matrix matched standards improved the results for a range of certified reference materials.

Halickz and Brenner (66), analysed silicate rocks and their glasses, and clay minerals by ICP-AES. They found that for the silicate materials, the particle sizes, which were dependent on grinding times, were inadequate to control reliably the analytical calibration functions. Analyte signal intensity ratios did not reach a maximum as a function of grinding times, and calibration functions were not consistent for all rock standards. The introduction of clay minerals, despite some difficulties encountered in nebulising the sample, was acceptable. The clay mineral suspensions appeared to be sufficiently small (0.5 - 2 μm) to achieve adequate transport to the plasma.

The analysis of kaolin has been performed (67, 68), and it was found that to prevent blockage, nebuliser design was important. The nebuliser did not however effect the particle size distribution. This size distribution is significantly effected by the spray chamber design and

critically effected by the injector tube diameter. The optimum inner tube diameter proved to be 4 mm i.d., which enabled particles as large as 16 μm to reach the plasma. This however, caused instability in the plasma. Consequently a single pass spray chamber and a 3 mm i.d. injector tube were recommended for practical use. This enabled particles up to 8 μm diameter to be introduced into the plasma and be completely atomised. Particles above this diameter were found to be only partially atomised. Several other factors were found to influence the analytical performance, e.g. the dispersants which prevent agglomeration may also cause partial precipitation. They must therefore be matrix matched with the standards. The effects of viscosity were found to cause non-linear calibration curves with high solids content slurries (> 7-8% m/v).

The analysis of coals (69, 70,) by slurry atomisation into an ICP-AES proved problematic. The analytical performance was greatly affected by the inability to grind the samples down to a sufficiently small particle size distribution. The use of variable step size simplex optimisation identified the most important parameters for atomisation efficiency to be the particle size distribution, slurry concentration and sample uptake rate.

The use of flow injection as a method of introducing slurries into an ICP-AES, has been successfully demonstrated (71). A mini spray chamber proved to be the

optimum design for the spray chamber, due to the decrease in sample dispersion. The introduction of a 500 µl sample injection gave a sensitivity equivalent to that obtained by continuous nebulisation. An injector tube diameter of 3 mm i.d. enables the signal to be enhanced by a factor of two compared with the signal obtained using an injector tube of diameter 1.5 mm i.d. Excellent agreement was obtained with certified reference materials with good precision.

Fundamental studies on the analysis of refractory slurries by ICP-AES (72), have identified that transport and atomisation effects may lead to reduced recoveries of some analyte elements. The refractory ores contain a wide variety of minerals, which when ground subtle variations in particle sizes for different minerals of different hardnesses may be disguised within narrow particle size ranges. These minerals may segregate during nebulisation to produce these low recoveries. The particle size is therefore deemed to be critical, with the samples required to have particle sizes below 5 µm for refractory samples and 3 µm for bulk materials. This would account for the low recoveries due to transportation and possibly atomisation effects in some studies. The five slurries analysed in this study show comparable mass transfer effects with solutions, when the particle sizes were below these figures. Plasma operating conditions were also shown to be important in the atomisation process. A decrease in the nebuliser gas flow increases the residence

time in the plasma and increasing the atomisation efficiency.

The use of ICP-MS for the determination of trace analytes in slurries was first discussed by Williams et al. (73). Analysis was performed on a number of soils and industrial catalysts and the results compared with those obtained by slurry nebulisation ICP-AES and conventional procedures. The nebulisation of 1% slurries was found to cause cone blockage after about thirty minutes, and methods such as decreasing the concentration, resulted in elements at very low levels being undetected. The maximum solids content that could be tolerated and the use of techniques such as flow injection were not discussed. However, the results obtained show good agreement with the other techniques and certified values for all the elements studied except for aluminium, which was found to be about ten per cent low, possibly due to the nature of the refractory aluminium oxides which can withstand the plasma temperature.

The use of slurry atomisation ICP-MS for coals (74), showed good agreement with certified values, again with the exception of aluminium. The fact that the particle size distributions showed a contribution from material of a diameter greater than 10 μm, suggests that coal is particularly suitable for this method. The introduction of slurries of up to 1% m/v, did not cause any cone blockage effects, suggesting that ICP-MS may be more tolerant of high solids than had been previously thought.

Gervais and Salin (63), used a desolvation technique to dry the slurries before analysis by ICP-AES. They found this acted to increase the signal intensities of both the slurries and the aqueous standards by factors of about three and eleven, respectively. However, despite these increases, detection limit improvements were marginal due to an increase in the noise. They found it was necessary to use a continuous tubular injector tube to reduce fluctuations in the plasma and that the injector-gas composition appeared to have a major effect on the particle decomposition capability of the plasma.

1.4.2 **Laser ablation**

The direct analysis of solid samples, both conducting and non-conducting, by laser ablation before introduction into an ICP, provides many advantages over other techniques. The dissolution of many solid samples is often difficult and time consuming involving the use of hazardous and expensive chemicals, and runs the risk of incomplete dissolution, the introduction of contaminants and the loss of volatile analytes. The use of other solid sampling techniques are also problematic. The production of slurries may involve large grinding times with the introduction of contaminants from the grinding medium, and possible problems with precision. Spark methods are generally only associated with conducting solids, and suffer from poor reproducibility, slow sample throughput

and standards matching (64). The formation of discrete signals using electrothermal vaporisation, causes problems with some instrumentation and there is also a loss of some analytes, and so the technique may not be practical for many samples. The use of direct insertion techniques, has not been fully investigated but problems are expected with complex matrices, selective volatilisation and the production of standards (65).

The laser process depends upon stimulated emission, as distinct from spontaneous emission. In stimulated emission an excited state is stimulated to emit a photon by presence of radiation of the same frequency, and the more photons there are present, the greater the probability of emission. For this process to work the existence of a metastable excited state is required, the lifetime of which being long enough for it to participate in stimulated emission. The other requirement is for the presence of a greater population in this metastable state than in the lower state where the transition terminates. At thermal equilibrium the opposite is true, therefore, a population inversion must be achieved. This population inversion is normally caused by a process called pumping, the inversion is caused indirectly through an intermediate state, I. The molecule is excited to I then gives up some of its energy non-radiatively and changes to lower state, A. The laser transition is the return from A to the ground state. In practice, I, is a range of states all of which can convert to A. The I state is reached by an

intense flash of light or pumping.

If the optical cavity is obstructed in lasing systems which have high energy levels with relatively long lifetimes it is possible to improve energetic processes, resulting in a large proportion of the active species raised to state I. At the same time the transition from A to the ground state is suppressed. If at the peak of excitation the obstruction is removed the random processes, which take place over a period of 100-500 μsecs, will be released in a giant pulse, with a pulse width much shorter than the uncontrolled system. This process is called Q-switched mode, so called because the shutter changes the quality (Q) of the resonant cavity. Without obstruction a lasing system is said to be free running or to be fixed-Q (fixed quality resonant cavity).

The use of laser ablation involves the pulsing of a high energy beam at the surface of a sample which causes vaporisation of part of the sample. It was first proposed as a method of sample introduction in atomic spectrometry soon after the invention of the ruby laser by Maiman (76) in 1960. Thompson et al. (77), used a laser inductively coupled plasma microprobe, a laser microprobe and an ICP-AES, for the analysis of steels. The ruby laser used, delivered pulses of 1.0 s and was only able to run in Q-switched mode, producing large craters (300 μm). Reasonable results were obtained by this procedure with variance of less than two per cent, for the major

elements. A series of steel standards enabled calibration curves to be obtained which were linear over at least three orders of magnitude. The detection limits obtained were similar to those obtained by dissolution ICP-AES. The main disadvantage of this system was the single pulse nature, which produced a transient signal for each shot. The size of the crater and the amount ablated meant that the position of the laser shot had to be moved after each firing. It was concluded that while the technique was excellent for major element analysis, it was not possible for trace metals due to inhomogeneity of the sample and transportation problems.

The use of a ruby laser, capable of running in either Q-switched or fixed Q-mode was investigated by Carr and Horlick (78), for the analysis of aluminiums and brasses. They investigated the variation in the signal intensity caused by the variation of a number of parameters including the number of laser shots, and the operation mode. They found no differences in the times and shapes of the signal between elements. The laser repetition rate proved to be optimum at eight seconds which gave a signal intensity twice as good as that obtained for a four second repetition rate. The analytical performance using fixed-Q is much better than that obtained with Q-switched, this is mostly due to the amount of sample ablated, 500 μg compared with 25 μg which also meant the results were less susceptible to inhomogeneity. Detection limits were found to be in the sub-nanogram range. It was also found that

there were some matrix effects, particularly for the aluminium samples, caused by the laser ablation.

Ishizuka and Uwamino (79), used a ruby laser to analyse steels by ICP-AES. They found that there was a linear increase in signal as the laser power was increased in Q-switched mode and that focussing of the laser was very important, particularly when the laser was in fixed-Q mode. They all found that the smaller the spot size the better the analytical performance. The length of the carrier tube, from the ablation cell to the plasma torch, proved to be very important with the laser in Q-switched mode, probably due to the smaller amount of material ablated. The calibration curves were linear over two to three orders of magnitude. The detection limits were in the low picogram range with better results using the laser in fixed-Q mode. The precision was found to be similar in both laser modes.

Gray (80), was the first to describe the use of laser ablation as a method of sample introduction into an ICP-MS. The most serious problems arose from the nature of the mass spectrometry system. The peak arrival rate of the sample is very high and of short duration causing problems in the detection recording system. The transient nature of the signal also causes problems for a scanning instrument. It was also found that sample concentrations produced by 0.5 to 13 laser shots was sufficient to result in some deposition on the cones. It was possible to

obtain a nearly steady state signal with repetition rates of 3 Hz, which would extend the period over which the signal could be collected, although this was not possible with the type of laser used. The analytical performance of the instrument was poor, with detection limits much poorer than with solution nebulisation, and poor precision. However, there were some advantages particularly for isotope ratio work.

The first use of an Nd : YAG (Neodymium : Yttrium Aluminium Garnet ($Y_3Al_5O_{15}$)), laser was described by Arrowsmith (81). The laser was capable of running in single pulse or at a repetition rate of 10 Hz, which produced a continuous signal. This signal could be maintained over long periods by the translation of the sample. The analytical performance of the system was good, with linear calibration curves over four orders of magnitude, for steels. The detection limits were in the range of 0.2 - 2 $\mu g\ g^{-1}$ in the solid and precision of less than five per cent.

The use of a Nd : YAG laser system which is capable of being run in Q-switched mode with variable repetition rates, or fixed-Q mode in a roster, has now been used for the analysis of steels (82), carbonate materials (83), uranium and thorium in aluminium (84) and trace elements in solid plastics (85).

The optimum conditions for the analysis of trace

impurities in steels (82), were found to be focussed for fixed-Q mode and focussed 4 mm above the surface for Q-switched mode. In Q-switched mode, the energy density was so high that the beam is capable of ionising the argon atmosphere to form a plasma. When the target surface is below the focal point a high proportion of the laser energy is lost forming the plasma. The ion yield is increased when the laser beam is defocussed above the focal point. the laser energy loss, to plasma formation is less and therefore the plasma has a greater area of contact. It was found that fixed-Q mode is optimum for the analysis of trace metals and Q-switched mode for non-metallics and high boiling point metals. The analytical precision obtained using fixed-Q mode were better than those obtained using Q-switched mode. This is because the amount ablated in fixed-Q mode is larger and more stable than that obtained in Q-switched mode.

The analysis of carbonate materials (83), by laser ablation proved problematic because of the difficulties in obtaining adequate standards. The use of pressed powder standards of the carbonates proved to be inhomogeneous, although using a true internal standard (Ca^{44}), produced linear calibration curves over at least three orders of magnitude. The precision was however poor. The use of fused glass standards showed better analytical precision and no matrix effects were observed. The use of laser ablation as a method of obtaining spatial information has also been investigated for the analysis of the shell walls

of marine bivalves for changes in analyte ratios, which occur due to salinity and temperature variations and for the presence of inorganic pollutants (83).

1.5 Temperature measurements

The amount of information obtained from spectroscopic observation of an ICP discharge is relatively small. A number of parameters such as, temperature and electron number density, can be obtained if equilibrium and plasma mechanisms are considered. Although this information is not sufficient to describe every process occurring in the plasma a knowledge of the temperature and electron number density can aid our understanding of many analytical applications (86).

A plasma contains many types of neutral or ionised species, either excited or in their ground state. A knowledge about the role and density of these species is necessary to understand the plasma fully. As well as the presence of electrons, neutral (Ar) and ionised (Ar^+) argon are present. The neutral argon may be excited (Ar^*) and the lowest levels are either resonant levels or metastable. Molecular excited (Ar^*_2) and ionised (Ar_2^+) have also to be considered. The injected analyte species occurs in a number of forms (M, M^+, M^{2+}, M^*, M^{*+} ...) depending on the respective ionisation and excitation energies. Negative ions may also be present. The kinetic energy of the plasma may be high enough to atomise every species, and some radicals will exist (OH, N_2, N_2^+, CH, CN ...), this is especially true for the introduction of organics.

The temperature, T, can be defined in classical gas thermodynamics by its relationship to the mean kinetic energy, E_{kin}, of the particles;

$$E_{kin} = \frac{3}{2} (kT)$$

where K is the Boltzmann constant. This equation assumes that all the species have the same mean kinetic (or translational) energy. In a plasma it is difficult to define a single temperature, the different temperatures will be defined according to the parameters observed.

A large number of separate temperature measurements can therefore be defined including, translational or kinetic temperature, excitation temperature, rotational temperature, ionisation-recombination temperature, electron temperature, radiation temperature and Norm temperature. The classification and the equations used in these measurements are discussed in detail by Mermet (87).

The ionisation-recombination temperature (T_{ion}) is defined from the Saha and Boltzmann equations. The Saha equation states that for an equilibrium constant, $s_{e,p}$ we have

$$S_{z,p} = 2\frac{g_p}{g_q} \frac{(2 \pi m_e)^{3/2}}{h^3} (KT_i)^{5/2} \exp \frac{(-(E_p - E_q) - E)}{KT_i}$$

where m_e is the electron mass,

h, Plancks constant,

E_p-E_q, energy difference between levels p and q,
E, lowering of the ionisation energy for species z,
T_i, the ionisation energy
g_p and g_q the statistical weights for species p and q.

The Boltzmann distribution states that the ratio of number densities of either atoms or ions in two energetically bound states p and q is given by

$$\frac{n_p}{n_q} = \frac{g_p}{g_q} \exp \frac{(-(E_p-E_q))}{KT_{exc}}$$

where n_p and n_q are the populations of particles in states p and q respectively,
E_p and E_q the excitation energies of the two states p and q (with $E_p > E_q$),
T_{exc} is the excitation temperature of the species.

The number density of atoms or ions in state p (n_p) relative to the total number density (n_t) is given by

$$\frac{n_p}{n_t} = \frac{g_p}{Q(t)} \exp \left(\frac{-E_p}{KT_{exc}} \right)$$

where Q(t) is the partition function of the species (88). The partition function can be calculated from the J-values (89).

These equations can be combined to produce

$$\frac{n^{2+}}{n^{+}} = \frac{4.83*1015}{n_e} T_{ion}^{3/2} \frac{g^{2+}}{g^{+}} \exp \frac{-E_{ion}}{KT_{ion}}$$

where n^{2+} and n^{+} are the population levels for the second ionisation and first ionisation level respectively and g^{2+} and g^{+} the degeneracies of the element in its second ionisation and first ionisation level respectively.

In using this calculation, the assumption is made that the plasma is in local thermal equilibrium (LTE), however it may be demonstrated that this is not the case. The deviation of the plasma from LTE is discussed fully by Boumans (89).

A study of the effect of desolvation on the spatial distribution of electron density (90,91), found that the elimination of water from the aerosol flow decreased the overall electron density. There was found to be little change 16 mm above the load coil, but a very large decrease 4 mm above the load coil. The change in excitation conditions experienced by an analyte under dry aerosol sample introduction conditions was not apparent from the data. The electron density in the normal analytical zone was essentially the same for both conditions, so that the excitation conditions should remain broadly similar.

Tang and Trassey (92) investigated the role of water on the excitation temperature of the plasma. They found that the most important role of water in the ICP is the

hydrogen contribution to thermal conductivity. The hydrogen from the water greatly enhances the thermal conductivity and dominates the energy transfer process from the plasma to the sample.

Walters and Barnardt (52), investigated the role of desolvation and hydrogen addition on the excitation features of an ICP. In both cases there was an improvement in the analytical performance, due to the increase in ionisation temperature, electron densities and axial intensity which causes an increase in the net spectral line intensities leading to lower detection limits. the apparent contradiction between the increase in electron density observed after desolvation and the decrease observed by Caughlin and Blades (91) is explained by the fact that Cauglin and Blades completely eliminated the water content. In this case an optimum amount of water is introduced into the nebuliser gas. This explanation is also used to explain the temperature decrease observed by Tang and Trassey (92). Walters and Barnardt (52) do agree that hydrogen is responsible for better energy transfer in the plasma.

Fister and Olesik (93), investigated the role of the desolvating droplet in the plasma, finding a variation in the vertical atom emission profiles, and also a greater deviation from LTE with a narrow injector tube. Alder et al. (94), also investigated the influence of water vapour on the excitation and ionisation temperature measurements,

finding a decrease in the temperatures of at least 500 K when water was removed. There was also variation with the viewing height, with both temperatures decreasing with increased viewing height and the differences increasing.

1.6 Aims of This Study

Plasma spectrometry is a major technique for the determination of elemental composition. Methods for the analysis of aqueous and some organic solutions are in many cases well established, but the application of plasma spectrometry to more difficult materials is often severely restricted by their physical and chemical properties. The objective of this study is to design and develop sample introduction techniques and instrumentation for plasma spectrometry to extend the application of the technique to more difficult materials.

Particular emphasis is placed on samples which are only available in small quantities and others difficult to analyse by conventional means due to safety, practical or economic reasons. Such samples include volatile organics, unstable species in volatile organics and samples difficult to dissolve.

2. INSTRUMENTATION AND MISCELLANEOUS MATERIALS

2.1 VG Plasmaquad II Inductively Coupled Plasma - Mass Spectrometer

The VG PlasmaQuad II ICP-MS instrument (VG Elemental, Winsford, Cheshire, U.K.) was subjected to minor modifications for a number of experiments. The on-board mass flow controller which normally meters the nebuliser gas flow and allows the mixing of the nebuliser gas flow was not used. The nebuliser gas flow was metered using an external mass flow controller (Tylene U.K., Swindon, U.K.) which was fed directly from the output of a Signal gas blender (Signal Instrument Company, Camberley, U.K.). The removal of part of the side of the instrument and the torch box enabled the placement of the sample introduction system on the outside of the instrument with the ability to connect the sample introduction system directly to the plasma torch.

2.2 Kontron S35 Inductively Coupled Plasma Atomic Emission Spectrometer

The Kontron S35 (Kontron GmbH, Eching, FDR) ICP-AES consists of a monochromator consisting of a 0.6 m Czerny-Turner type which utilises a 2400 lines mm^{-1} holographic grating. The wavelength is selected using an optical angle encoder which enables wavelength selection to be accurate to 1/10000 of a degree or 0.0015 nm. The

spectrometer is enclosed and kept at a constant temperature (37 $\pm$ 0.1 ^{o}C). Plasma viewing is by means of a periscope which allows observation from 0 - 60 mm above the load coil. Both the periscope and spectrometer are computer controlled.

The ICP torch used is of the demountable Greenfield type mounted in a four turn, water cooled copper coil. The RF generator is a 3.5 kW 27.12 MHz crystal tuned system. The gas flows were metered using mass flow controllers, some modification was made to enable the introduction of mixed gases into the nebuliser gas flow by means of a Signal gas blender (Signal Instrument Company, Camberley, U.K.). In this case the nebuliser gas was controlled externally using a mass flow controller (Tylene, U.K., Swindon, U.K.).

2.3 Signal Gas Blender

The mixing of gases for introduction into the nebuliser gas flow was performed using an Signal Gas Blender (Signal Instrument Company, Camberley, Surrey, U.K.). The instrument relies upon a constant differential pressure across the orifice. The gas flow is therefore determined by the orifice geometry, pressure difference, temperature and density of the gas.

The whole flow assembly is enclosed in a thermostatically controlled box. the calibration of the instrument is obtained by addition of a trace of propane which is

measured using a flow ionisation detector which is calibrated against a primary standard. The composition of the gas mixture is repeatable to within 2% of the set point.

There is a pressure drop of 25 psi across the blender. Consequently an input pressure of 95 psi is normally used to ensure an output of 70 psi.

3. ANALYSIS OF ORGANICS BY ICP-MS AND ICP-AES

3.1 Introduction

The great majority of samples introduced into an ICP are inorganic in form and normally introduced in an aqueous solution. there are, however, many instances where it is either impossible, or difficult, to introduce samples in this form. Some samples are in organic solutions and it may not be advantageous to extract these into an aqueous system, examples include, solvent extractions, high performance liquid chromatography, organic vapours (e.g. coupled GC-ICP) and samples directly dissolved or occurring in organic solvents.

It is the latter area which is of particular interest in this study. The direct introduction of organics into an ICP, has been performed for a large number of different solvents, including alkenes (26,27,31), alcohols (26,29,32), alkanes (26, 30,32), MIBK (28, 100) and diethyl ether (26,30). The ICP-MS has been used for a smaller variety of samples including white spirit (35), fuel oil (35), xylene (36) and ethanol (37).

3.2 Determination of Trace Metals in Organics by ICP-AES

3.2.1 Introduction

The nebulisation of organic solvents is relatively straightforward, indeed volatile solvents produce fine aerosols with greater efficiency than water, however, the transportation of the solvent from the nebuliser to the plasma is problematic due to the physical characteristics of each solvent used. The major factors affecting the droplet size distributions are considered to be surface tension, viscosity, evaporation rate, solvent density and vapour pressure (102). The first two of these, surface tension and viscosity, affect the primary droplet size and the others affect the droplet size changes between the nebuliser and the plasma. One of the consequences of this is the requirement to matrix match the standards.

The tolerance of a plasma to a large number of organic solvents (26), was investigated in terms of the "limiting aspiration rate" of the solvent. This was defined as the rate at which a solvent could be introduced into a plasma, with the plasma remaining stable and no carbon build up for one hour. In general a correlation was found between high evaporation factors and low limited aspiration rates.

The effect of thermostatically controlling the aerosol at low temperature has also been investigated (28-30). The temperature region within which aerosol cooling can be

applied advantageously was found to lie between the maximum tolerable aerosol temperature and the optimum aerosol cooling temperature. The range between these two temperatures depended on the solvent. For most solvents the optimum signal to background ratio has been found to be close to the optimum aerosol cooling temperature. Above this optimum temperature the background increases and the analyte intensity decreases to the point where the plasma is unstable. Below this optimum point the analyte tends to become trapped in the condenser.

These authors (28-30) found that the solvents had a two fold effect on the plasma. Firstly the evaporation rate caused a shift in the droplet size distribution, which affected the rate at which the analyte was delivered to the plasma. There was also an effect on excitation conditions in the plasma as a result of the solvent vapour pressure.

A thermostatically controlled spray chamber (39) was used for the analysis of a number of solvents. A number of parameters were optimised by a variable step size simplex procedure. It was found that there was no direct relationship between the solvents studied and the operating conditions. Some general conclusions were made, for solvents of higher volatility a lower nebuliser gas flow rate and spray chamber temperature are preferable and that the maximum signal to background ratio was obtained using lower forward powers.

The shows some the problems encountered by the introduction of volatile organic solvents. A smaller droplet size is obtained but also a high solvent plasma loading. This means that to prevent plasma instability a method or methods are required to limit the volume of solvent reaching the plasma.

3.2.2 Experimental

The solvents used in these experiments were Aristar grade (BDH, Dorset, U.K.). Standards were prepared either from organometallic standards (Conostan, MBH Analytical Ltd., Barnet, Herts., U.K.) of organometallic salts (Spectrosol cyclohexylbutyric acid salts, BDH, Dorset, U.K.).

The spray chamber used was of the Scott type double pass design, jacketed to allow the circulation of a cooling fluid. Temperature control was achieved by means of an open propanol reservoir into which was immersed a recirculation pump, with a heating element (Techam Tempunit, Techne, Cambridge, U.K.) to pump the cooling/heating fluid around the system. Cooling was achieved using a refrigeration unit (Grant CC15, Grant Instruments, Barrington, Cambridge, U.K.) and by the addition of liquid nitrogen. Propan-2-ol was used as the pumped fluid.

3.2.3 Results and Discussion

The introduction of volatile organic solvents into a plasma for ICP-AES, is complicated by high solvent transport efficiency which can lead to plasma instability or even to extinction of the plasma. There are a number of ways of preventing this high transport efficiency, two methods are to decrease the sample uptake rate or to cool the spray chamber.

Both of these methods were used for the introduction of methanol into an ICP to determine the trace metal composition. The plasma operating conditions, for this analysis, are shown in Table 3.2.3.1. They were obtained by univariate searches using the emission lines (251.611 nm and 212.412 nm) as a reference.

These conditions were used to determine a number of trace metals in methanol. The detection limits obtained for these elements are shown in Table 3.2.3.2.

The equation used for the calculation of the detection limits was:

$$C_L = 3(RSD)_B \frac{(Co)}{S/B}$$

where C_L = detection limit, $(RSD)_B$ = relative standard deviation of the background, Co = analyte concentration

TABLE 3.2.3.1 THE OPERATING CONDITIONS USED FOR THE DETERMINATION OF TRACE METALS IN METHANOL

Forward power	1.25 kW
Coolant gas flow	25 l min^{-1}
Auxiliary gas flow	0.6 l min^{-1}
Nebuliser gas flow	1.6 l min^{-1}
Viewing height	10.6 mm
Temperature of spray chamber	$-4^{o}C$
Sample uptake rate	0.67 ml min^{-1}

TABLE 3.2.3.2 DETECTION LIMITS OBTAINED FOR THE DETERMINATION OF TRACE METALS IN METHANOL USING ICP-AES

Analyte	Detection limits/μg ml^{-1}	
	Direct Nebulisation	Flow Injection*
Si	7	2
Cu	8	2
V	7	3
Mn	12	4.15

* 300 μl sample loop

and S/B the signal to background ratio.

The results obtained for the direct introduction of the methanol into the ICP are compared with those obtained, under the same operating conditions, apart from the sample uptake rate, which was increased from 0.67 ml min^{-1} to 2.5 ml min^{-1}, for the flow injection of the methanol into an aqueous carrier stream. The sample loop size used for this experiment was 300 μl, this was chosen because it was the maximum volume which when injected did not appear to cause plasma instability.

The results show that the use of flow injection enables a marked improvement in the detection limits to be obtained. This nearly correlates with the change in sample uptake rate and hence transport of the analyte to the plasma. The uptake rate increased from 0.67 ml min^{-1} to 2.5 ml min^{-1} which represents an increase by a factor of 3.7. The detection limits obtained from silicon showed an improvement by a factor of 3.5.

A similar procedure was performed for the determination of trace metals in hexane by ICP-AES. The optimum conditions were obtained by the variable step size simplex procedure. The following parameters were optimised; forward power, coolant gas flow, auxiliary gas flow, nebuliser gas flow, viewing height, temperature of spray chamber, sample uptake rate and oxygen addition. The criterion of merit was the signal to background ratio and the analyte used for this optimisation was copper.

A similar procedure was performed for the determination of trace metals in hexane, by ICP-AES. The operating conditions, used for both the direct nebulisation and the flow injection of the hexane into the plasma are shown in Table 3.2.3.3.

The decrease in both the temperature of the spray chamber and the uptake rate of the solvent compared with the methanol conditions after the optimisation is due to the volatility of the sample. The evaporation factor, E, for methanol is 47.2 $\mu m^3/s$ compared with 298 $\mu m^3/s$ for hexane at 25^{o}C (12).

The temperature of the spray chamber (-19^{o}C) meant that for the flow injection experiments the use of a carrier stream of water was no longer appropriate, because of the freezing of the water in the spray chamber. Consequently 2-ethoxy ethanol was used as the carrier stream. This solvent was selected as carrier because of its lower vapour pressure and its intrinsically high level of oxygen. The flow injection loop volume used was 150 μl.

This level of oxygen is important, because the introduction of hexane caused carbon deposition on the torch. A low flow of oxygen was added to the nebuliser gas flow, to prevent this deposition by combustion of the carbon. The introduction of oxygen proved not to be necessary for the flow injection studies.

TABLE 3.2.3.3 THE OPERATING CONDITIONS USED FOR THE DETERMINATION OF TRACE METALS IN HEXANE BY ICP-AES

Forward power	1.65 kW
Coolant gas flow	22 l min^{-1}
Auxiliary gas flow	1.0 l min^{-1}
Nebuliser gas flow	1.2 l min^{-1}
Viewing height	11.4 mm
Temperature of spray chamber	-35 ^{o}C
Sample uptake rate	
(i) Direct nebulisation	0.5 ml min^{-1}
(ii) Flow injection	2.5 ml min^{-1}
Oxygen addition	4.5% v/v

The results from these experiments are shown in Table 3.2.3.4. These detection limits, once again show the advantage of the use of flow injection. There is once again a marked improvement between the results. The decrease in the sample loop volume, compared with the hexane results (Table 3.2.3.2), does not appear to affect these results. The improvement is slightly greater than can be explained by the relative transport efficiencies. The sample uptake rate increases from 0.5 ml min^{-1} for direct nebulisation of the solvent to 2.5 ml min^{-1} for the flow injection of the solvent or an increase by a factor of five. The detection limit for copper improves from 12 $\mu g\ ml^{-1}$ to 2 $\mu g\ ml^{-1}$ or by a factor of six. This may be partly due to the expected detrimental effect on the plasma caused by the introduction of oxygen.

The introduction of diethyl ether also required the addition of a low flow of oxygen to prevent carbon build up on the torch. This solvent is significantly more volatile than hexane, with an evaporation factor of 771 $\mu m^3/s$ compared with that for hexane of 298 $\mu m^3/s$ at 25°C (12). This will clearly increase analytical problems with the solvent. The system was optimised using a variable step size simplex procedure (101) for the determination of trace metals in diethyl ether by ICP-AES. The criterion of merit used was the signal to background ratio and the parameters optimised were the forward power, the viewing height above the load coil, the nebuliser gas flow rate

Table 3.2.3.4 DETECTION LIMITS OBTAINED FOR THE DETERMINATION OF TRACE METALS IN HEXANE USING ICP-AES

Analyte	Detection limits/μg ml^{-1}	
	Direct Nebulisation	Flow Injection*
Si	10	2
Cu	12	2
V	11	2
Mn	15	3

* 150 μl sample loop

and the spray chamber temperature. A particular line was selected to represent atomic lines of a low to medium ionisation potential ("soft") and a line with a high first or second ionisation potential ("hard") according to the criteria of Boumans and Lux-Steiner (100), ("soft" Cu I 324.754 nm and "hard" Mn II 257.610 nm). The results for this optimisation procedure are shown in Table 3.2.3.5. Univariate searches around the optima were performed to illustrate the importance of each parameter on the sensitivity (Figures 3.2.3.1 - 3.2.3.4).

The optimal conditions obtained for the forward power (Fig. 3.2.3.1) appear to contradict earlier work by other workers, which showed organic solvents required an increase in forward power compared with aqueous solutions, to reach an optimum (23, 25,29,30). The work of Evans et al. (101), however, found a decrease in power was required for a wide variety of solvents and concluded that it was the effect of including other parameters in the optimisation; particularly the combined effects of lower nebuliser gas flow and spray chamber temperature, which results in a much reduced solvent load to the plasma.

The nebuliser gas flow (Figure 3.2.3.2), proved to be a critical parameter. This is due to the spatial effects in the plasma. By decreasing the nebuliser gas flow the optimum will move to lower down in the plasma, where the electron number density is significantly increased (91). This effect of the electron number density is more

TABLE 3.2.3.5 OPTIMUM CONDITIONS FOR THE DETERMINATION OF TRACE METALS IN DIETHYL ETHER BY ICP-AES

System	Line		Optimum
Cooled spray chamber	Cu(I)	Forward Power/kW	1.38
		Height above load coil/mm	43.26
		Carrier gas/ l min^{-1}	1.25
		Temperature/^{o}C	>-40
	Mn(II)	Forward Power/kW	1.73
		Height above load coil/mm	14.15
		Carrier gas/ l min^{-1}	0.88
		Temperature/^{o}C	>-40

FIG 3.2.3.1: NORMALISED SBR VS FORWARD POWER DIETHYL ETHER INTO AN ICP-AES

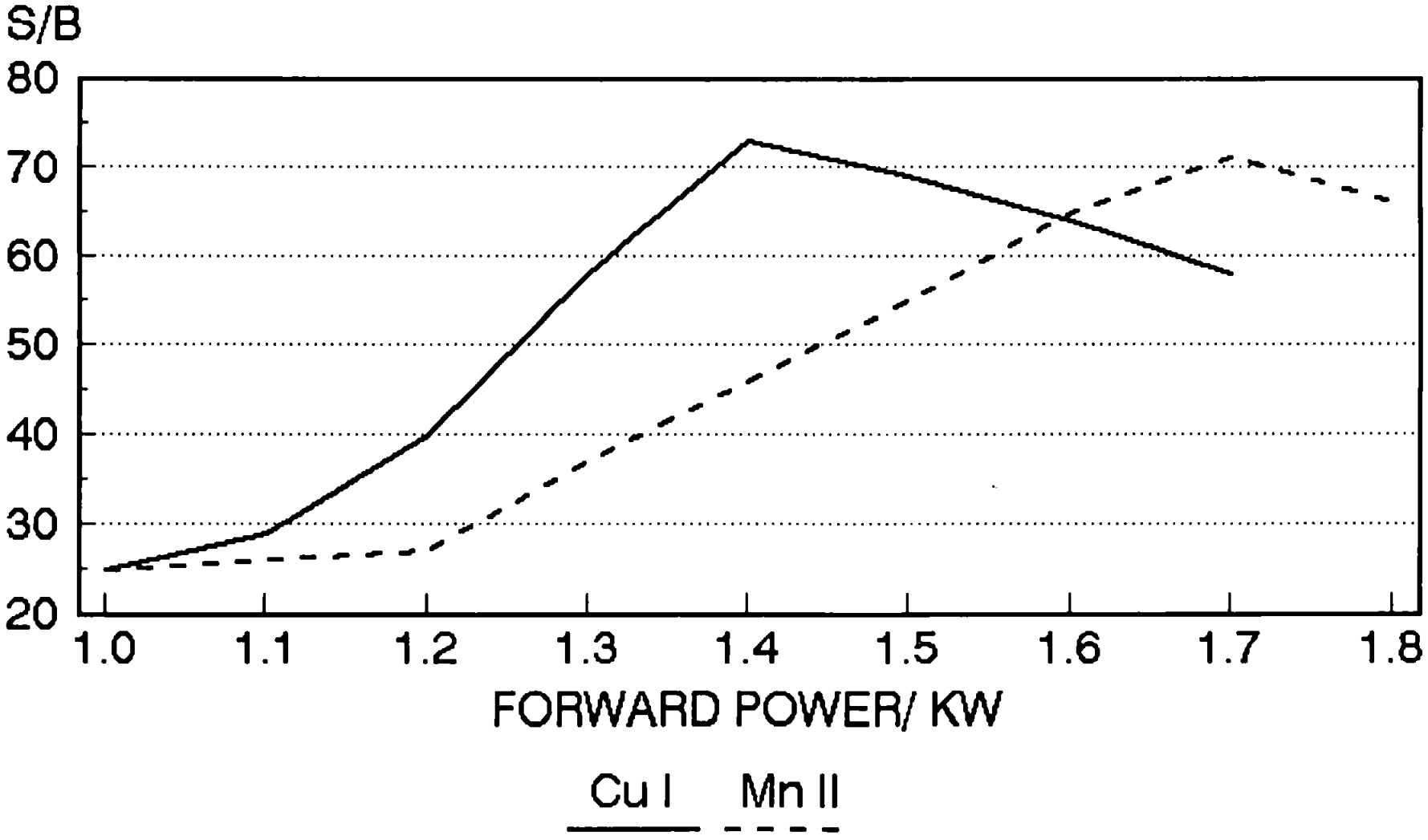

FIG 3.2.3.2: NORMALISED SBR VS NEBULISER GAS DIETHYL ETHER INTO AN ICP-AES

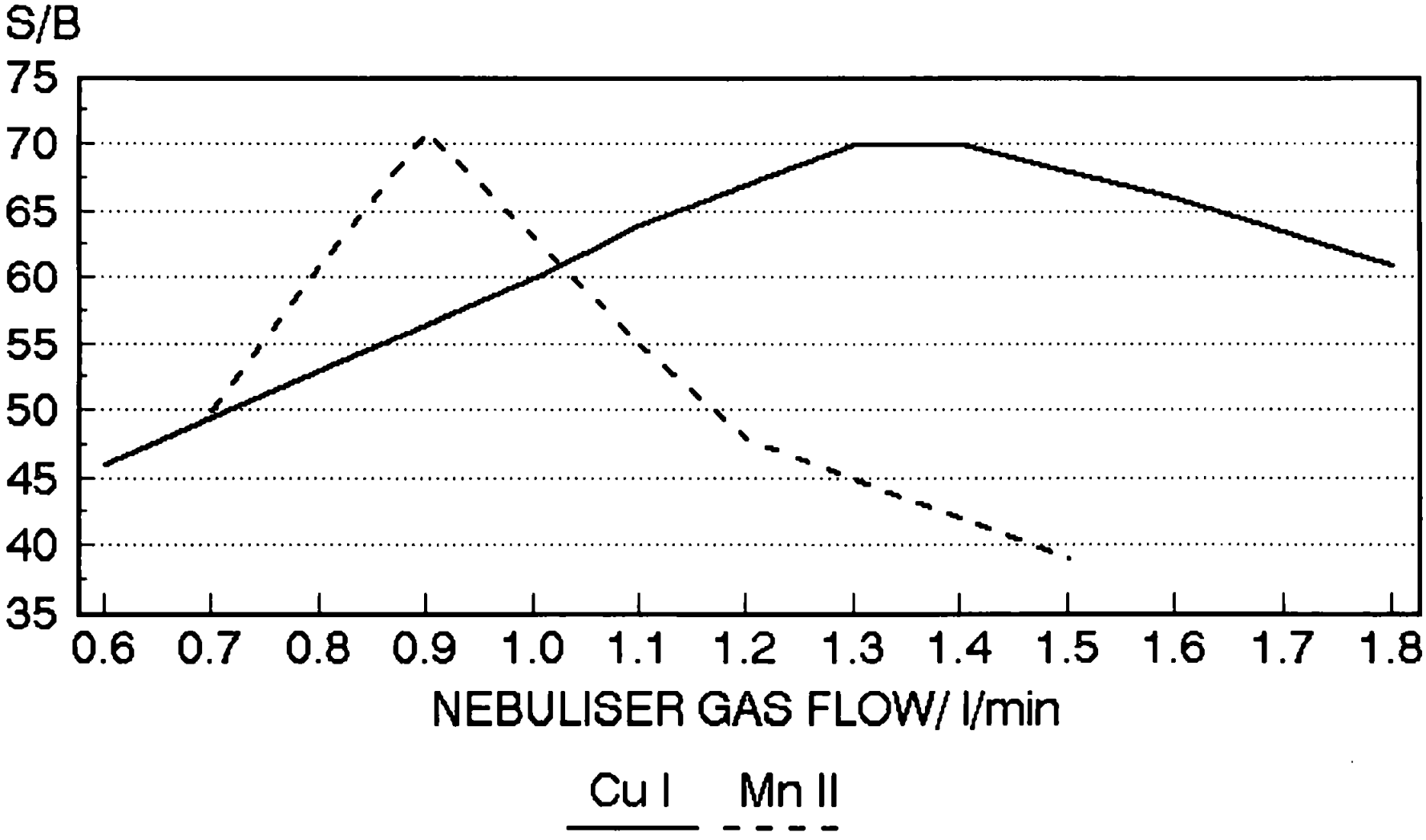

FIG 3.2.3.3: NORMALISED SBR VS VIEWING HEIGHT DIETHYL ETHER INTO AN ICP-AES

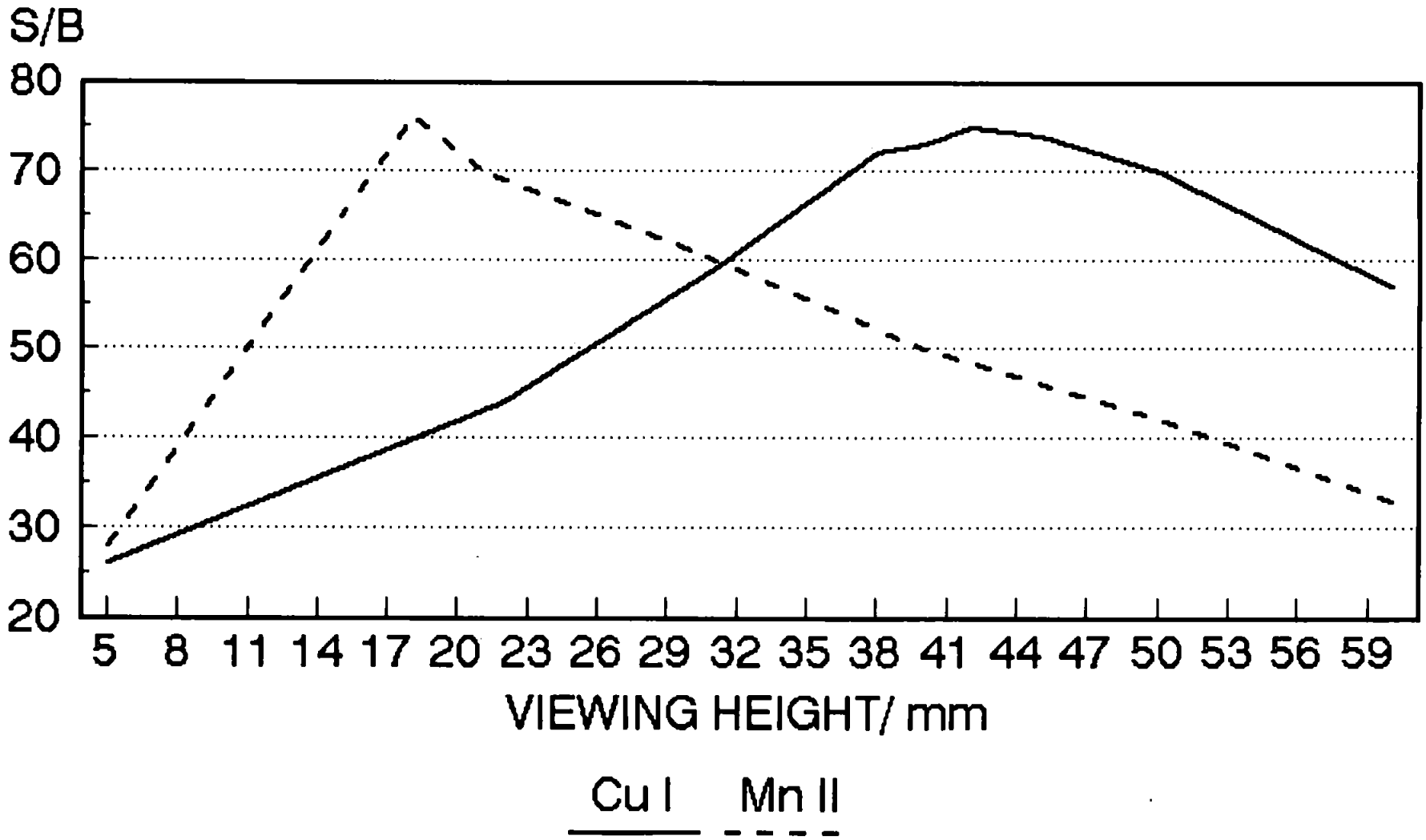

FIG 3.2.3.4: NORMALISED SBR VS TEMPERATURE OF SPRAY CHAMBER DIETHYL ETHER INTO AN ICP-AES

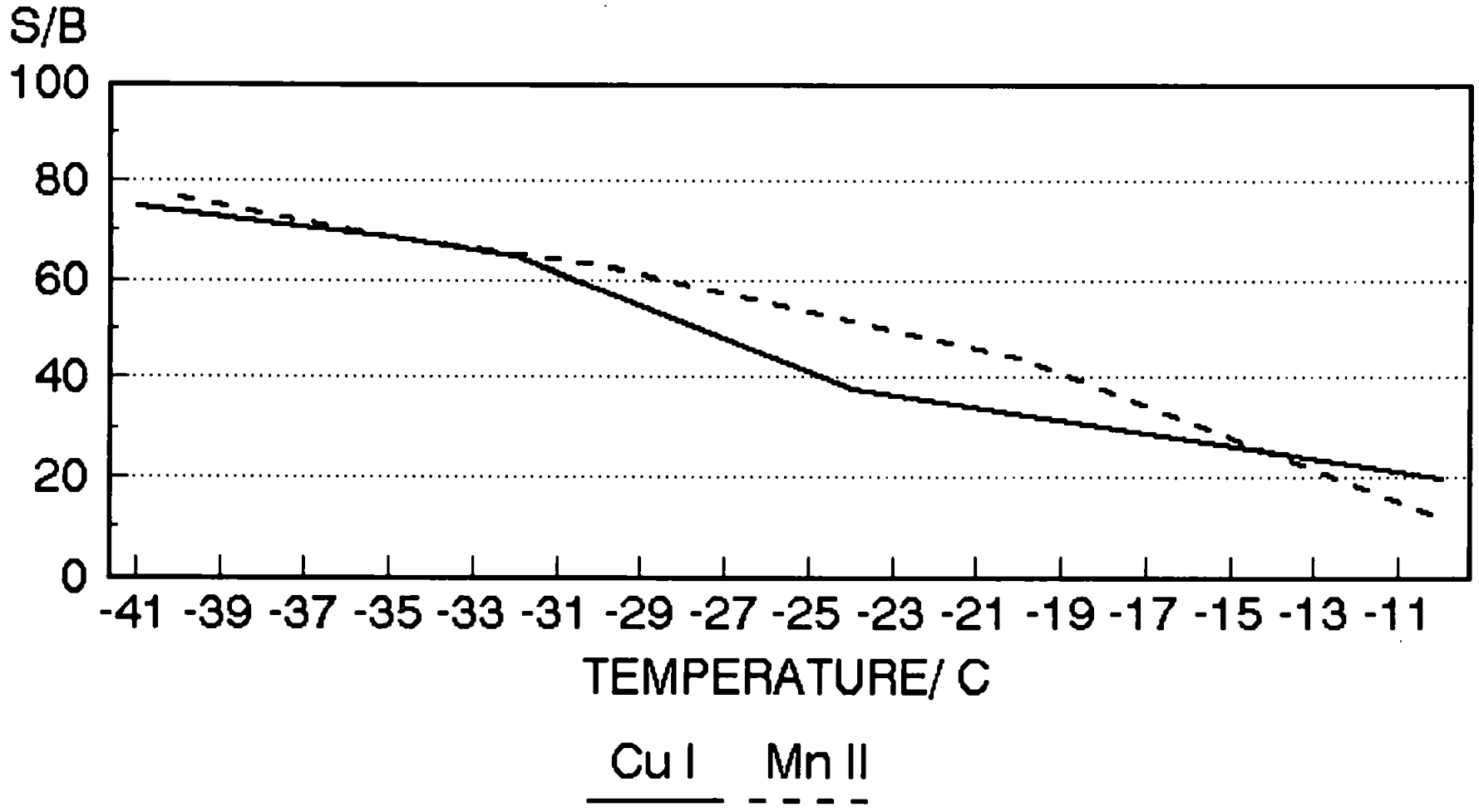

important for the hard lines (e.g. manganese) than for the soft lines because of the increased energy required to cause atomisation.

The viewing height also proved to be important for this work (Figure 3.2.3.3). The relationship between the parameters, particularly forward power and the nebuliser gas flow greatly affects the optimum viewing height. The well-documented use of lower viewing heights for hard lines compared with soft lines, is supported by this study using organic solvents.

The temperature of the spray chamber (Figure 3.2.3.4), did not reach an optimum for the introduction of diethyl ether. There is a steady increase in the SBR, with a decrease in temperature, for both the hard and the soft lines. Further work on this parameter was prevented by the inability to maintain a constant temperature below $-40^{o}C$.

The use of flow injection as a method of introducing small volumes of diethyl ether into the plasma was investigated. the carrier stream used was 2-ethoxy ethanol. The effects on the detection limits of using different sized sample loops was investigated and the results along with those obtained by continuous nebulisation are shown in Table 3.2.3.6.

It can clearly be seen that the effect of the use of flow

TABLE 3.2.3.6 DETECTION LIMITS OBTAINED USING ICP-AES FOR THE DETERMINATION OF TRACE METALS IN DIETHYL ETHER USING FLOW INJECTION

	Line	Detection limits ($\mu g\ l^{-1}$)
Continuous nebulisation	Cu(I)	10
	Mn(II)	15
Sample loop volume/μl		
300	Cu(I)	13
	Mn(II)	17
100	Cu(I)	9
	Mn(II)	13
50	Cu(I)	2
	Mn(II)	2

injection is to improve the detection limits compared with continuous nebulisation. Decreasing the volume of the volatile solvent entering the plasma using smaller sized sample loops improved the sensitivity for both the analytes investigated. By lowering the amount of diethyl ether entering the plasma, the stability of the plasma was considerably improved, which also enabled an increase in the uptake rate. In addition, there was a decrease in memory effects aided by faster throughput of the solvent. Not only did the peaks have a better shape, with smaller sample loops there was a notable improvement in the relative standard deviations (Table 3.2.3.7), which act to improve the detection limits.

TABLE 3.2.3.7 RELATIVE STANDARD DEVIATIONS OBTAINED FOR THE DETERMINATION OF TRACE METALS IN DIETHYL ETHER BY FLOW INJECTION ICP-AES

Sample loop volume/μl	Standard Concentration /μg l^{-1}	Relative Standard Deviation	
		CuI	MnII
50	10	3.9	4.5
	50	3.8	4.5
	100	3.6	4.8
100	10	4.9	6.4
	50	4.8	6.6
	100	4.6	6.8
300	10	6.2	8.3
	50	7.1	8.3
	100	6.4	9.1

n = 10

3.3 Determination of Trace Metals in Organics by Inductively Coupled Plasma - Mass Spectrometry

3.3.1 Introduction

The problems encountered in the introduction of organic solvents, particularly volatile organic solvents, for inductively coupled plasma - mass spectrometry are similar to those encountered with the introduction of organics for ICP-AES. The major problems are caused by the effects of high solvent loading in the plasma, which may lead to plasma instability, which means methods are required to lower this loading.

The problems associated with the introduction of organics into the ICP-MS, which differ from those encountered with an ICP-AES, are due to the nature of the coupling between the ICP and the mass spectrometer. Without the introduction of a low flow of oxygen into the nebuliser gas flow, carbon deposited on the sampling cones may rapidly block the orifice preventing extraction of the ions from the plasma. The other novel factor is the effect of the organic solvent on the ion lens system used to focus the ion beam onto the detector.

3.3.2 Experimental

The solvents used in these experiments were of Aristar grade (BDH, Dorset, U.K.). Standards were prepared either from organometallic Standards (Conostan, MBH Analytical Ltd., Barnet, Herts.) or organometallic salts (Spectrosol cyclohexylbutyric acid salts, BDH, Dorset, U.K.).

The spray chamber used was of the Scott type double pass design, jacketed to allow the circulation of cooling fluid. Temperature control was achieved by use of a recirculation system, supplied with the spectrometer, which pumped cooling/heating fluid around the system. Cooling was achieved by the refrigeration system supplied with the recirculation system and/or by the addition of liquid nitrogen. Propan-2-ol was used as the pumped fluid.

3.3.3 Results and Discussion

The introduction of organic solvents for ICP-MS, is complicated by the necessity to add a low flow of oxygen to the nebuliser gas flow to prevent the build up of carbon on the cones and the effect of the organics on the ion lenses. Both these effects can be partially removed by preventing large amounts of solvent reaching the plasma, for example by cooling the spray chamber, this will however effect the sensitivity of the technique. Consequently care must be taken to prevent cone blockage

and the effects of carbon on the lenses.

The introduction of methanol into the plasma, was achieved by using a slow uptake rate, and the cooling of the spray chamber. The conditions used for this are shown in Table 3.3.3.1. The instrument was optimised for the determination of a wide range of analytes. The detection limits obtained for these analytes are shown in Table 3.3.3.2.

Flow injection was once again used to facilitate the introduction of the organic into the plasma. For the flow injection of methanol a carrier stream of 2-ethoxy ethanol was used. This is because of the lower spray chamber temperature used for the analysis by ICP-MS compared with ICP-AES, which prevents the use of water as a carrier stream. The flow injection loop size volume used in this experiment was 100μl.

The results indicate that the introduction of organic solvents for ICP-MS is possible. The stability of the plasma is clearly of importance in obtaining good analytical data. The use of flow injection improves this stability, by introducing smaller volumes of the volatile organic into the plasma. This results in a great improvement in the detection limits obtained using flow injection compared with those obtained using direct nebulisation.

TABLE 3.3.3.1 THE OPERATING CONDITIONS USED FOR THE DETERMINATION OF TRACE METALS IN METHANOL BY ICP-MS

Forward power	1.75 kW
Coolant gas flow	17.5 l min^{-1}
Auxiliary gas flow	1.0 l min^{-1}
Nebuliser gas flow	0.7 l min^{-1}
Sampling Depth	2.2 mm
Temperature of spray chamber	-30^{o}C
Sample uptake rate	0.8 ml min^{-1}

TABLE 3.3.3.2 DETECTION LIMITS OBTAINED FOR THE DETERMINATION OF TRACE METALS IN METHANOL BY ICP-MS

Analyte	Detection limits/ng ml^{-1}	
	Direct Nebulisation	Flow Injection*
Cu	14	9
V	8	4
Mn	9	4
Pb	12	8

* 100μl

The introduction of diethyl ether into the plasma is complicated by its extreme volatility. The cooling of the spray chamber below -40°C, was found not to be feasible as it proved impossible to keep the temperature constant. The use of a peristaltic pump was also problematic because the low uptake rates required meant that the pulsing effects of the pumping was a problem.

The variable step size simplex procedure was used to optimise the system for the determination of copper in diethyl ether by ICP-MS. The optimum conditions obtained are shown in Table 3.3.3.3. These conditions were used to obtain the detection limit for copper in diethyl ether which is shown in Table 3.3.3.4 compared with those obtained using flow injection. The volume of the flow injection loops was varied to give an idea of the effect of the diethyl ether on the plasma.

These results show that there was an improvement in the detection limits obtained, when small volume flow injection loops were used with an optimum of about 50 μl. This was partly due to the fact that the sample uptake rate can be increased from about 0.05 ml min^{-1} to 0.7 ml min^{-1}, which minimised the effect of the peristaltic pump on the results, and the fact that the stability of the plasma was improved because of the decrease in the total amount of the volatile solvent entering the plasma.

TABLE 3.3.3.3 OPTIMUM CONDITIONS OBTAINED FOR THE DETERMINATION OF COPPER IN DIETHYL ETHER BY ICP-MS

Forward power	1.91 kW
Coolant gas	17.75 l min^{-1}
Auxiliary gas flow	1.10 l min^{-1}
Nebuliser gas flow	0.75 l min^{-1}
Spray chamber temperature	-40^{o}C
Sample uptake rate	0.05 ml min^{-1}

TABLE 3.3.3.4 DETECTION LIMITS OBTAINED FOR THE DETERMINATION OF COPPER IN DIETHYL ETHER BY ICP-MS

Method of Introduction		Detection limit/ng ml^{-1}
Direct nebulisation		27
Flow injection	300 μl	28
	100 μl	14
	50 μl	10
	25 μl	18

Conclusion

It is clear therefore that the introduction of volatile organics for ICP-MS is feasible, but problematic. These problems are mostly due to the effect of the high transport efficiency of the solvents which causes high solvent vapour loading. This leads to plasma instability. This can be partially offset by the cooling of the spray chamber, but at low temperatures the stability may be poor; or by decreasing the sample uptake rate, which may lead to pulsing effects from the pump. The use of flow injection enables a smaller amount of the volatile organic solvent to enter the spray chamber and hence the plasma and by using small sample volumes the uptake rate may be able to be increased leading to less pulsing effects and an improvement in the detection limits. Flow injection also decreases the analysis time, because not only is the uptake rate increased but washout times dramatically decreased.

CHAPTER 4

ANALYSIS OF ORGANICS AFTER DESOLVATION

4.1 Introduction

One of the major problems associated with the analysis of volatile organic solvents, is caused by the high solvent loading which can cause plasma instability or even extinguish the plasma. The method described in Chapter 3, to prevent this instability involved the cooling of the spray chamber and decreasing the sample uptake rate. Both of these methods have problems associated with them and have no effect on the enhancement of the signal. For the most volatile solvents the cooled spray chamber and low uptake rates still provide poor analytical performance. This is because it is difficult to stabilise the spray chamber temperature at the low temperatures required and because of the effect of pulsing by the peristaltic pump at low pump speeds.

Clearly it would be advantageous to have a method of reducing much of the solvent from reaching the plasma, without removal of the analyte. Such a method is the use of a desolvation interface between the nebuliser and the plasma torch. This consists of a method of producing a solvent vapour, normally by heating of the spray chamber, and a condenser which will cause the vapour to condense back to a liquid and be removed from the gas flow.

4.2 Experimental

A desolvation device incorporating thermoelectric devices, to cool the condenser was constructed. These thermoelectric devices, (Peltier Coolers, Melcar CPI4-127-066, Trenton, N.J., U.S.A.), are obtained by arranging n- and p- type materials in couples. The passage of current due to the indicated applied voltage will cause the top surface to be cooled and the bottom surface to be heated, while reversal of current will cause reversal of the direction of heat flow (102).

The Peltier coolers were placed on an aluminium block (100 x 35 x 35 mm), into which a glass tube was placed complete with a drain, connected to a peristaltic pump (Fig. 4.2.2.1). Water cooled copper plates were placed on the outside of the Peltier coolers in order to remove the excess heat and lower the temperature of the cool side. The temperature difference between the two plates of the Peltier cooler could be varied by changing voltage or current from the power source. A schematic diagram of the condenser is shown in Figure 4.2.1.

This condenser was placed between a heated spray chamber and the plasma torch. The spray chamber was of the ARL type (ARL, Crawley, U.K.), and heated using heating tape (Electrothermal Engineering Ltd., Southend-on-Sea, Essex, U.K.).

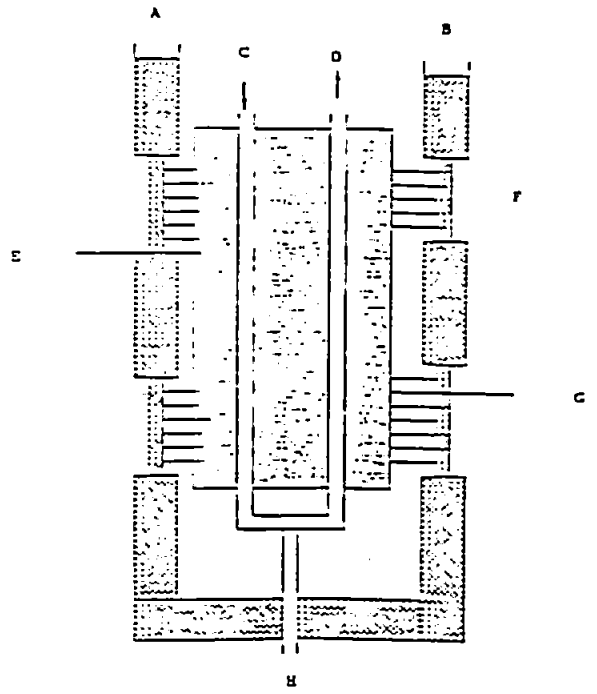

A - COOLANT IN
B - COOLANT OUT
C - FROM NEBULISER
D - TO PLASMA
E - ALUMINIUM BLOCK
F - COOLED COPPER PLATE
G - PELTIER COOLER
H - DRAIN

FIG 4.2.1: SCHEMATIC DIAGRAM OF DESOLVATION CONDENSER

The standards were obtained using organometallic standards (Conostan, MBH Analytical Ltd., Barnet, Herts., U.K.) or organometallic salts (Spectrosol cyclohexylbutyrate salts, BDH, Poole, Dorset, U.K.). The solvents used were Aristar grade (BDH, Poole, Dorset, U.K.).

4.3 **Results and Discussion**

The desolvation system described was optimised by the variable step size simplex procedure for the determination of trace metals in diethyl ether by ICP-AES. The criterion of merit used was the signal to background ratio. The optimum conditions are shown in Table 4.2.3.1.

The desolvation system was found to remove seventy per cent of the solvent introduced. The desolvated solvent when analysed showed levels of the analyte to be below the detection limit (0.6 ng ml^{-1} for Cu^{63}).

To illustrate the importance of all the parameters optimised univariate searches were performed around the optimum (Figs. 4.2.3.1 - 4.2.3.4).

The optimum conditions obtained for both the forward power (Fig. 4.2.3.1) and the viewing height (Fig. 4.2.3.3) are similar to those obtained when using a cooled spray chamber (Fig. 3.2.3.1 and Fig. 3.2.3.2). This is probably to be expected because, although the majority of the solvent has been removed by the desolvation system, the

TABLE 4.2.3.1 OPTIMUM CONDITIONS FOR THE DETERMINATION OF TRACE METALS IN DIETHYL ETHER BY ICP-AES USING A DESOLVATION SYSTEM

Analyte	Parameter	Optimum
Cu(I)	Forward Power	1.43 kW
	Height above load coil	43.3 mm
	Nebuliser gas flow	1.4 l min^{-1}
	Temperature	<-40°C
Mn(II)	Forward power	1.7 kW
	Height above load coil	14.2 mm
	Nebuliser gas flow	0.9 l min^{-1}
	Temperature	<-40°C

FIG 4.2.3.1: NORMALISED SBR VS FORWARD POWER USING DESOLVATION DIETHYL ETHER INTO AN ICP-AES

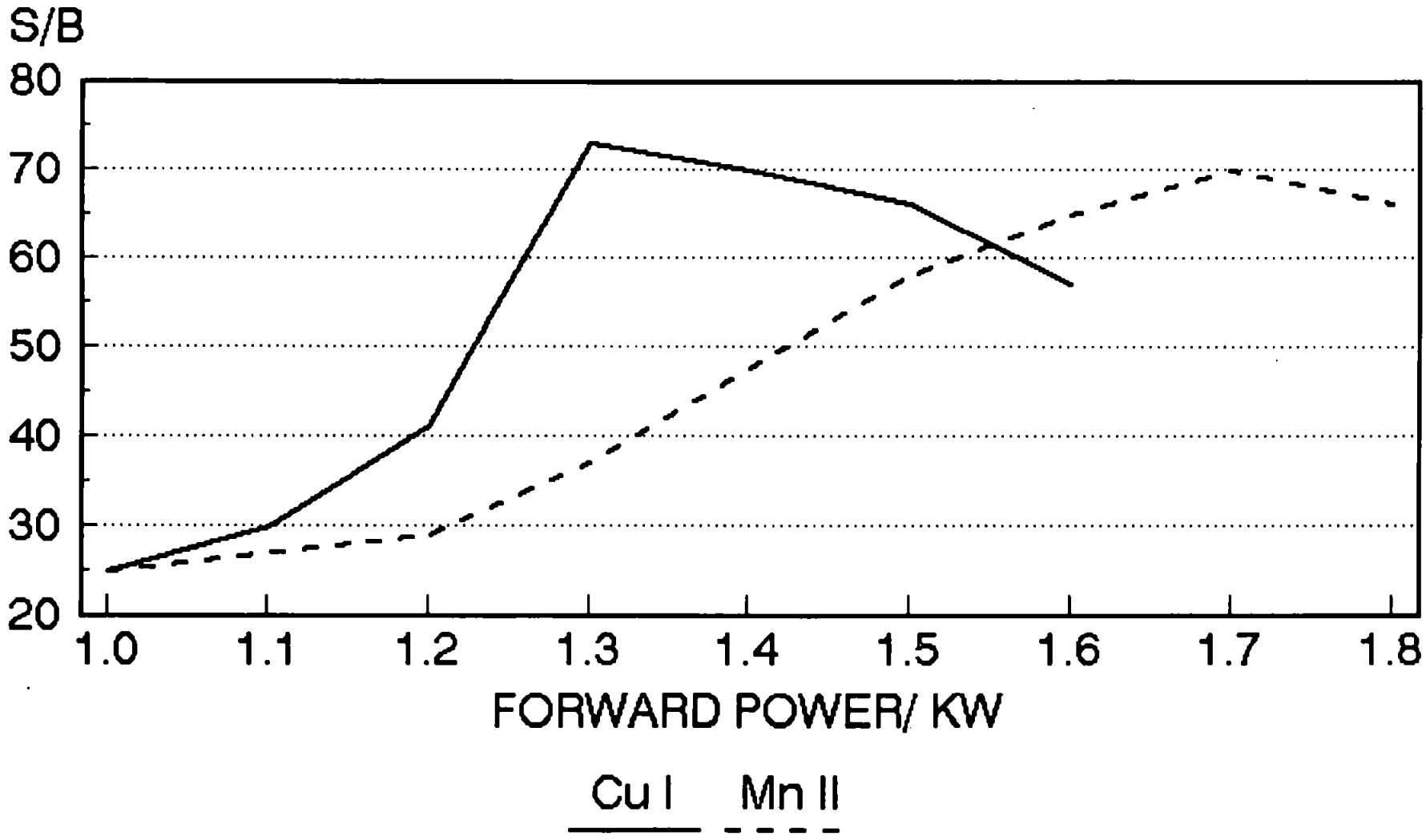

FIG 4.2.3.2: NORMALISED SBR VS VIEWING HEIGHT USING DESOLVATION DIETHYL ETHER INTO AN ICP-AES

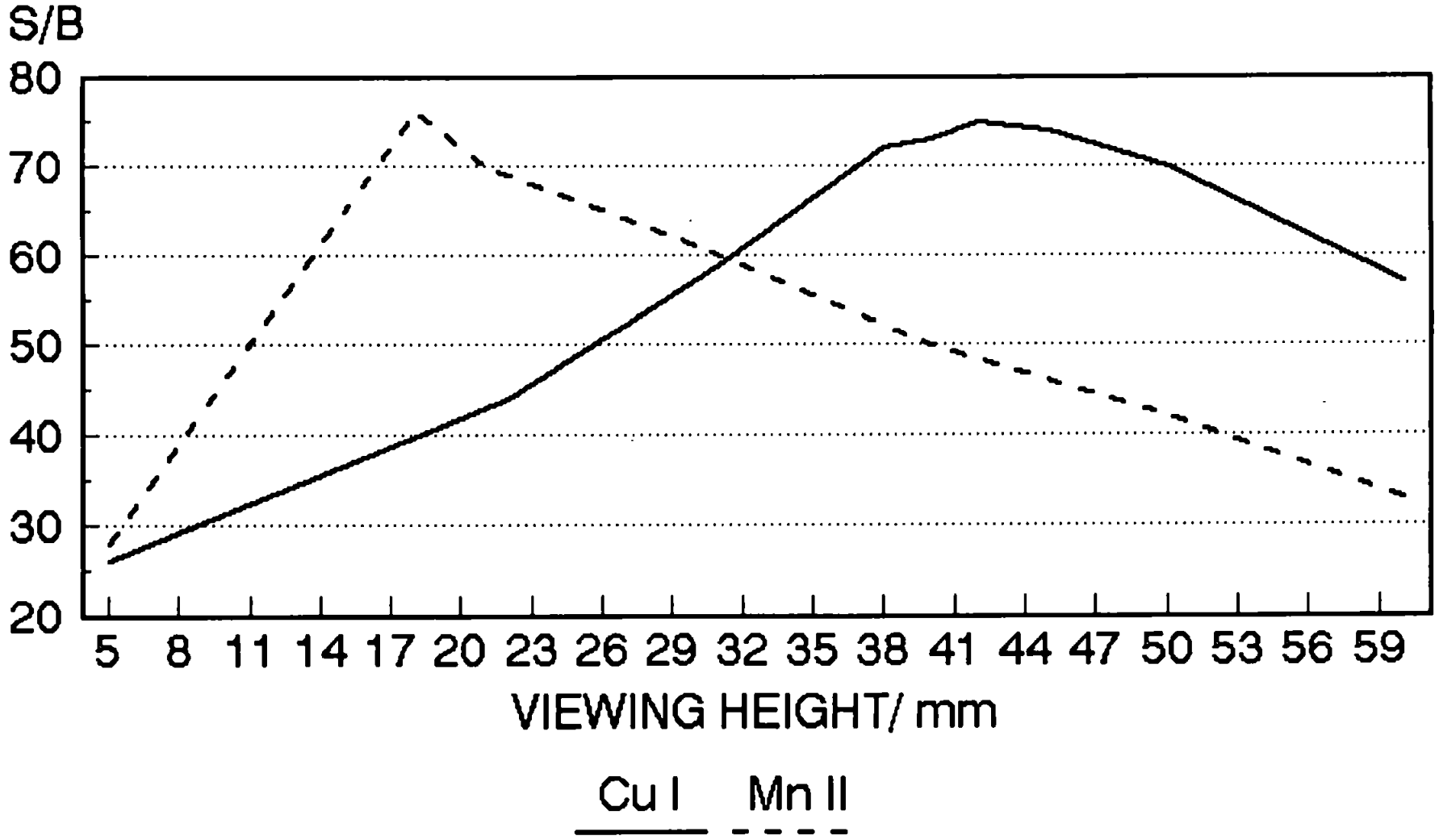

FIG 4.2.3.3: NORMALISED SBR VS NEBULISER GAS USING DESOLVATION DIETHYL ETHER INTO AN ICP-AES

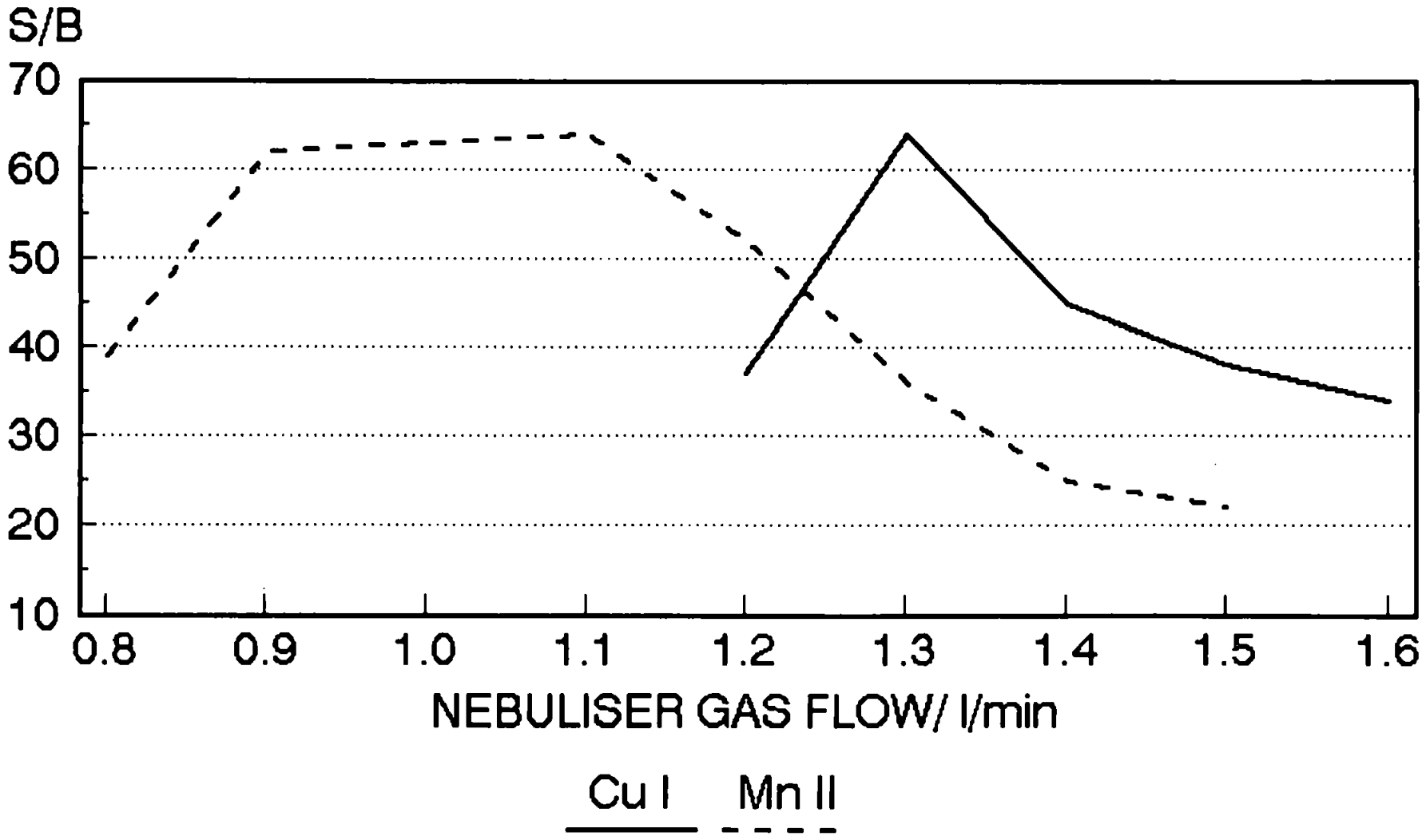

FIG 4.2.3.4: NORMALISED SBR VS TEMPERATURE OF DESOLVATION CONDENSER DIETHYL ETHER INTO AN ICP-AES

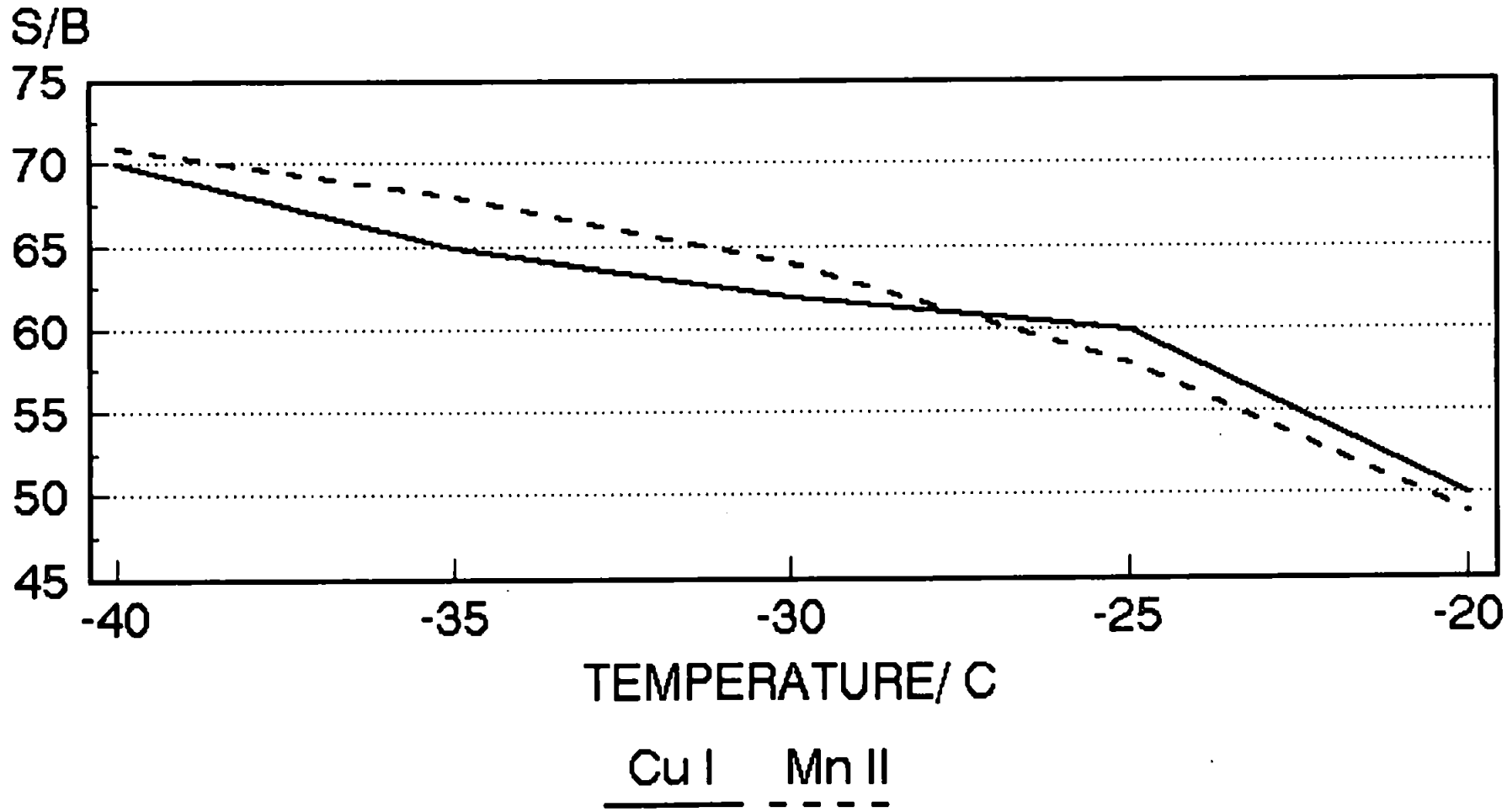

total amount of solvent entering the plasma is similar because of the fact that the sample uptake rate was increased from 0.05 ml min^{-1} to 0.15 ml min^{-1}. This means that the sample uptake rate has increased by a factor of three. The system being seventy per cent efficient the equivalent solvent loading to the cooled spray chamber is ninety per cent. Consequently the operating conditions would be expected to change little.

The effect of the nebuliser gas flow (Fig. 4.2.3.3) proved to be very important for the desolvation of the solvent. It would be expected that the lower optimum gas flow would be required compared with a cooled spray chamber, to increase the residence time in the interface and hence the desolvation efficiency. It appears, however, that the spatial effects in the plasma are of more importance. The lower the nebuliser flow the greater the electron number density will be and hence the effects on the atomisation of the analytes (91). This is particularly true for the "hard" lines (e.g. manganese) where the analyte is more difficult to atomise and consequently a larger electron number density is required. We have, therefore a lower optimum nebuliser gas flow for the "hard" line compared with the "soft" line.

The results obtained for the temperature, relate to the temperature at the centre of the desolvation device, are shown in Figure 4.2.3.4. This indicates that an optimum was not reached. This was due to the inability to control

the condenser temperature below a figure of -40°C. The temperature drop across the peltier cooler having reached the maximum possible (approx. 50°C). Clearly the use of a recirculation system which enables the outside of the Peltier cooler to decrease in temperature would enable a decrease in the condenser temperature. This proved to be more difficult than envisaged, because of the difficulties in maintaining a large enough volume of cooled liquid over the cooling plates to remove the heat from the Peltier coolers more effeciently. Using nitrogen cooled propanol recirculated over the copper plates gave only a marginal improvement in the condenser temperature. It is expected, however, that the signal to background ratio would continue to improve with decreasing condenser temperature.

The effect on the detection limits of using the desolvation interface is shown in Table 4.3.3.2. The results are compared with those obtained using a cooled spray chamber. There is clearly a marked improvement in the results obtained between the two methods. This is due to a number of factors; the desolvation device by removing most of the solvent does not remove as much of the analyte, hence the solvent entering the plasma has a higher relative analyte concentration. There is also an increase in the solvent uptake rate which will again increase the total analyte entering the plasma, this increase is only from 0.05 ml min^{-1} to 0.15 ml min^{-1} or a factor of three. The detection limits showed an improvement by a factor of between seven and a half and

TABLE 4.2.3.2 DETECTION LIMITS OBTAINED FOR THE DETERMINATION OF TRACE METALS IN DIETHYL ETHER BY ICP-AES

System	Line	Detection limit/$\mu g\ l^{-1}$
Desolvation	Cu(I)	1
	Mn(II)	2
Cooled spray chamber	Cu(I)	10
	Mn(II)	15

ten. The rest of this improvement is due to the decrease in the noise, from the peristaltic pump and an increase in the transport efficiency of the analytes.

In the previous chapter it was shown that the use of flow injection led to improved detection limits when introducing a volatile organic solvent into an ICP. The carrier stream used was 2-ethoxy ethanol, because of its lower volatility compared with diethyl ether and its intrinsically high oxygen to carbon ratio. The effect on the detection limits of varying the sample loop volume is shown in Table 4.2.3.3. There was an improvement in the detection limits caused by a decrease in sample size. This was due to the fact that the sample uptake rate was increased from 0.15 ml min^{-1} to 0.3 ml min^{-1} (300 μl loop, 1.5 ml min^{-1} (100 μl loop) and 1.8 ml min^{-1} (50 μl loop). These improvements in the sample uptake rate correlate well with the improvements in the detection limits obtained. The increase in the sample uptake rate also gave sharper and better defined peaks. The improvement using the desolvation device was not as marked, as in the work with a cooled spray chamber (see Table 3.2.3.6). The detection limits obtained using the cooled spray chamber showed an improvement by a factor of six when flow injection was used this compares with an improvement by a factor of nearly two in the work with the desolvation system.

The desolvation system, with slight modification, was

TABLE 4.2.3.3 DETECTION LIMITS OBTAINED FOR THE DETERMINATION OF TRACE METALS IN DIETHYL ETHER BY FLOW INJECTION ICP-AES

Sample loop volume /μl	line	Detection limit /μg ml^{-1}
300	Cu(I)	5
	Mn(II)	7
100	Cu(I)	1
	Mn(II)	3
50	Cu(I)	0.6
	Mn(II)	1.5

incorporated into the ICP-MS system and evaluated for the introduction of diethyl ether. The system was optimised by the variable step size simplex procedure for the analysis of both copper and silicon. The criterion of merit used was the signal to background ratio and the parameters optimised were forward power, nebuliser gas flow, coolant gas flow and the temperature of the desolvation systems condenser. The results are shown in Table 4.2.3.4.

As a measure of the relative importance of each parameter, a number of univariate searches were performed around the optimum, holding all the other parameters constant except the one under investigation (Figs. 4.2.3.5 - 4.2.3.8). The determination of silicon was found to be possible when using the desolvation system because of the large decrease in the interference caused by the polyatomic ion CO^+ at m/z 28. The isotopic ratios obtained using peaks at m/z 29 and 30 were, after using background correction, the natural abundance and the results were reproducible.

The results obtained for optimisation of the introduction of diethyl ether, into the ICP-AES instrument, showed that a lower forward power was found to be optimum compared with aqueous solutions. However, in the case of ICP-MS, an increase in forward power was required to reach the optimum (Fig. 4.2.3.5). This was possibly due to the spatial temperature phenomena being less important in ICP-MS.

TABLE 4.2.3.4 OPTIMUM CONDITIONS OBTAINED FOR THE DETERMINATION OF TRACE METALS IN DIETHYL ETHER USING ICP-MS AFTER DESOLVATION

Analyte	Parameter	
Cu	Forward Power	2.00 kW
	Nebuliser gas flow	0.71 l min^{-1}
	Coolant gas flow	17.6 l min^{-1}
	Condenser temperature	<-40^{o}C
Si	Forward power	1.86 kW
	Nebuliser gas flow	0.67 l min^{-1}
	Coolant gas flow	17.3 l min^{-1}
	Condenser temperature	-40^{o}C

FIG 4.2.3.5: NORMALISED SBR VS FORWARD POWER USING DESOLVATION DIETHYL ETHER INTO AN ICP-MS

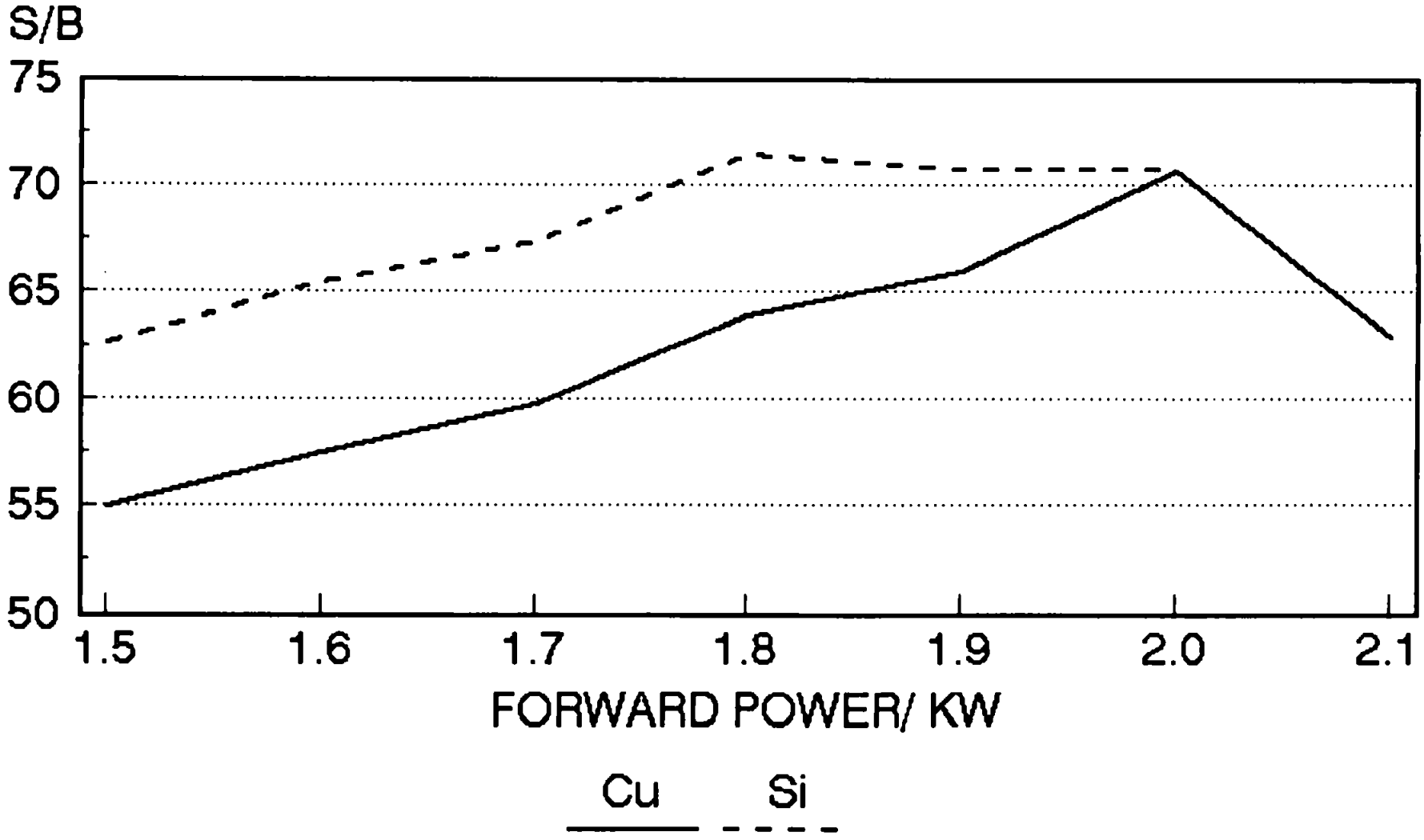

FIG 4.2.3.6: NORMALISED SBR VS NEBULISER GAS USING DESOLVATION DIETHYL ETHER INTO AN ICP-MS

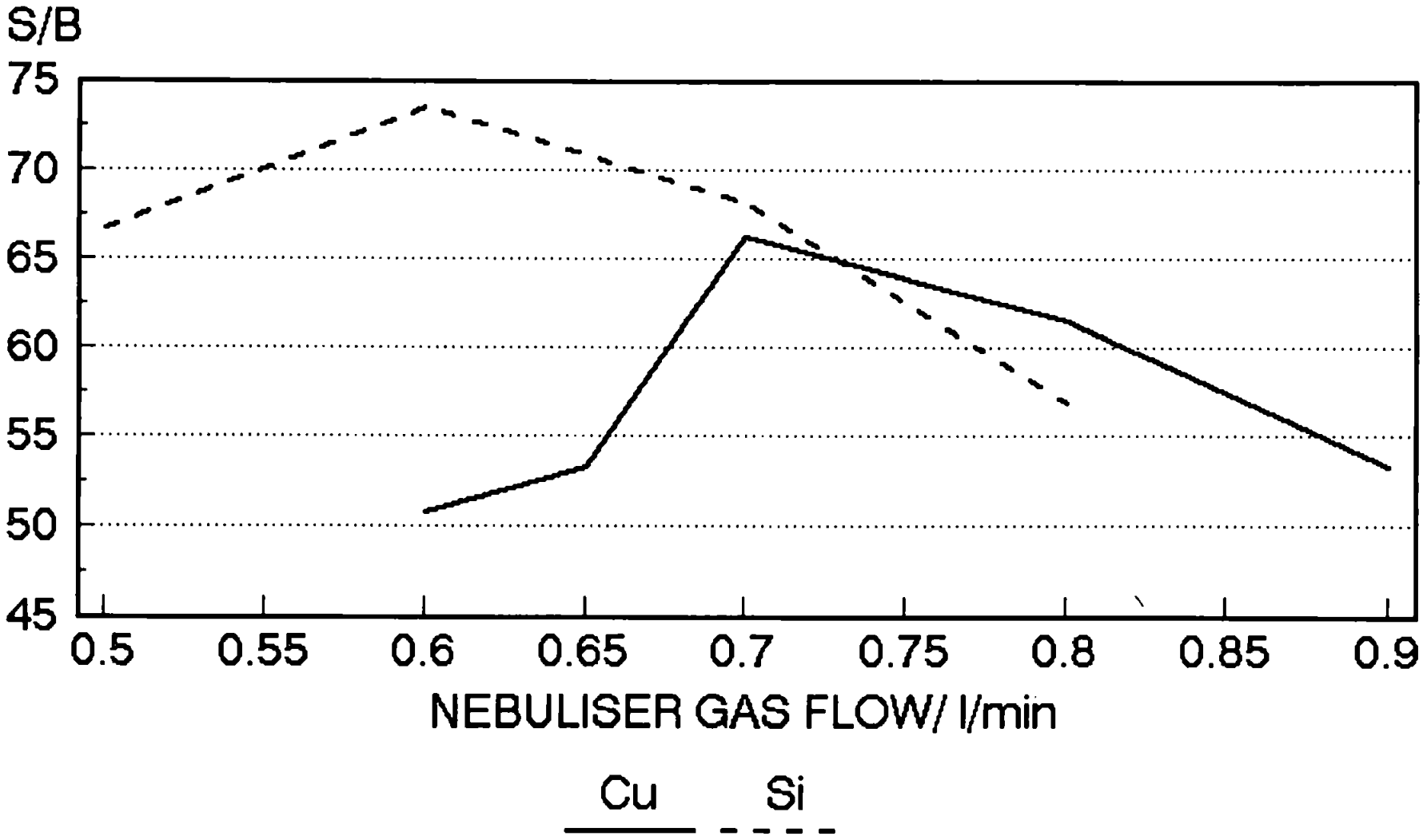

FIG 4.2.3.7 NORMALISED SBR VS COOLANT GAS FLOW USING DESOLVATION DIETHYL ETHER INTO AN ICP-MS

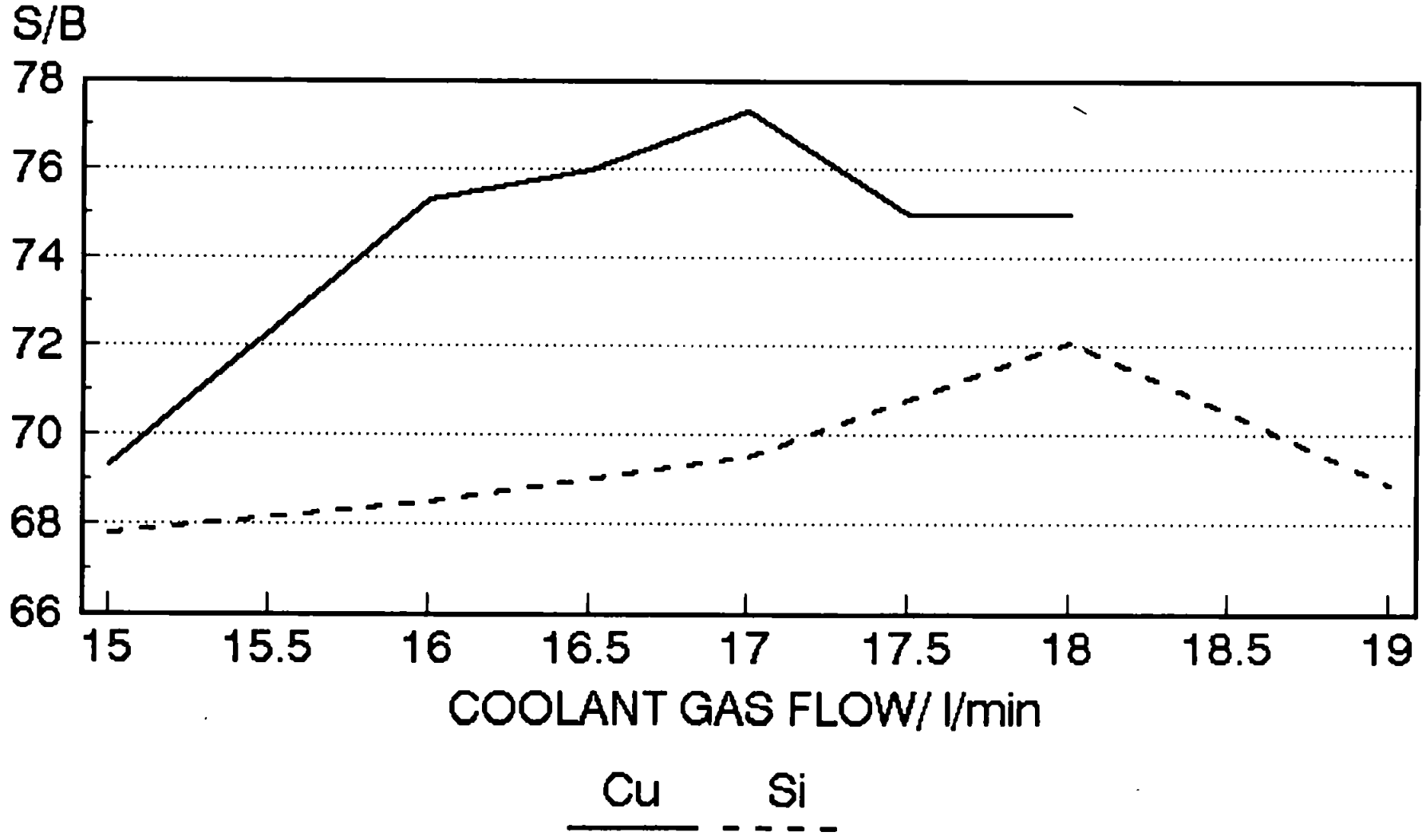

FIG 4.2.3.8: NORMALISED SBR VS TEMPERATURE OF DESOLVATION CONDENSER DIETHYL ETHER INTO AN ICP-MS

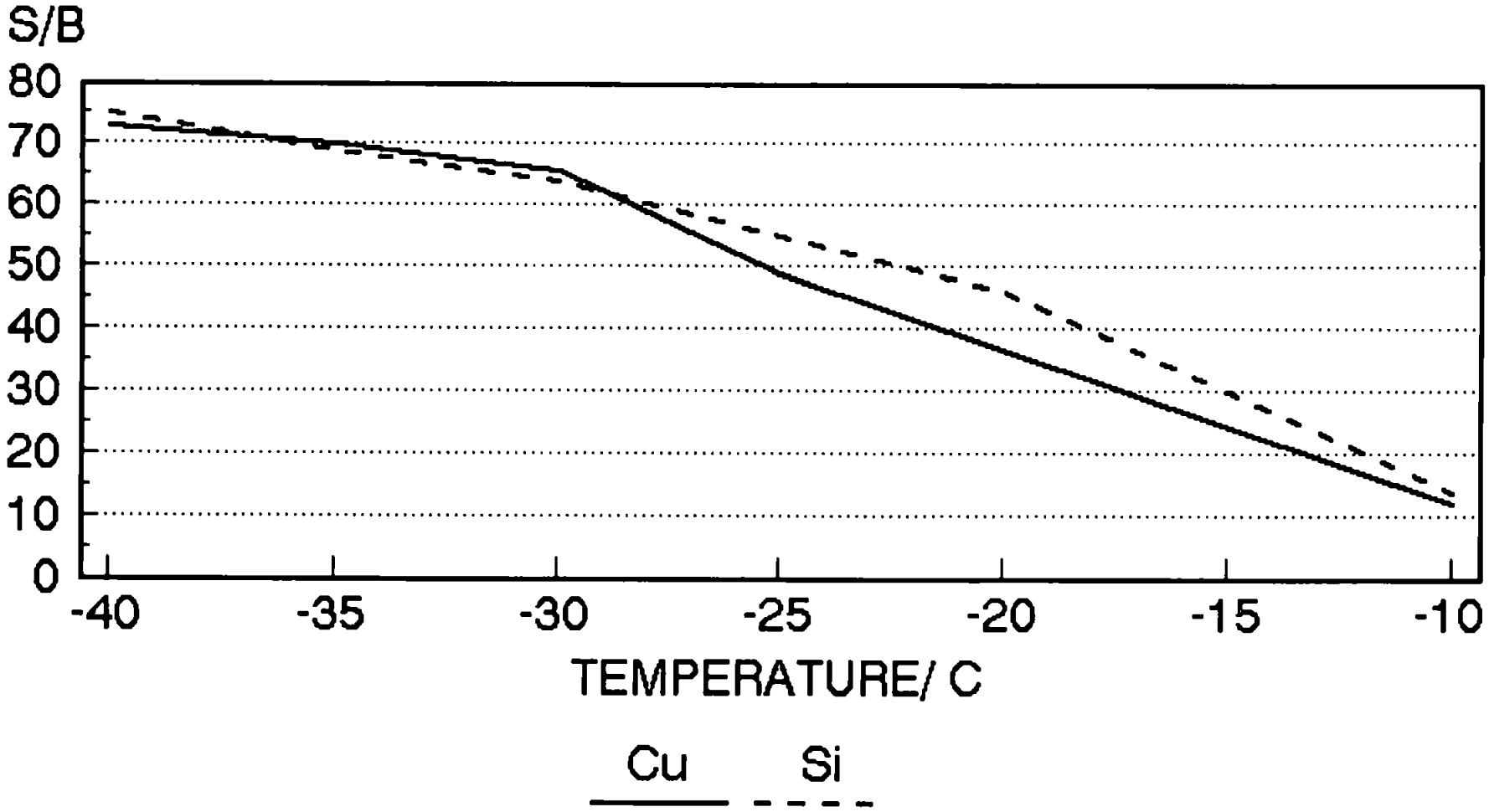

The nebuliser gas flow (Fig. 4.2.3.6), has a sharp optimum comparable with those obtained using ICP-AES. The actual flow rate is less than that normally associated with aqueous samples. This is probably due to the increased solvent removal efficiency caused by the longer residence time in the condenser caused by the lower gas flows.

The coolant gas flow (Fig. 4.2.3.7), has a much greater effect on the signal intensity for the introduction of desolvated organics into an ICP-MS than either aqueous or non-desolvated organics. This may be due to the effect of the slightly lower nebuliser gas flows which will have on the spatial effects of the plasma. This will lead to a much higher electron number density compared with either aqueous or non-desolvation organic introduction. The coolant gas may be acting to compensate for this change.

The temperature of the condensation stage of the desolvation system could not be kept constant below about $-40^{o}C$. Consequently no optimum value was obtained (Fig. 4.2.3.8), for this parameter.

The detection limits were calculated for a number of analytes and the results compared with those obtained using a cooled spray chamber. The results are shown in Table 4.2.3.5. Using the cooled spray chamber it was not possible to obtain a detection limit for silicon because of the effect on the CO^{+} interference. Clearly there is a marked improvement in sensitivity between the two

TABLE 4.2.3.5 DETECTION LIMITS OBTAINED FOR THE DETERMINATION OF TRACE METALS IN DIETHYL ETHER BY ICP-MS

System	Element	Detection limit ($\mu g\ l^{-1}$)
Desoluation	Cu	1.2
	Si	1.0
	Mn	0.6
	V	0.6
	Pb	1.1
Cooled Spray Chamber	Cu	27
	Mn	14
	V	15
	Pb	24

systems due to an increase in the stability of the plasma resulting from the decreased solvent loading. In particular the determination of silicon at low $\mu g\ l^{-1}$ levels was possible. The use of flow injection, was again investigated as a means of lowering the volume of volatile organic solvent entering the plasma, 2-ethoxy ethanol was used as the carrier stream. The effect of using different size sample loops was also investigated and the results shown in Table 4.2.3.6. Again the stability of the plasma increased with a decrease in solvent loading, facilitating an increase in the sample uptake rate, which improved the detection limits. This increase in sample uptake rate also produced better shaped flow injection peaks (Fig. 4.2.3.9), with less tailing and a decrease in sampling time resulting in decreased memory effects.

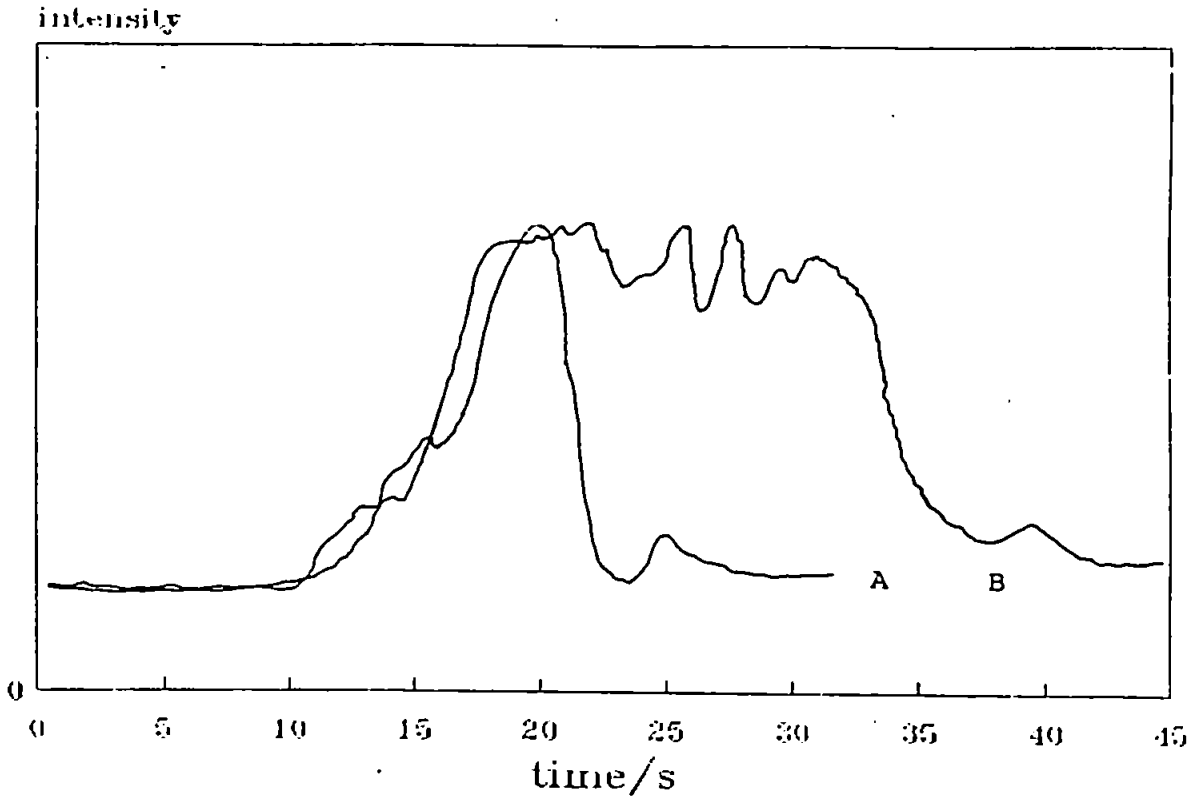

FIG 4.2.3.9: PROFILES OF FLOW INJECTION PEAKS INJECTION OF 80µg/ml Si IN DIETHYL ETHER IN A CARRIER STREAM OF 2-ETHOXY ETHANOL

A = 50µl
B = 300µl

Conclusion

The use of desolvation to remove some or most of a solvent reaching a plasma has a number of effects. The solvent loading of the plasma is decreased increasing the plasma stability and hence the analytical performance. The sample uptake rate may be increased to minimise the effects of the pumping on the performance, without losing plasma stability. This enables analytical performance to be comparable with that obtained for aqueous operation. The use of flow injection may also enhance the analytical performance by decreasing the amount of volatile solvent entering the plasma, it is also advantageous due to the rapid sample throughput of the method and a decrease in memory effects.

The temperature obtained in the condenser by the Peltier coolers, is comparable with the temperature obtained in cryogenic systems which use solid carbon dioxide. The advantages of the Peltier system compared with this method are clear. The Peltier system is easily controlled and the temperature can be varied, the Peltier coolers are solid state and hence require no handling problems and the entire system is easily demountable because of its relatively small size.

CHAPTER 5

ANALYSIS OF ORGANICS USING FLOW INJECTION WITH A CARRIER STREAM OF DILUTE NITRIC ACID

5.1 Introduction

The introduction of organic solvents into an ICP is problematic because the enhanced transportation of the solvent causes high solvent loading. This high solvent loading can cause plasma instability and even extinguish the plasma. The use of flow injection has been shown to decrease this solvent loading if the carrier stream used is less volatile than the solvent being investigated. Additionally, by decreasing the sample loop volume, the uptake rate may be increased without an effect on the plasma stability.

The carrier stream which will cause the plasma no instability is the use of an aqueous carrier stream. Thus flow injection of organics into this will enable only the organic solvent to detrimentally effect the plasmas stability. The use of small volumes of organics may enable the plasma to remain stable throughout the procedure.

The use of membrane dryer tubes to desolvate both aqueous and organic solvents has been reported (52-54). This technique utilises a thin membrane to separate the nebuliser gas from a counter flow of dry argon. The

solvent is purged through the membrane resulting in a drier nebuliser gas entering the plasma. The system reaches stability rapidly and is easy to operate.

5.2 **Experimental**

The membrane drier tube (MD-250-12P) was supplied by Perma Pure Products Ltd.,(Toms River, N.J., U.S.A.). A schematic diagram of the membrane drier tube is shown in Figure 5.2.1. All solvents used were Aristar grade (BDH, Poole, Dorset, U.K.). The standards were prepared from Conostan organometallic solutions (MBH Analytical Ltd., Barnet, Herts., U.K.) or organometallic salts (Spectrosol cyclohexylbutyrate salts, BDH, Poole, Dorset, U.K.).

SCHEMATIC DIAGRAM OF MEMBRANE DRYING TUBE

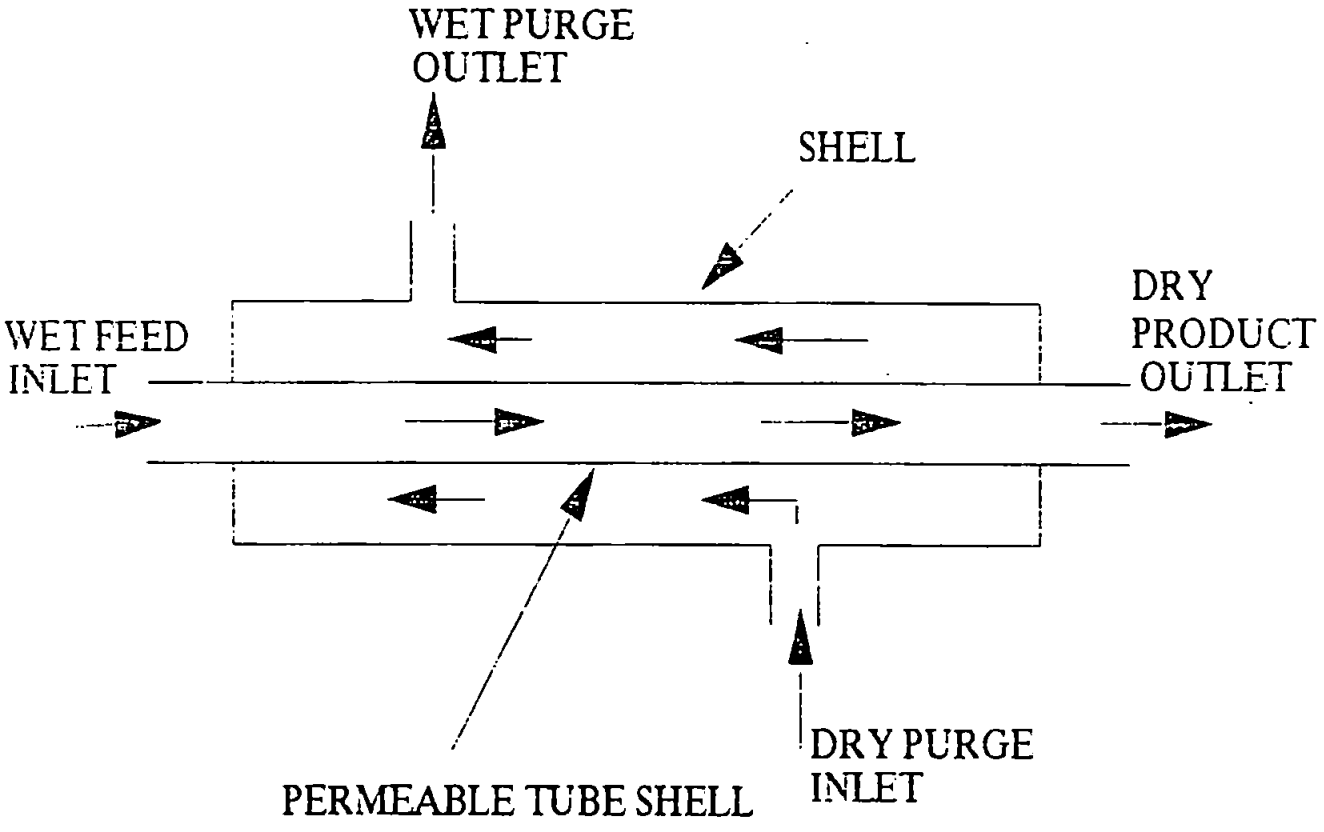

FIG 5.2.1: SCHEMATIC DIAGRAM OF MEMBRANE DRYING TUBE

5.3 Results and Discussion

Using the flow injection system, small volumes of diethyl ether (10 - 25 μl) were introduced into a carrier stream of dilute nitric acid (2%), at uptake rates of 1 - 4 ml min^{-1}. It was found that despite the small volume of organic solvent injected, carbon deposition on the cones caused a suppression of the signal. This was overcome by addition of a low flow of oxygen (5.5% v/v) into the nebuliser gas. Using the oxygen addition, sharp flow injection peaks were obtained for all the elements investigated at 100 ng ml^{-1} levels. It was noted that the reflected power showed an increase as the solvent "plug" entered the plasma, giving a maximum of between 35 W and 40W, prior to returning to the background level of 5W.

The system was optimised for the analysis of indium (m/z 115, 100 μg ml^{-1}) in diethyl ether, using the variable step size simplex procedure (Table 5.3.1). For these experiments 25 μl of sample was injected into the ICP-MS.

Univariate searches were performed around the optimum obtained (Fig. 5.3.1 - 5.3.5). The nebuliser gas flow rate (Fig. 5.3.1) has a sharp optimum at a slightly higher position than that obtained previously from the direct nebulisation of diethyl ether into the ICP-MS previously (Section 3.2.3).

The distance of the torch from the sampling cone (Fig.

TABLE 5.3.1: OPTIMAL CONDITIONS OBTAINED BY THE VARIABLE STEP SIZE SIMPLEX PROCEDURE FOR THE DETERMINATION OF INDIUM IN DIETHYL ETHER

Nebuliser gas flow/ l min^{-1}	0.79
Torch distance/mm	1.22
Forward power/kW	1.78
Oxygen addition/% v/v	5.86
Uptake rate/ml min^{-1}	3.56

FIG 5.3.1: NORMALISED PEAK AREA VS NEBULISER GAS DIETHYL ETHER BY FI-ICP-MS WITH A CARRIER STREAM OF DILUTE NITRIC ACID

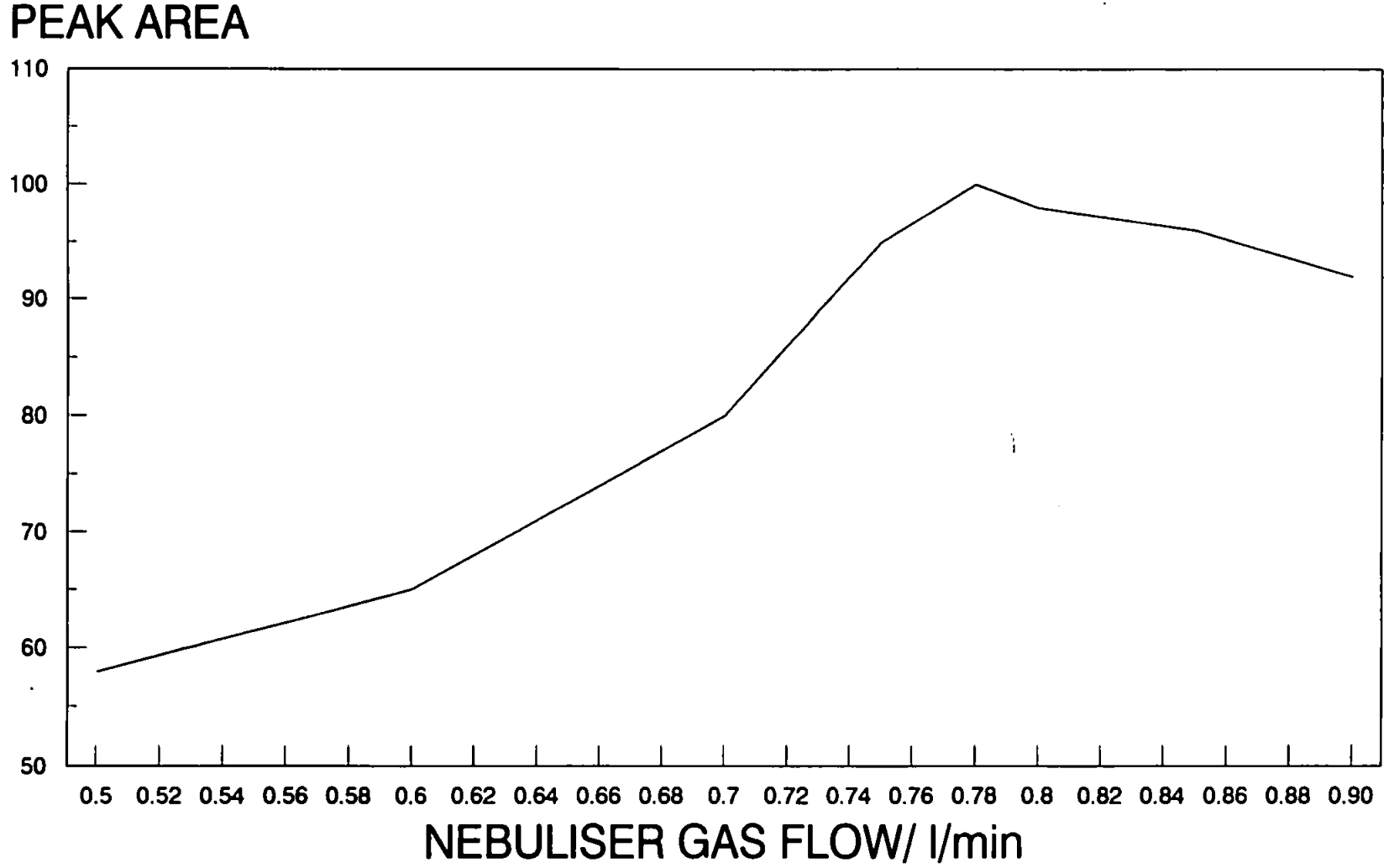

FIG 5.3.2:NORMALISED PEAK AREA VS TORCH DISTANCE DIETHYL ETHER BY FI-ICP-MS WITH A CARRIER STREAM OF DILUTE NITRIC ACID

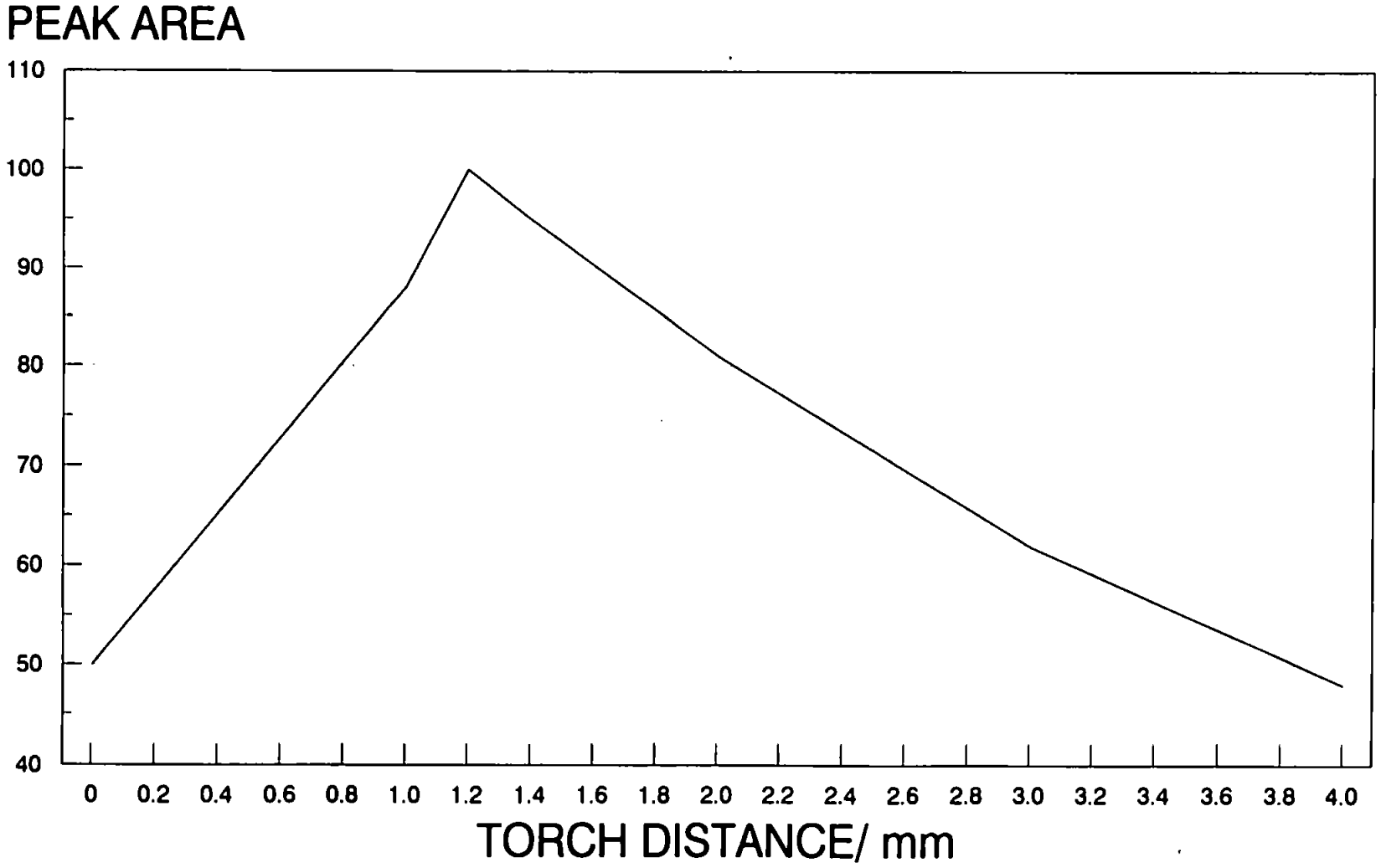

FIG 5.3.3: NORMALISED PEAK AREA VS FORWARD POWER DIETHYL ETHER BY FI-ICP-MS WITH A CARRIER STREAM OF DILUTE NITRIC ACID

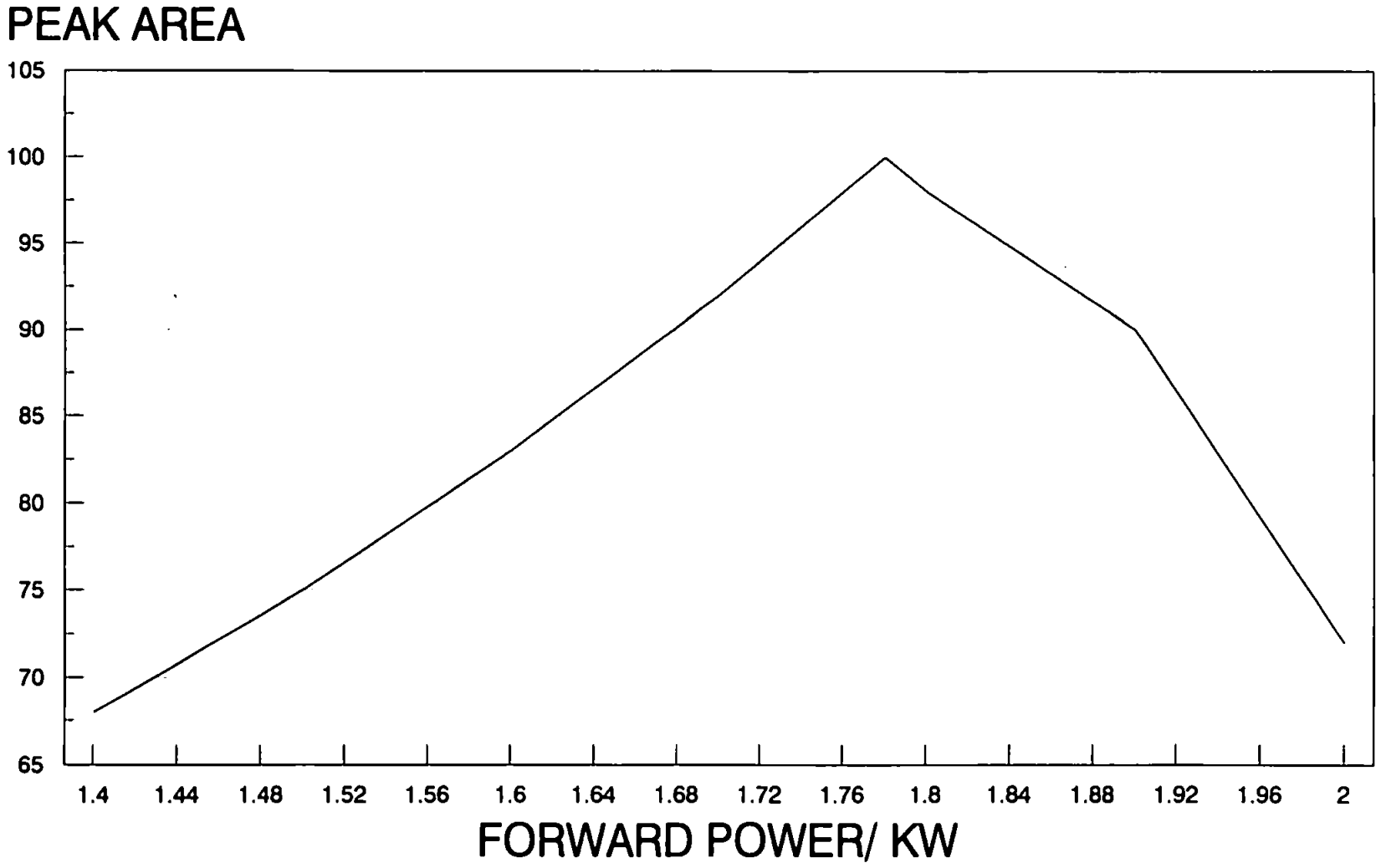

FIG 5.3.4: NORMALISED PEAK AREA VS OXYGEN DIETHYL ETHER BY FI-ICP-MS WITH A CARRIER STREAM OF DILUTE NITRIC ACID

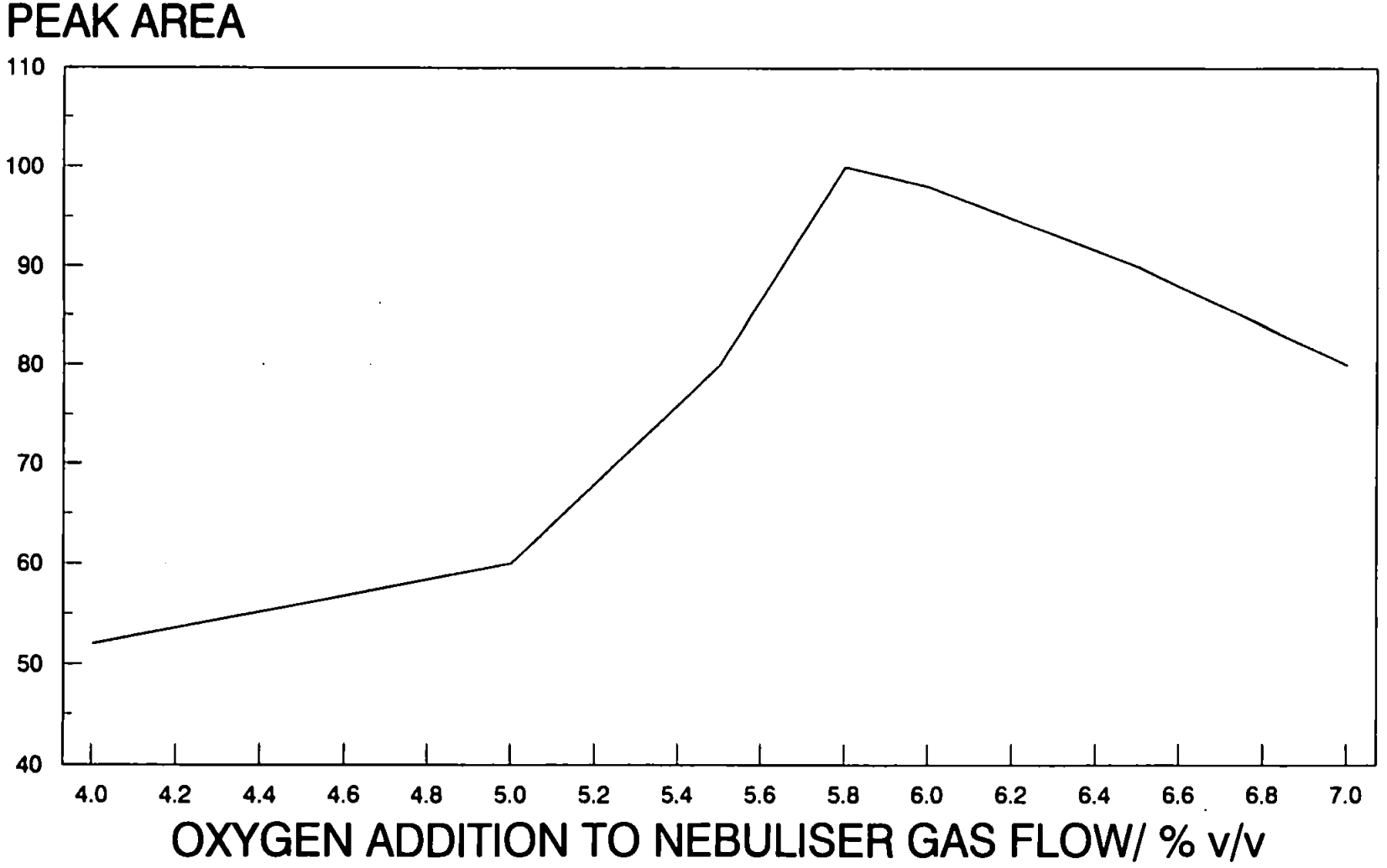

FIG 5.3.5: NORMALISED PEAK AREA VS UPTAKE RATE DIETHYL ETHER BY FI-ICP-MS WITH A CARRIER STREAM OF DILUTE NITRIC ACID

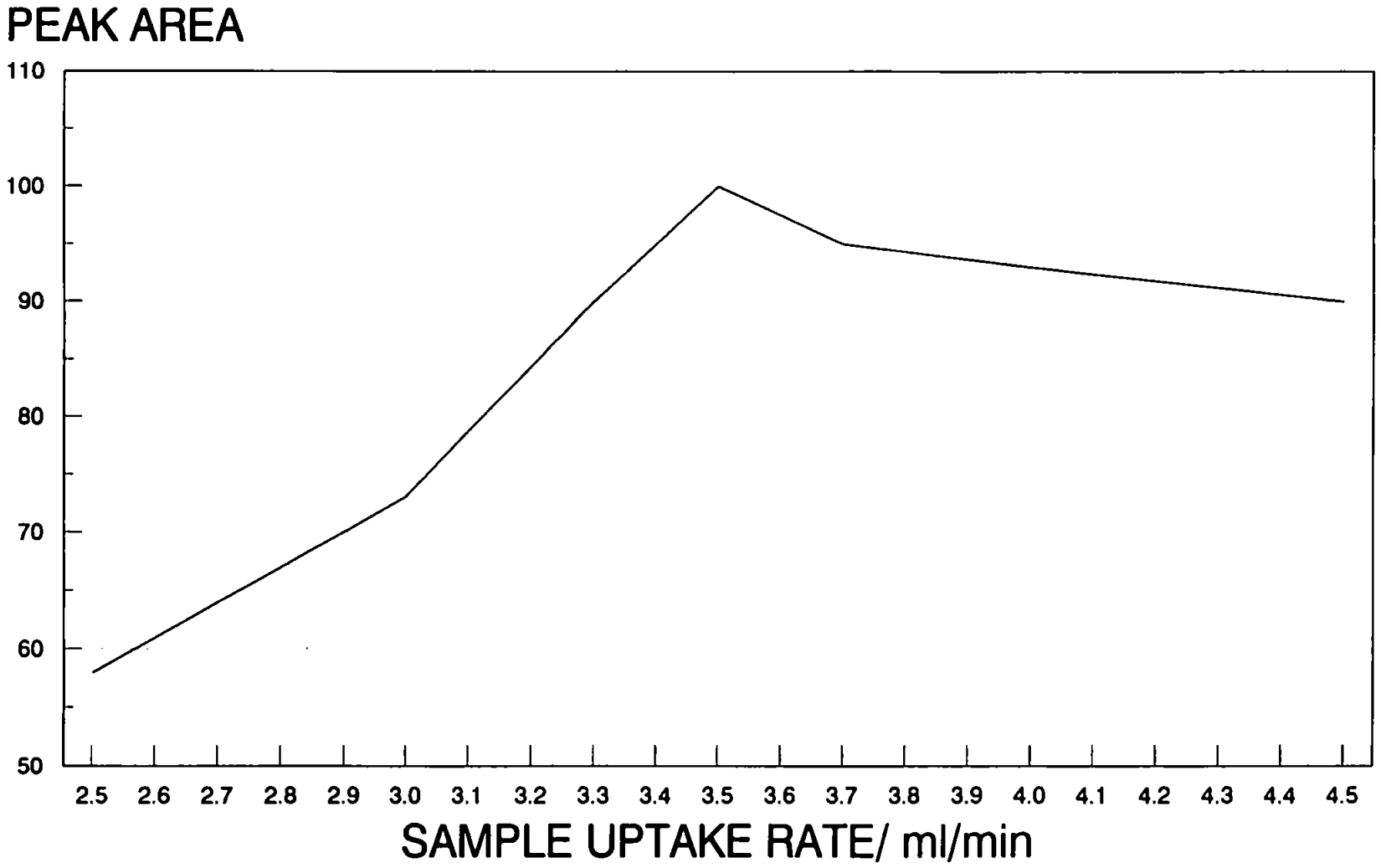

5.3.2) was related to the nebuliser gas flow rate, with an optimum similar to that obtained for direct nebulisation.

The forward power (Fig. 5.3.3) is higher than that required for aqueous samples with the optimum at a similar value to direct nebulisation (see section 3.2.3).

The addition of oxygen to the nebuliser gas (Fig. 5.3.4) appears to be an important parameter. Below about 5.5% v/v there is evidence of carbon deposition on the cones, but above the optimum there is a decrease in sensitivity caused by the detrimental effect of the oxygen on the plasma.

The sample uptake rate (Fig. 5.3.5) is much higher than that used for direct nebulisation of the solvent which is typically about 0.05 ml min^{-1}.

A membrane drying tube was placed between the spray chamber and the plasma torch to reduce the solvent load. The membrane drier tube removes some of the solvent vapour, organic and aqueous, from the nebuliser gas. This device, 30 cm long with a diameter of 0.7 cm containing a hydroscopic membrane 30 cm long with a diameter of 0.3 cm, removes the solvent by purging through the membrane using a counter flow of dry argon. It was found that a counter flow of twice the nebuliser gas flow was required for optimum efficiency. Above this rate there was no noticeable improvement in efficiency. Modification of the

instrument enabled part of the side of the cover and the torch box to be removed. This enabled the spray chamber to be placed outside the instrument and the membrane drier tube to be placed between it and the torch.

The detection limits for both copper and indium (Table 5.3.2) show a marked improvement, compared with those obtained without the use of a membrane drying tube. The membrane drying tube improves the detection limits of the technique by reducing the background signal, without affecting either the size or shape of the peaks.

Another important effect of the incorporation of the membrane drier tube into the system was the decrease in reflected power, as the "plug" of diethyl ether entered the plasma. This implied it would be possible to increase the sample volume size, without causing plasma instability. The results obtained from experiments using increased sample volume sizes (Table 5.3.3), confirm that the sample volume could be significantly increased when the drier tube was incorporated. It should be noted, however, that the increase in reflected power obtained using a sample volume of 175 μl, prevents long term use.

The determination of other analytes (e.g. Al, Cu, In, Pb and Zn), in diethyl ether, using the increased sample volumes enabled the detection limits to be improved to facilitate determination of low to sub- ng ml^{-1} levels. The results together with those obtained from analytes in

TABLE 5.3.2: DETECTION LIMITS FOR Cu AND In IN DIETHYL ETHER BY FI-ICP-MS USING A CARRIER STREAM OF DILUTE NITRIC ACID

Analyte	Membrane Separator	Detection limit/ng ml^{-1}
In	yes	0.9
	no	4.9
Cu	yes	1.4
	no	4.0

3 σ detection limits

TABLE 5.3.3: THE EFFECTS OF SAMPLE VOLUME ON THE DETECTION LIMITS OF INDIUM IN DIETHYL ETHER

Sample volume/μl	Detection limit ng ml^{-1}
25	3.61
50	0.85
100	0.15
175	0.03

3 σ detection limits

dilute nitric acid (2%) using the same size sample volume (50 μl) are shown in Table 5.3.4. Whilst there is a slight difference in detection limits between the two sets of results, the difference is not as great as would normally be associated with using similar organic samples.

The introduction of methanol was also investigated, the use of the membrane drier tube enabled the uptake rate of methanol for direct nebulisation to be increased from about 0.7 ml min^{-1} to 2 ml min^{-1}. This increase in transportation will obviously have an effect on the sensitivity of the technique.

A comparison of the results obtained for the analysis of trace metals is shown in Table 5.3.5. The detection limits obtained clearly show the advantages of the use of a membrane drier tube. Flow injection, in this case 50 μl loops were used, also has an advantageous effect on the quality of the analytical data obtained.

Conclusion

The use of a membrane drier tube, particularly when allied to the use of flow injection, provides a reliable method of removing much of the volatile organic solvent, before it reaches the plasma causing instability and having a detrimental effect on the quality of the results. The membrane itself is robust and its non-mechanical nature prevents breakdown.

TABLE 5.3.4: DETECTION LIMITS OBTAINED FOR Al, Cu, In, Pb, AND Zn IN DIETHYL ETHER AND DILUTE NITRIC ACID USING FI-ICP-MS WITH A CARRIER STREAM OF DILUTE NITRIC ACID

Analyte	Detection limit/ng ml^{-1}	
	Ether	2% HNO_3
Al	0.52	0.50
Cu	1.4	1.0
In	0.85	0.81
Pb	0.91	0.85
Zn	1.3	0.93

3 σ detection limits

TABLE 5.3.5: DETECTION LIMITS OBTAINED FOR THE DETERMINATION OF TRACE METALS IN METHANOL BY ICP-MS

Analyte	Membrane Drier Tube	Detection limits/ng ml^{-1}	
		Direct Nebulisation	Flow Injection[+]
Al	No	5	1
Cu	No	8	2
In	No	4	1
Pb	No	7	2
Zn	No	7	2
Al	Yes	0.6	0.4
Cu	Yes	1.1	0.7
In	Yes	0.9	0.6
Pb	Yes	1.0	0.7
Zn	Yes	1.4	1.1

[+] 50 μl sample loop

CHAPTER 6

ANALYSIS OF REACTIVE ORGANOMETALLIC SAMPLES

6.1 Introduction

Alkyl compounds of a variety of elements, primarily from groups II and III, are employed in the preparation of complex semiconductors by the process of metal organic chemical vapour deposition (MOCVD) (40, 41). Many of these organometallics are pyrophoric and react with air and water. The reactions are often vigorous and produce a range of toxic products (42). Although the samples can be stabilised in organic solvents, typically diethyl ether, contamination is a major problem. Contamination at the level of 1 $\mu g\ ml^{-1}$ can completely alter the physical, chemical and optical properties of the resultant semiconductor chips. Consequently sophisticated analytical techniques are required for their analysis.

The literature contains few reports of methodology for the analysis of trace contaminants in such organometallics and most have been concerned primarily with the analysis of trimethylgallium, normally involving the decomposition of the sample. Barnes et al., (43-45) analysed trimethylgallium by two separate methods. In the first the non-volatile impurities were analysed after decomposition in 0.5 M hydrochloric acid at a temperature of -78^{o} C, followed by direct nebulisation into an ICP-AES

spectrometer. Inorganic compounds in an aqueous medium were used as standards. The second method involved the direct analysis of the trimethylgallium by the exponential dilution technique which enabled the volatile impurities, such as silicon and zinc to be analysed. Barnes et al., (46) also analysed trimethylaluminium using a decomposition method. In this case the use of acids caused a very vigorous reaction, so that the sample was decomposed in 95% ethanol, before direct analysis by ICP-AES again using inorganic compounds in an aqueous medium as standards.

Jones et al., (47) used an unspecified decomposition procedure for the analysis of volatile impurities in trimethylgallium, trimethylaluminium and trimethylindium by ICP-AES. Direct analysis of electronic grade gas has been reported using an inductively coupled plasma - mass spectrometer (ICP-MS) (48). Other reports include the decomposition of organometallics prior to analysis e.g. trimethylgallium by graphite furnace atomic absorption spectrometry (49), dimethylzinc by gas chromatography (50) and dimethylcadmium by gas chromatography - mass spectrometry (51).

6.2 Experimental

The membrane drying tube (MD-250-12P) was obtained from Perma Pure products Ltd. (Toms River, N.J., U.S.A.). All standards were prepared from Conostan organometallic standards (MBH Analytical Ltd., Barnet, Herts., U.K.) or organometallic salts (Spectrosol cyclohexylbutyrate salts, B.D.H., Poole, Dorset, U.K.). The spray chamber used was a Scott type double pass and the nebuliser a v-groove high solids 'Ebdon' nebuliser (P.S.Analytical, Sevenoaks, Kent, U.K.).

6.3 Results and Discussion

The introduction of small volumes (25 μl) of diethyl ether by flow injection into a carrier stream of dilute nitric acid was optimised for the determination of indium. The optimisation was performed using a variable step size simplex procedure and the results are shown in Table 6.3.1.

These optimum conditions were used for the analysis of trace metal impurities in trimethylgallium etherate (TMG). TMG is known to react vigorously in the presence of water or carbon dioxide, however when stabilised in diethyl ether to form an etherate, this reaction proved to be fairly slow. In this work the small internal area of the pump tube (i.d. 0.5 mm) and the hydrophobic nature of

TABLE 6.3.1: OPTIMAL CONDITIONS OBTAINED BY THE VARIABLE STEP SIZE SIMPLEX PROCEDURE FOR THE ANALYSIS OF INDIUM IN DIETHYL ETHER BY FI-ICP-MS

Nebuliser gas flow/ l min^{-1}	0.79
Torch distance/mm	1.22
Forward power/kW	1.78
Oxygen addition/% v/v	5.86
Uptake rate/ml min^{-1}	3.56

the ether, resulted in little reaction between the two phases during carriage to the nebuliser. In addition there was no evidence of any reaction in the spray chamber. Initially copper and indium were determined under these optimum conditions and the calibration curves obtained are shown in Figures 6.3.1 - 6.3.2 respectively. These calibration curves show the effects of the high background caused by the organic solvent which results in an intercept on the signal axis and in poor sensitivity.

A membrane drying tube, was placed between the spray chamber and the plasma. The membrane drying tube device contained a hydroscopic membrane through which the solvent was purged into a counter flow of dry argon. The flow rate of the dry argon was twice that of the nebuliser gas flow rate. This system was used for the analysis of TMG, where 50 μl of the TMG was flow injected into a carrier stream of dilute nitric acid (2% v/v). The results for this are shown in Table 6.3.2.

To calibrate the samples a series of organometallic standards were made up in diethyl ether. Since the effect of the trimethylgallium matrix on the plasma is unknown, however, it was not possible to assume the results obtained were accurate. In order to assess whether the use of such standards is justified, a number of standard addition calibrations were performed, the results for which are shown as percentage recoveries. The results obtained are compared with the results using standards in

FIG 6.3.1: CALIBRATION CURVE FOR COPPER IN DIETHYL ETHER USING FI-ICP-MS WITH A CARRIER STREAM OF DILUTE NITRIC ACID

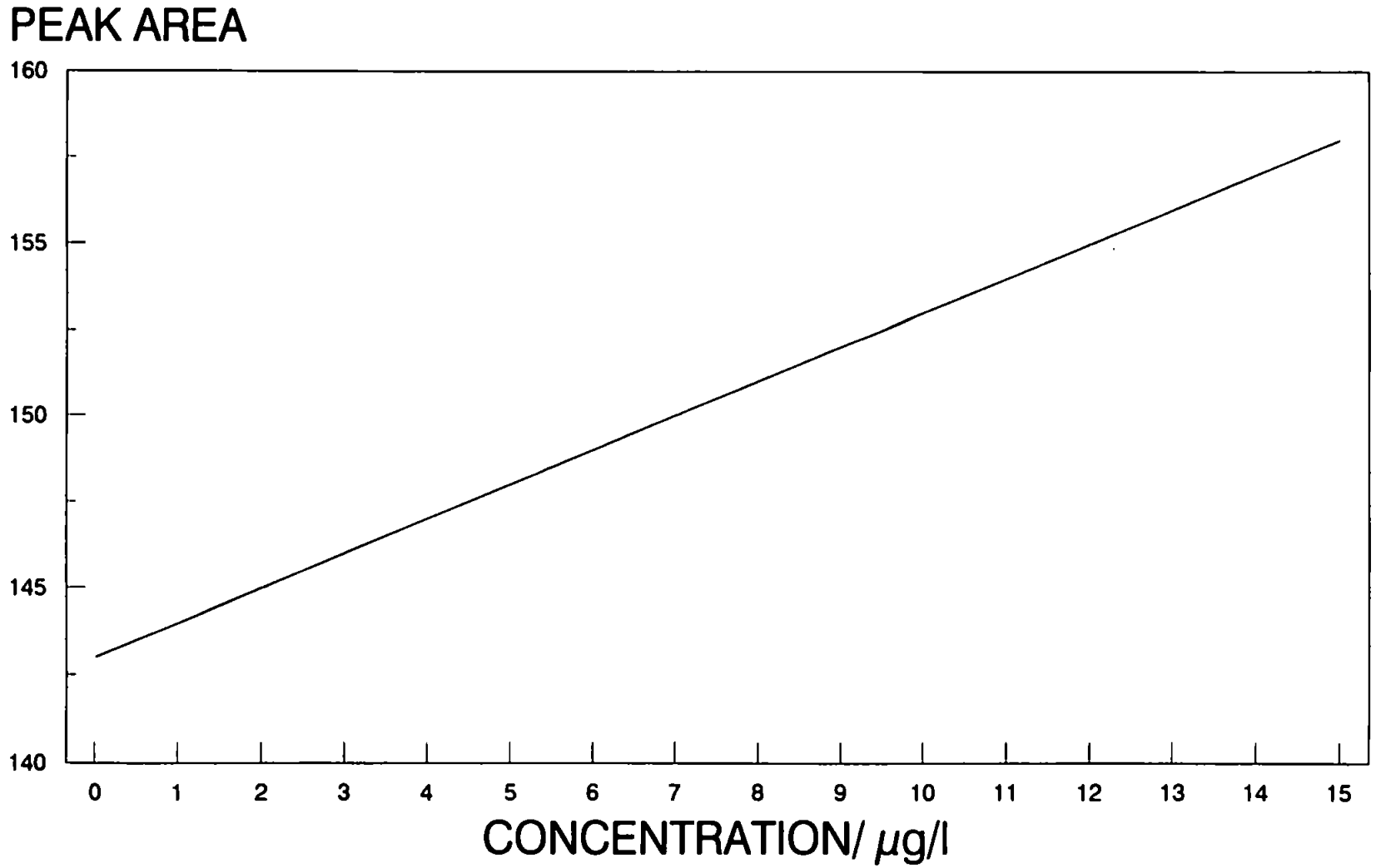

FIG 6.3.2: CALIBRATION CURVE FOR INDIUM IN DIETHYL ETHER USING FI-ICP-MS WITH A CARRIER STREAM OF DILUTE NITRIC ACID

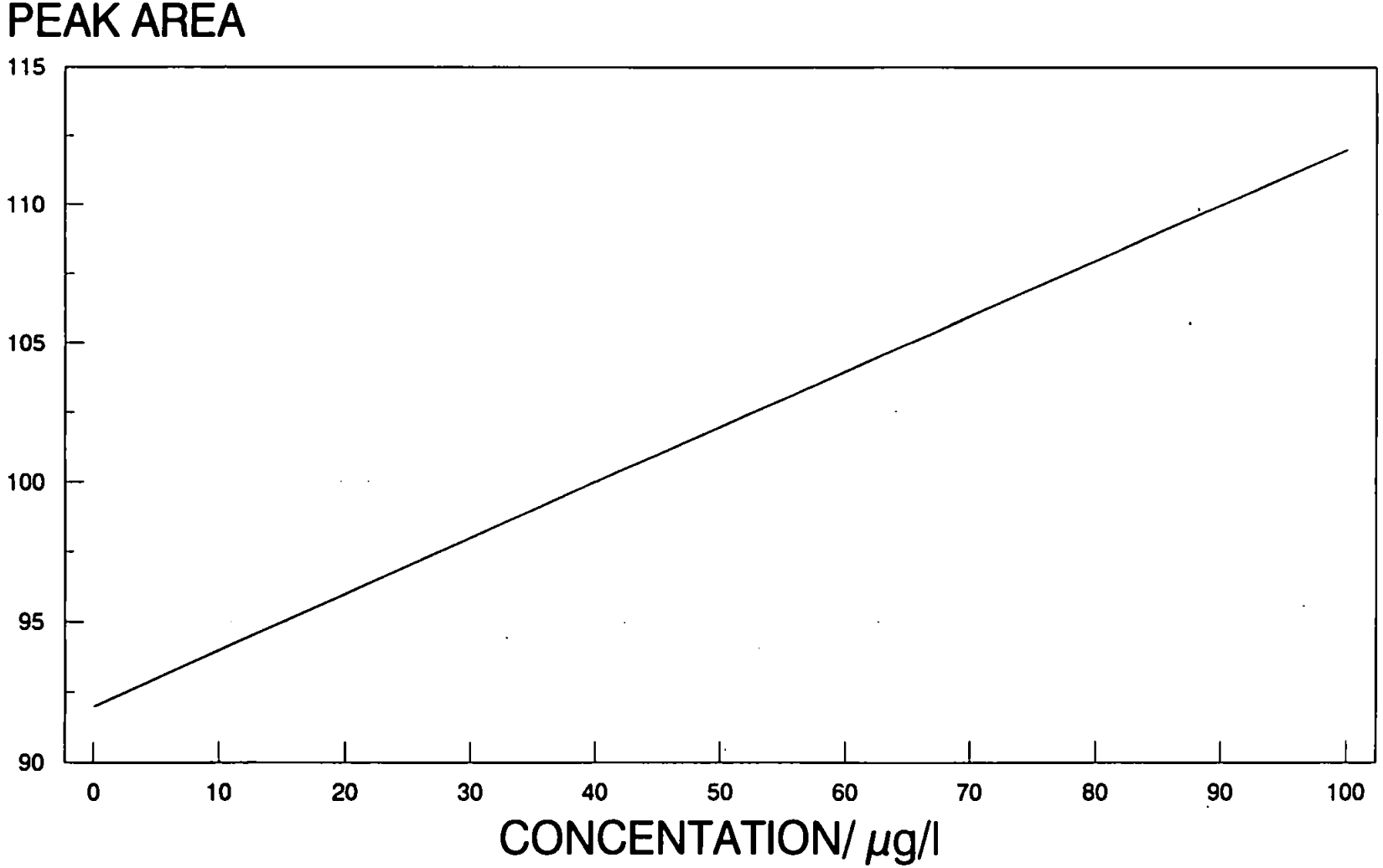

TABLE 6.3.2: ANALYSIS OF TRIMETHYLGALLIUM IN DIETHYL ETHER BY FI-ICP-MS USING A CARRIER STREAM OF DILUTE NITRIC ACID

Analyte	Concentration^{+}/ng ml^{-1}	Recovery^{+}/%
Al	23.3 ± 2.1	107.6 ± 10.3
Cu	8.2 ± 0.8	95.4 ± 10.0
In	61.4 ± 6.5	94.8 ± 10.2
Pb	96.1 ± 10.7	104.2 ± 12.5
Zn	77.0 ± 7.8	92.6 ± 8.6

$^{+}$ 3 σ precision

Table 6.3.2. The relative standard deviations were of the order of 3-4%.

The results show reasonable agreement between the two methods of calibration and indicate that the effect of the trimethylgallium matrix on the plasma was not sufficient to prevent the use of standards made up in diethyl ether for calibration. Clearly this makes the analysis of TMG easier, and indeed safer, by reducing the amount of TMG required for the analysis.

The optimum conditions obtained for the analysis of small volumes of diethyl ether injected into a carrier stream of dilute nitric acid (Table 6.3.1) were also used for the analysis of methyllithium in diethyl ether. In addition the analysis of methyllithium by direct nebulisation was also performed using the same conditions, although in this case a slower sample uptake rate was required to retain plasma stability (0.5 ml min^{-1}).

The addition of small volumes of the methyllithium into the carrier stream of dilute nitric acid (2%) did initially cause some blockages in the pump tubing, as a result of hydrolysis at the interface between the acid and the methyllithium. However, by increasing the concentration of the acid to 10% such blockages were prevented. Clearly there was some reaction at the interface of the two phases although the hydrophobic nature of the diethyl ether prevented the acid from

reacting with all but the surface of the organic phase. The increase in the acid concentration increased the rate of reaction, and thus prevented build up of the intermediate solid which caused the blockage. Alternatively, the problem may be overcome by direct nebulisation of the methyllithium into the ICP-MS instrument.

The determination of the trace metal impurities present in methyllithium was performed using the two methods described. Calibration was achieved using organometallic standards diluted in diethyl ether. The results obtained show a reasonable agreement between the two analyses (Table 6.3.3) and indicate that either method may be used. However, the use of the flow injection technique does have some advantages over direct nebulisation, owing to the increased speed of analysis and the decrease in washout times. The memory effects, using direct nebulisation of methyllithium, may be severe. In both cases the relative standard deviation was between 3-4%.

Since these results assumed that the matrix effects of the methyllithium did not affect the results, and that the use of standards in diethyl ether was justified, a check was made by hydrolysing the methyllithium. The hydrolysis procedure involved the addition of methyllithium (12.5 ml) slowly (0.6 ml min^{-1}) to ice cold concentrated hydrochloric acid (12.5 ml). After the reaction was completed the sample was heated (60^{o}C) on a hot plate for

TABLE 6.3.3: ANALYSIS OF METHYLLITHIUM IN DIETHYL ETHER BY ICP-MS

Analyte	Flow Injection/ng ml^{-1}	Direct nebulisation/ ng ml^{-1}
Fe	17.6 ± 1.6	16.8 ± 1.8
Co	23.5 ± 2.4	24.2 ± 2.9
Cu	29.2 ± 3.3	30.1 ± 3.4
Mo	89.5 ± 8.6	88.9 ± 8.7
Cd	170.2 ±18.4	160.2 ±18.8
In	78.6 ± 8.0	80.4 ± 8.6
Ba	73.2 ± 8.1	67.3 ± 8.0
Pb	87.2 ±10.2	82.1 ±11.1

3 σ precision

two hours to remove any residual diethyl ether and the samples made up to volume with dilute nitric acid.

The samples of hydrolysed methyllithium were analysed by ICP-MS, with calibration using standard additions. These results (Table 5.3.4) show reasonable agreement with the results obtained for the methyllithium in diethyl ether. This suppports the use of organometallic standards made up in diethyl ether for calibration.

Conclusion

It is clear that the analysis of reactive samples, such as trimethylgallium and methyllithium, dissolved in volatile organic solvents may be readily achieved using the technique of flow injecting small samples into a carrier stream of an aqueous nature. The use of flow injection improves the analysis time, because of the faster throughput of samples, decreased washout times and reduced memory effects. It also improves the detection limits and the precision of the analysis.

TABLE 6.3.4: RESULTS OBTAINED FOR THE ANALYSIS OF HYDROLYSED METHYLLITHIUM USING ICP-MS

Analyte	Concentration/ng ml^{-1}
Fe	15.3 ± 1.0
Co	24.2 ± 1.8
Cu	31.2 ± 2.5
Mo	94.0 ± 8.9
Cd	163 ±13
In	75.1 ± 6.3
Ba	65.8 ± 5.6
Pb	90.0 ± 6.4

3 σ precision

CHAPTER 7

ANALYSIS OF DESOLVATED SLURRIES

7.1 Introduction

The analysis of solid samples by slurry atomisation - inductively coupled plasma - atomic emission spectrometry (SA-ICP-AES) and slurry atomisation - inductively coupled plasma - mass spectrometry (SA-ICP-MS), has become a widely accepted technique for the analysis of a large number of sample types, particularly geological materials (64-73). One of the major problems associated with this technique is the requirement to reduce the particle size of the sample prior to analysis, so that the atomisation efficiencies are comparable with those obtained for the aqueous standards. Ebdon et al. (67, 69), quote a figure of below 5 μm for refractory materials and 3 μm for bulk material for the atomisation efficiencies to be the same. This requirement to produce small particle size slurries often leads to long grinding times and thus negates the time advantages when compared with dissolution techniques for many samples. These figures for particle size include the water jacket associated with the particle, not the size of the dry particle as it leaves the preheated zone of the plasma. The effect on the plasma caused by the necessity to desolvate the water droplet surrounding the particle before atomisation and the subsequent loss of energy in the plasma caused by this process, has not been considered. Consequently it was considered that

desolvating the slurry, prior to entry into the plasma would have a beneficial effect on the atomisation process, and lead to a possible increase in the particle size which could be atomised efficiently.

Ebdon et al.(105), also investigated the aerosol size distributions from solutions and slurries that exit various points in single and double pass spray chambers, using a phase/Doppler - shift laser spray analyser. The results for both population diameter and percentage volume diameter distributions were recorded and used to elucidate information about the mechanisms of aerosol formation, transportation and sample loss. The population distributions of the primary aerosol from a high solids Ebdon nebuliser were found to be essentially monomodal, covering the range < 1 to 36μm, the bulk being below 20μm. The mean and mode diameters were of the order 7 to 10μm. The volume distribution was multimodal and shows weighting toward the larger particle sizes with a mean of the order 10 to 13μm. Increasing the gas flow acted to increase the fraction of fine particles in the aerosol. The effect of a spray chamber on these distributions caused some modifications. A single pass spray chamber concentrated the larger particles and particle coagulation effects appeared to be present. The addition of an injector to the spray chamber also caused modification resulting in a loss of the larger particles. A 3mm injector allowed a greater fraction of the larger particles through compared with a 2mm injector, at all the gas flows investigated.

Studies performed on a double pass spray chamber showed that aerosols exiting the inner pass had similarities to those of the primary aerosol. This also proved to be the case for the aerosol exiting the spray chamber with population (9.7μm) and volume (12.8μm) mean diameters compared with 9.5μm and 12.9μm respectively for the inner pass at a flow rate of 0.75l min^{-1}. The addition of an injector caused a decrease in the population mean and mode diameter range (5 to 7μm) and a reduction in the distribution range with a 2mm injector. It was found that aerosols formed from 1% (m/v) slurries showed no significant differences from those formed from solution, under the same gas flow conditions.

The effects on the plasma due to the desolvation of the water droplet surrounding the particle before atomisation, and the loss of energy caused by this process, has not been considered in previous studies. Consequently desolvation of the slurries prior to entry into the plasma may have a beneficial effect on the atomisation process. This may reasonably be expected to lead to an increase in the particle size with respect to both the transportation to, and atomisation by the plasma.

7.1.1 Analysis of Certified Reference Materials

The use of desolvation for the analysis of geological material, by ICP-AES has been investigated by Gervais and Salin (63). Although they found a marked increase in the response signal of the instrument after desolvation, they found only a marginal increase in the sensitivity due to an increase in the relative background signal. They also observed a marked increase in slope for the calibration curve for the aqueous standards than was obtained for the slurries. The effect of the injector tube diameter was not discussed, although previous work had indicated that an optimum of about 3 mm is required (67-72).

Tang and Trassey (92), reported that the desolvation of aqueous samples increased the analytical performance. The use of an ultra-sonic nebuliser enabled more control over the droplet size range entering the plasma, and it was found that desolvation caused the average droplet size to decrease to 3 μm from about 5 μm when desolvated at 150^{o}C. This reduction in particle size had an effect on both the transport efficiency and the plasma conditions.

There has been no reports in the literature concerning the introduction of dry slurries into an ICP-MS.

7.2 **Experimentation**

7.2.1 Instrumentation

Slurry preparation

The slurries were prepared by the bottle and bead wet grinding method (68) which used 2-3 mm glassed (vitrified) zirconia beads (Glen Cresson, Stanmore, U.K.) shaken with the samples within polyethylene containers using a laboratory flask shaker. Triton X-100 (1% v/v) was used as the dispersant, unless otherwise stated.

The size distribution of the slurries was measured using a Coulter counter (TA II Multi Channel Particle Counter, Coulter Electronics Ltd., Harpendon, Herts., U.K.) and laser diffraction (2600/3600 Particle Sizer VA.1, Malvern Instruments Ltd., Malvern, U.K.).

The Coulter Counter determines the number and size of particles suspended in an electrolyte, by the particles passing through an orifice, on either side of which are immersed electrodes. The changes in resistance, caused by the particles as they pass through the orifice, generate voltage pulses. The amplitudes of these pulses are proportional to the volume of the particles. These pulses are amplified, sized and counted and from the derived data the size distribution may be determined (94).

The laser diffraction technique is based upon measurements of the forward diffracted light from a disperse suspension. The angle of diffraction is inversely proportional to the particle size and the intensity of the diffracted beam at any angle is a measure of the mean projected areas of the particles of a specific size (94).

The in-flight solids collections were performed using a cascade impactor (Mark III Particle Sizing Stock Sampler, Andersons Samplers, Atlanta, GA., U.K.). Total sampling of the aerosols was conducted isokinetically using a metered draw through the impactor from a 380 W laboratory compressor.

The cascade impactor contains nine jet plates, each with a pattern of precision-drilled orifices, separated by spacers. The orifices on each plate are arranged in concentric circles which are offset on each succeeding plate. The size of the orifices are the same for any given plate, but smaller for each succeeding plate. As the sample is drawn through the sampler at a given flow rate, the jets of air flowing through any particular plate direct the particulates towards the collection area on the downstream side of the plate. The decreasing orifice sizes from plate to plate mean that the gas velocity increases. Whenever the velocity imparted to a particle is sufficiently great, its inertia will overcome the aerodynamic drag of the airstream and become impacted on the collection plate (94).

7.2.2 Results and Discussion

The desolvation device described in Chapter 4 with slight modification was used to desolvate both aqueous standards and slurries before analysis by ICP-MS. The ICP-MS operating conditions are shown in Table 7.3.1. The results from this modification are compared with those obtained for the same samples without desolvation. During desolvation the spray chamber was heated to a temperature of 102^{o}C with little variation over time (< 0.5^{o}C). The condenser was kept at a temperature of -2^{o}C also with little variation over time (< 0.5^{o}C). To lower the condenser temperature further risked the possibility of blockage or long washout times as the vapour formed a solid on the walls.

Using a Karl-Fischer titration , the efficiency of the desolvator was measured as 90%. The Karl-Fischer method for determination of water involves the use of the Karl-Fischer reagent, which is composed of iodine, sulphur dioxide, pyridene and methanol. The water is collected in the methanol, which is titrated against the other reagents. The end point employed in this technique involves an electrometric system.. Two stationary electrodes are immersed in the solution, which is mechanically stirred, a small potential is passed between them (0.1-0.2V) and the current that flows is followed as a function of the volume of added reagent. The end point is marked by a sudden rise is the current (94).

TABLE 7.3.1 OPERATING CONDITIONS

ICP Conditions	
Cooling gas flow	14.0 l min^{-1}
Auxiliary gas flow	1.0 l min^{-1}
Nebuliser gas flow	0.95 l min^{-1}
Mass Spectrometer Conditions	
Mass range	2-245 amu
Dwell time	320 us
Number of channels	2048
Number of scans	100

The transport efficiency after desolvation was 4.9% compared with an efficiency without desolvation of 2.2%.

The results from the initial experiment for the reference materials; SO-1 soil (CANMET, Ottawa, Canada) and SARM-18 coal (MINTEK, Randburg, Rep. South Africa) are shown in Table 7.3.2. The samples used in this experiment were shaken for eight hours and the particle size distribution determined using a Coulter Counter. The results revealed that 98.4% and 55.9% respectively for SO-1 and SARM-18 fell below 4 μm.

Table 7.3.2 shows that using either a wet or dry slurry, the results are within 10% of the expected values and mostly within the confidence limits of the reference materials.

The exceptions, particularly manganese and nickel have oxide interferences on the isotopes analysed. One of the advantages of desolvation is the removal of most of the oxide, hydroxide and hydrogen polyatomic interferences.

It should also be noted that the desolvation of the samples caused an improvement in the sensitivity. This improvement appears to be due mostly to the improvement in transport efficiency, although the removal of the solvent also appears to improve the atomisation efficiency.

TABLE 7.3.2 RECOVERIES OBTAINED WITH AND WITHOUT DESOLVATION FOR SAMPLES SO-1 AND SARM-18

I) SARM-18

Analyte	Certified Values /$\mu g\ g^{-1}$	Recoveries/% Non-Desolvated	Desolvated
V	23	91.3 ± 8.1	100.0 ± 4.4
Cr	16 ± 2	100.0 ± 7.5	108.8 ± 4.1
Mn	22 ± 1	-[1]	86.4 ± 4.5
Co	6.7± 1.2	95.5 ± 6.8	106.4 ± 3.3
Ni	10.8± 0.7	-[2]	95.4 ± 4.1
Cu	5.9± 0.7	93.2 ± 6.8	98.1 ± 4.3
Zn	5.5± 1.3	96.4 ± 7.1	108.2 ± 3.6
Sr	44 ± 2	93.2 ± 7.4	100.1 ± 4.6
Ba	78 ± 7	92.3 ± 7.4	102.6 ± 3.9
La	10 ± 3	90.0 ± 5.2	110.0 ± 2.8

II) SO-1

V	139 ± 8	92.8 ± 7.4	105.0 ± 4.9
Cr	160 ±15	98.1 ± 8.2	106.9 ± 4.6
Mn	890 ±30	90.4 ± 4.0	97.5 ± 3.5
Co	32 ± 3	96.6 ± 3.3	106.6 ± 3.1
Ni	94 ± 7	86.2 ± 5.1	105.3 ± 4.9
Cu	61 ± 3	98.4 ± 8.1	95.1 ± 5.3
Zn	146 ± 5	102.7 ± 4.1	104.8 ± 4.1
Ba	879 ±47	93.3 ± 3.5	95.2 ± 2.9
Pb	21 ± 4	90.5 ± 4.8	80.9 ± 2.4

Standard deviations quoted as 3 σ

[1] high level of potassium caused interference as KO
[2] high level of calcium caused interference as CaO

These results give little information about the effects of particle size on the recoveries. In order to elicit more information about particle size effects, a series of slurries were prepared over a range of grinding times (half hourly intervals from 0 to 2 hours). The sample used was SO-1. The slurries were analysed both with and without desolvation. The particle size distribution, measured by the Coulter Counter is shown in Figure 7.3.1, and the results obtained for the recoveries are shown in Figures 7.3.2 - 7.3.10.

These graphs clearly show that there is a difference in the efficiencies between the two methods of sample introduction. The use of desolvation enables recoveries of 100% to be obtained after about 30 minutes grinding compared with the one hour required for the non-desolvated slurry. In particle size terms this corresponds to "cut off" points of about 8μm for desolvated slurries and about 4 um for non-desolvated slurries. This assumes there is no atomisation of particles above either 8 μm or 4 μm respectively for desolvated and non-desolvated slurries and 100% atomisation for those particles below these figures. It is, of course, unlikely that this is rigorously the case.

To obtain both transport and atomisation efficiencies for smaller particle size bandwidths, a cascade impactor was used to fractionate the SO-1 sample. In this study the bands around the perceived "cut off points were of

FIG 7.3.1: PARTICLE SIZE DISTRIBUTION FOR SO-1 DIFFERENT GRINDING TIMES

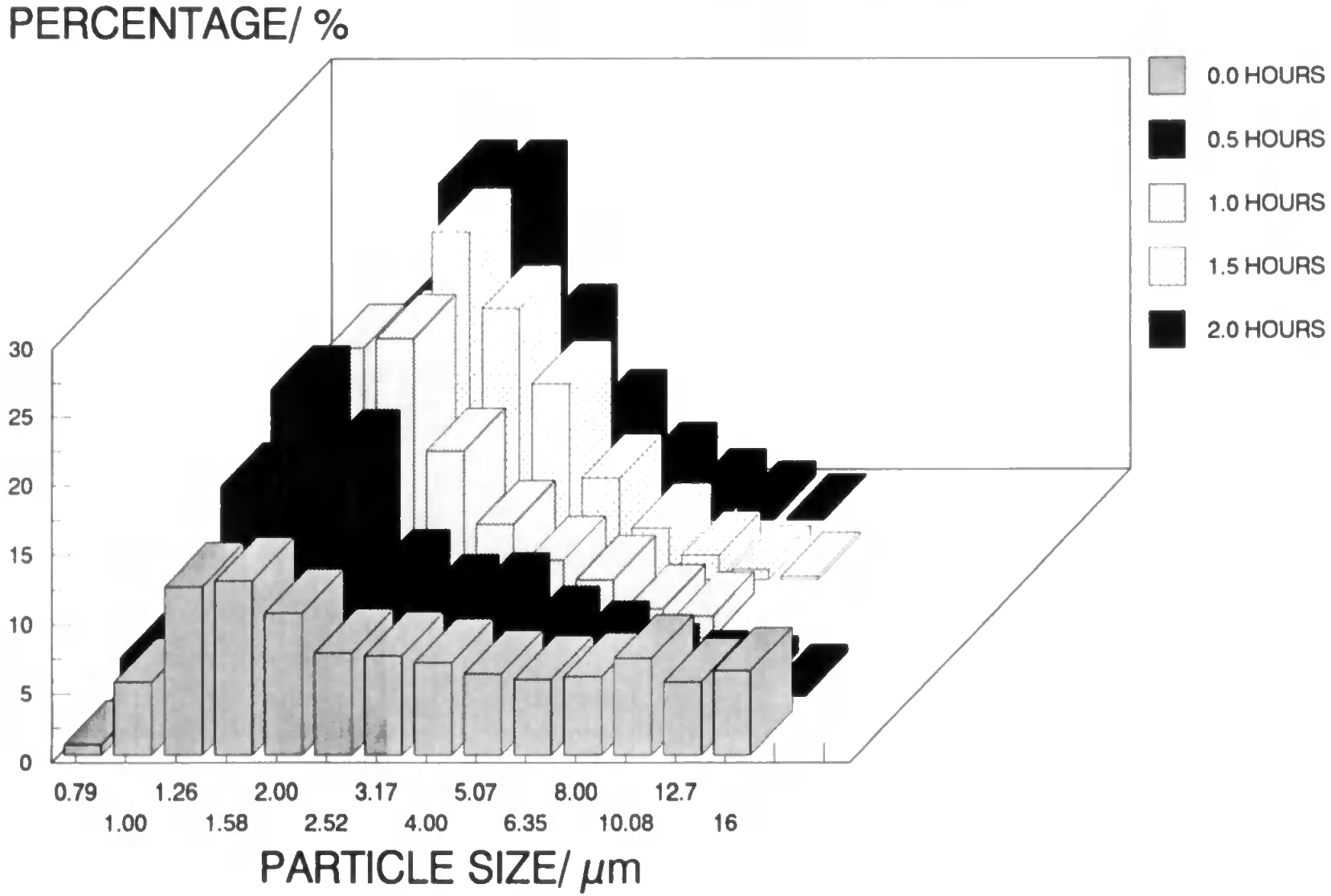

FIG 7.3.2: VANADIUM WITH AND WITHOUT DESOLVATION DIFFERENT GRINDING TIMES

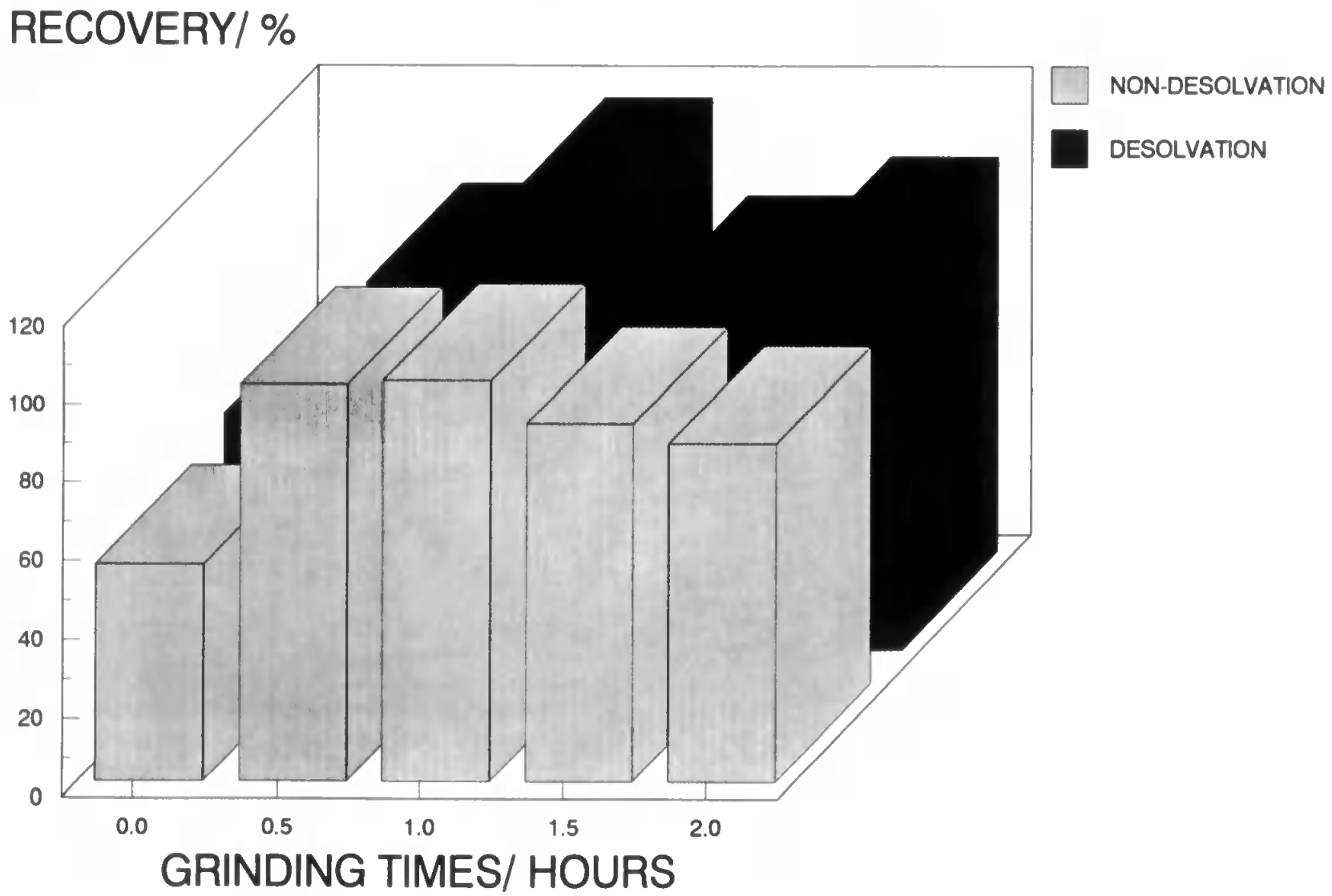

FIG 7.3.3: CHROMIUM WITH AND WITHOUT DESOLVATION DIFFERENT GRINDING TIMES

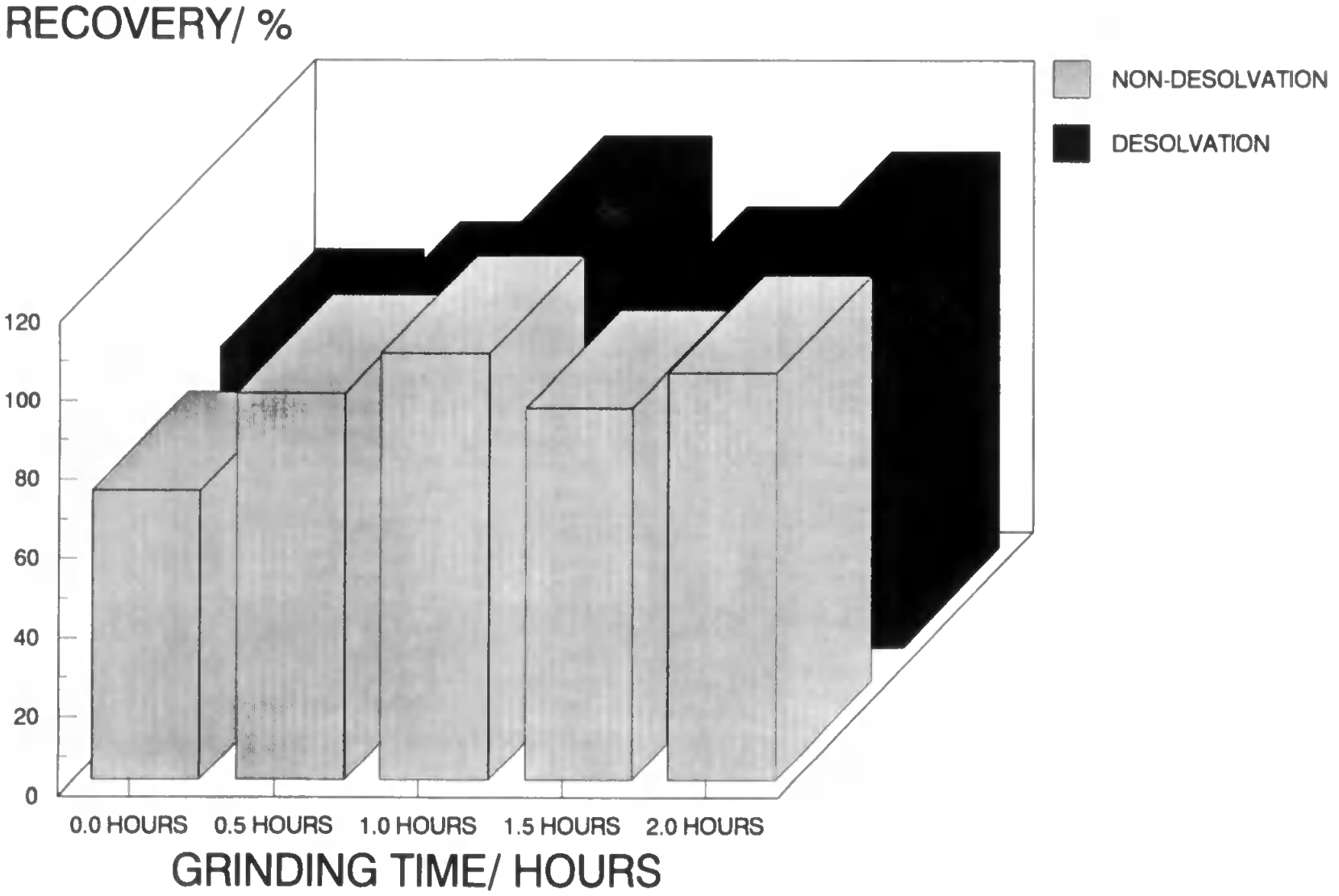

FIG 7.3.4:MANGANESE WITH AND WITHOUT DESOLVATION DIFFERENT GRINDING TIMES

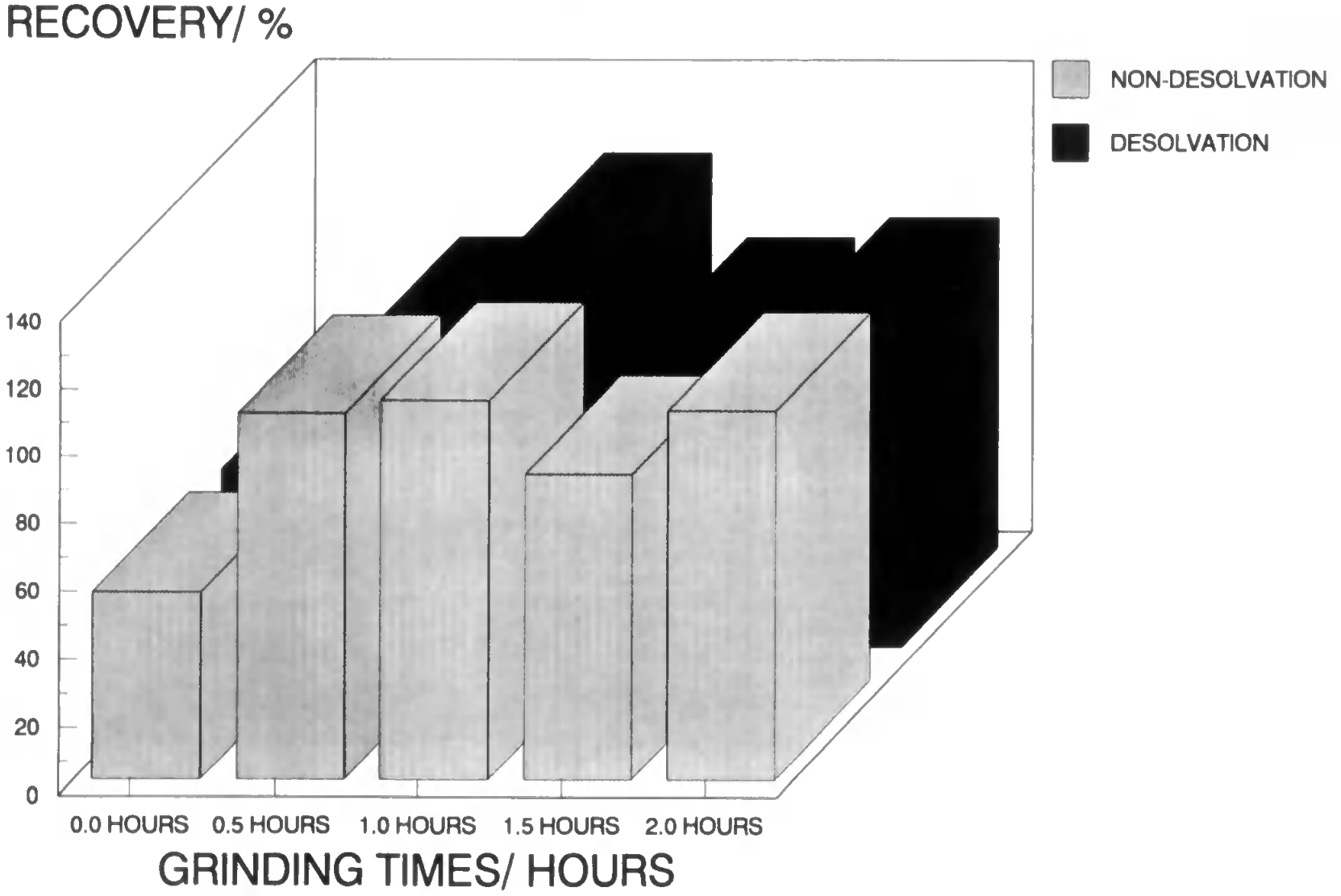

FIG 7.3.5: COBALT WITH AND WITHOUT DESOLVATION DIFFERENT GRINDING TIMES

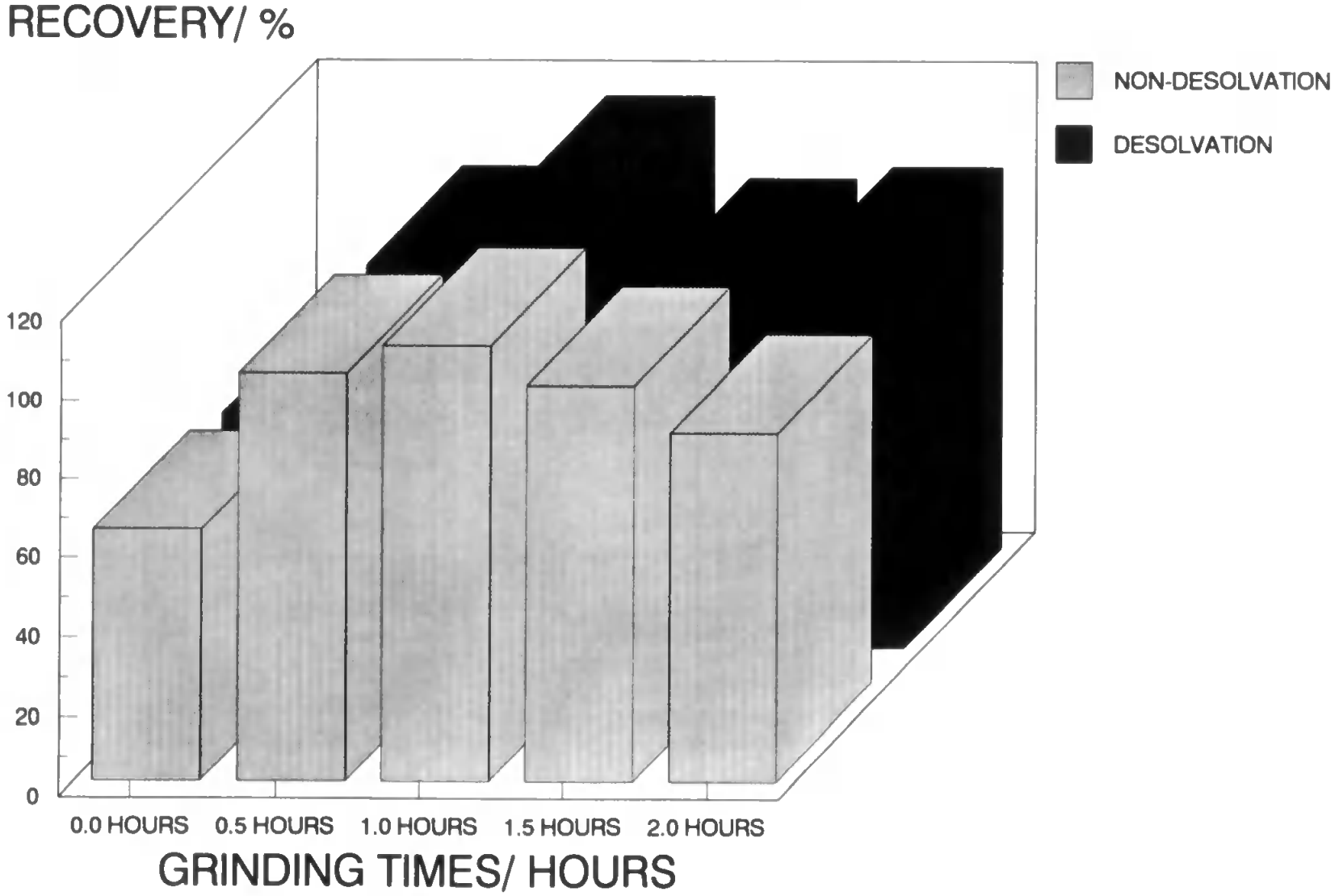

FIG 7.3.6: NICKEL WITH AND WITHOUT DESOLVATION DIFFERENT GRINDING TIMES

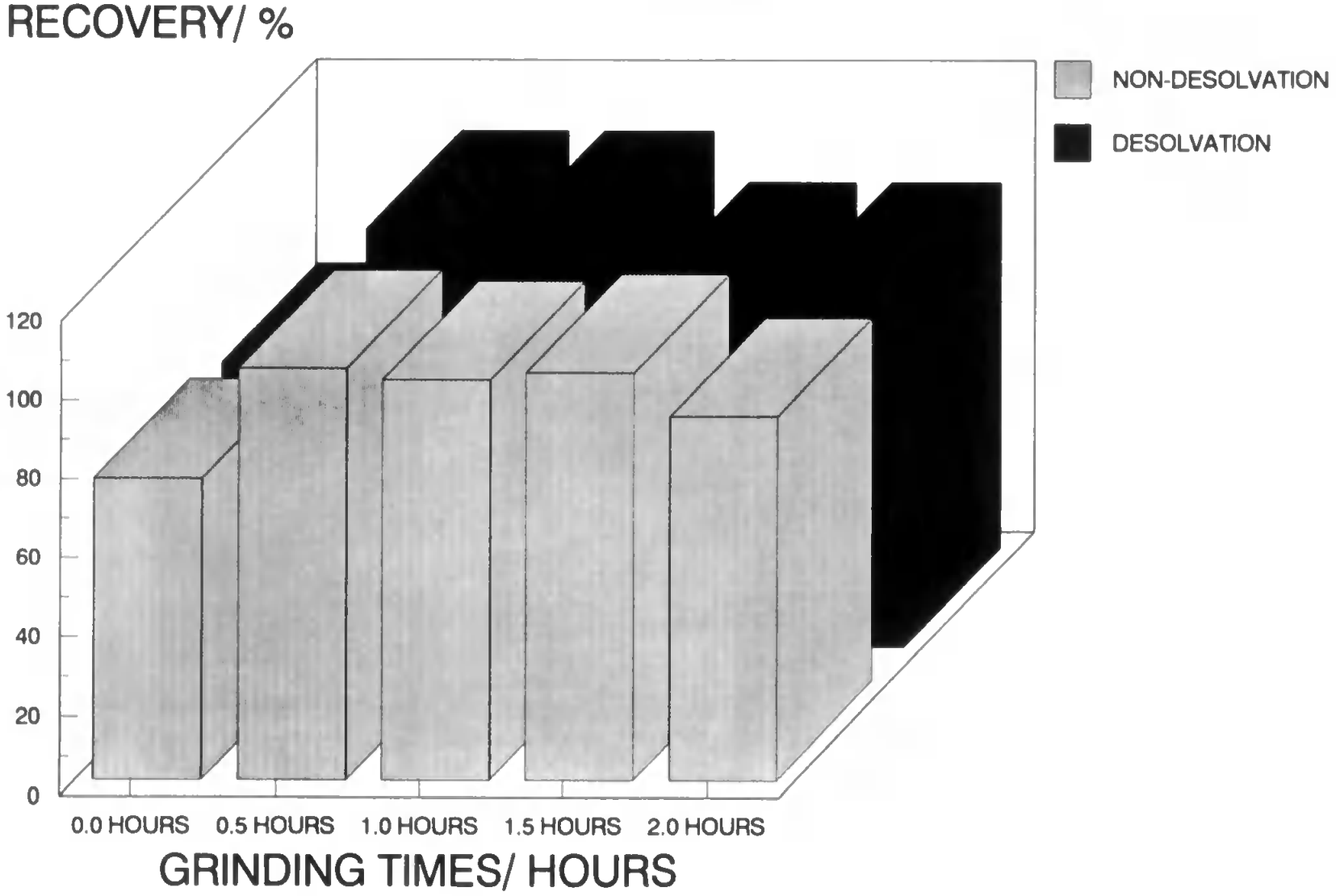

FIG 7.3.7: COPPER WITH AND WITHOUT DESOLVATION DIFFERENT GRINDING TIMES

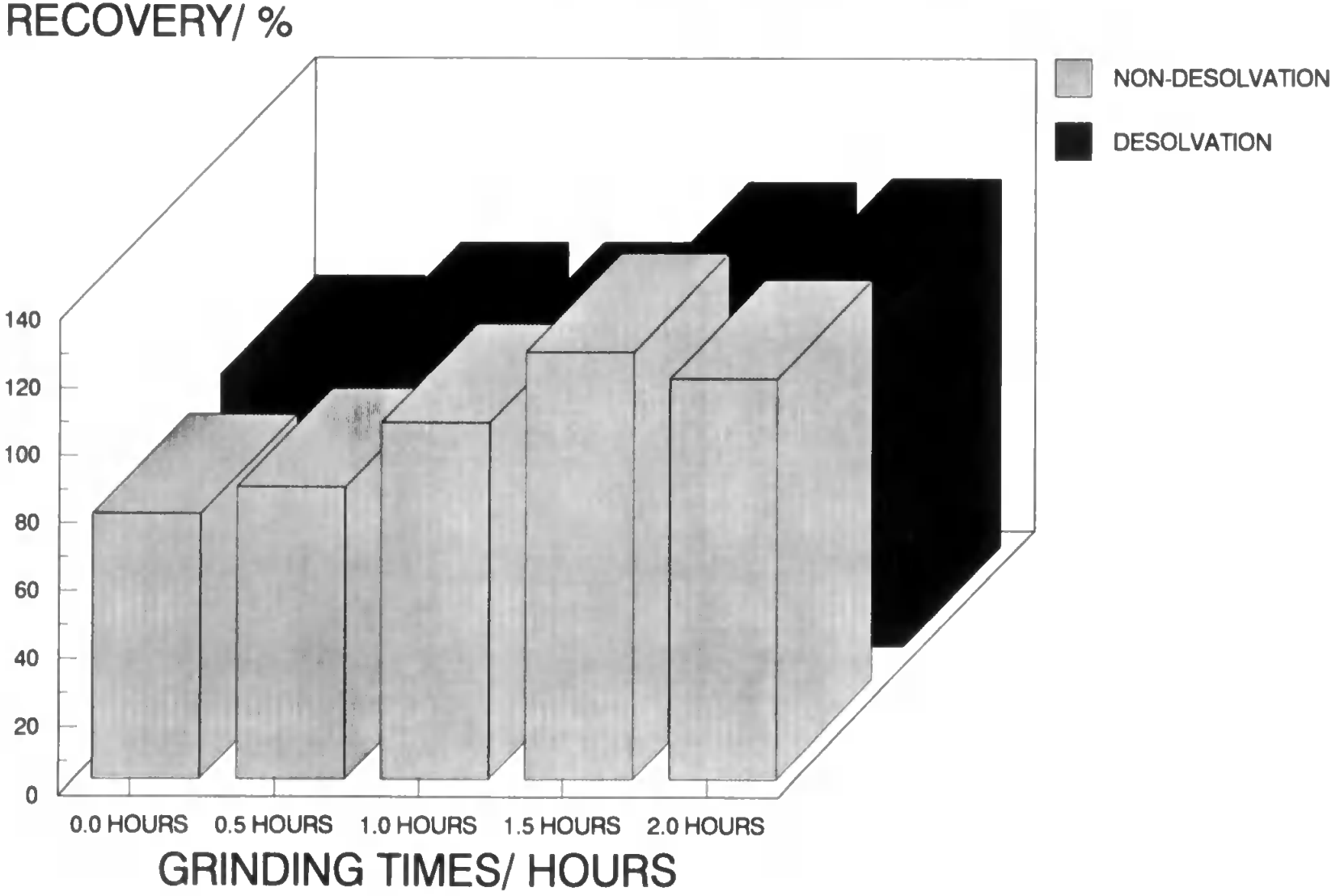

FIG 7.3.8: ZINC WITH AND WITHOUT DESOLVATION DIFFERENT GRINDING TIMES

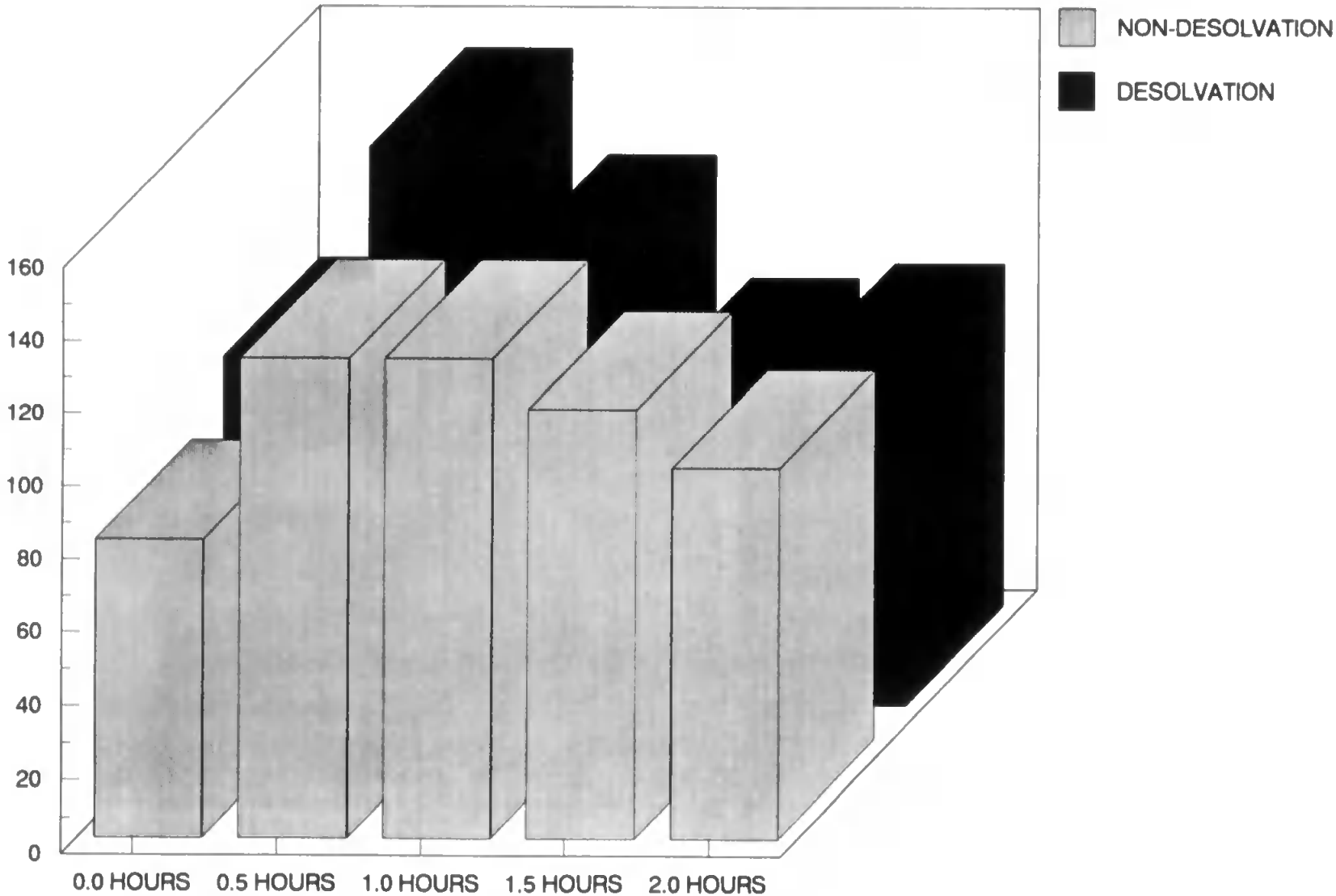

FIG 7.3.9:STRONTIUM WITH AND WITHOUT DESOLVATION DIFFERENT GRINDING TIMES

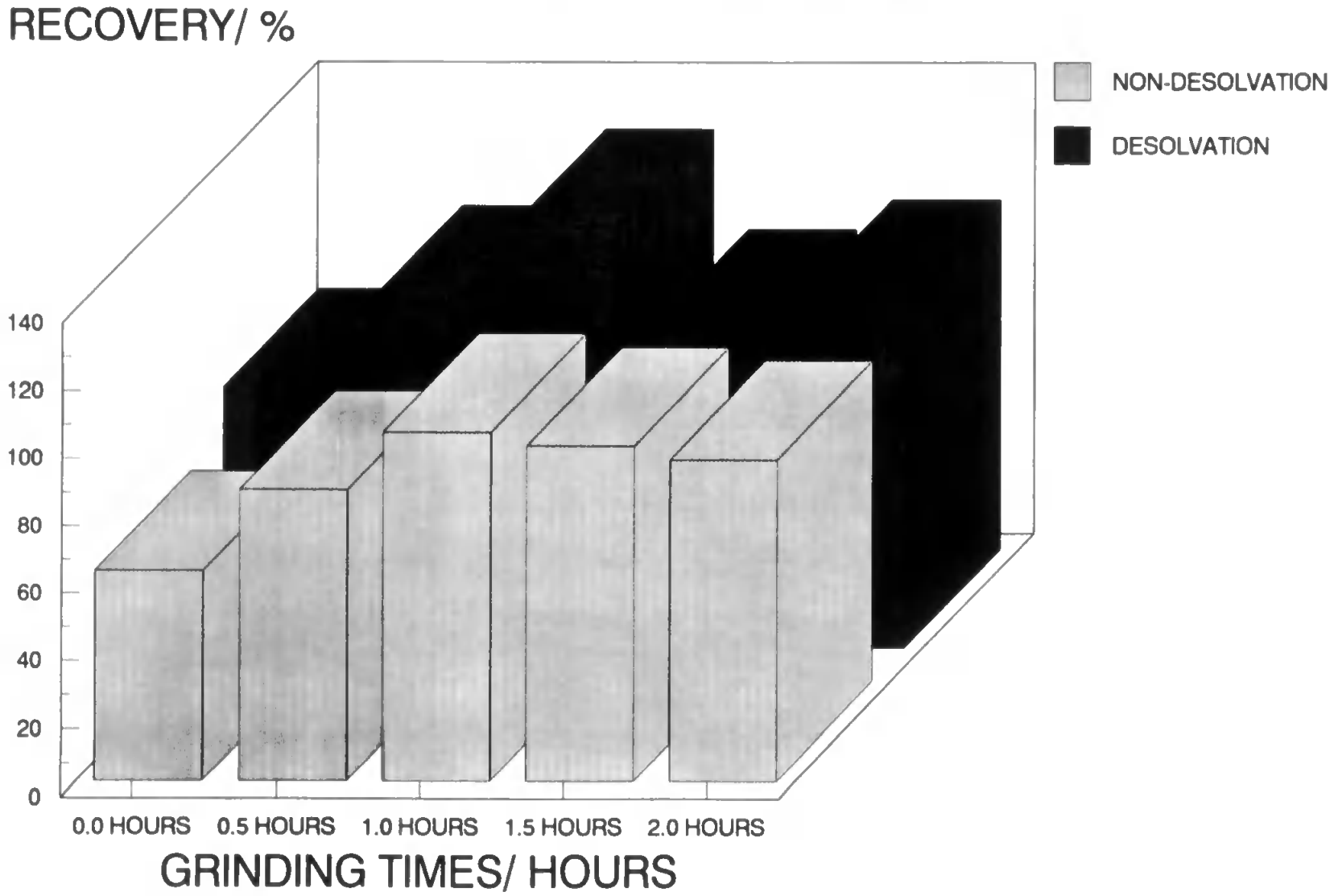

FIG 7.3.10: BARIUM WITH AND WITHOUT DESOLVATION DIFFERENT GRINDING TIMES

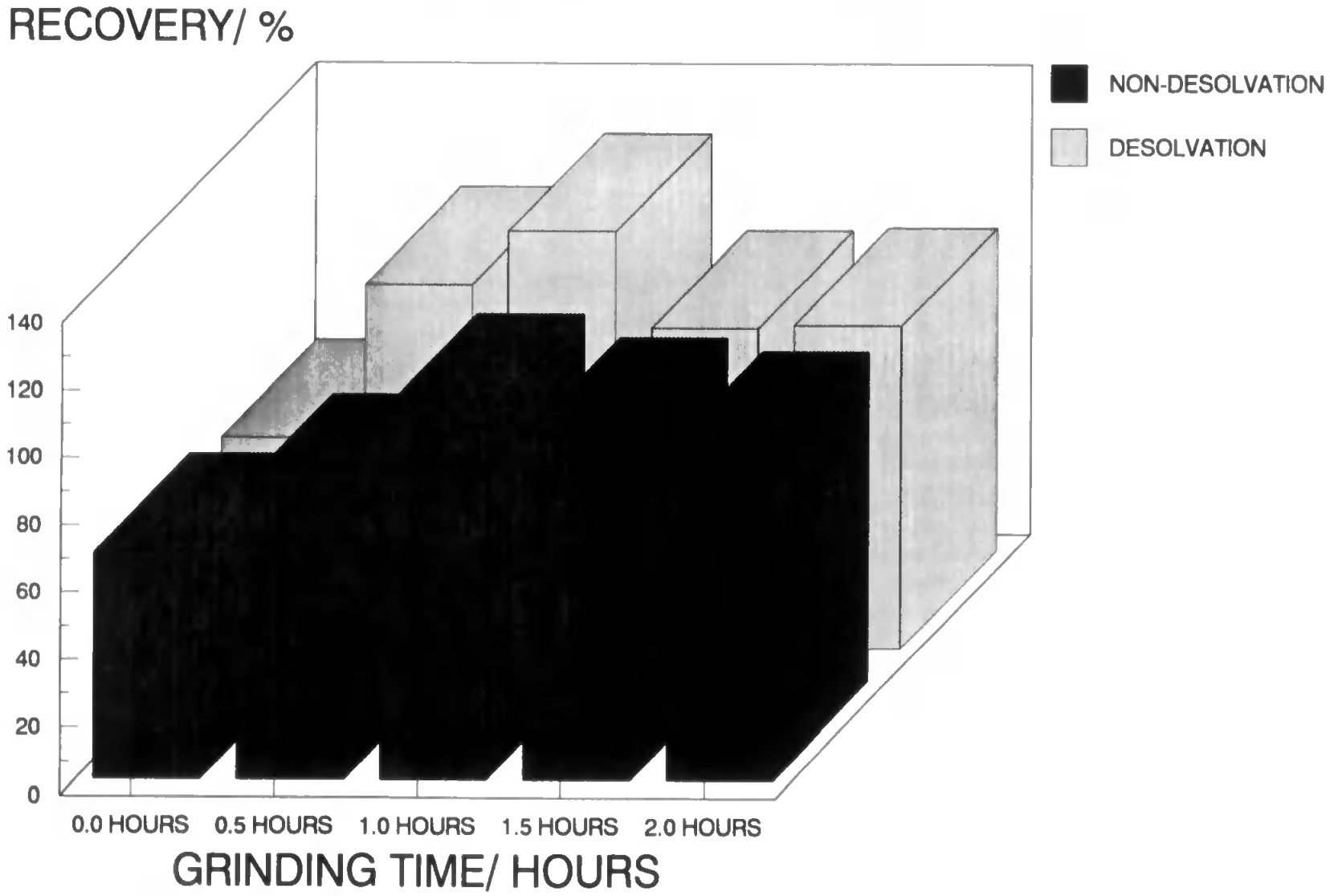

particular interest.

The results from these experiments are shown in Figures 7.3.11 - 7.3.16. In the four bandwidths shown the mode and mean point are in the same band.

These graphs (Figs. 7.3.11 - 7.3.16, indicate that there is not only a great difference between the desolvated and non-desolvated samples, but also a marked dependence on the element analysed. It is clear that there is not a sharp "cut off" point at a particular particle size. This is probably due to a number of factors, including the geological nature of the sample, transport efficiencies, residence times and the assumptions used in the particle size measurements that the particles are spherical. These factors will effect the atomisation efficiencies of the different elements, particularly since different elements will be intrinsically associated with different minerals with different grinding characteristics. There is no correlation between atomisation efficiencies and atomisation energies.

The homogeneity of the sample is important in understanding some of the effects described above. In order to elicit information on the homogeneity of sample SO-1, sub-samples were dissolved using a microwave digestion procedure after fractionation using the cascade impactor. This procedure involved the addition of concentrated nitric acid (3 ml, Aristar, BDH, Dorset,

FIG 7.3.11:VANADIUM WITH AND WITHOUT DESOLVATION AFTER FRACTIONATION

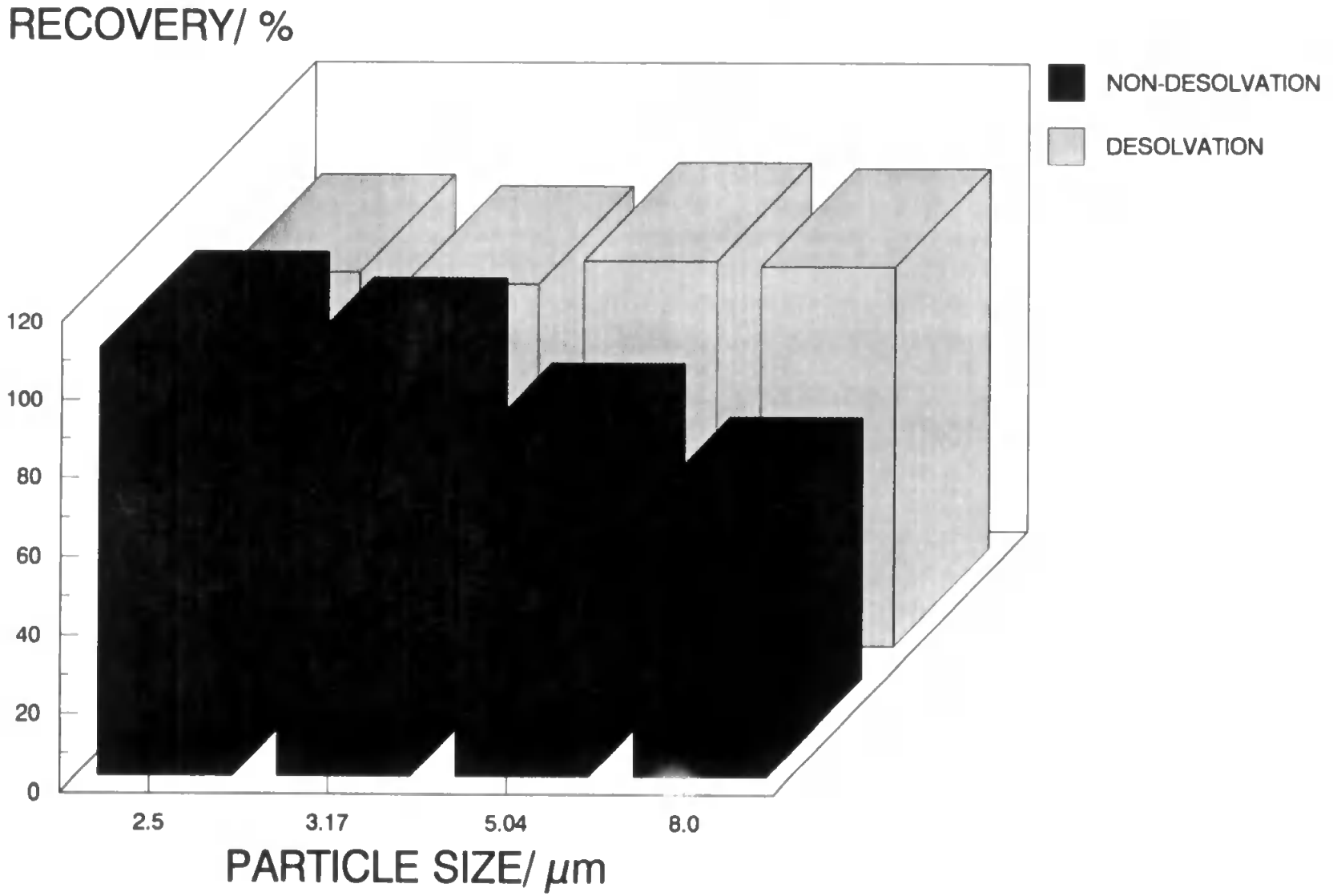

FIG 7.3.12:CHROMIUM WITH AND WITHOUT DESOLVATION AFTER FRACTIONATION

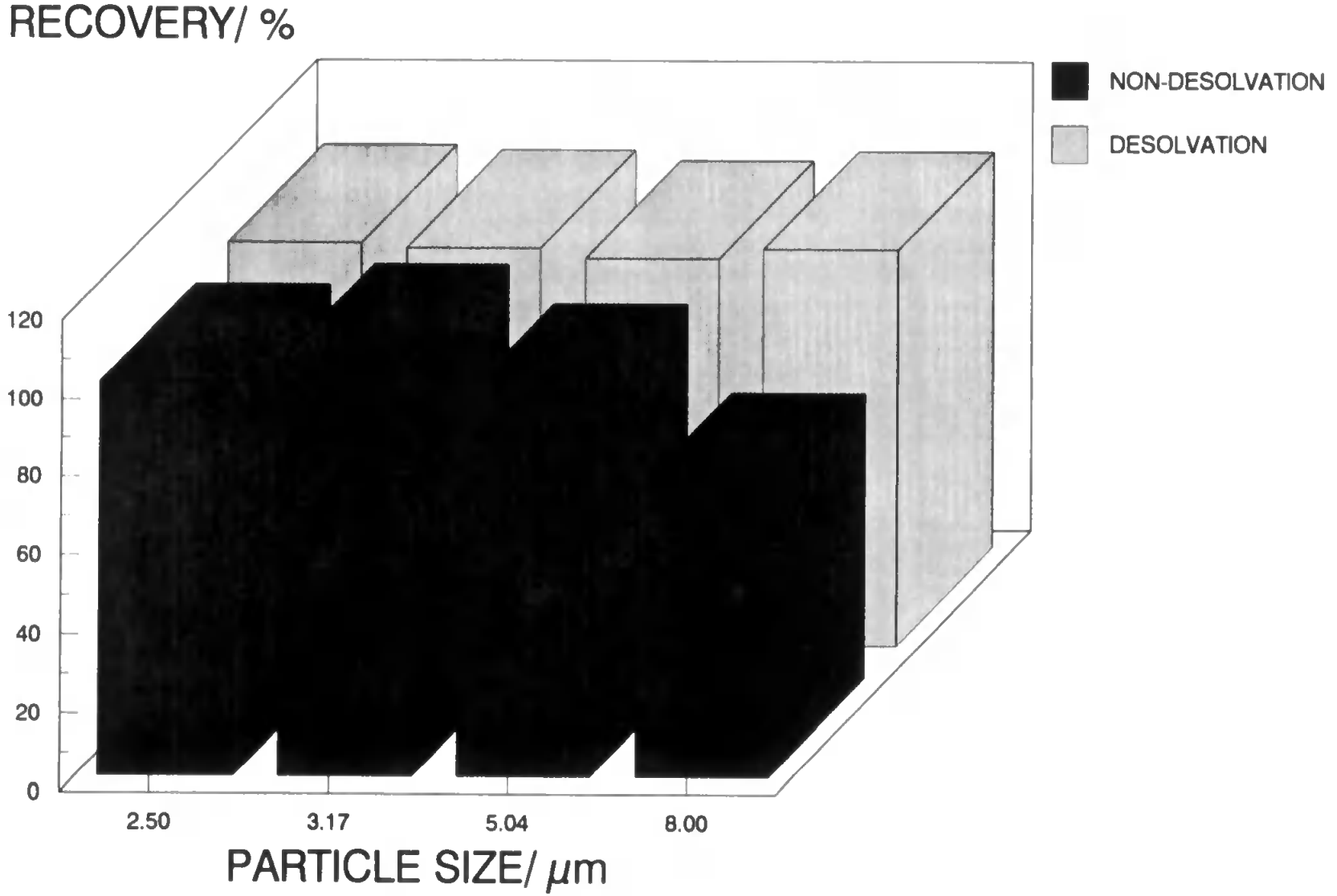

FIG 7.3.13: COBALT WITH AND WITHOUT DESOLVATION AFTER FRACTIONATION

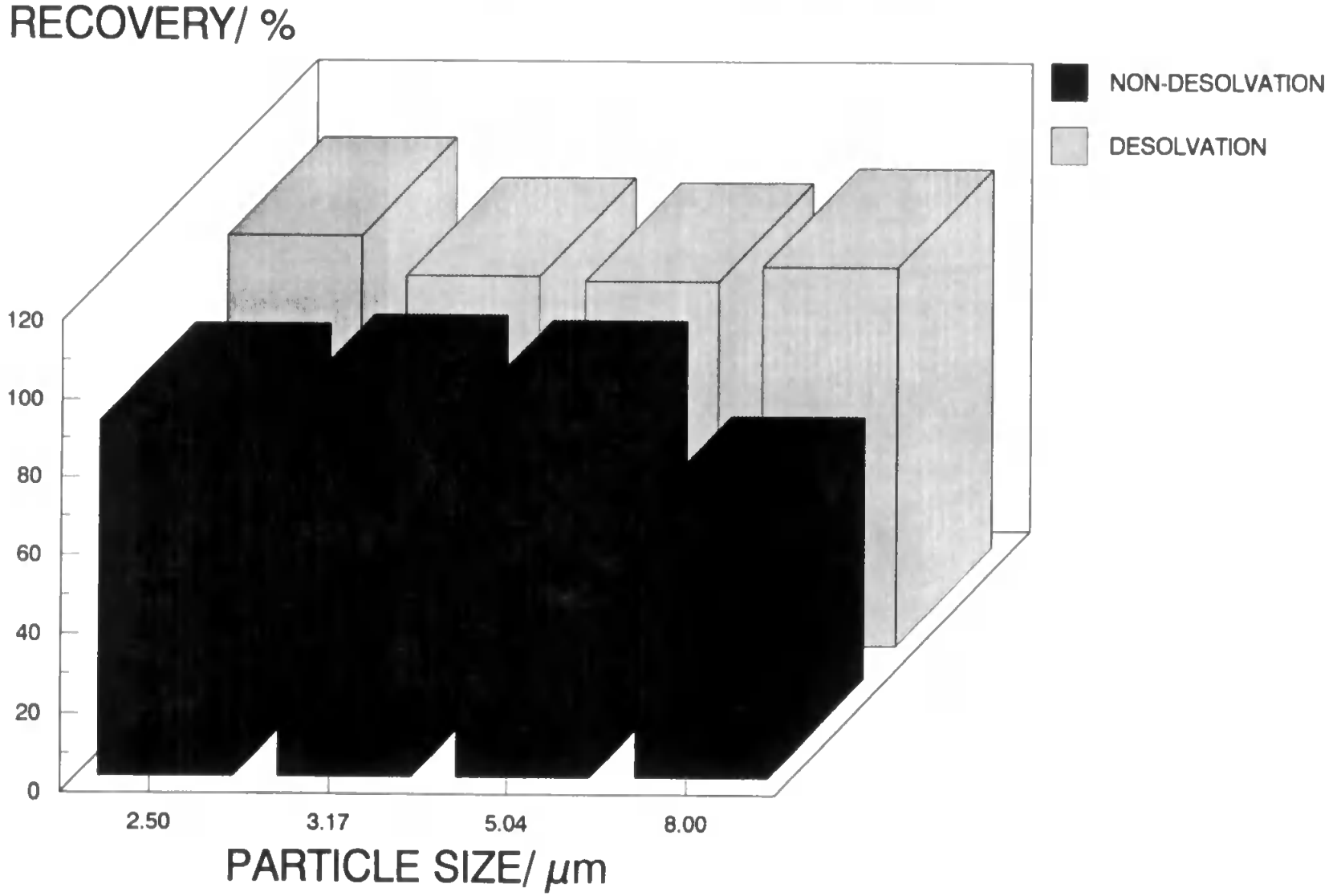

FIG 7.3.14: COPPER WITH AND WITHOUT DESOLVATION AFTER FRACTIONATION

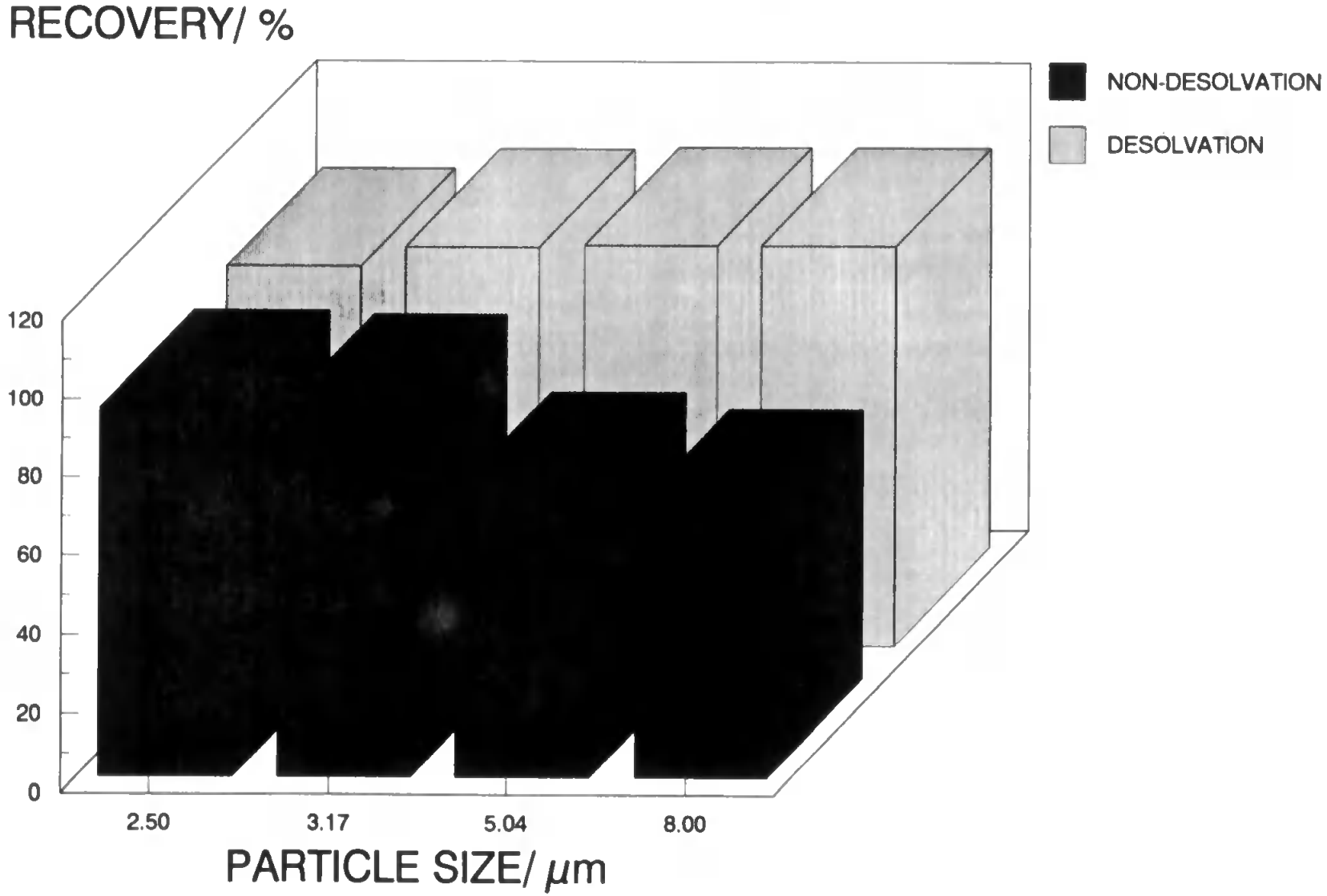

FIG 7.3.15: STRONTIUM WITH AND WITHOUT DESOLVATION AFTER FRACTIONATION

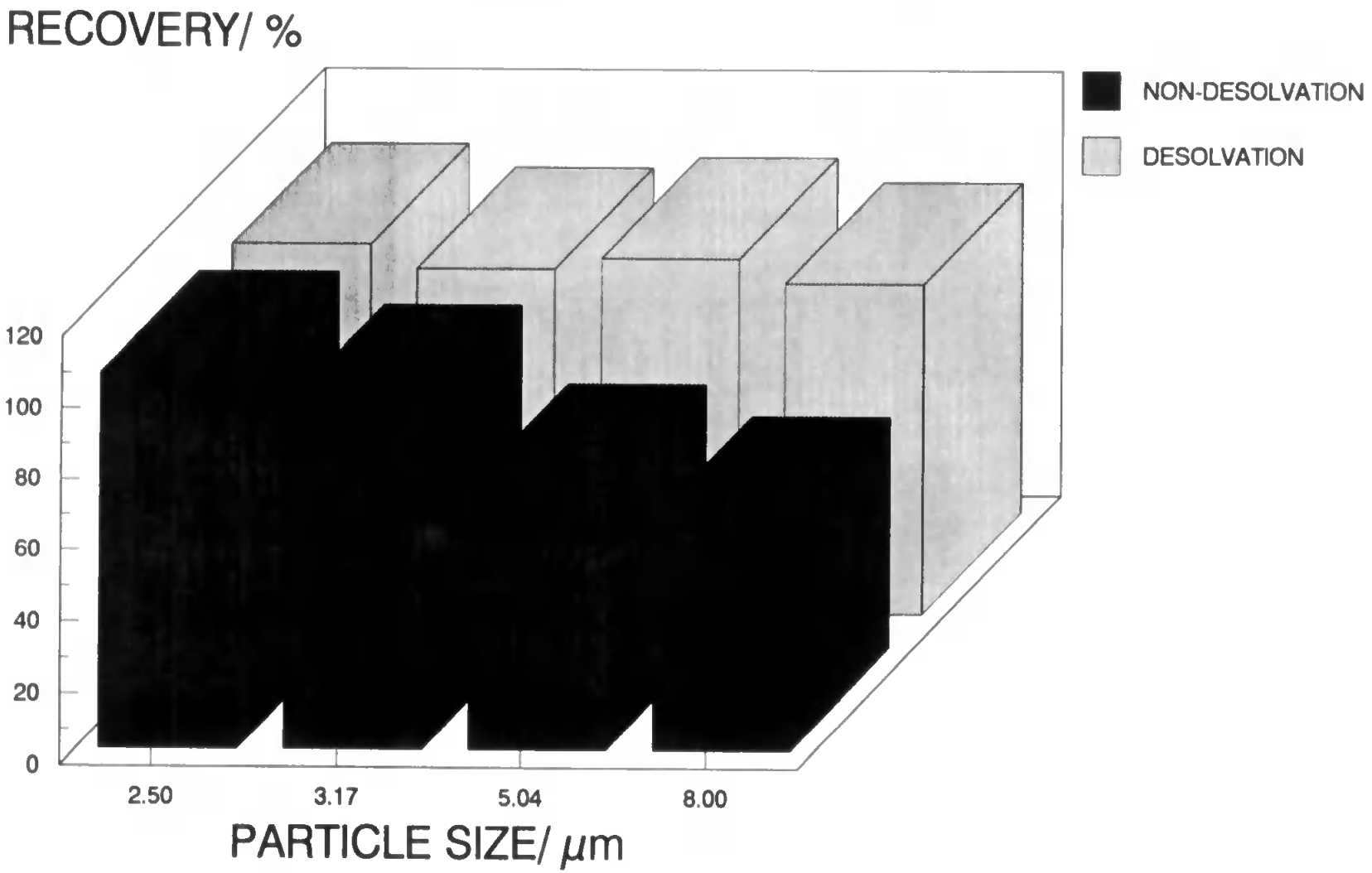

FIG 7.3.16: BARIUM WITH AND WITHOUT DESOLVATION AFTER FRACTIONATION

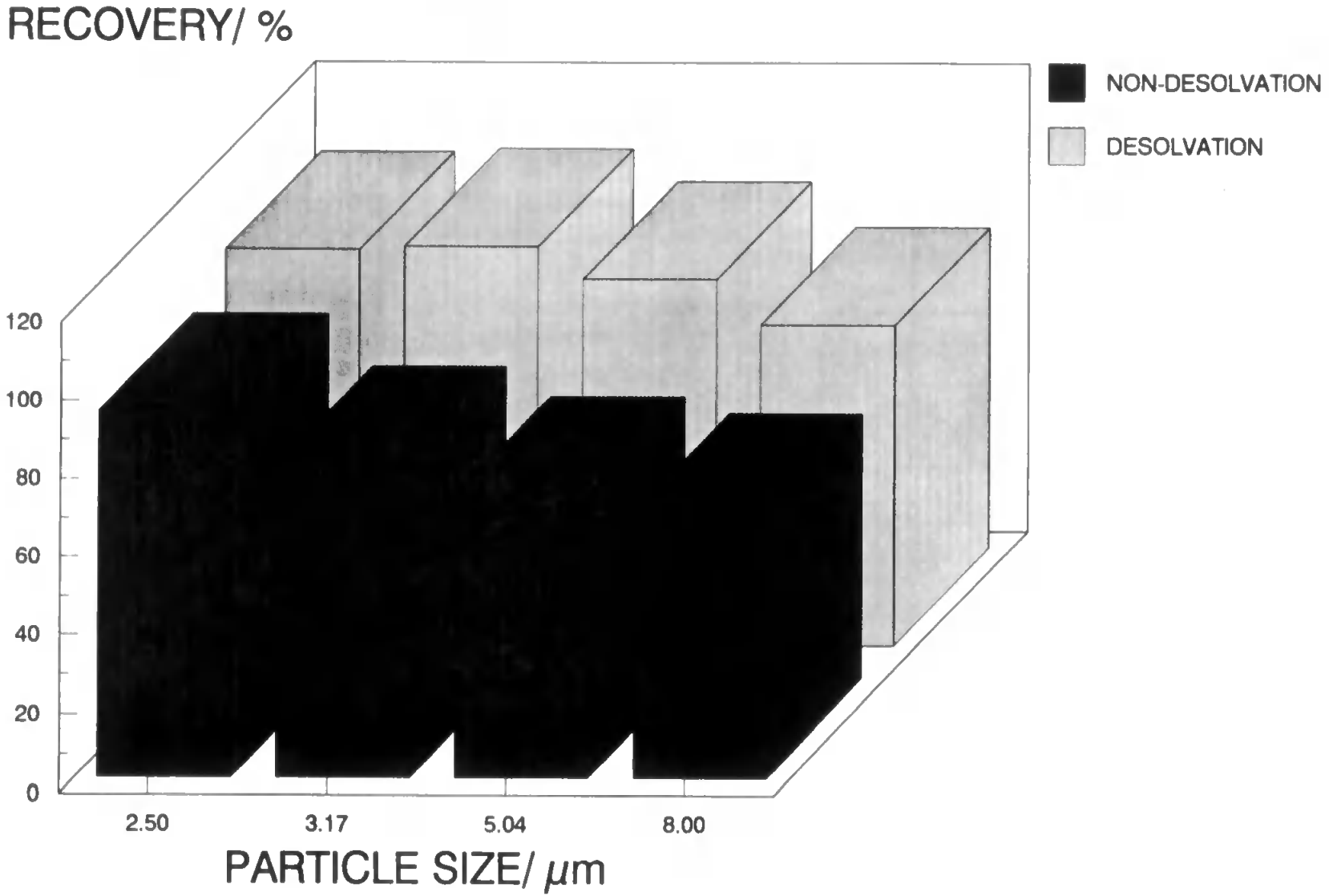

U.K.) to the carefully weighed samples placed in a microwave bomb. This was followed by microwaving at 140W for five minutes, to remove the organic fraction from the sample. The microwave bomb was then cooled and the pressure released. Hydrofluoric acid (2 ml, 20% v/v, Aristar, BDH, Dorset, U.K.) was added and the sample microwaved at 70W for twenty minutes. The bomb was then cooled and the pressure released. The hydrofluoric acid was evaporated off using a heating plate and the samples placed in volumetric flasks and made up to 100 ml with dilute nitric acid (2% v/v).

The resulting digests were analysed by ICP-MS and the results compared with those obtained following slurry atomisation - ICP-MS (Figures 7.3.17 - 7.3.21). These results indicate that the dissolution of the samples gave recoveries that were comparable with those obtained for the desolvated slurry atomisation results. The similarity, with the possible exception of copper (Figure 7.3.19), indicates that the differences in recoveries over the particle size range are partly due to the inhomogeneity of the samples rather than the atomisation efficiency of the plasma. These results give evidence that the "cut off" points for desolvated samples is about 8 μm, and that for non-desolvated samples is about 3 μm. It is also evident that these values are due to the transport efficiency rather than atomisation efficiency.

Throughout the above study Triton X-100 (1% v/v) was used

FIG 7.3.17: VANADIUM AFTER FRACTIONATION AND DISSOLUTION

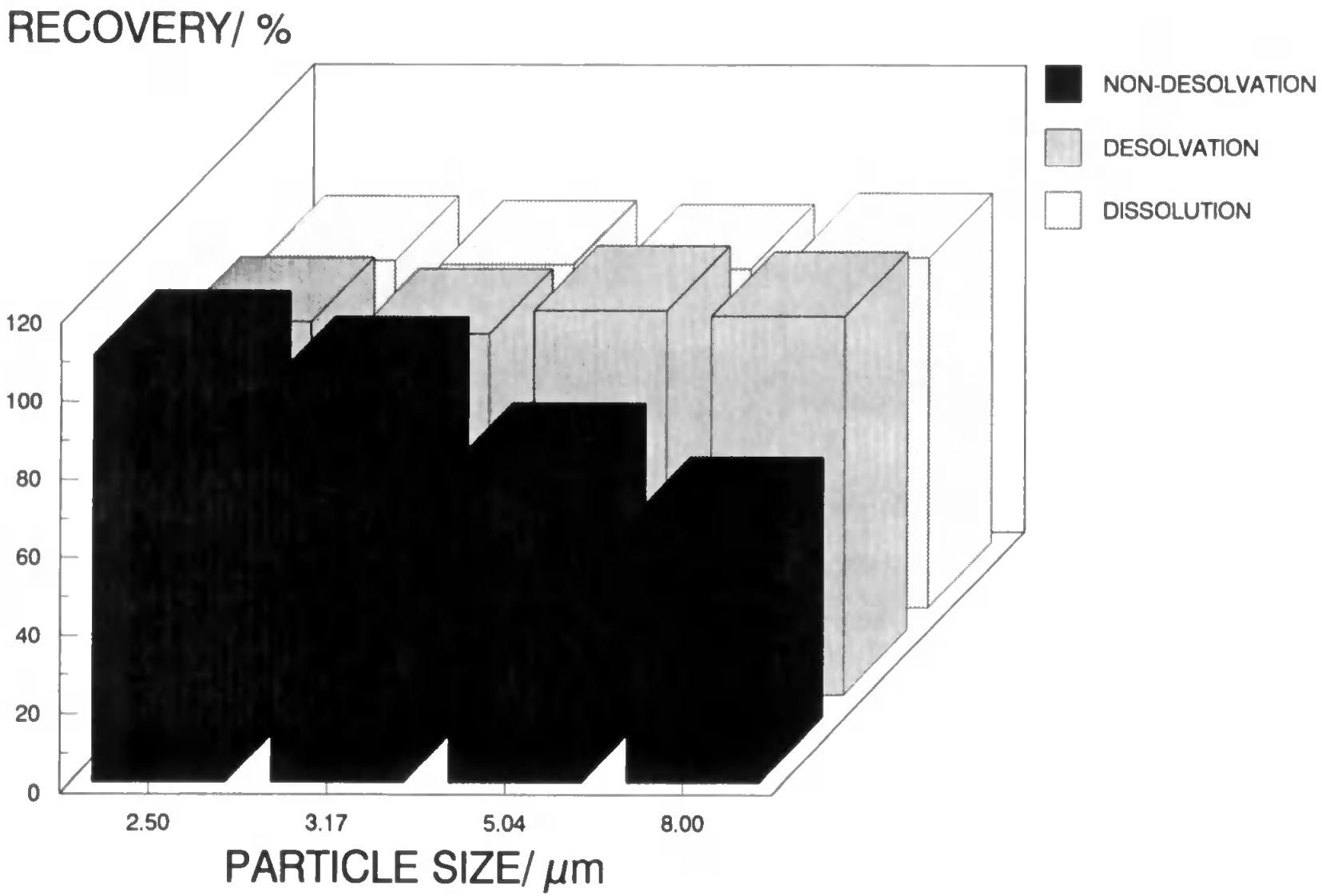

FIG 7.3.18: COBALT AFTER FRACTIONATION AND DISSOLUTION

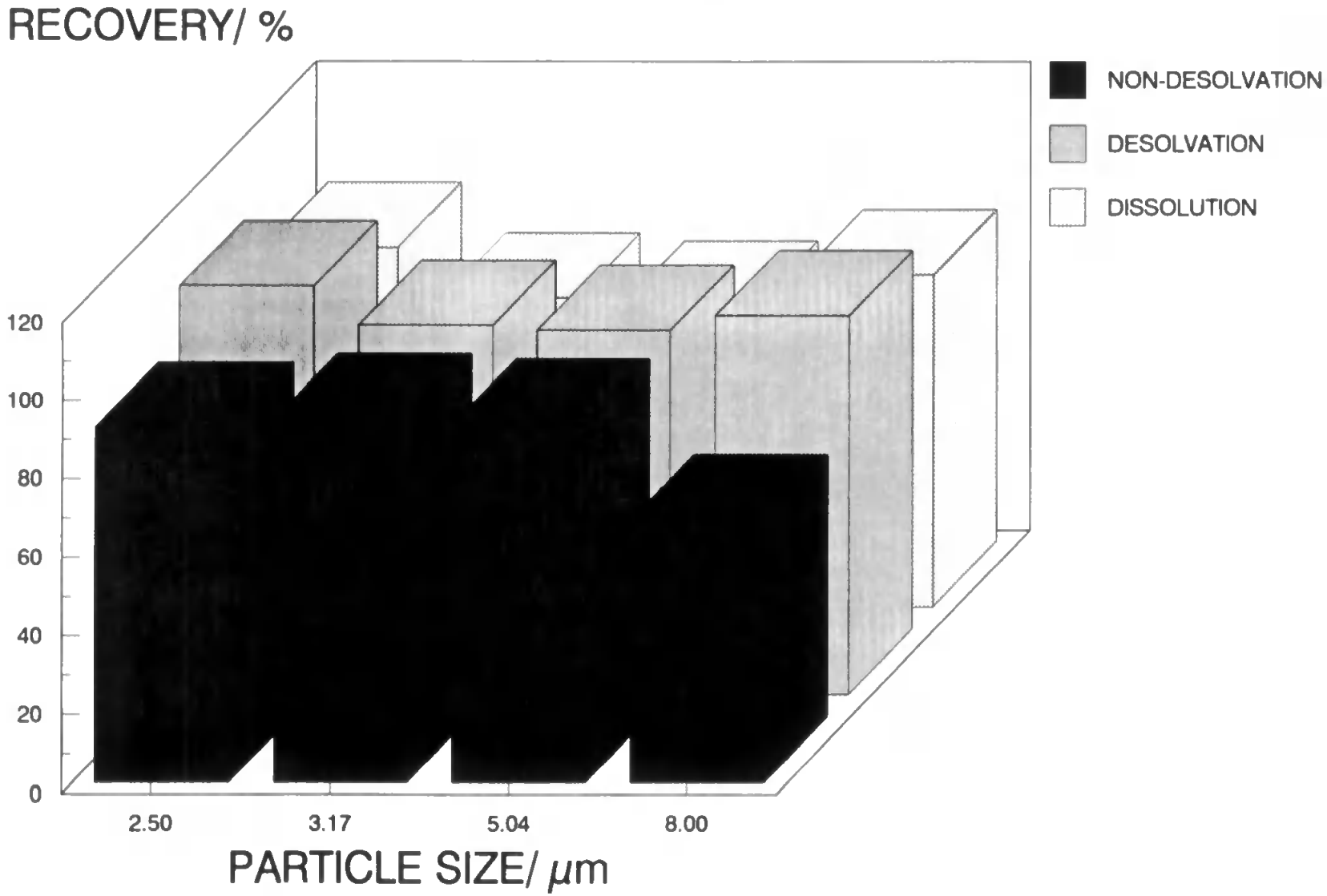

FIG 7.3.19: COPPER AFTER FRACTIONATION AND DISSOLUTION

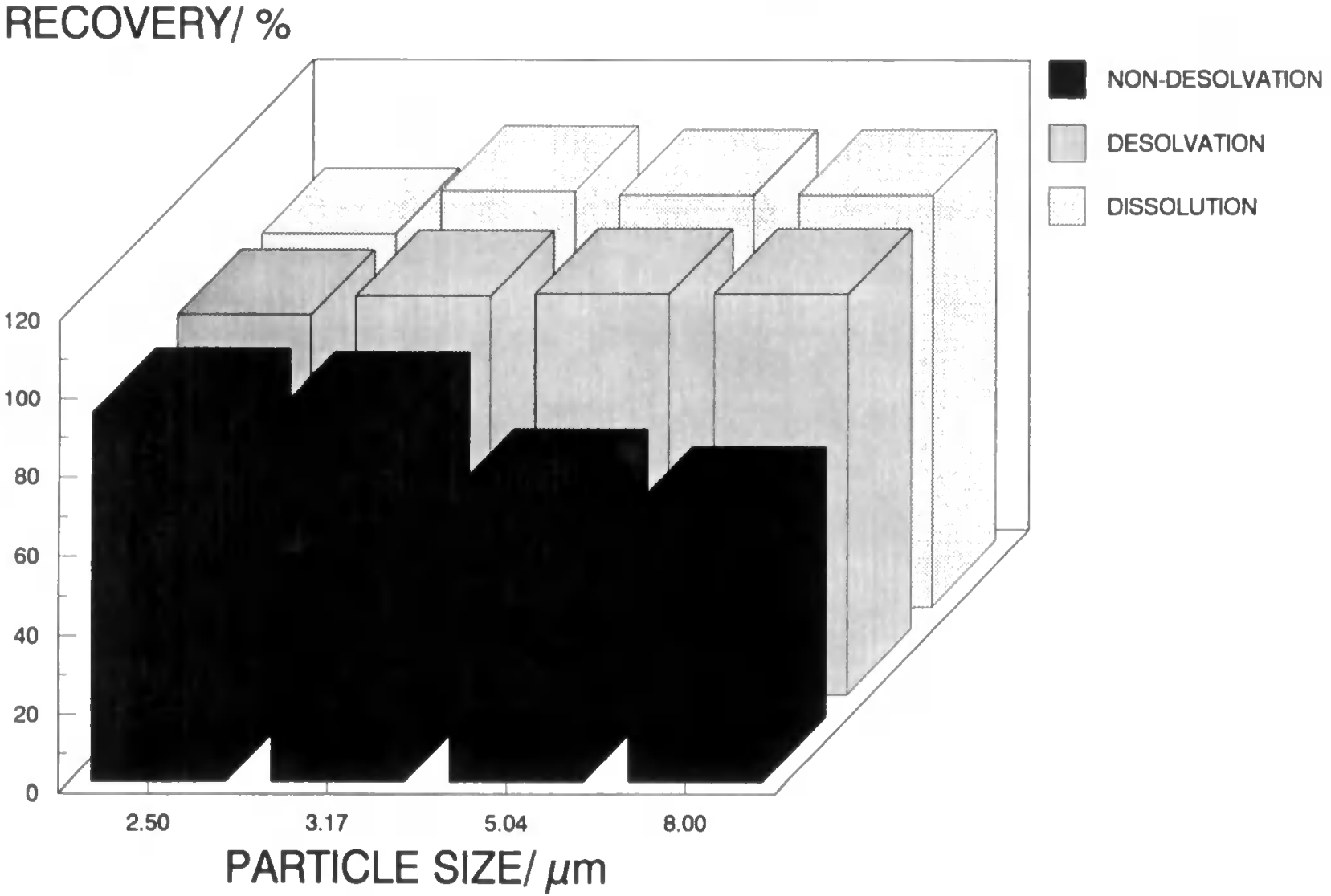

FIG 7.3.20: STRONTIM AFTER FRACTIONATION AND DISSOLUTION

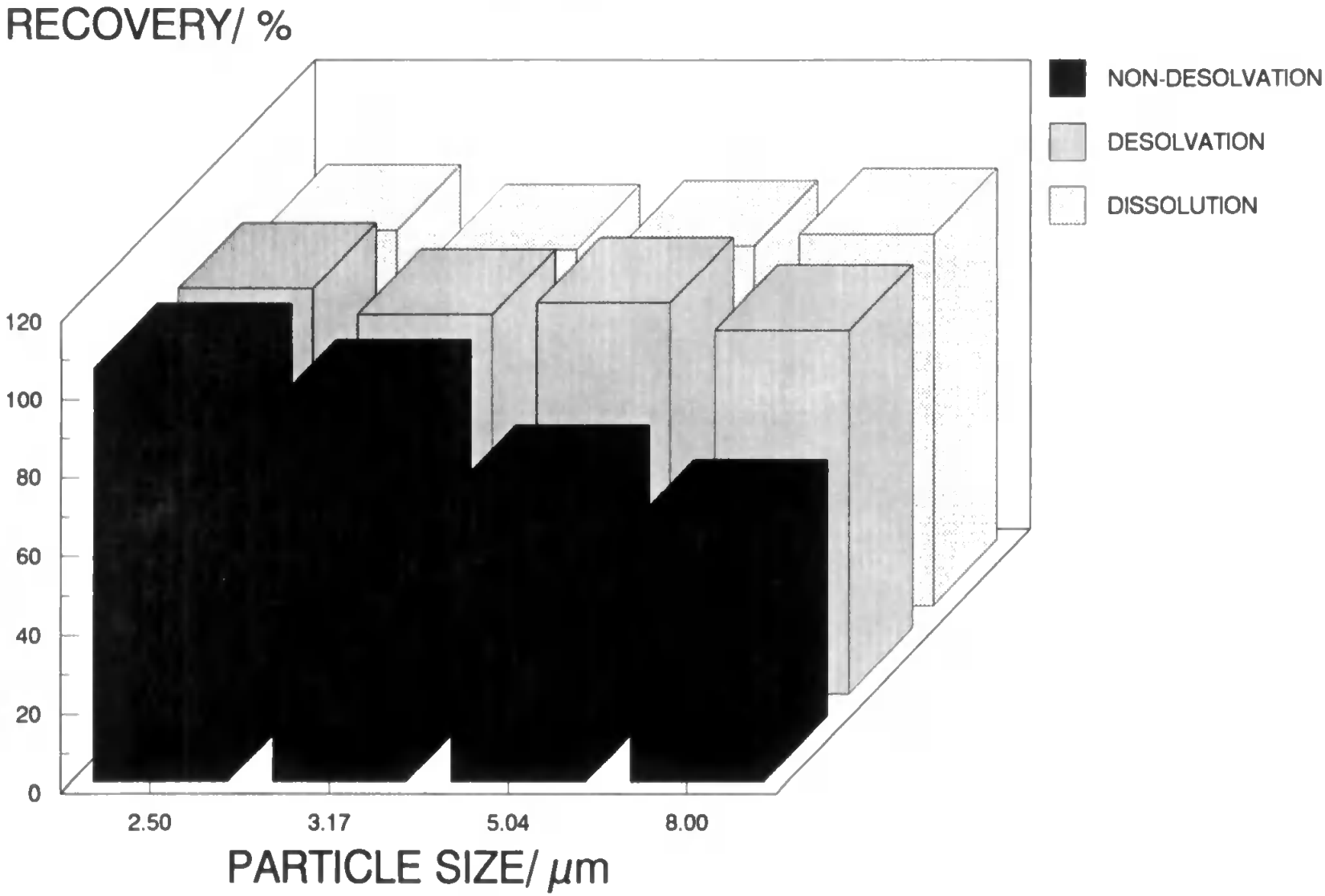

FIG 7.3.21: BARIUM AFTER FRACTIONATION AND DISSOLUTION

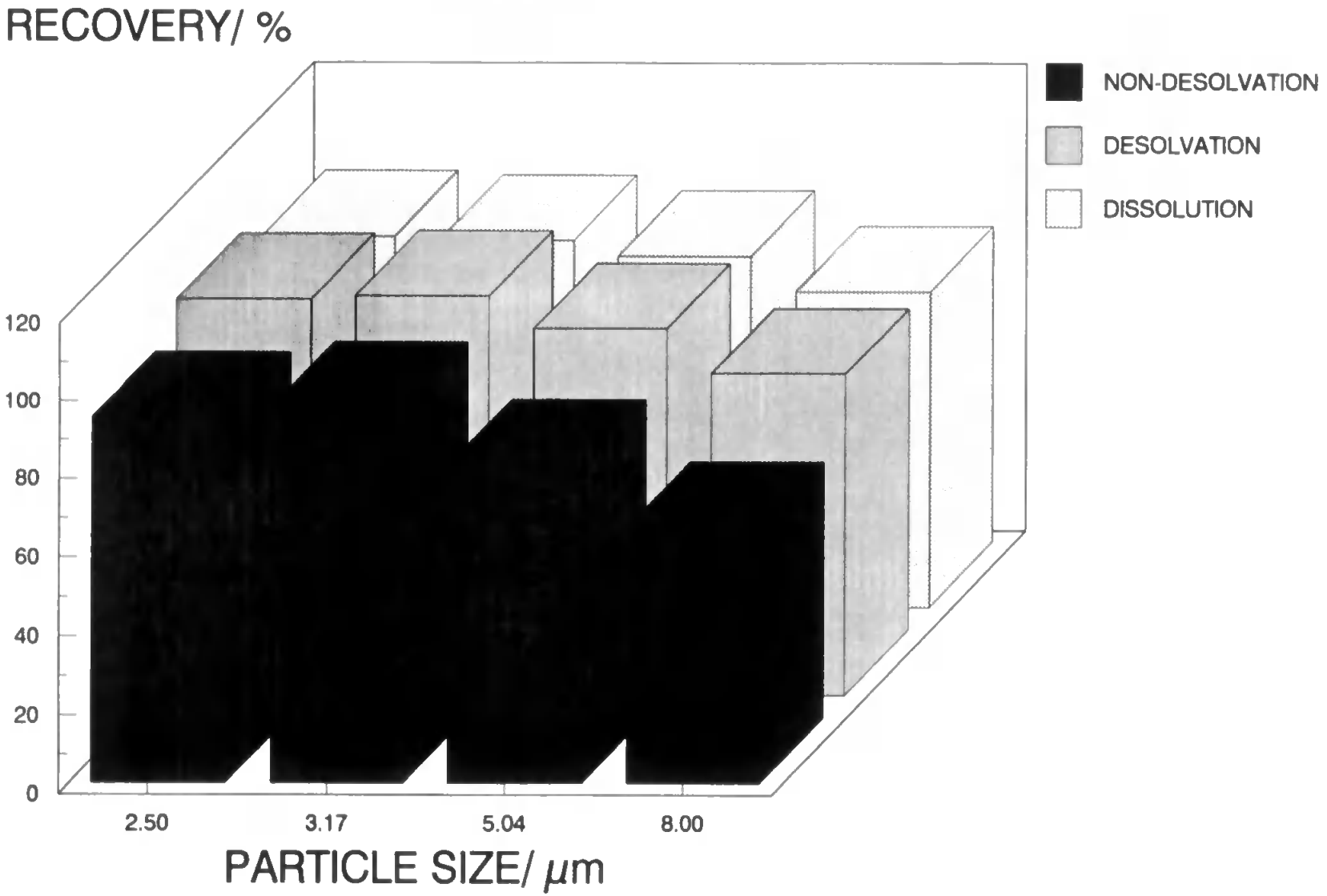

as a dispersant and this may have some effect on the results. Consequently the experiments involving different grinding times were repeated using tetra sodium pyrophosphate (1% m/v) as the dispersant. Results obtained using this dispersant were compared with the results obtained using Triton X-100, and a statistical f-test used. This evaluation showed that the use of different dispersants may have an effect on the results obtained for non-desolvated slurries. In this case there was a twenty per cent chance of the two sets of results being different. The results for the desolvated slurry showed that there was a 95% certainty that they were the same. Clearly, the fact that a large amount of the solvent is being removed when the sample is desolvated means that the effect of the dispersant will be greatly reduced.

The effect of desolvation, is then, to enhance the analyte signal for both aqueous standards and also the slurry sample. One measure of the degree of enhancement is to compare the ratio of the desolvated with the non-desolvated calibration curve slopes. To achieve this a series of slurry standards of varying concentrations were prepared and analysed both with and without desolvation. The calibration curves were then plotted and the slopes obtained. The gradients were compared with a series of aqueous standards analysed both with and without desolvation. The average improvement in the gradient for aqueous solutions is 6.4 compared with 7.4 for the

slurries, and clearly shows that desolvation of the sample improves the response more for slurries than for aqueous solutions.

Thus the use of desolvation for the analysis of slurries, acts not only to increase the transport efficiency, but also enhances the sensitivity of the technique. Importantly however the analyte signal increases slightly more for the slurry than the aqueous standards. The other factor to note is the ability to analyse large particle sizes. It would appear that if a particle of 8 μm or less reaches the plasma then it is likely to be atomised.

7.3 Analysis of precious group metals

7.3.1 Introduction

The analysis of the precious group metals (PGM's) is complicated by the difficulties encountered in bringing some of the elements into solution. The dissolution procedures are time consuming and often involve the use of hazardous and expensive chemicals. The introduction of contaminants and the loss of volatile species may also be a problem.

A procedure which would not involve extensive sample pretreatment would therefore be beneficial. The use of slurries was therefore considered. Although the metals are hard they are also brittle (94), and consequently would be expected to grind down fairly well.

7.3.2 **Iridium**

7.3.2.1 Experimental

The instrument used in this study was an inductively coupled plasma - mass spectrometer (VG Plasmaquad II+, VG Elemental, Winsford, Cheshire, U.K.). A De Galan nebuliser was used in conjunction with a Scott type double pass spray chamber.

The slurries were prepared by the bottle and bead method (68). Samples of Iridium (1g) were shaken for sixteen hours with zirconia beads (10 g). Triton X-100 (1% v/v) was used as a dispersant. The resultant slurry was made up in volumetric flasks at different concentrations (0.1, 0.2, and 0.5% m/v).

A blank was prepared by the same process although omitting the addition of sample.

Standards were prepared from an iridium standard solution and standard addition (5, 10 and 15 $\mu g\ ml^{-1}$) used for calibration. The iridium standard was also analysed for any impurities. In all cases 100 $\mu g\ ml^{-1}$ of indium was added to the samples to act as internal standard.

The analysis of the standard, by standard addition, found most of the impurities to be less than 1 $ng\ ml^{-1}$, the exception being copper (10 $ng\ ml^{-1}$) and platinum (7 ng

ml^{-1}).

7.3.2.2 Results and Discussion

Two samples of the iridium were prepared (Ir60 and Ir961), and the results obtained by slurry atomisation ICP-MS compared with indicative values. The indicative values were obtained by DC arc spectroscopy (J. Matthey PLC, Sonning Common) and had standard deviations of the order of ten percent. The particle size distributions are shown graphically in Figure 7.3.2.1.

The results obtained for the sample Ir60 are shown in Table 7.3.2.1. Two sets of results are given: the first was obtained using the iridium argide peak (m/z = 231) as an internal standard, and the second obtained using indium as an internal standard. All the results shown were obtained after blank subtraction and are for a 0.1% m/v slurry.

The results show that there is a reasonable agreement between the results obtained by the two methods of internal standardisation and with the indicated values. The major difference is found with copper and platinum, and is possibly due to the effect of the large amount of impurities of these elements in the iridium standard solution.

The use of an intrinsic internal standard ($IrAr^+$) appears

FIG 7.3.2.1: PARTICLE SIZE DISTRIBUTION FOR IRIDIUM

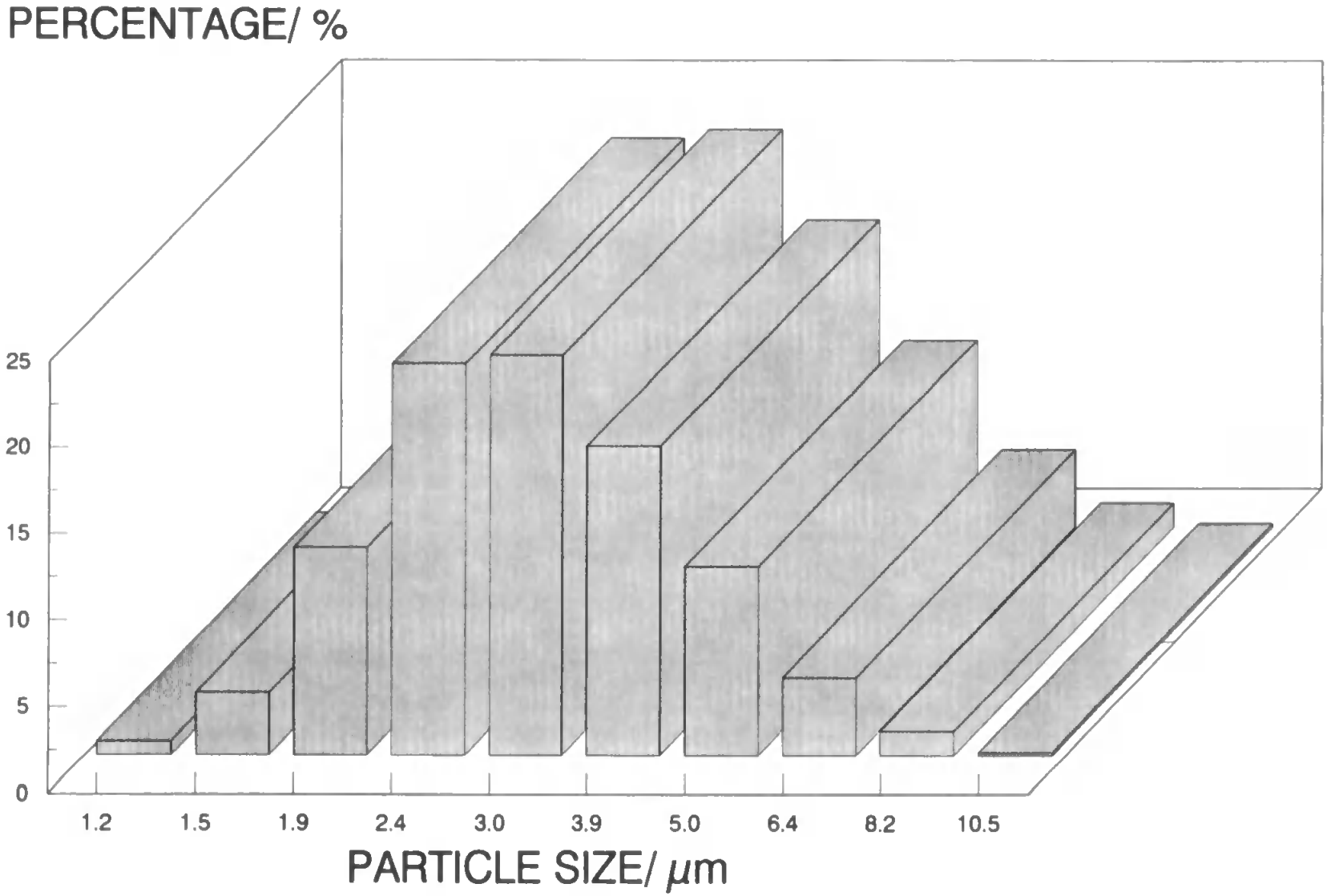

TABLE 7.3.2.1 RESULTS FOR THE ANALYSIS OF THE IRIDIUM SAMPLE IR60 BY SLURRY ATOMISATION-ICP-MS

$\mu g\ g^{-1}$

Analyte	Indicative Value	Internal Standard	
		In	IrAr
Mg	10	5.8 ± 0.4	6.2 ± 1.4
Al	1	1.3 ± 0.1	0.9 ± 0.0
Ti	<1	0.9 ± 0.1	1.0 ± 0.0
V	2	0.7 ± 0.3	1.0 ± 0.0
Cr	<1	1.3 ± 0.5	1.0 ± 0.2
Mn	<1	3.8 ± 1.0	1.1 ± 0.1
Fe	6	5.2 ± 1.1	7.4 ± 0.7
Ni	1	1.3 ± 0.4	1.0 ± 0.0
Cu	<1	12.8 ± 0.6	9.7 ± 0.1
Zn	10	7.5 ± 2.1	5.6 ± 1.9
Ru	5	4.7 ± 0.5	3.7 ± 0.4
Rh	<1	0.1 ± 0.0	0.1 ± 0.0
Pd	<1	-	0.3 ± 0.0
Ag	<1	0.3 ± 0.1	-
Pt	1	-	0.7 ± 0.0
Au	<1	0.2 ± 0.0	0.1 ± 0.0

to give better quality results compared with those obtained using the added internal standard. This would seem to indicate that the addition of an element to the solution does not act in the same way as the analytes in the slurry and consequently the iridium standards may also be expected to vary in the same way.

Using the instrument in extended dynamic range mode, in order to protect the detector, the total counts for both iridium isotopes in the iridium solutions were compared with the counts obtained for the slurries. This study showed that the two samples gave very similar totals and therefore it can be concluded that the solution and the slurry (0.1%) have a similar effect on the plasma. However, the introduction of more concentrated slurries (0.2% m/V) had a detrimental effect on the plasma. The correlations obtained for the solutions was poor and there was evidence of cone blockage caused by the iridium condensing on the sampling cone. The results obtained were therefore unsatisfactory with large standard deviations.

The results obtained for Ir961 are shown in Table 7.3.2.2. The internal standard used for this work was $IrAr^+$. The results for this sample appear to be slightly worse than those obtained with the previous sample. There is poor accuracy for magnesium, iron and zinc as well as copper and platinum. The iron, magnesium and zinc suffer from interferences on the peaks analysed, although these

TABLE 7.3.2.2 RESULTS OBTAINED FOR THE ANALYSIS OF IRIDIUM SAMPLE IR961 BY SLURRY ATOMISATION-ICP-MS

Analyte	Indicative Values	Obtained
Mg	<1	2.1 ± 0.6
Al	<1	1.7 ± 0.2
Ti	<1	1.3 ± 0.1
V	2	1.4 ± 0.2
Cr	<1	0.9 ± 0.1
Mn	1	0.8 ± 0.0
Fe	10	8.2 ± 0.2
Ni	<1	0.3 ± 0.0
Cu	<1	0.3 ± 0.0
Zn	10	8.3 ± 0.5
Ru	70	79.2 ± 6.6
Rh	300	276.0 ± 7.6
Pd	<1	0.9 ± 0.4
Ag	<1	0.5 ± 0.1
Pt	<1	1.0 ± 0.1
Au	-	0.2 ± 0.1

interferences should also apply to the standard solution.

It is clear therefore that samples of iridium metal which are ground so that the majority of particles are < 4 μm will give reasonable agreement with indicated values. Consequently the technique of slurry atomisation is feasible for the analysis of trace metals contaminants in iridium and may give reasonable results with good precision.

This is particularly true when an intrinsic internal standard is used rather than an internal standard that is added. The detrimental effects on the plasma with the addition of a metal in this form, means that standards must be matrix matched, and thus negates some of the advantages of slurry atomisation. The long grinding times required to produce the small slurry particles are also a disadvantage.

7.4.3 **Palladium**

7.4.3.1 Experimental

Samples of palladium metal powder were ground by the bottle and bead technique (68), for various times (1, 2, 3 and 4 hours) to produce slurries with different particle size distributions. The slurries were then made up in volumetric flasks to produce 0.1 % m/v slurries. The dispersants used in this study was Triton X-100 (1% v/v).

The slurries were analysed by ICP-MS and the result compared with those obtained after dissolution of the palladium metal. This dissolution procedure involved the addition of the palladium sample (0.1 g) to a microwave bomb to which was also added concentrated nitric acid (5 ml) and hydrofluoric acid (1 ml). The samples were heated at 70 W for ten minutes, and then 140 W for 5 minutes. The bombs were then cooled and the pressure released. The hydrofluoric acid was removed by evaporation using a laboratory flask heater. The dissolved palladium was then washed into a volumetric flask using one of the dispersants and made up to the mark.

The palladium sample used was a palladium standard prepared in house by Johnson Matthey PLC, by the addition of 100 $\mu g\ g^{-1}$ standards in chloride solutions to the palladium metal sponge. The standards were then evaporated to dryness at 110^{o}C before being milled for

sixteen hours using a platinum ball mill. This was followed by stirring and homogenisation for sixteen hours. The standards were then reduced under 10% v/v hydrogen in nitrogen for two hours. They were finally treated at 500 ^{o}C for three hours to remove the chloride and milled for a further sixteen hours in the platinum ball mill.

The standards were analysed in three different laboratories, using ICP-AES after dissolution. The results obtained for the platinum impurities in the palladium sponge is significantly higher than that added to the sponge, due to the effects of the platinum balls in the milling process.

The desolvation device, described in chapter 3, was used to obtain dry slurries.

7.4.3.2 Results and Discussion

The particle size distributions obtained for each of the various grinding times are shown graphically in Figure 7.4.3.1.

Each of the palladium slurries were analysed by ICP-MS and the results obtained compared with those obtained for the dissolved palladium. In each case the dissolved palladium results were considered to represent one hundred per cent recovery and so the slurry results are therefore compared to this figure. The slurries were analysed by two distinct methods, the first involving direct nebulisation into the plasma and secondly after desolvation of the sample. The minor palladium isotope (m/z = 102) was used as an internal standard for this work.

The results for these two methods are compared in Figures 7.4.3.2 - 7.4.3.8 and it can be seen that significantly better recoveries are obtained for the desolvated samples when compared with the non-desolvated samples. This appears to be due to both an increase in the transport and the atomisation efficiencies, caused by the spatial charge effects in the plasma. Since no energy was required to desolvate the particle prior to atomisation. The palladium sample was considered homogeneous, therefore the pattern should remain constant for each of the trace analytes investigated. This is broadly supported by the

FIG 7.4.3: PARTICLE SIZE DISTRIBUTION FOR PALLADIUM

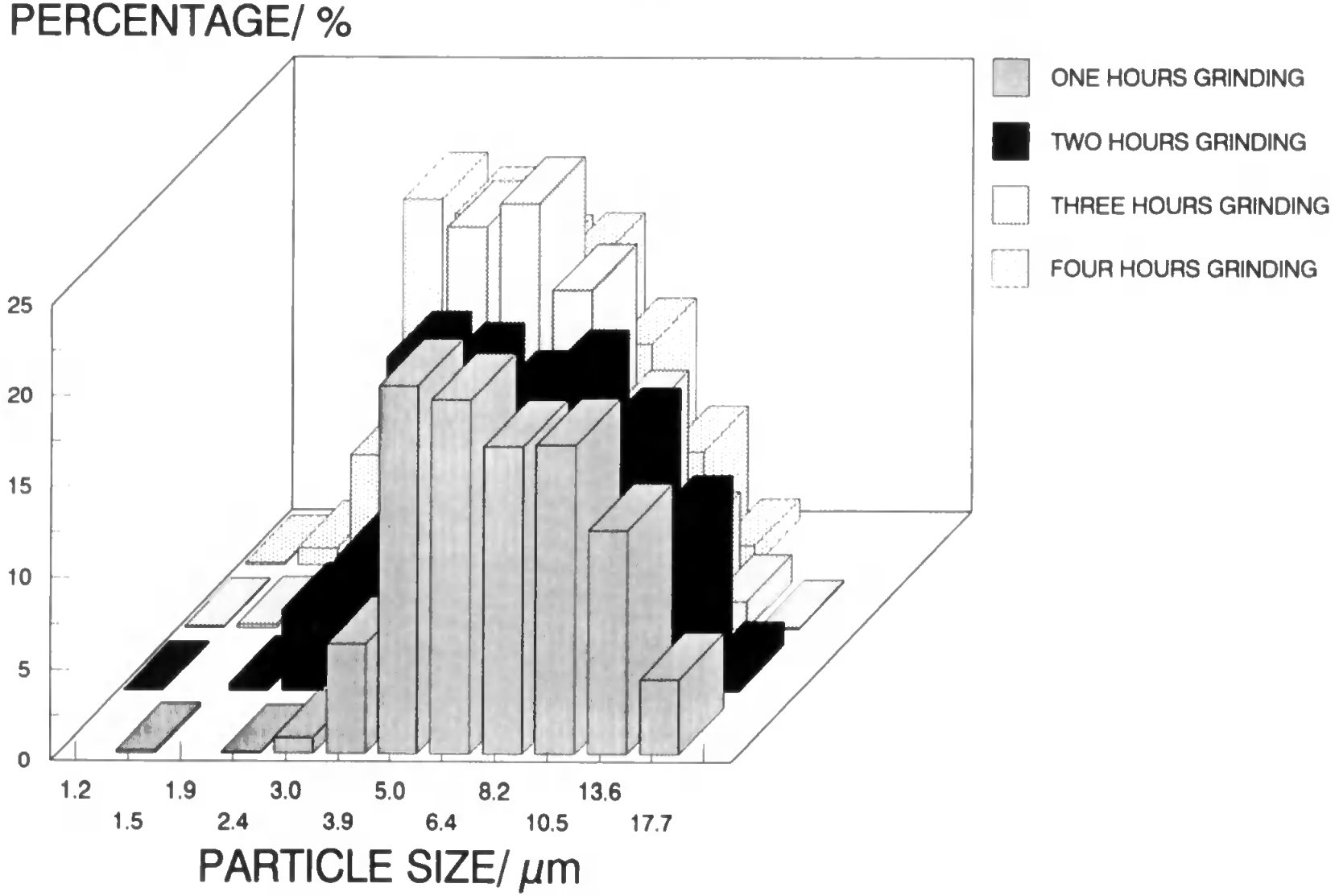

FIG 7.4.3.1: MAGNESIUM RECOVERY WITH AND WITHOUT DESOLVATION PALLADIUM SAMPLE

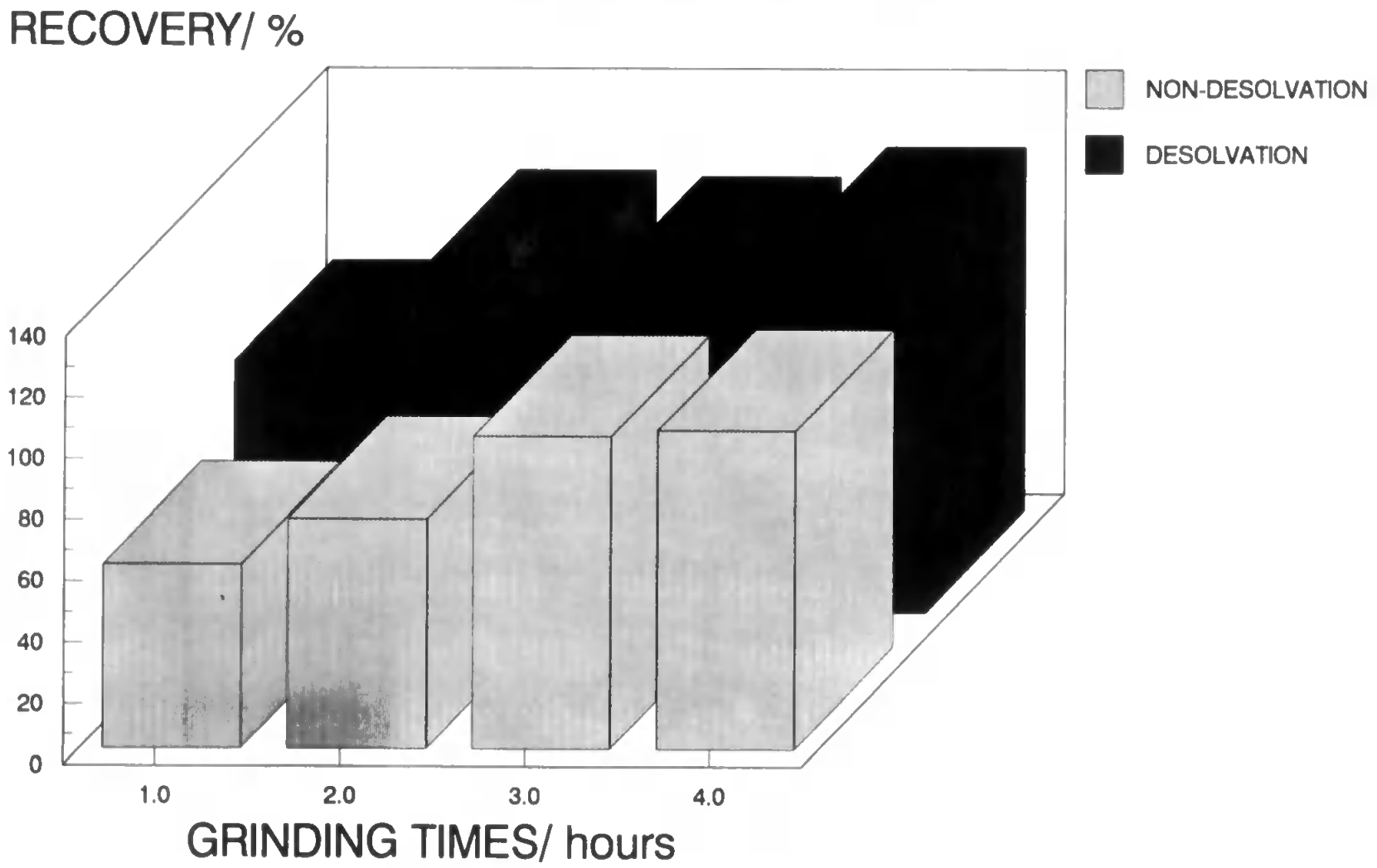

FIG 7.4.3.2: NICKEL RECOVERY WITH AND WITHOUT DESOLVATION PALLADIUM SAMPLE

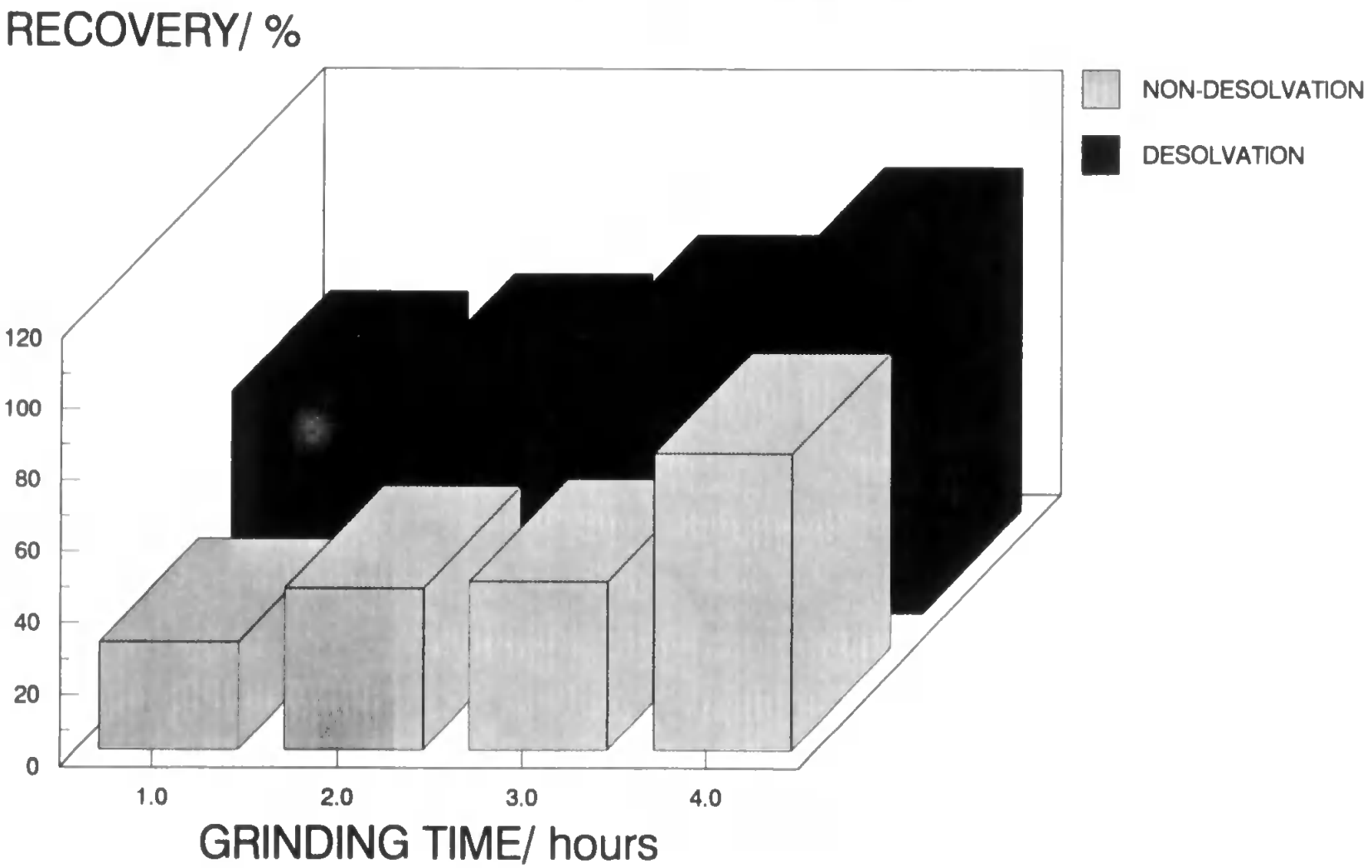

FIG 7.4.3.3: COBALT RECOVERY WITH AND WITHOUT DESOLVATION PALLADIUM SAMPLE

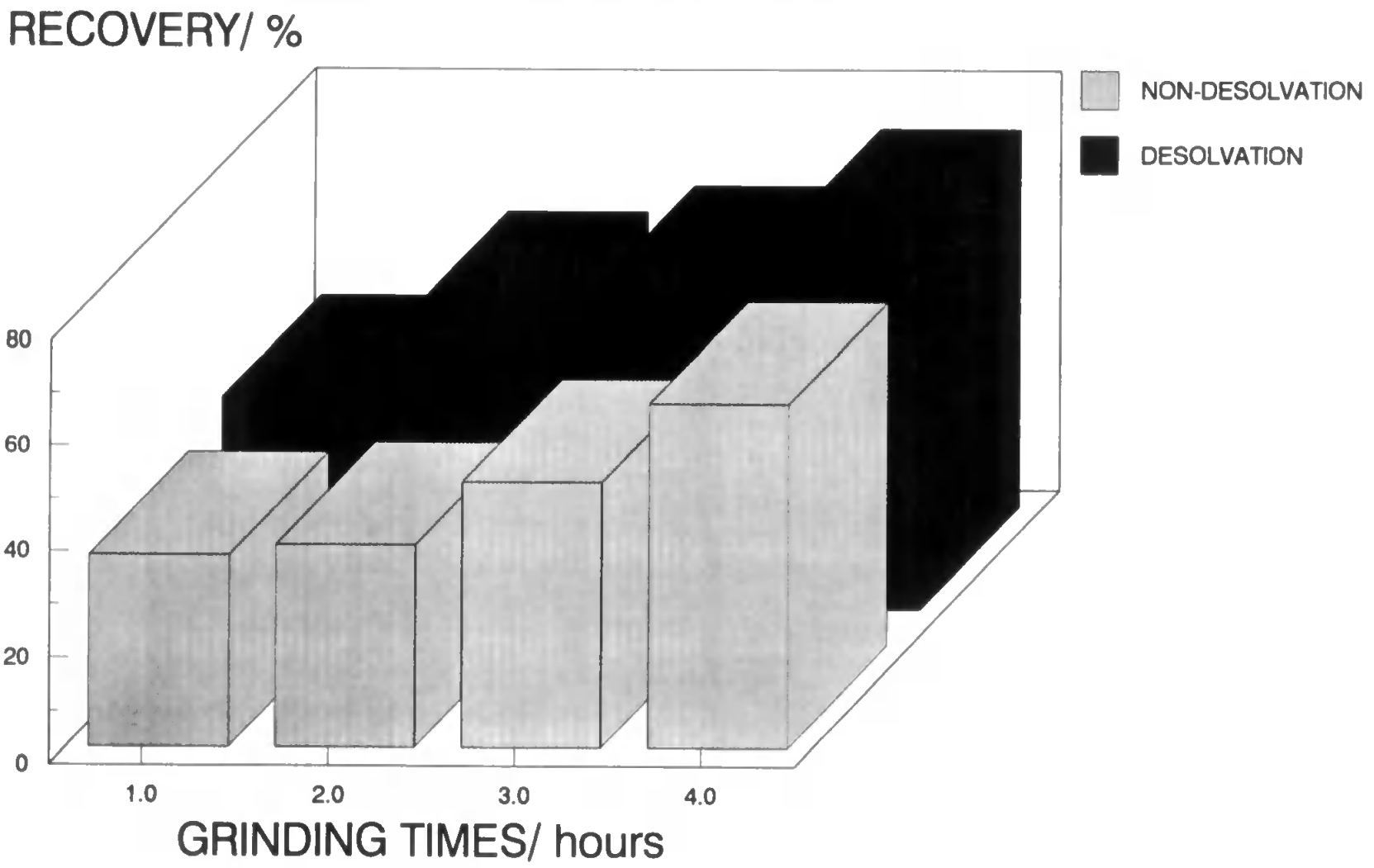

FIG 7.4.3.4: COPPER RECOVERY WITH AND WITHOUT DESOLVATION PALLADIUM SAMPLE

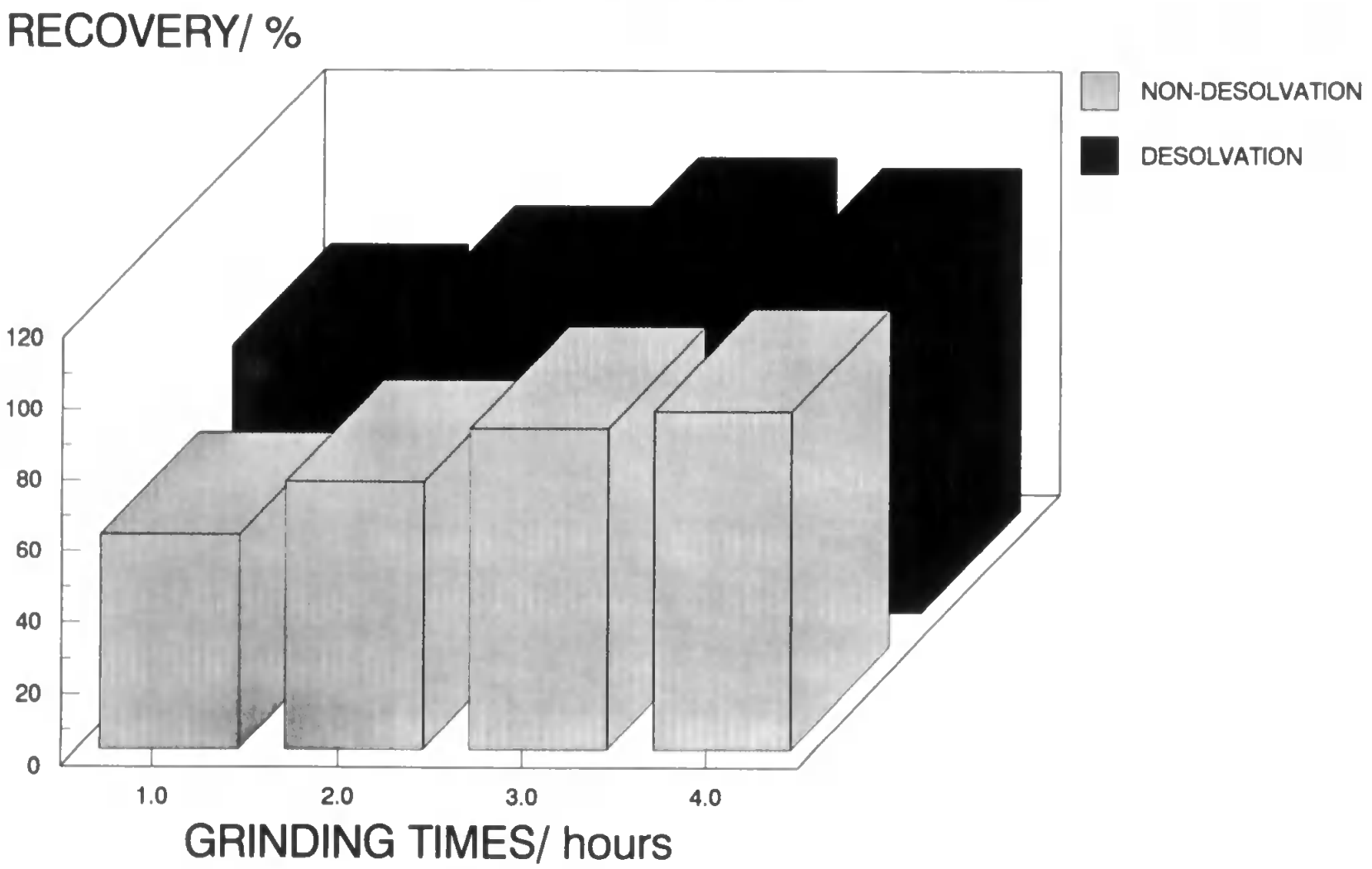

FIG 7.4.3.5: ZINC RECOVERY WITH AND WITHOUT DESOLVATION PALLADIUM SAMPLE

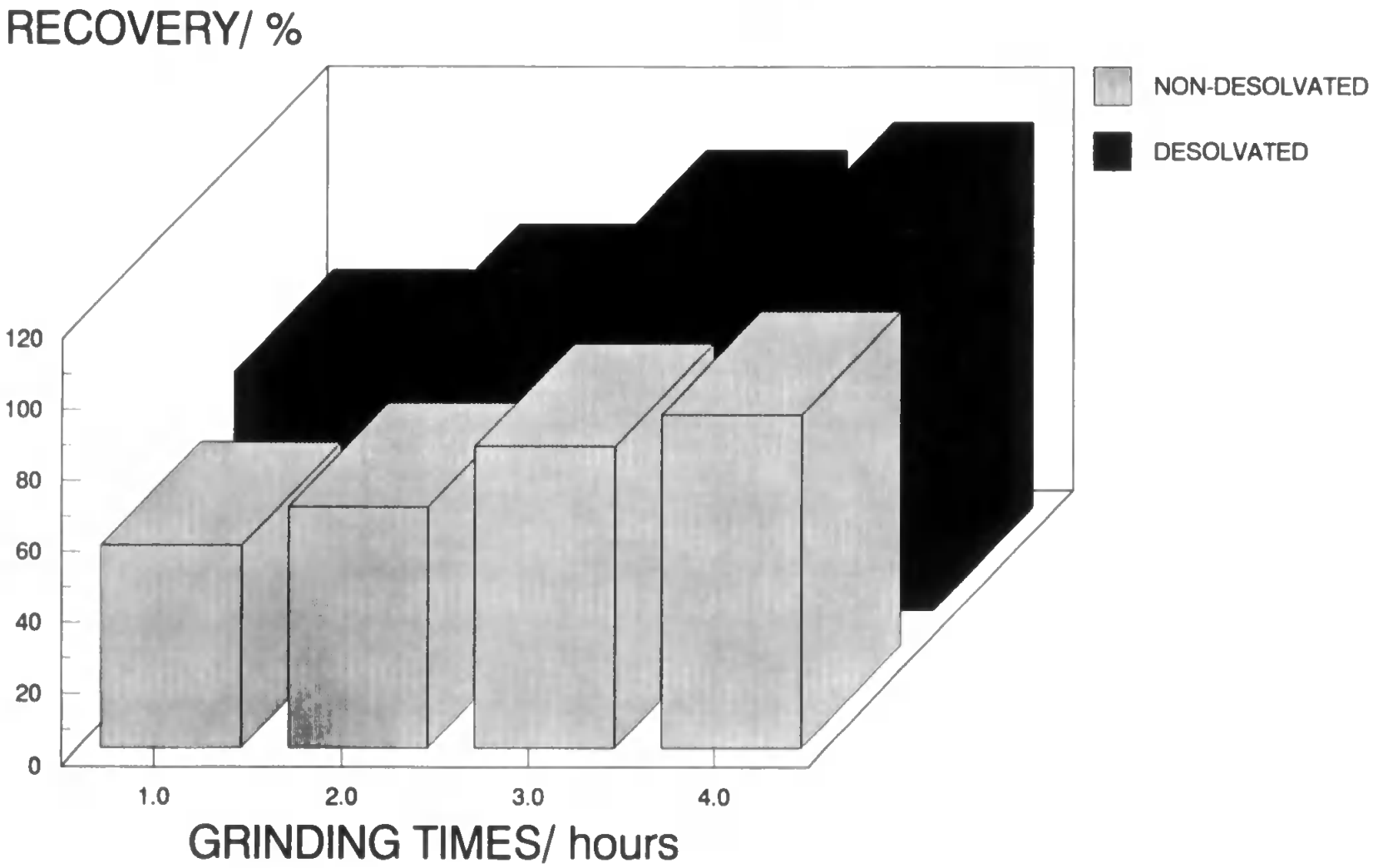

FIG 7.4.3.6: ANTIMONY RECOVERY WITH AND WITHOUT DESOLVATION PALLADIUM SAMPLE

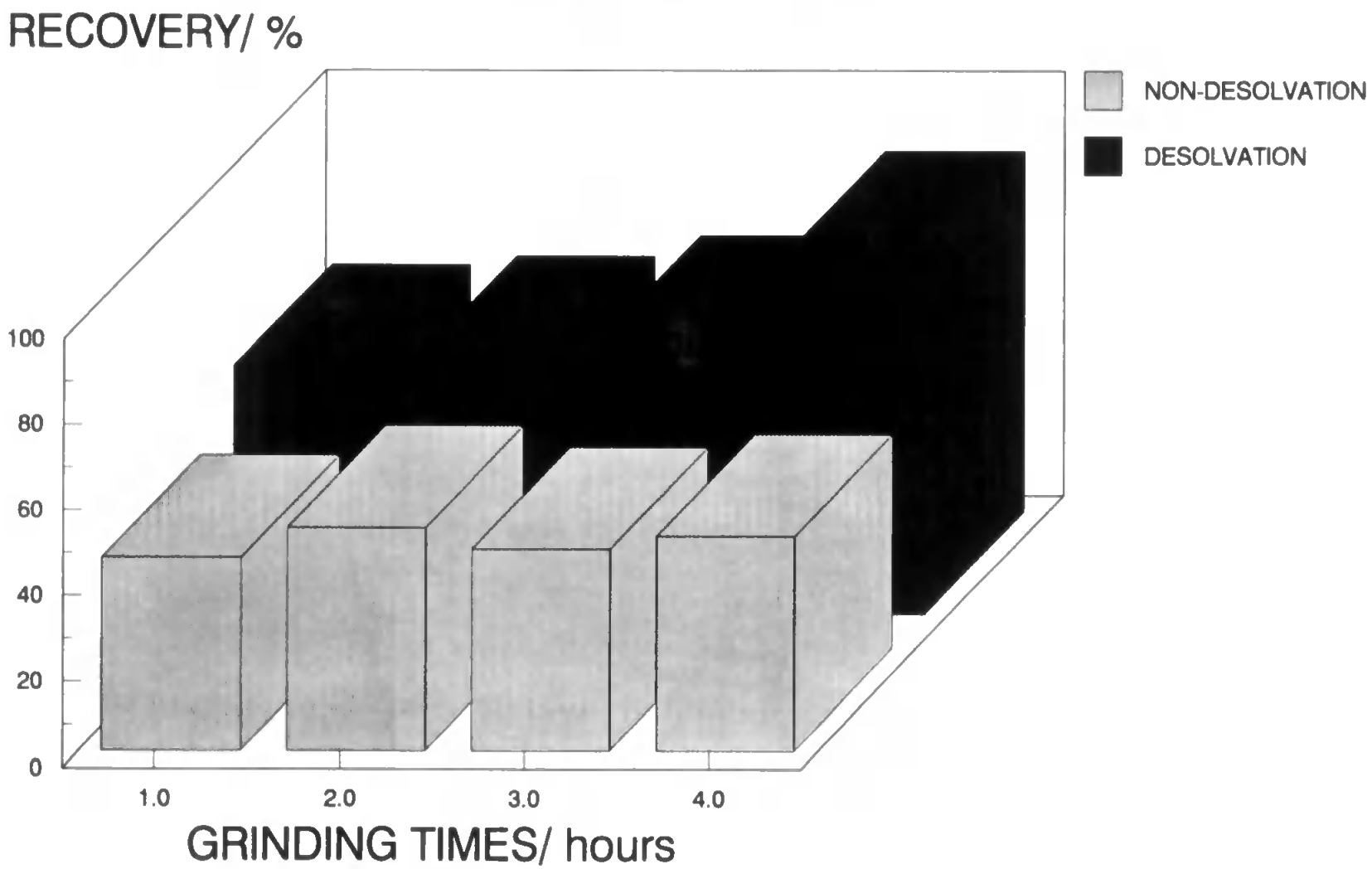

FIG 7.4.3.7: GOLD RECOVERY WITH AND WITHOUT DESOLVATION PALLADIUM SAMPLE

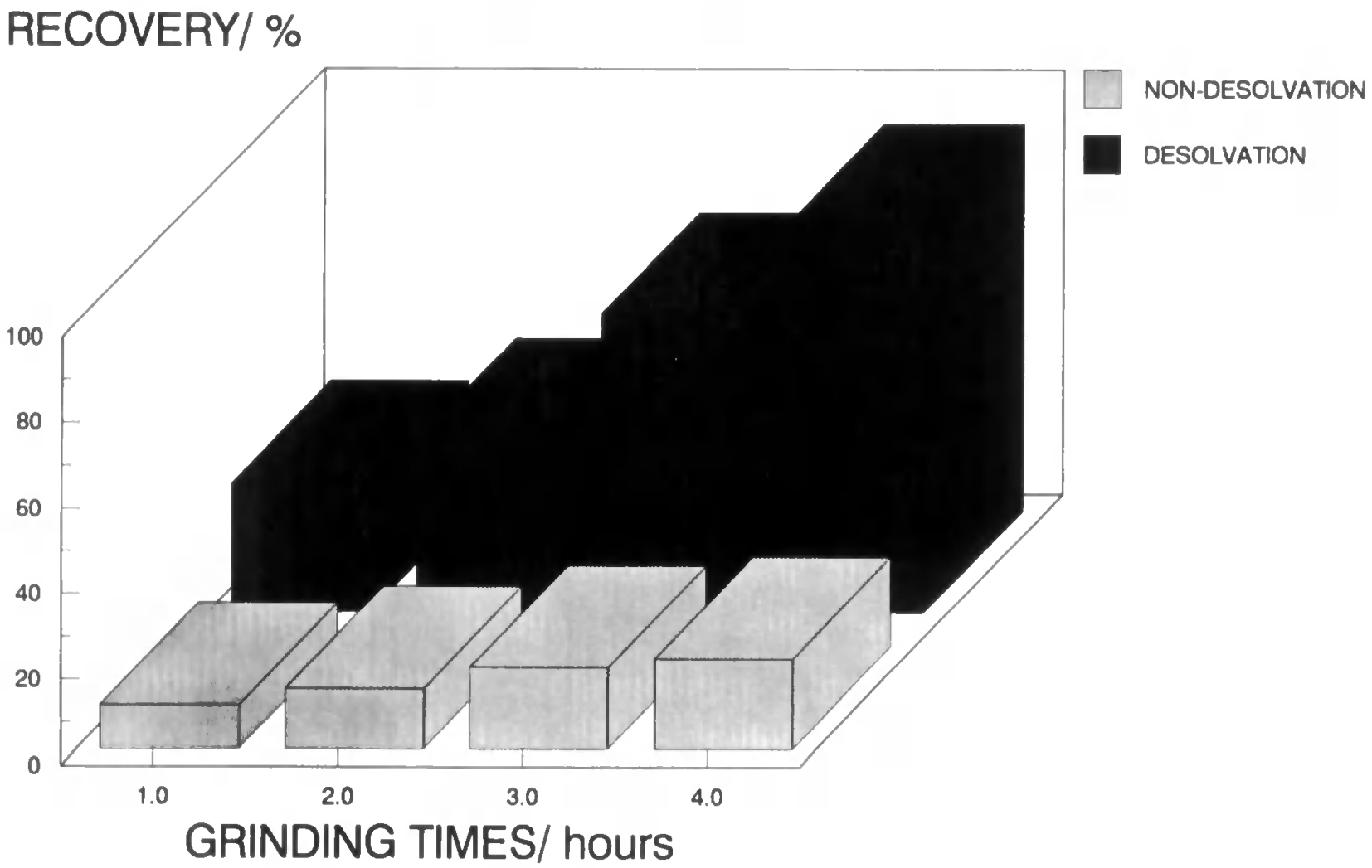

FIG 7.4.3.8: BISMUTH RECOVERY WITH AND WITHOUT DESOLVATION PALLADIUM SAMPLE

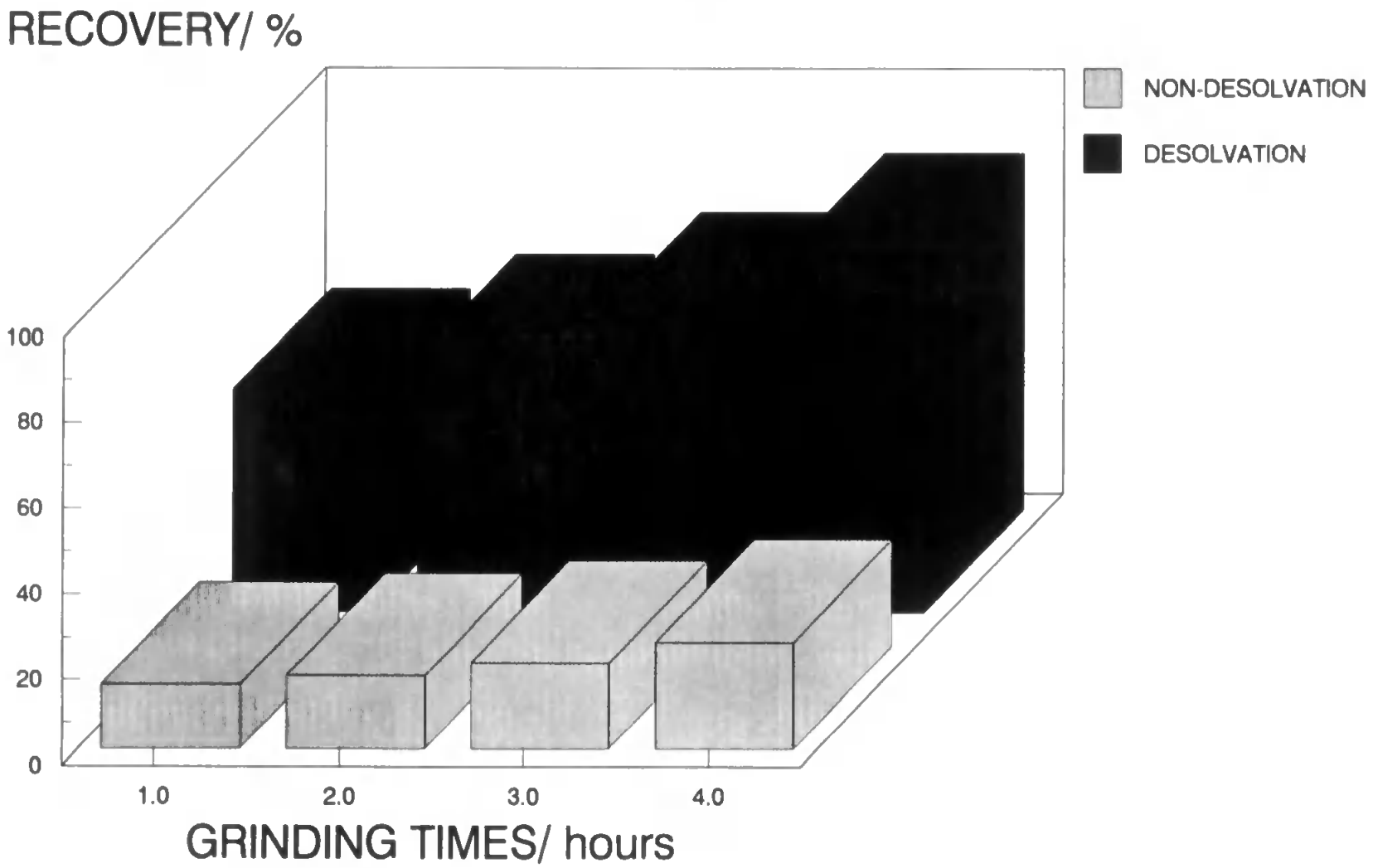

experimental work. Figures 7.4.3.2 to 7.4.3.8. do not show the standard deviations of the results, which were normally in the range three to six per cent.

If the graphs in Figures 7.3.3.2 to 7.3.3.8 are compared with the particle size results Figure 7.4.3.1 it can be seen that when the slurries are desolvated, particles of about 10 μm can be both transported to, and atomised by the plasma. This compares with a figure of about 5 μm for the non-desolvated slurry. This ability to both transport and atomise slurry particles which are far larger than those introduced without desolvation enables the grinding times in slurry preparation to be significantly decreased without a detrimental effect on the analytical performance.

The effect of the dispersant, particularly for the desolvated samples appears to be small. This observation was checked using the statistical f-test (96). This test showed that for the desolvated results there was a greater than ninety five per cent chance of the results being similar; although there was less certainty in the case of the non-desolvated sample which had a less than ninety per cent chance of being the same. The difference between these results probably reflects the large amount of dispersant which is removed by the desolvation procedure.

7.4 OVERALL CONCLUSIONS

The results for the analysis of both iridium and palladium show that the use of slurry atomisation as a method of introducing powdered metals into the ICP-MS is feasible. The technique does however require the grinding of the samples into a suitable particle size range, which may take a considerable period of time and thus negate some of the advantages associated with this technique. The use of desolvation prior to the introduction of slurries into the ICP-MS greatly increases the transport efficiency associated with the technique, enabling larger particles to reach the plasma. Once such particles reach the plasma they appear to be totally atomised and ionised. The removal of the aqueous coating surrounding the particles prior to analysis also means that less plasma energy is required in this desolvation process. This in turn enables larger particles to be fully analysed and thus enable reduced grinding times to be used.

CHAPTER 8

ANALYSIS OF PRECIOUS GROUP METALS BY LASER ABLATION

8.1 Introduction

The analysis of the platinum group metals (PGM's) is complicated by the difficulty involved in bringing them into solution. The dissolution procedures for these elements are often time-consuming and involve the use of hazardous and often expensive chemicals. In addition, there is also the possibility of loss of volatile analytes and the introduction of contamination.

Consequently a method which does not involve a long sample pretreatment step has a number of advantages for routine analysis of such samples. One such technique is the use of a laser to ablate material from the solid sample. The ablated material is carried to the ICP-MS in an argon carrier stream where the sample is ionised and subsequently analysed. The major problem associated with the technique of laser ablation - inductively coupled plasma - mass spectrometry (LA-ICP-MS), is associated with the precision, which is often poor due to the varying amounts of sample ablated (82,83). The problem is made worse by the difficulty in obtaining good matrix matched standards, especially if an isotope of the main matrix element is required as a true internal standard (84). The use of "true" internal standards helps to negate some of the problems associated with cone blockage caused by the

ablated solid.

8.2 **Experimental**

8.2.1 Instrumentation

The inductively coupled plasma - mass spectrometer used was a PlasmaQuad II + (VG Elemental, Wilton, Cheshire, U.K.) equipped with a VG Laserlab. The Laserlab, utilised a Nd:YAG laser operating at 1064 nm. It was capable of running in either fixed-Q or Q-switched mode with a repetition rate of up to 14 Hz. A standard VG sampling chamber was used and the ablated material was carried to the plasma using a 4 mm i.d. poly(vinyl)chloride tube. A 2 way 3-port valve enabled the cell to be purged with argon prior to sample changing.

8.2.2 Standards

The standards for this work were prepared in-house by the addition of 100 $\mu g\ g^{-1}$ of standard chloride solutions to the precious group metal sponges, followed by evaporation to dryness at 110^{o}C before being milled for sixteen hours using a platinum ball mill. This was followed by stirring and homogenisation for sixteen hours. The standards were then reduced under 10% v/v hydrogen in nitrogen for two hours, and then treated at 500^{o}C for three hours to remove the chloride. Finally the standards were milled for a further sixteen hours in the platinum ball mill.

The standards were analysed in three different laboratories, using inductively coupled plasma - atomic emission spectrometry, following dissolution. The result obtained for the platinum is significantly higher than that added to the sponge, due to the effects of the platinum cylinders used in the milling process.

8.2.3 Sample Preparation

All of the standard and sample discs were prepared using an evacuated KBr disc press (13 mm i.d.). The sponge (2g) was weighed out and added to the press and put under a pressure of two tonnes for five minutes followed by a pressure of ten tonnes for a further five minutes.

8.2.4 Sample Dissolution

To make a full comparison of the results obtained by the laser ablation - inductively coupled plasma - mass spectrometry samples of the sponges were dissolved, prior to analysis by ICP-MS.

8.2.4.1 Palladium

A sample of the sponge (0.1 g) was carefully weighed into a microwave bomb and concentrated nitric acid was added (10 ml, Aristar BDH, Dorset, U.K.). The bombs were placed in a microwave oven (CEM Microwave Technology Limited, Buckingham, U.K.) and microwaved for ten minutes at a pressure of 200 psi. The dissolved metal was washed into volumetric flasks and made up to 100 ml with 18 MΩ distilled water.

8.2.4.2 Rhodium

A sample of gold metal (3 g, 99.99% pure, Johnson Matthey, Royston, Hertfordshire, U.K.) was placed in a beaker and heated with a mixture of concentrated nitric acid and concentrated hydrochloric acid (2:1, 20 ml, Aristar BDH, Dorset, U.K.) and made up with 18 MΩ water (40 ml). This was placed on a hot plate at a temperature of 120°C until all the gold had dissolved. The sample was evaporated down to the point where gold started to precipitate out. Hydrochloric acid (1:1) was added to redissolve the gold and the sample again evaporated down. This procedure was repeated four times. The gold chloride produced by this method was made up to produce a 3% solution.

A sample of this 3% solution (0.1 g, of gold, 3.33 ml) was placed in a beaker and the rhodium sponge added (0.1 g) along with concentrated hydrochloric acid (10 ml). The

beaker was placed on a hot plate (150^{o}C), covered with a watch glass, and left for four hours. The liquid was then carefully decanted into a volumetric flask, leaving the gold and unreacted rhodium. This unreacted rhodium was reacted with more gold chloride (0.03 g, 1 ml) and concentrated hydrochloric acid (10 ml) and left for a further four hours. At this point all of the rhodium had reacted and the solution was transferred to the volumetric flasks after filtering to remove the gold precipitate.

8.2.5 Operating Conditions

The operating conditions are shown in Table 8.1. The ion lenses were optimised for the determination of silver (m/z 107) in the Q-switched mode operating at 4 Hz.
The results obtained in the Q-switched mode are for samples preablated for three minutes.

TABLE 8.1 OPERATING CONDITIONS

ICP Conditions:-

Coolant gas flow	14.0 l min^{-1}
Auxiliary gas flow	0.8 l min^{-1}
Nebuliser gas flow	0.83 l min^{-1}
Forward power	1.6 kW

Mass Spectrometer Conditions:-

Mass range	2-245 m/z
Dwell time	80 μs
Number of channels	2048
Number of scans	400

Laser Ablation Conditions:-

Voltage	775 V
Number of irradiation	
Fixed-Q pulse mode	10 shots
Q-switched pulse mode	4 Hz for 1 minute

8.3 Results and Discussion

8.3.1 Analysis of Rhodium

Optimisation of the plasma and laser operating conditions was achieved using univariate searches keeping the other parameters constant. The major factors affecting the sensitivity were the forward power, nebuliser gas flow and the laser voltage which is related to the laser power. Three elements were used in the univariate searches; cobalt (m/z 59), platinum (m/z 198) and lead (m/z 208). Three other masses were also used; the doubly charged rhodium peak (m/z 51.5), the rhodium argide peak (m/z 143) and the background (m/z 113).

The results obtained for the univariate search on the forward power are shown in Figure 8.1. There is a clear increase in the response as the power increases from 1.2 kW to 1.6 kW, followed by a slight decrease above this point. There was also an increase in the ions detected which continued to increase up to 1.8 kW; there was no noticeable increase in the background signal. Work on the introduction of desolvated slurries (see Chapter 9.) showed that there is a decrease in the electron number density when using a dry plasma caused largely by the removal of the hydrogen. By increasing the forward power the temperature of the plasma increases and this should improve the ionisation efficiency of the plasma and hence the response. This previous work also indicated that the

FIG 8.1: EFFECT OF FORWARD POWER ON RESPONSE ANALYSIS OF RHODIUM

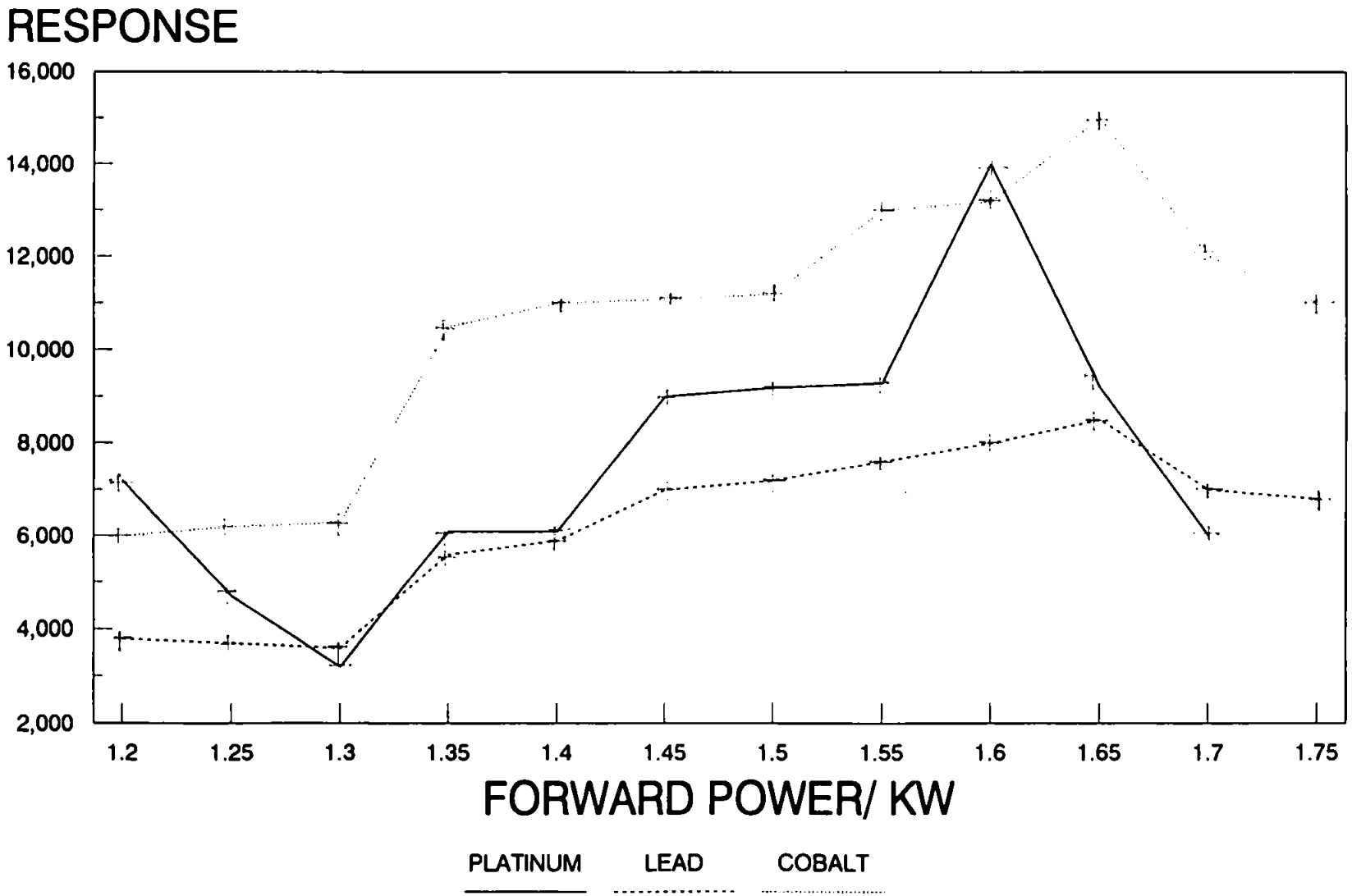

increase in forward power increases the formation of other species, and thus supports these findings.

The nebuliser gas flow, shown in Figure 8.2 affects the residence time in the plasma and hence the ionisation efficiency. Consequently this parameter proves to be critical in the optimisation of the instrument. The results indicate that there is little difference between the results obtained and those expected for the introduction of aqueous samples. This non-divergence may be due to the nature of the ablated material which enters the plasma or the effect caused by the requirement to nebulise the aqueous sample.

The laser voltage will affect the amount of material ablated and so if increased will cause an increase in the instrument response. This can be clearly seen in Figure 8.3 which shows a sharp increase in the signal between 650 and 750 volts, where a plateau appears to be reached, indicating that there is a maximum in the amount of material that can be ablated or successfully introduced to the plasma. The results obtained for the high voltages also showed an increase in the standard deviations obtained, indicating that the power coupling is such that inconsistent amounts of sample are being ablated. Consequently, a setting of 775 volts was used for the rest of the study which enabled most of the possible material to be ablated without an increase in the standard deviation.

FIG 8.2: EFFECT OF NEBULISER GAS ON RESPONSE ANALYSIS OF RHODIUM

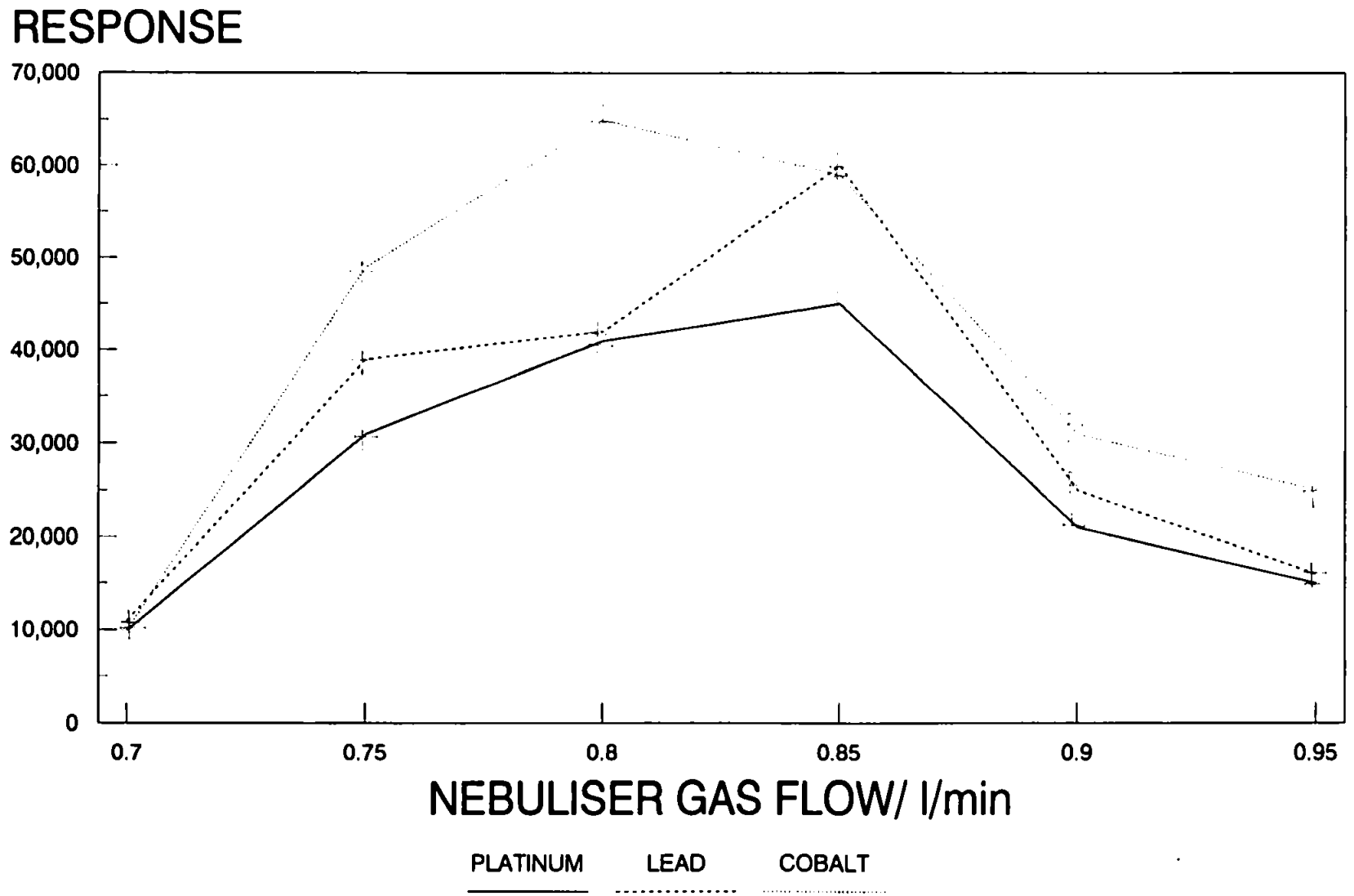

FIG 8.3: EFFECT OF LASER VOLTAGE ON RESPONSE ANALYSIS OF RHODIUM

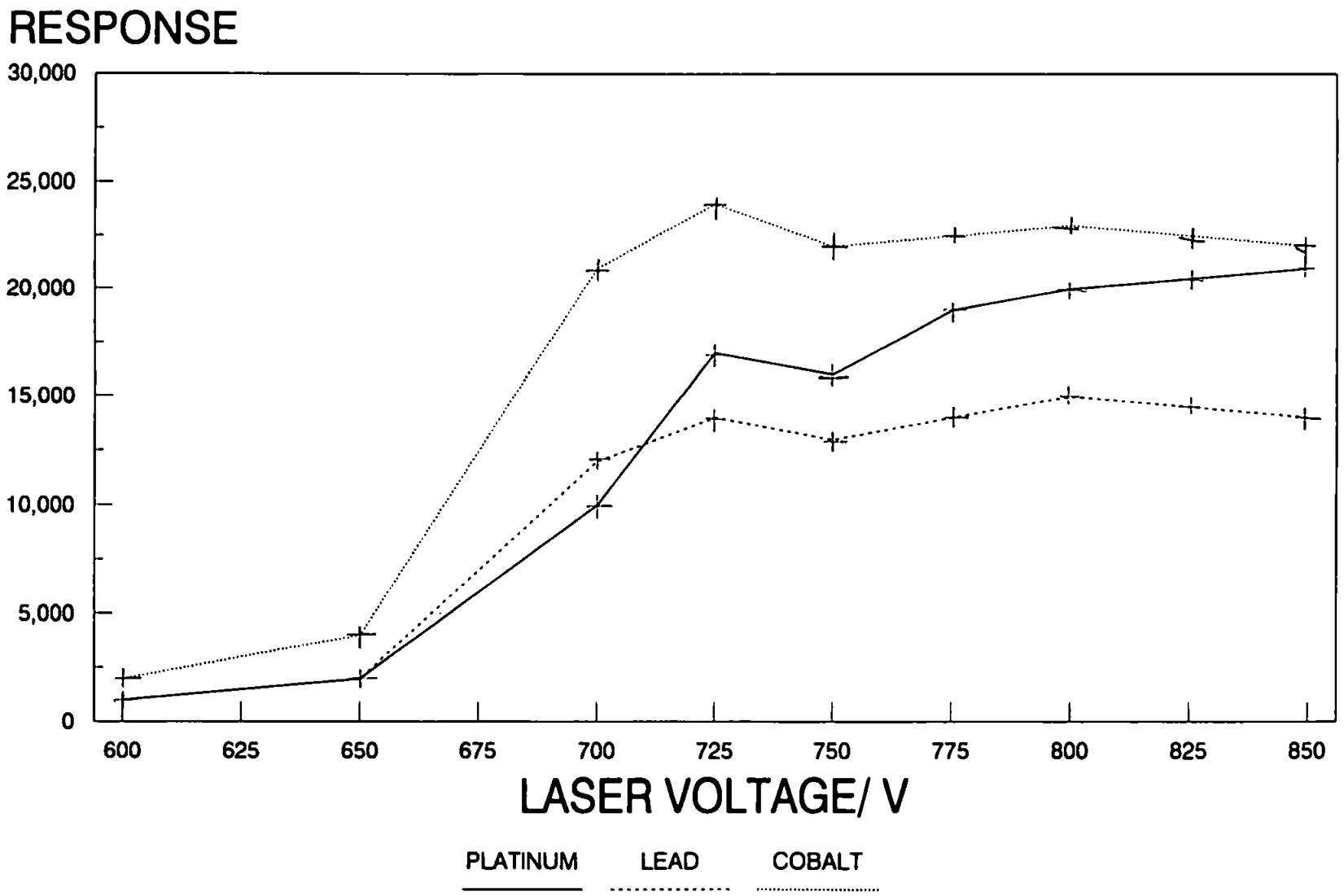

In the fixed-Q mode of operating the laser beam was focussed on the surface of the samples. However in the Q-switched mode of operation the coupling of the laser beam with the conducting metal will greatly affect the results obtained and this coupling will be affected by the focussing of the laser. The effects on both the accuracy and precision caused by the amount of defocussing are shown in Figures 8.4 - 8.9 for one of the rhodium samples. The results are compared with those obtained for the same sample after dissolution. The distinction is made that negative defocussing is used when the laser is focussed below the surface of the sample and positive defocussing when the laser is focussed above the surface.

The effects of focussing the laser on the surface of the sample is clearly detrimental to the results obtained, and give a very large standard deviation. The coupling of the laser and the sample, with a large amount of energy focussed on a very small area causes a large variation in the amount of material ablated. By defocussing the laser the power is dissipated over a larger area which causes a decrease in the total amount of material ablated, although the amount ablated is more consistent. Consequently a compromise between an improvement in the standard deviation and the total amount of material ablated is required. The value used for the rest of the experimentation was -10 mm.

FIG 8.4: EFFECT OF FOCUSSING IN Q-SWITCH MODE DETERMINATION OF MAGNESIUM IN RHODIUM

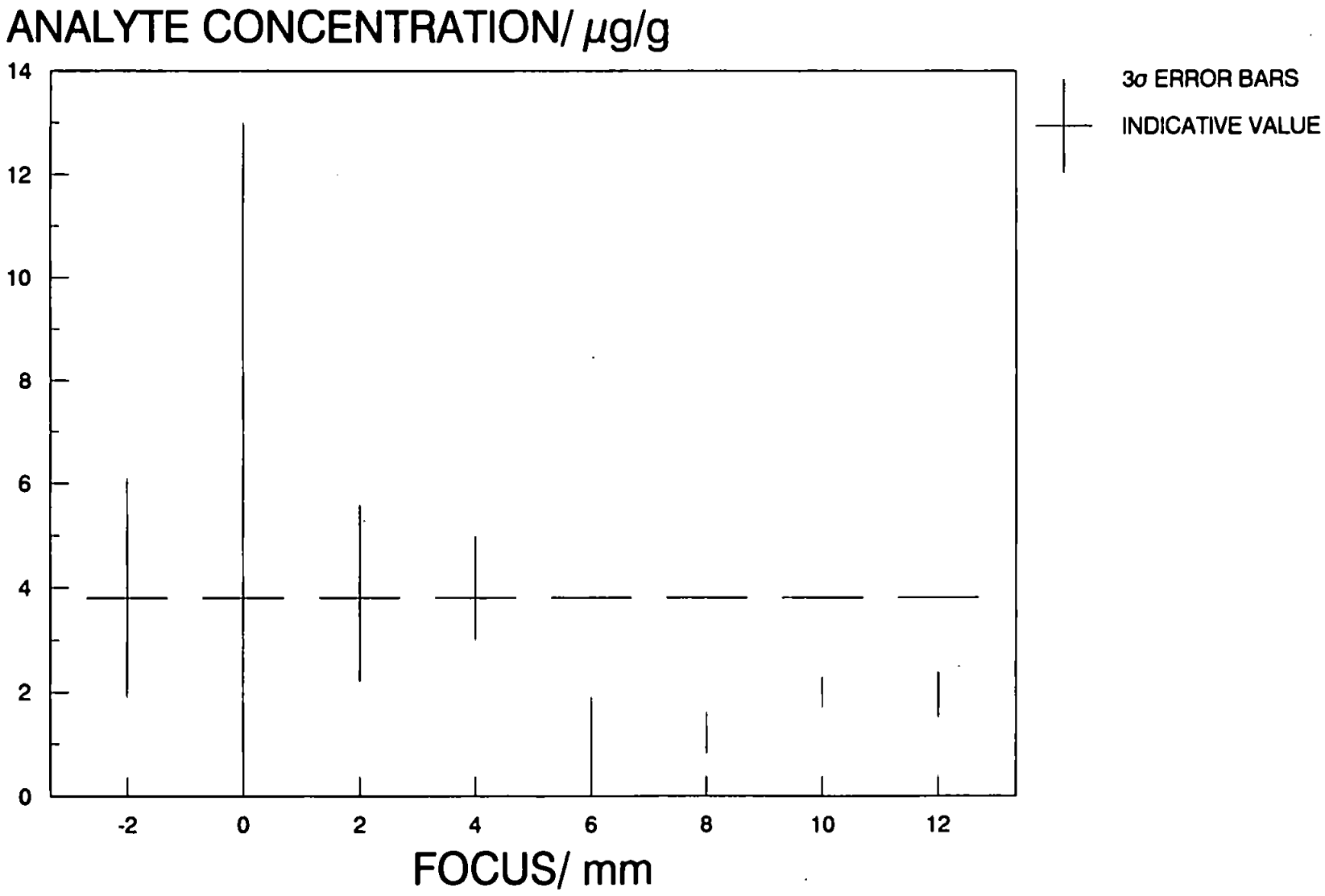

FIG 8.5: EFFECT OF FOCUSSING IN Q-SWITCH MODE DETERMINATION OF IRON IN RHODIUM

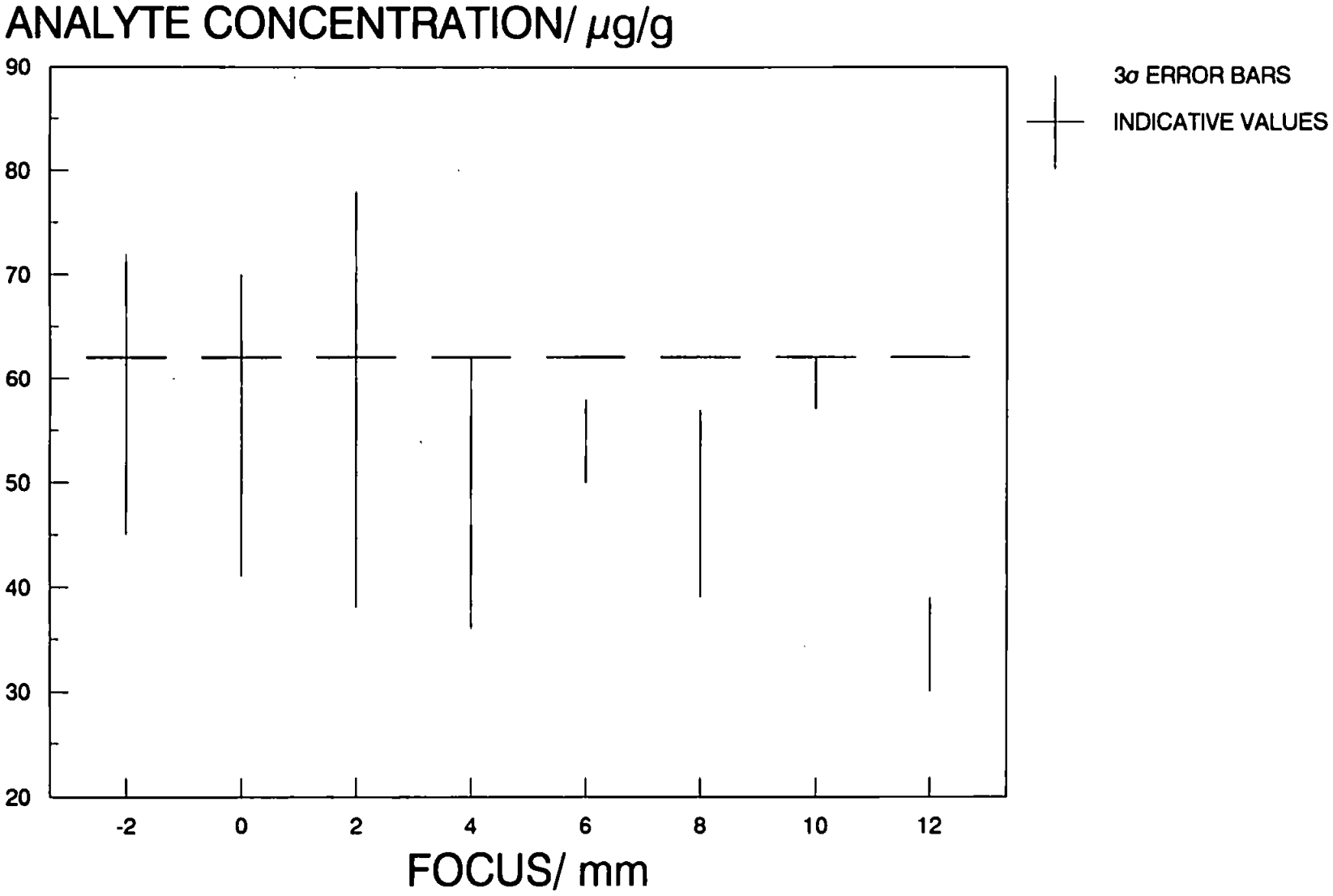

FIG 8.3: EFFECT OF FOCUSSING IN Q-SWITCH MODE DETERMINATION OF NICKEL IN RHODIUM

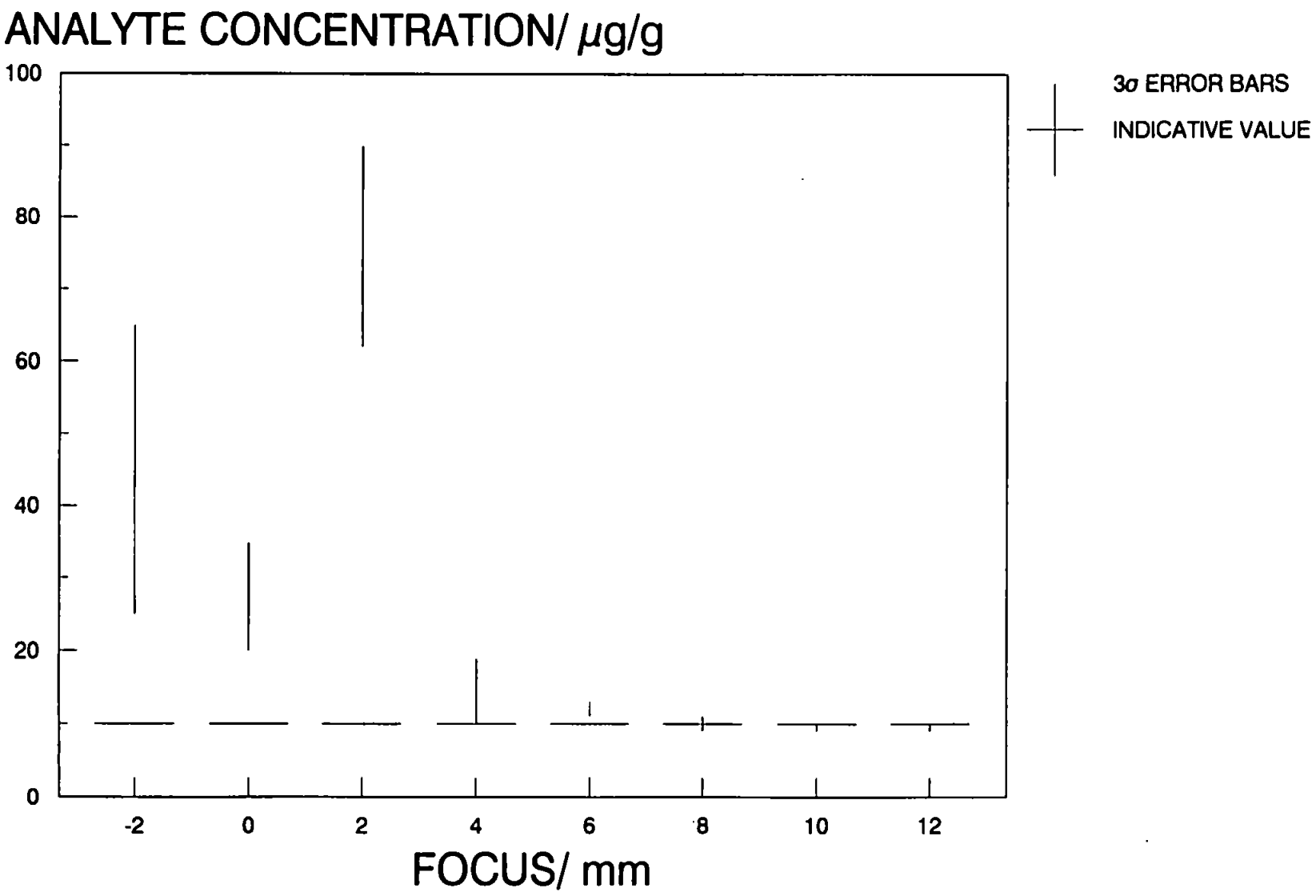

FIG 8.7: EFFECT OF DEFOCUSSING IN Q-SWITCH MODE DETERMINATION OF RUTHENIUM IN RHODIUM

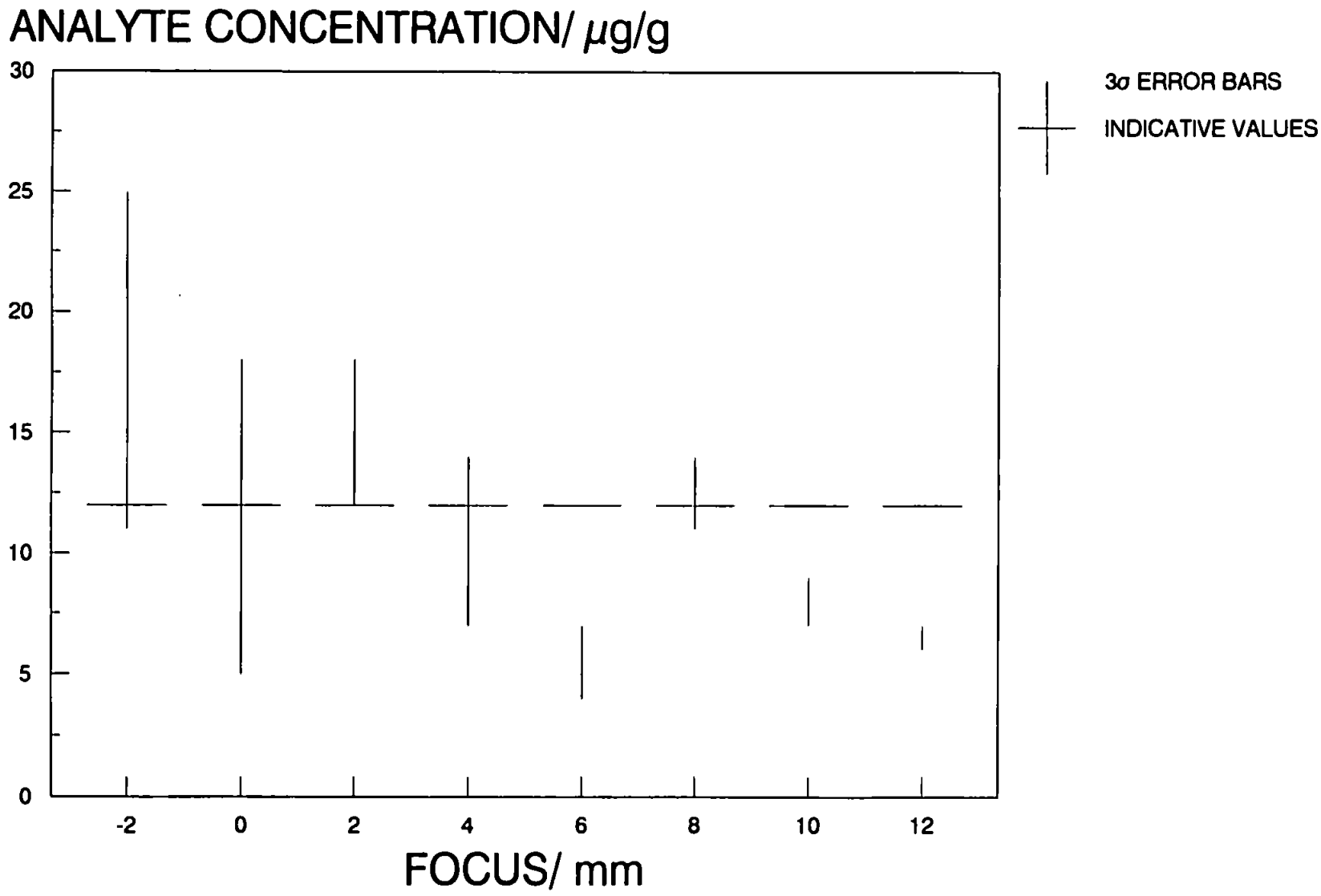

FIG 8.8: EFFECT OF FOCUSSING IN Q-SWITCH MODE DETERMINATION OF PALLADIUM IN RHODIUM

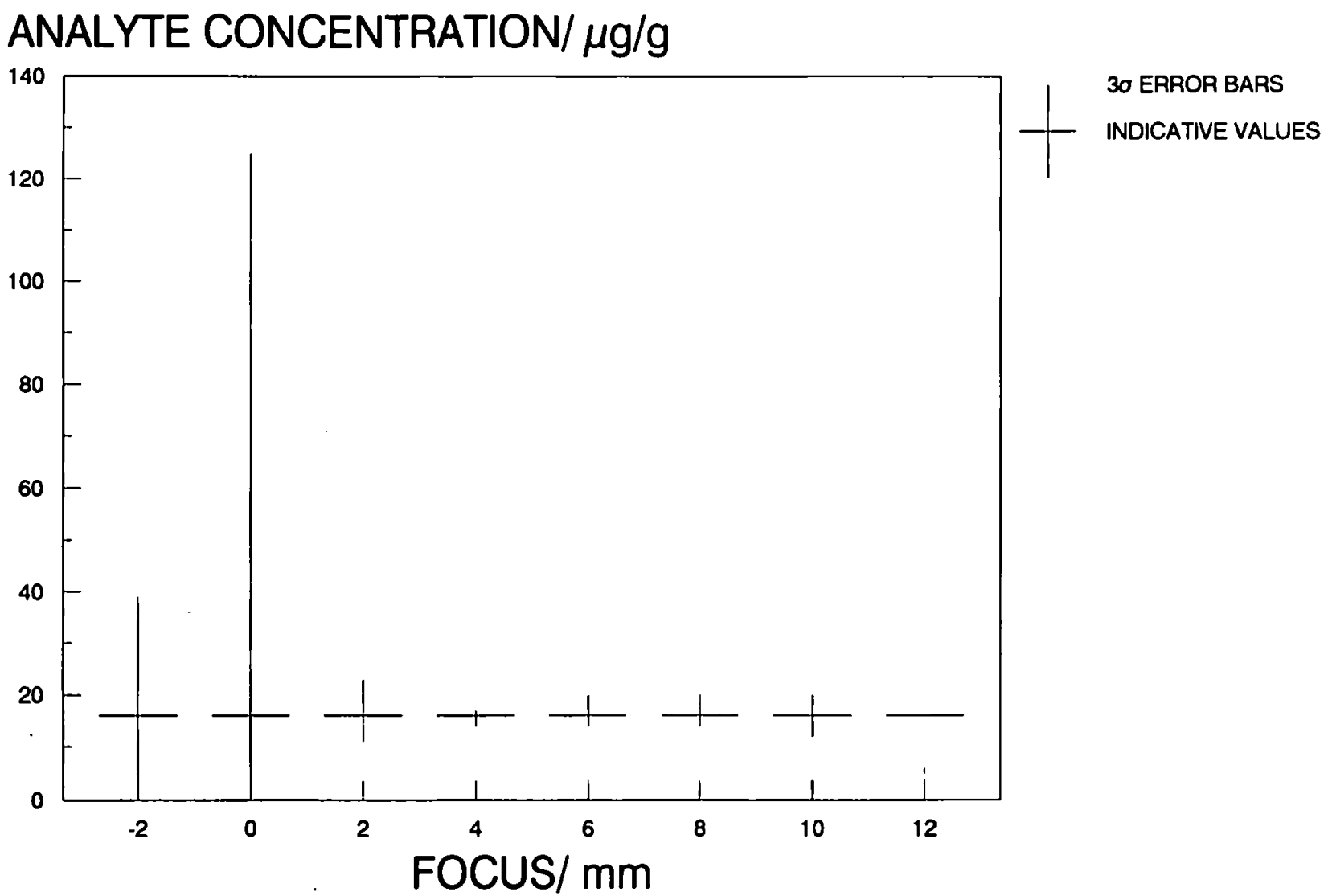

FIG 8.9: EFFECT OF FOCUSSING IN Q-SWITCH MODE DETERMINATION OF IRIDIUM IN RHODIUM

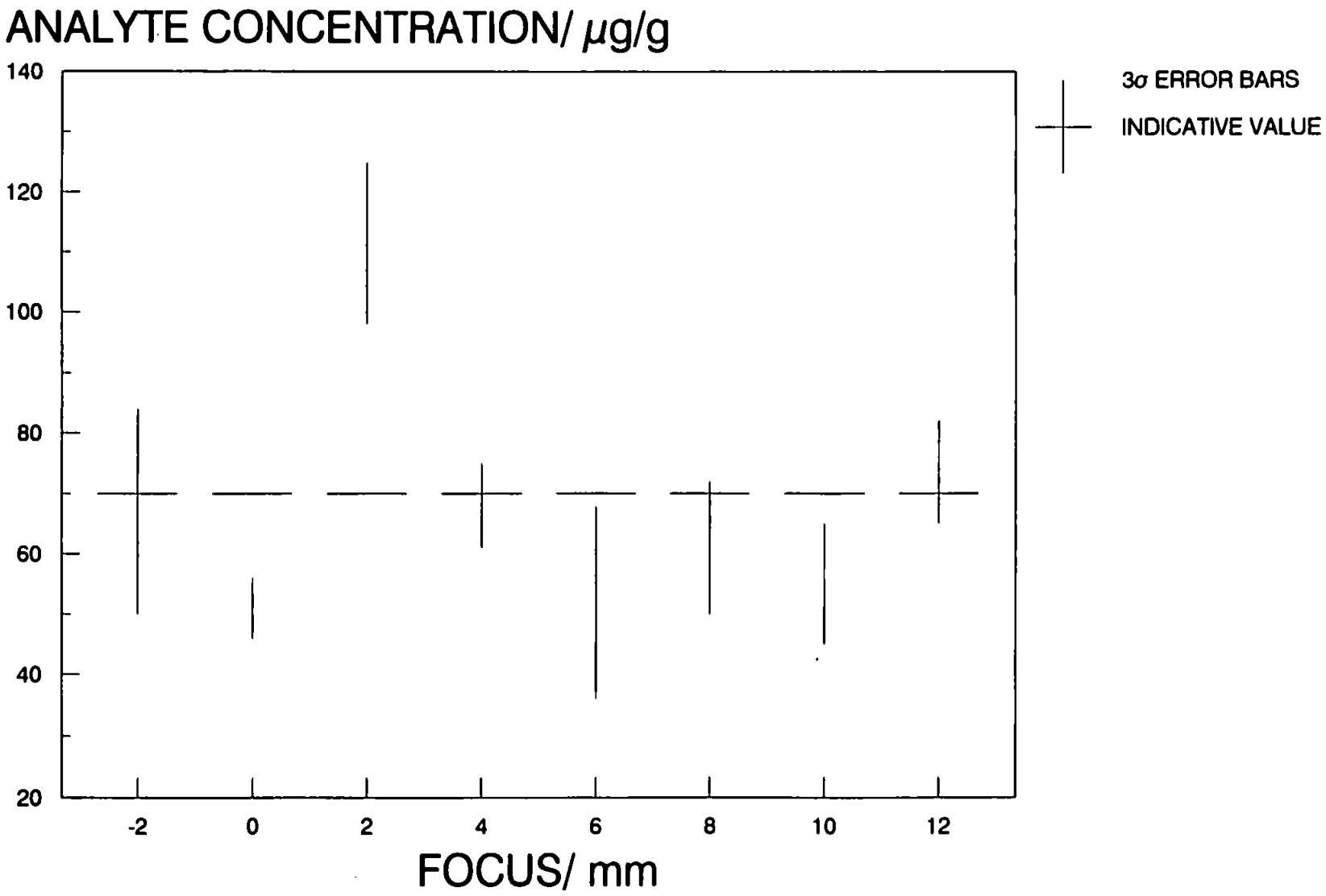

The conditions described were used for the analysis of two rhodium samples, 111 and 139, by laser ablation - inductively coupled plasma - mass spectrometry, in both fixed-Q and Q-switched modes. These results (Table 8.2) were compared with those obtained following dissolution of the sample by the method described in Section 8.2.4. Indicative results were obtained by DC arc spectrometry. For LA-ICP-MS analyses the rhodium argide peak (m/z 143) was used as an internal standard, which proved better than those obtained using either the rhodium doubly charged peak (m/z 51.5) or in the absence of an internal standard. The results show good agreement between those obtained by laser ablation and those after the sample was dissolved prior to analysis by inductively coupled plasma - mass spectrometry. The large amount of nickel and silver present in the gold used in the dissolution procedure prevented the results for these two elements being obtained.

A statistical test, the f-test, was performed on the results and this showed that in most cases there is a confidence level of greater than 95% that the results are the same. The exceptions were the results for magnesium, cobalt and ruthenium when the laser was in Q-switched mode for the sample 111; and magnesium iron and lead with the laser in Q-switched mode for sample 139. These results show that both better precision and better accuracy is obtained in laser ablation - inductively coupled plasma - mass spectrometry, when the laser is in fixed-Q mode.

TABLE 8.2 RESULTS OBTAINED FOR RHODIUM BY LASER ABLATION -ICP-MS AND AFTER DISSOLUTION BY ICP-MS

i) Rhodium 111

		Concentration/$\mu g\ g^{-1}$		
Analyte	Indicative	Fixed-Q	Q-switched	Dissolution
Mg	10	3.0±0.2	2.0±0.4	3.5±1.1
Fe	60	58.0±9.3	59.4±2.8	63.1±1.7
Ni	10	7.8±0.7	10.8±2.5	-[1]
Co	6	1.8±0.3	2.5±0.4	2.4±0.2
Ru	6	10.1±1.3	8.5±1.0	11.9±1.1
Pd	1	16.6±4.6	15.8±4.9	16.4±1.2
Ag	<1	0.8±0.2	0.5±0.1	-[2]
Ir	40	55.7±3.2	53.0±9.8	69.2±3.4
Pb	<1	2.0±0.0	1.9±0.1	2.1±0.2

ii) Rhodium 139

		Concentration/$\mu g\ g^{-1}$		
Analyte	Indicative	Fixed-Q	Q-switched	Dissolution
Mg	8	2.7±0.7	3.0±1.1	3.8±0.4
Fe	40	48.0±3.0	45.6±8.8	59.5±1.1
Ni	7	6.3±1.8	8.3±1.4	-[1]
Co	3	3.1±0.7	1.2±0.4	2.6±0.6
Ru	4	10.8±1.5	7.9±1.4	12.5±1.1
Pd	<1	5.4±2.4	7.8±1.4	10.7±1.4
Ag	<1	0.1±0.0	0.2±0.1	-[2]
Ir	30	79.4±8.1	82.4±7.6	84.2±3.1
Pb	90	24.2±2.4	14.9±3.8	24.1±1.0
Bi	<1	0.0±0.0	0.1±0.0	0.3±0.1

uncertainty expressed as 1 σ

[1] ArO interference

[2] Isotopes not resolved from rhodium matrix

8.3.2 Analysis of Palladium

The optimum conditions obtained for rhodium were used in the analysis of two samples of palladium (Table 1). The effect of defocussing the laser for analysis by laser ablation in Q-switched mode was investigated (Figures 8.10 - 8.14). The values obtained were compared with the results obtained after dissolution of the sample. These figures show a similar pattern to those obtained for the rhodium samples. For the analysis of palladium the laser was focussed 10 mm below the sample.

The results obtained for the analysis of the two palladium samples, 243 and 197, in both fixed-Q and Q-switched mode were also compared with the results obtained after dissolution of the sample prior to analysis by inductively coupled plasma - mass spectrometry (Table 8.3). The results indicate good agreement between the methods. In this case the results shown were obtained using the minor palladium isotope peak (m/z 102) as an intrinsic internal standard, which proved better than using either the palladium argide peak (m/z 148) or the palladium doubly charged peak (m/z 54).

The use of the f-test showed that in most cases the results had a certainly of greater than 95% that they were the same. The exceptions were magnesium in fixed-Q mode and gold in Q-switched mode for sample 243; and platinum

FIG 8.10: EFFECT OF FOCUSSING IN Q-SWITCH MODE DETERMINATION OF MAGNESIUM IN PALLADIUM

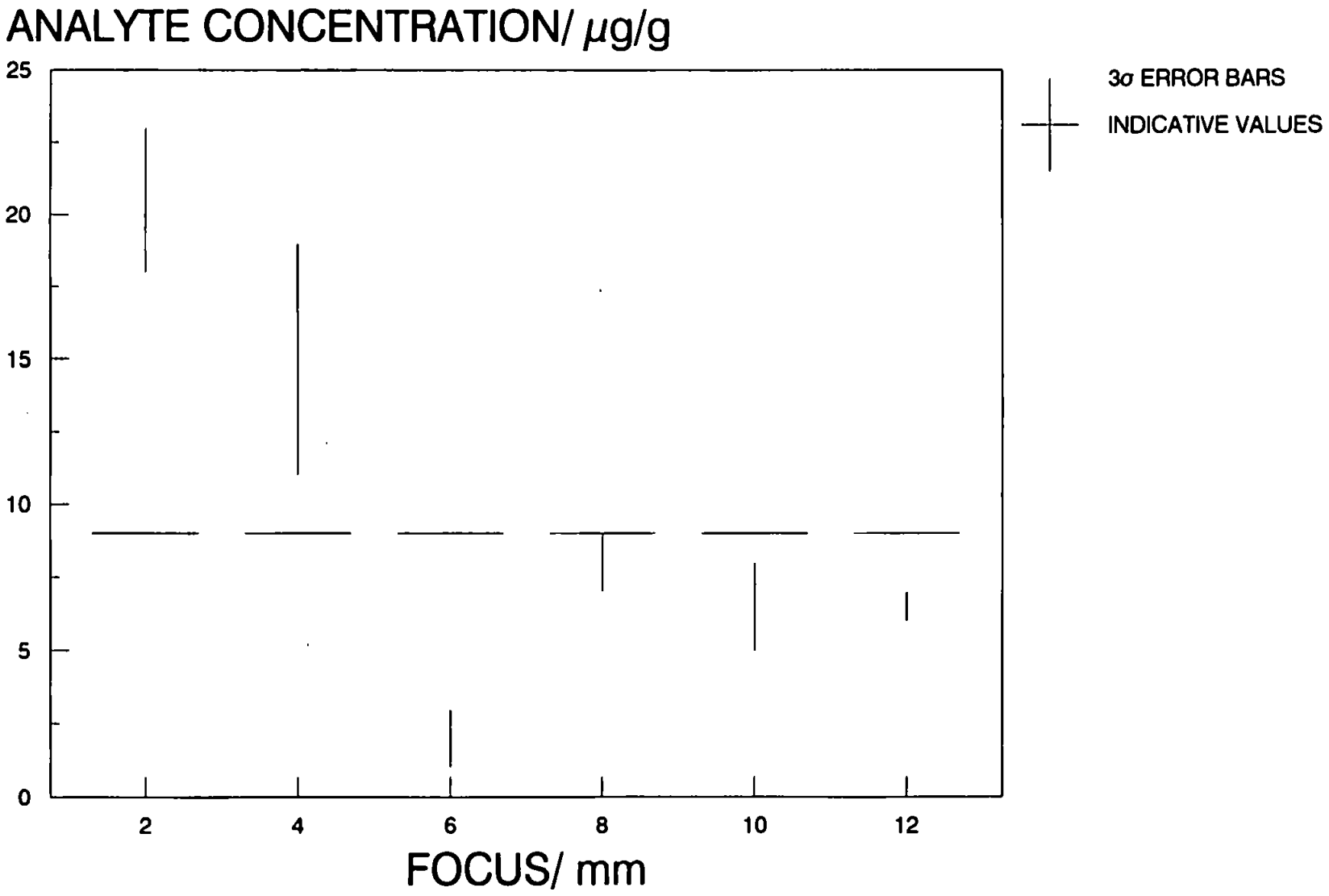

FIG 8.11: EFFECT OF FOCUSSING IN Q-SWITCH MODE DETERMINATION OF IRON IN PALLADIUM

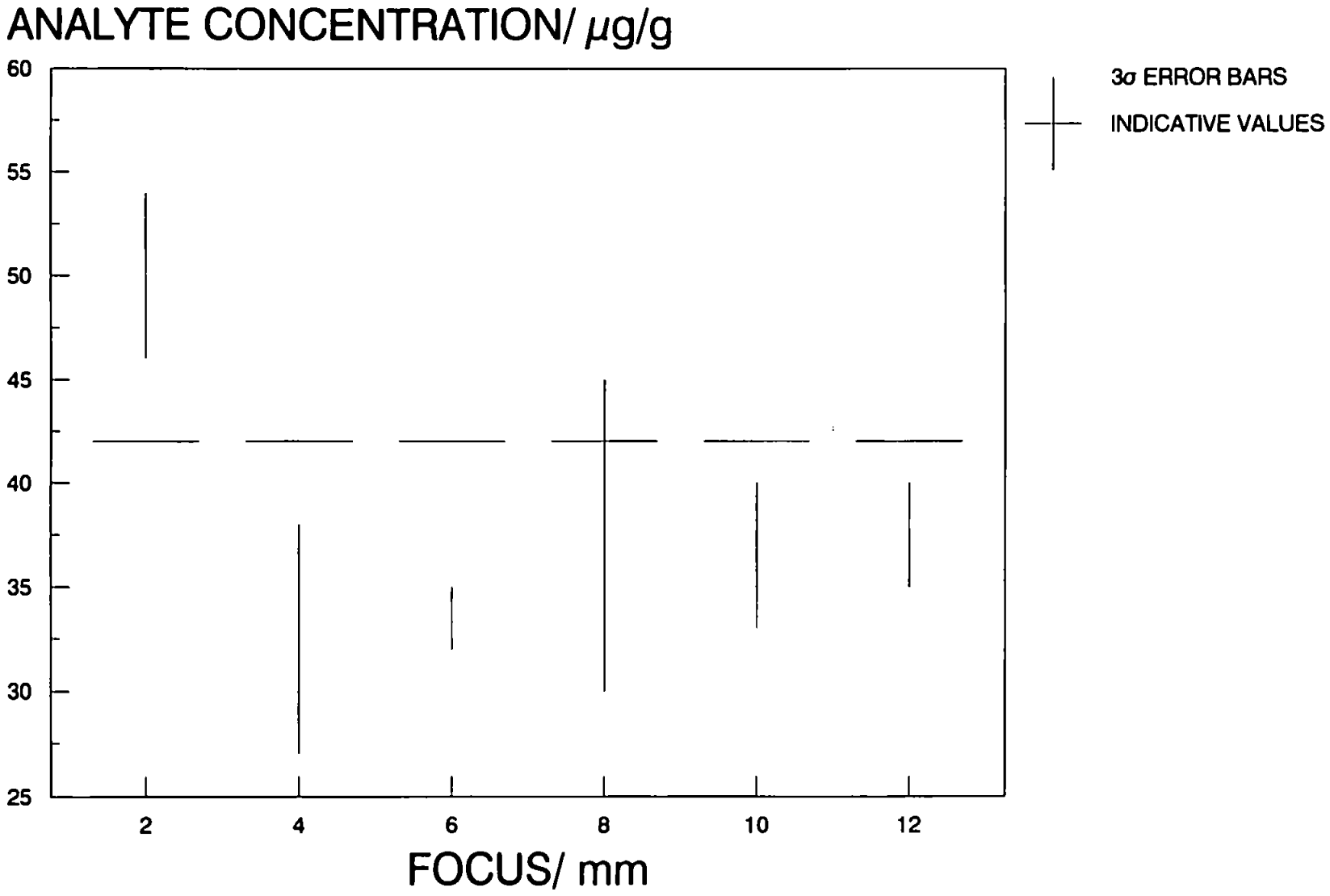

FIG 8.12: EFFECT OF FOCUSSING IN Q-SWITCH MODE DETERMINATION OF NICKEL IN PALLADIUM

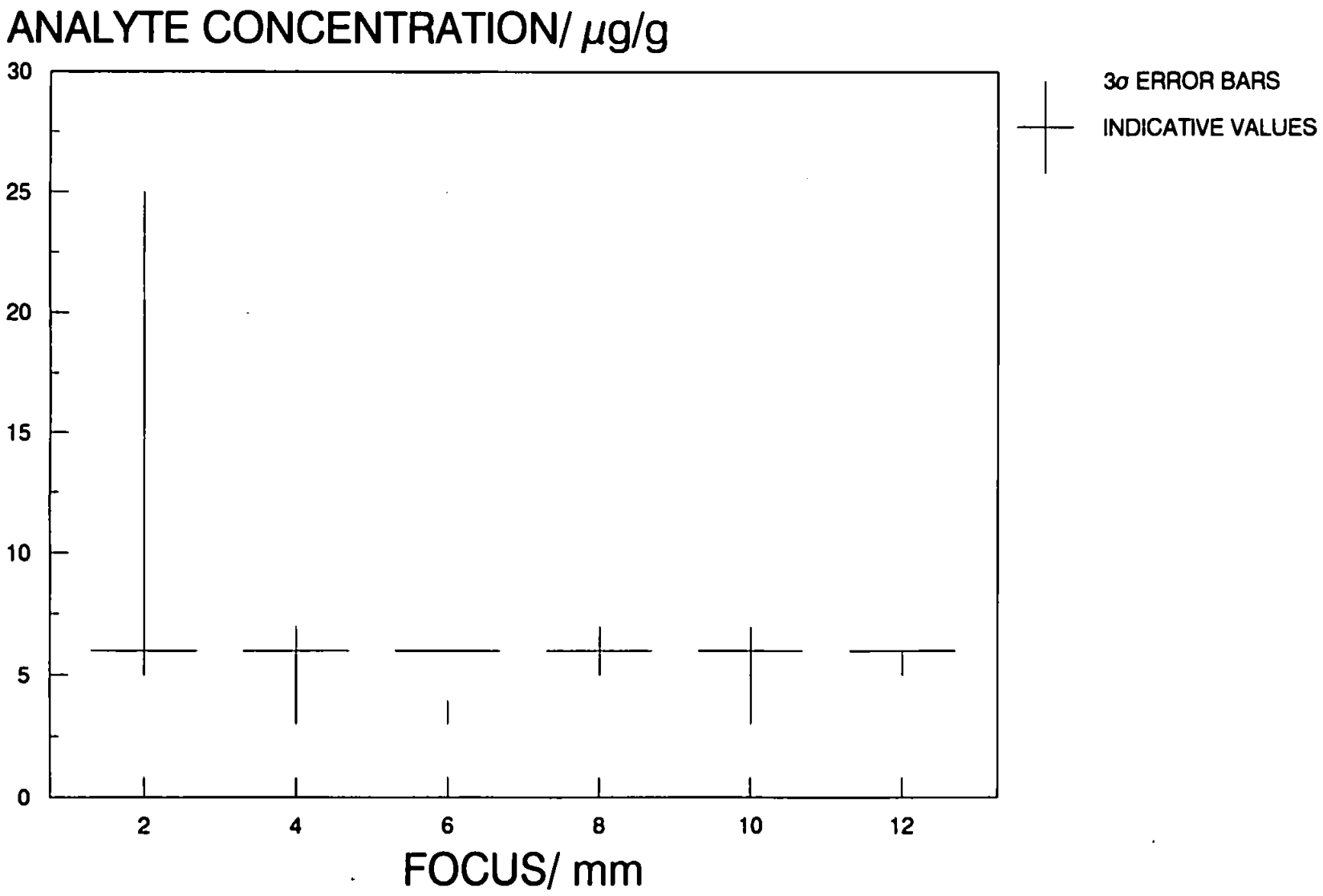

FIG 8.13: EFFECT OF FOCUSSING IN Q-SWITCH MODE DETERMINATION OF PLATINUM IN PALLADIUM

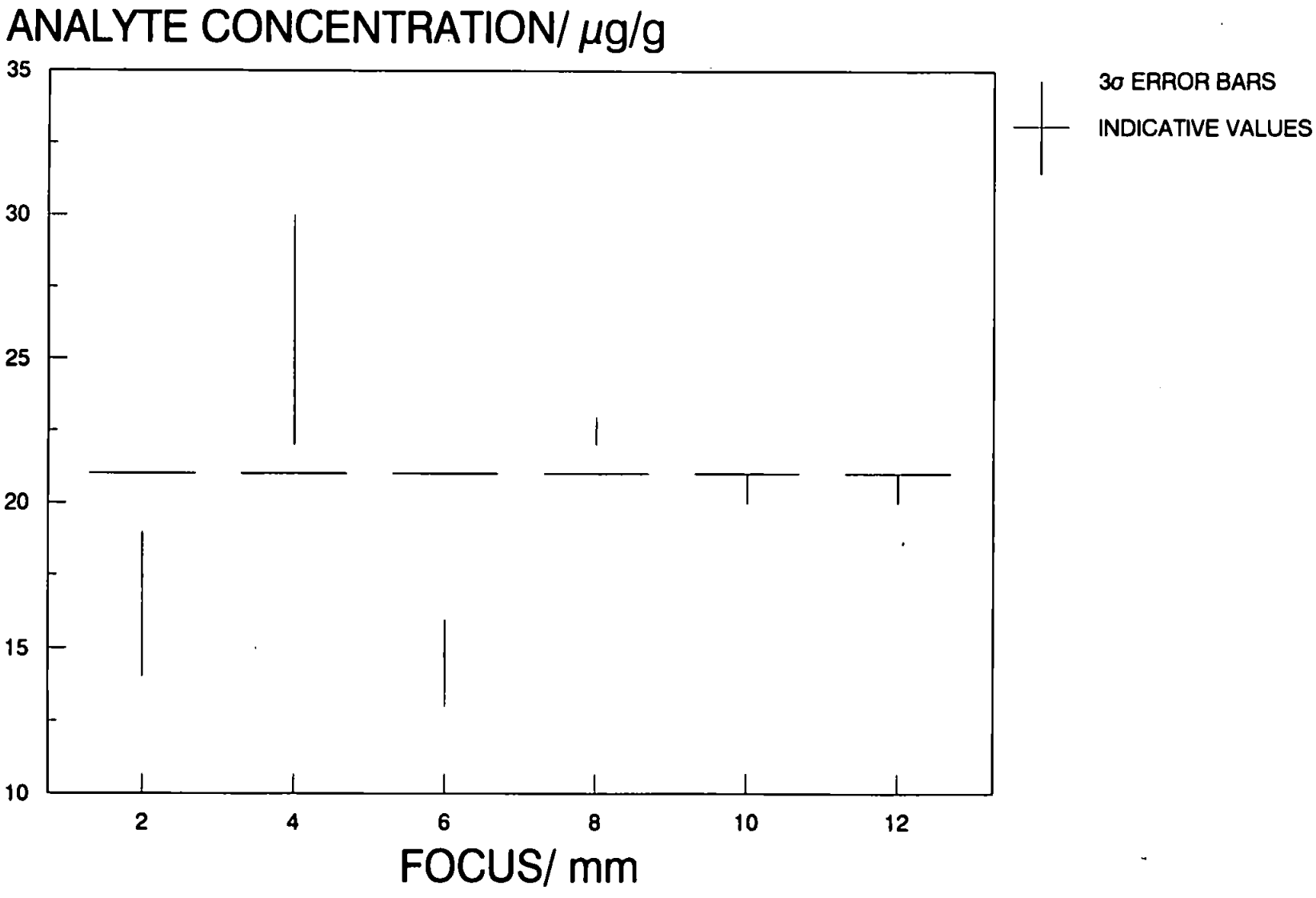

FIG 8.14: EFFECT OF FOCUSSING IN Q-SWITCH MODE DETERMINATION OF GOLD IN PALLADIUM

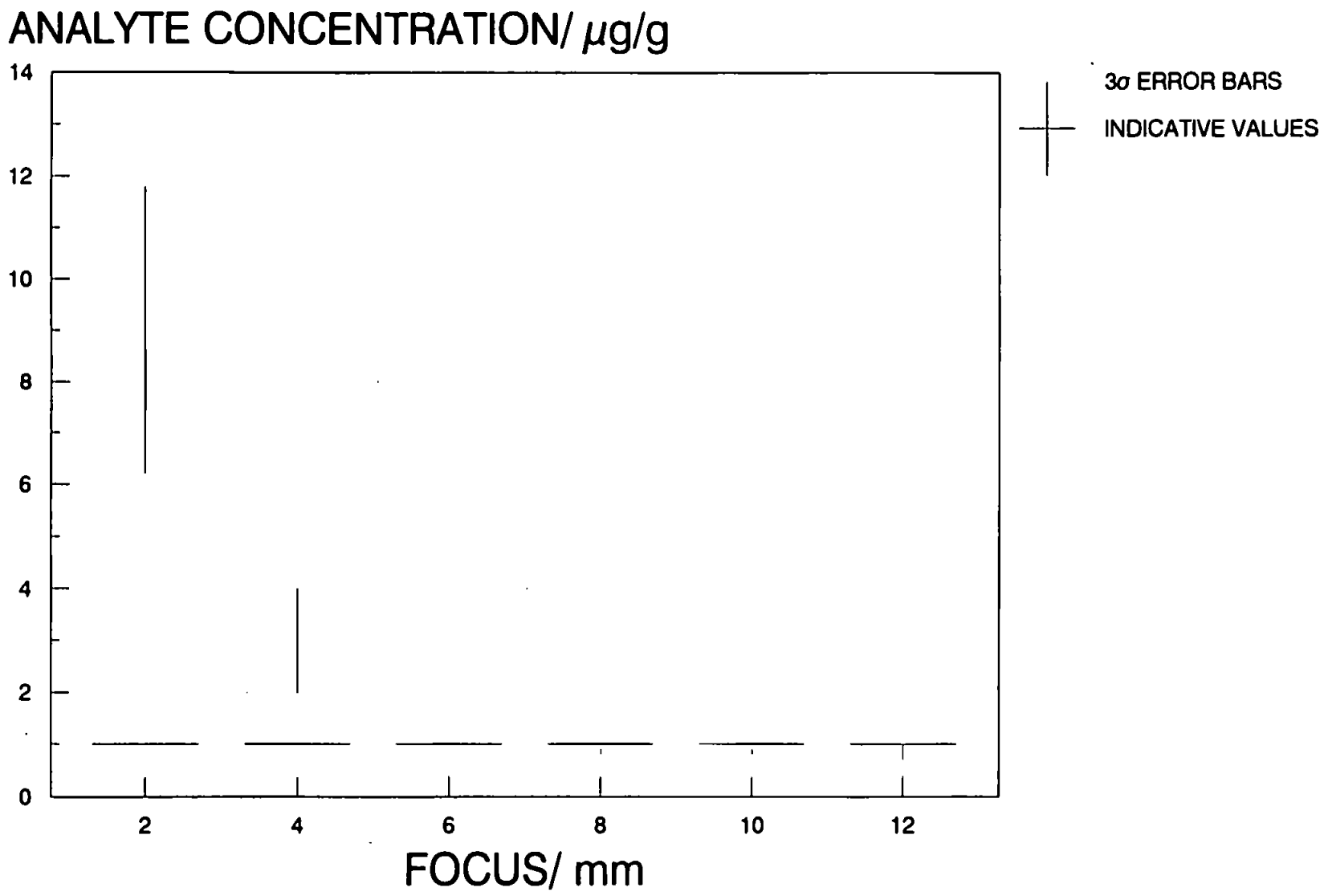

TABLE 8.3 RESULTS OBTAINED FOR PALLADIUM BY LASER ABLATION-ICP-MS AND AFTER DISSOLUTION BY ICP-MS

i) Palladium 243

		Concentration/$\mu g\ g^{-1}$		
Analyte	Indicative	Fixed-Q	Q-switched	Dissolution
Mg	14	7.6±0.7	14.9±4.1	8.9±0.5
Fe	71	37.6±3.9	38.1±8.0	42.5±1.8
Ni	7	5.3±0.7	6.5±1.3	5.7±0.3
Cu	3	4.0±0.5	3.1±0.3	4.0±0.4
Pt	3	24.3±2.5	27.0±10.0	21.1±1.1
Au	1	1.1±0.2	0.3±0.1	1.1±0.2
Pb	2	0.3±0.1	0.7±0.1	0.4±0.0
Bi	<1	0.2±0.0	0.3±0.1	0.1±0.0

ii) Palladium 197

		Concentration/$\mu g\ g^{-1}$		
Analyte	Indicative	Fixed-Q	Q-switched	Dissolution
Mg	14	15.4±1.1	15.6±1.3	15.6±1.7
Fe	99	51.3±4.8	46.7±7.9	58.4±2.5
Ni	3	3.4±1.8	3.6±0.3	5.0±0.4
Cu	24	25.9±0.9	25.0±1.2	23.5±1.1
Rh	25	19.9±1.7	17.6±2.7	-[1]
Ag	6	5.2±0.5	5.4±0.6	-[1]
Pt	3	11.0±0.7	8.2±0.90	10.9±0.5
Au	<1	1.0±0.1	0.8±0.1	1.0±0.2
Pb	<1	0.3±0.1	0.9±0.2	0.4±0.2

uncertainty expressed as 1 σ

[1] Isotopes not resolved from palladium matrix

and gold in Q-switched mode in sample 197. The results show that the use of the laser in fixed-Q mode gives far better results both in terms of precision and accuracy, compared with those obtained in the Q-switched mode.

The results for sample 197, following dissolution show the problem in determining rhodium and silver, due to overlapping of the palladium isotopes at m/z 102, 104, 106 and 108, which prevented resolution of the monoisotopic rhodium (m/z 103) or either of the silver isotopes (m/z 107, 109). These elements could be analysed by laser ablation because of the improvement in the resolution associated with the use of dry plasmas.

8.4 Conclusions

From the results obtained for both rhodium and palladium, it is clear that the use of the laser in fixed-Q mode provided the better quality results in terms of both accuracy and precision. It is also evident that the choice of an internal standard is important, with the best results being achieved using a minor isotope of the matrix element, although for monoisotopic elements the argide peak may also be used. The non-availability or difficulty in producing solid standards for use in laser ablation means that the use of this technique is still limited. The improved resolution encountered when using a dry plasma also means there are applications when the isotopes of interest may not be fully resolved from the matrix if analysed under wet conditions.

CHAPTER 9

DETERMINATION OF IONISATION TEMPERATURES IN THE PLASMA

9.1 Introduction

Calculations to obtain the spectroscopic temperatures of the plasma are complicated by the assumptions made in such calculations. The temperature of a plasma, T, can be defined in classical gas thermodynamics by the relationship with the mean kinetic energy, E_{kin}, of the particles (see Section 1.5). However, it is difficult to define a single temperature in a laboratory plasma. The various temperatures can be defined according to the physical phenomena that are observed. This means that a statement of temperature is a way of describing the energies of the various particles (87).

The translational, or kinetic temperature, T_{kin}, is obtained from use of the Maxwell distribution function, f(v), for the random velocity;

$$f(v) = 4\pi \left(\frac{m}{2\pi k T_{kin}} \right)^{3/2} \exp \left(\frac{-mv}{2kT_{kin}} \right)$$

where m is the mass of the particle considered.

The function defines the kinetic temperature as representing the temperature of the system in a state of complete thermodynamic equilibrium (CTE).

The motion of the emitting particles ensures that the central wavelength, y_0, appears to be shifted by $y - y_0$, by the Doppler effect.

The introduction of this effect into the equation leads to the following equation;

$$y - y_0 = 7.10 * 10^{-7} \; y_0 \; (T/M)^{1/2}$$

where T is expressed in Kelvin and M in atomic mass units (88).

The excitation temperature or electronic excitation temperature, T_{exc}, uses the Boltzmann distribution as the basis of the calculation. This distribution allows the definition of the population or number densities, n_j and n_k, of bound electrons of energy, E_j and E_k, with $k > j$, to be made;

$$\frac{n_k}{n_j} = \frac{g_k}{g_j} \exp -\frac{(E_k - E_j)}{kT_{exc}}$$

where g_k and g_j are the statistical weights of the two

levels, or the degeneracies, ($g = 2J + 1$).

k is the Boltzmann constant.

If the total number density, n, in the ionisation state is considered, we get;

$$n_k = \left(g_k \exp \frac{(-E_k)}{kT_{exc}} \right) Q(t)$$

where Q(t) is the internal partition function, defined as;

$$Q(t) = \Sigma_k g_k \exp \frac{(-E_k)}{kT_{exc}}$$

For low temperatures the value Q(t) is mostly near to the statistical weight, g_0, of the ground state. However, for higher temperatures (> 4000 K) this partition function may vary with the temperature and the electron number density. Formulae for these calculations have been published (89).

To obtain the rotational temperature, the Boltzmann equilibrium is used to define the line intensity formula;

$$I = \frac{(hc)}{4\pi y} An_k$$

where A is the transition probability (s^{-1}) for spontaneous emission.

By replacing n_k in the Boltzmann equation we obtain;

$$I = \frac{(hc)}{4\pi y} g_k A \frac{(n)}{Q(t)} \exp \frac{(-E)}{kT_{exc}}$$

A plot of ln (I/gA) versus E should be linear with a slope equal to -5040/T, when E is in electron volts (88).

For a transition J' - J'', a rotational line intensity and hence a rotational temperature, T_{rot}, can be calculated;

$$I = Dv^4 S \exp \frac{(-E_r)}{kT_{rot}}$$

where coefficient D contains the rotational partition function, the statistical weight and universal constants.
S is the oscillator strength
E_r the rotational energy.

The rotational energy is defined by;

$$E_r = B_v hcJ'(J'+1)$$

where B_v is the rotational constant belonging to the vibrational quantum number,v (87).

The electron temperature, T_e, can be calculated because after ionisation processes in the plasma the electrons are no longer bound, this means they are in nonquantitised levels. Many transitions, either free-free or free-bound

can occur. In the UV-visible part of the spectrum radiative recombination is the predominant process;

$$Ar^{+} + e^{-} \rightarrow Ar^{*} + h\nu$$

where v is the frequency.

This process leads to a continuum of which the intensity is a function of the wavelength namely;

$$\epsilon(Y,T) = c_1 \frac{n_e n^{+} z^2}{T_e 1/2_Y 2} \Gamma(Y,T,) \left(1 - \exp \frac{(-hc)}{kT} \right)$$

where z is the effective charge number
$\Gamma(Y,T)$ is a corrective factor (87).

The radiative field provides a radiation density U(T) which depends only on the radiation temperature, T_{rad}, and is given by the Planck function;

$$U(T)dy = \frac{(8\pi hc)}{y^5} . \left(\exp \frac{(dy/hy)}{kT_{rad}} \right)$$

THe norm temperature, T_{norm}, is the value of the excitation temperature for which a spectral line has a maximum intensity due to the competing effects of ionisation and excitation processes. It is a function of the total pressure and of plasma composition (87).

The plasma is often assumed to be in local thermal equilibrium (LTE) in order to make calculations less complicated. Deviations from LTE have been discussed by Blades (88). The concept of partial - LTE has also been reported (98,99), which states that a plasma is in LTE at the microscopic level.

One of the assumptions made in the introduction of slurries into an ICP is that aqueous standards can be used in the calibration process (see Section 1.4.1). For this to be the case the plasma conditions are assumed to be the same for both the samples and the standards. Clearly if the plasma temperatures measured for the introduction of samples and standards are different, then the plasma conditions are not the same. This would mean that the assumptions made about the introduction of slurries are no longer valid.

This argument also applies to the introduction of larger particles into the plasma. If the results obtained in Section 7.3 are valid, then the temperature of the plasma should remain constant for all the slurry particle size distributions investigated as well as the aqueous standards, when the slurries were desolvated.

The removal of water from the plasma, removes both hydrogen and oxygen from the thermal processes taking

place in the plasma. It is believed that, notably hydrogen, has a great effect on the thermal conductivity between the plasma and the analytes, increasing both the plasma temperatures and the atomisation efficiency (100,101). The effect of this change on the analytical performance is therefore, of great importance. The use of desolvation may be detrimental to the thermal conductivity in the plasma.

9.2 Experimental

The slurry used in these experiments (SO-1) was prepared as described in Section 7.2.

To calculate the ionisation temperature of the plasma, it was assumed that both the Saha and the Boltzmann equations can validly be used. This enabled the following equation to be used (15):

$$\frac{n^{++}}{n^{+}} = \frac{4.83 * 10^{15}}{n_e} T^{3/2} \frac{g^{++}}{g^{+}} \exp -E_i/kT$$

where n++ and n+ are the population levels for the second ionisation and first ionisation states respectively

n_e is the population of electrons

T is the ionisation temperature

E_i is the ionisation energy

k is the Boltzmann constant

g^+ and g^{++} are the degeneracies of the elements

In assuming that the plasma is in local thermal equilibrium (LTE), n_e and T are common for both the analyte and argon, the population ratio is therefore a function of the electron population, n_e.

By plotting ln $\frac{(n_p)}{(g_p)}$ against energy, E_i the slope of the line corresponds to -1/kT.

n_p is the population level, $\frac{n^{++}}{n^{+}}$

g_p the partition function, $\frac{g^{++}}{g^{+}}$

9.3 RESULTS AND DISCUSSION

Calculation of the ionisation temperature of the plasma provides information about the effect desolvation of the samples has on the plasma. Results obtained show that desolvation of the samples, whether aqueous or slurries, causes a decrease in the ionisation temperature (Table 9.3.1). This is considered to be due to the removal of hydrogen from the plasma, which has a major role in the thermal conductivity of the plasma and dominates the energy transfer process between plasma and sample (52). There is also a trend of increasing ionisation temperature with an increase in forward power. This is in agreement with previous work which indicates that not only is there an increase in the ionisation temperature (90), but also in the electron number density (91).

The effect of particle size, for the slurry calculations, shows that there is a trend towards a decrease in ionisation temperature with a decrease in particle size. This is particularly the case when the slurries are not desolvated. This effect is more difficult to quantify, particularly as there are some inconsistencies. It appears, however, that the relationship between the volume-diameter distribution and the population-diameter distribution is important, with a large number of small

TABLE 9.3.1: IONISATION TEMPERATURES CALCULATED USING AN INDUCTIVELY COUPLED PLASMA - MASS SPECTROMETER

SAMPLE			DESOLVATION	IONISATION TEMPERATURE/^{o}C
AQUEOUS	1300W		NO	6900
	1500W			7300
	1300W		YES	5400
	1500W			5900
SLURRY	1300W	0.0 HR	NO	6400
		0.5 HR		6300
		1.0 HR		6300
		1.5 HR		6300
	1500W	0.0 HR		7200
		0.5 HR		6700
		1.0 HR		6600
		1.5 HR		6500
SLURRY	1300W	0.0 HR	YES	5900
		0.5 HR		5500
		1.0 HR		5500
		1.5 HR		5600
	1500W	0.0 HR		5900
		0.5 HR		6500
		1.5 HR		5800

the plasma than a smaller number of large particles. This implies that the introduction of larger particles (>3μm) has less effect on the plasma than was previously expected. There is, however, variation in the results obtained and these differences may not be significant.

The trends shown in Figure 9.3.1, for the addition of hydrogen into the plasma, show as expected that the introduction of hydrogen into the nebuliser gas has a beneficial effect on the ionisation temperature. The addition of about 0.5% v/v hydrogen, to the argon nebulising the desolvated sample, brings the ionisation temperature above that calculated for the non-desolvated sample, with an optimum with the addition of about 1.25% v/v. Previous work (104), suggested that the excitation temperature should increase up to approximately 2-3% v/v hydrogen followed by a constant, but elevated temperature, up to about 5-6% v/v hydrogen. The temperature will then decrease returning to the initial value at about 10% v/v.

The effects of the hydrogen in the ICP, either from the decomposition of water or as a deliberate addition, appear to play a pivotal role in the energy transfer processes between the torus of the ICP and the central annular region. The thermodynamic properties of the hydrogen, particularly in terms of the heat capacity and the thermal

FIG 9.3.1 ADDITION OF HYDROGEN TO THE NEBULISER GAS FLOW EFFECT ON IONISATION TEMPERATURE AQUEOUS SAMPLE

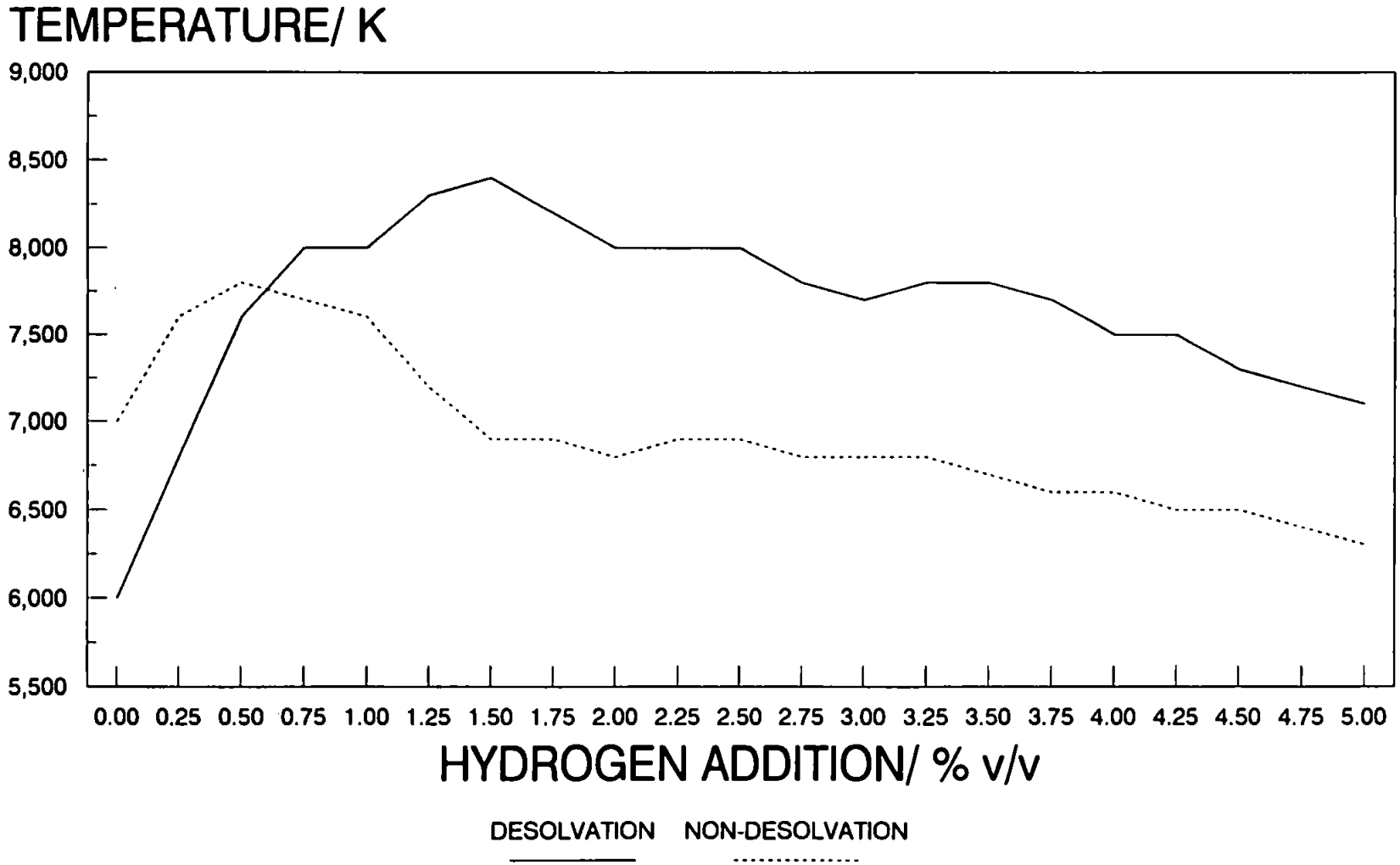

conductivity, reveal the reasons for this. Relatively small concentrations of hydrogen play a significant role in the energy transfer processes of the ICP.

If a conceptional model is considered, in which a simple heat transfer mechanism is assumed, the ICP can be visualised as a hot cylindrical tube, the torus, through which an inner gas flows. The total energy transfer will be determined by the thermal conductivity of the gas, the geometric contact area of the gas and the residence time (103).

Molecular hydrogen and atomic hydrogen have high thermal conductivities compared with argon, consequently the hydrogen will greatly effect the thermal conductivity in the torus. The specific heat capacity of molecular hydrogen is significantly greater than argon and therefore, acts to counter the increased thermal conductivity. By assuming ideal gas behaviour, then the specific heat capacity of atomic hydrogen is the same as argon. The specific heat capacities of argon and atomic hydrogen are independent of temperature, if electronic excited states are ignored, whilst molecular hydrogen is temperature dependent. The thermal conductivities of both forms of hydrogen are temperature dependent whilst argon is less temperature dependent (103).

The hydrogen added into the plasma, either as molecular hydrogen or in the form of water, will be dissociated to form atomic hydrogen. Despite, however, the higher specific heat capacities of molecular hydrogen, compared with atomic hydrogen or argon and the energy required to dissociate the hydrogen, or water, the very large increase in thermal conductivity provides an increase in the energy transfer and hence an increase in the temperature of the ICP.

This increase is however, limited by two mechanisms. An increase in the temperature of the plasma acts to increase the gas velocity in the inner tube, in the conceptual model, thus limiting the residence time in the plasma and hence energy transfer. The increased energy transfer will also tend to cause local cooling of the hot surface of the tube, extending this to the torus. This local cooling will cause a decrease in the degree of ionisation and conductivity of the plasma surface. To maintain the conductivity, the plasma will contract, causing a decrease in the geometric contact area and an increase in the gas velocity, caused by a decrease in the channel radius (103).

The addition of oxygen (Fig 9.3.2), has a less clear effect, and shows a similar trend for both the desolvated

and non-desolvated samples, with both having an optimum at about 0.25% v/v. The addition of the oxygen to the plasma does not have as great an effect on the energy transfer in the plasma, as hydrogen. This is due to the thermal conductivity of the oxygen. The thermal conductivity depends on the size and mass of the gas molecule, the specific heat capacity, C_v, and the temperature. The size and the mass of oxygen are clearly greater than that of hydrogen and the temperature we can consider to be constant. The thermal conductivity of oxygen is only slightly higher than argon, consequently the addition of oxygen into an ICP would be expected to have only a marginal effect on the total energy transfer.

To obtain optimum ionisation temperatures, the addition of hydrogen to the nebuliser gas at relatively high power after desolvation appears to be the most beneficial. The results obtained here show the importance of hydrogen addition when the samples are desolvated prior to analysis.

Some of these experiments were repeated using an inductively coupled plasma - atomic emission spectrometer, and the ionisation temperatures calculated. The results obtained showed good agreement. This seems to show that, at least for these samples and the analytes investigated, the doubly charged species are formed in the plasma. The

FIG 9.3.2 ADDITION OF OXYGEN TO THE NEBULISER GAS FLOW EFFECT ON IONISATION TEMPERATURE AQUEOUS SAMPLE

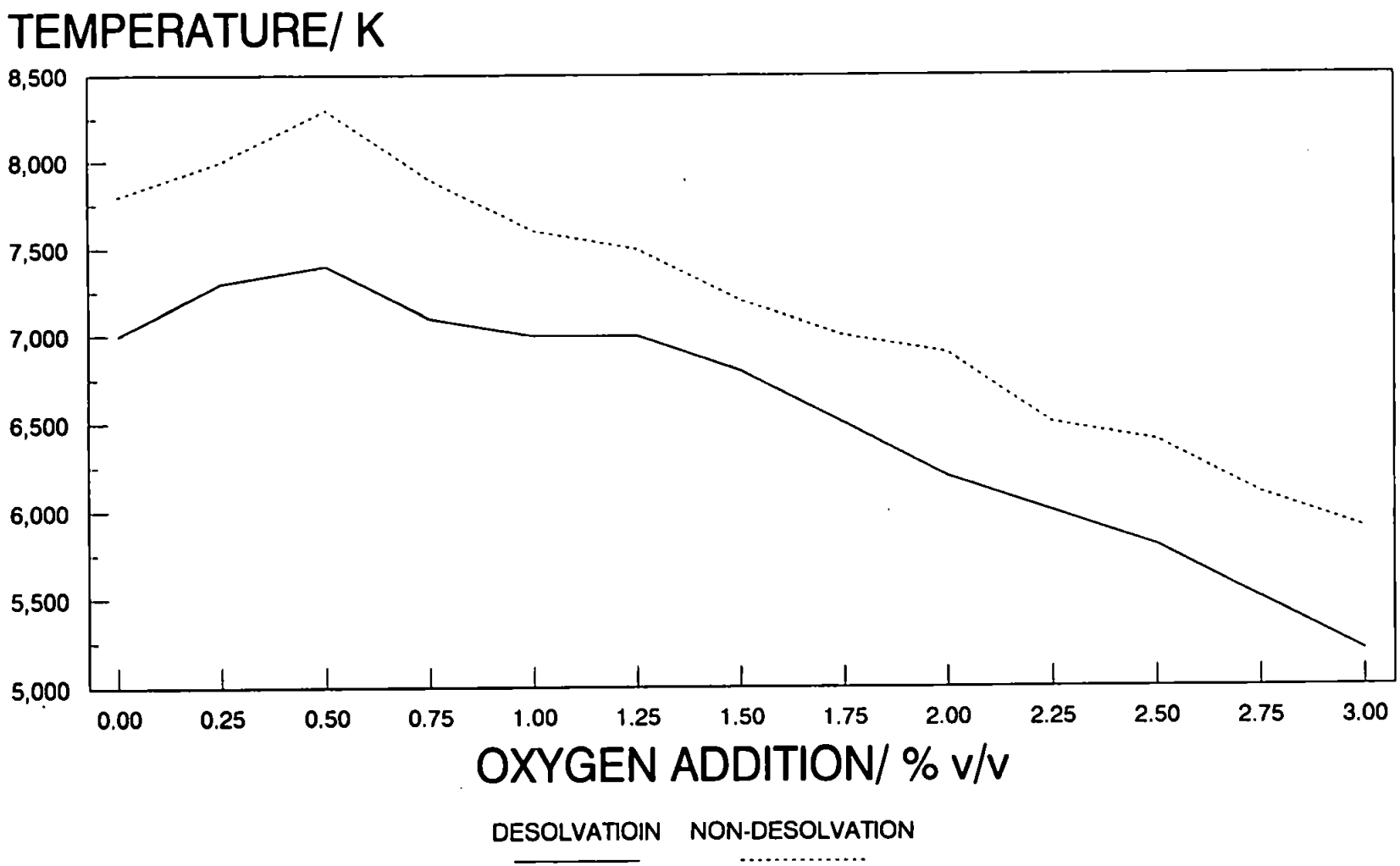

analytes used in these temperature calculations had low second ionisation energies. Clearly from empirical observation a number of species with high second ionisation energies form doubly charged species. It was considered beyond the scope of this study to consider the energies available in the plasma for the formation of doubly charged species.

9.4 EFFECTS ON THE PLASMA IONISATION TEMPERATURE DUE TO THE INTRODUCTION OF ORGANIC SOLVENTS

9.4.1 Introduction

Studies on the introduction of volatile organic solvents into an ICP are complicated by the effects on transport efficiency i.e. an improvement when compared with aqueous solutions, and the effects of the pyrolysis in the plasma. The effects on the plasma excitation conditions caused by the introduction of organic solvents have therefore, received little attention.

Measurements of the ionisation temperatures of the plasma during the introduction of organic solvents will give some indication of the excitation conditions, and the ease of which pyrolysis of the organic solvent takes place.

One of the requirements for the introduction of organics into an ICP-MS is a flow of oxygen into the nebuliser gas (5-6% v/v), to prevent the products of pyrolysis either blocking the cones or the torch. However, the introduction of oxygen into the nebuliser gas, at these levels, for the analysis of aqueous samples causes a decrease in the ionisation temperature (see Section 9.3). Consequently the introduction of oxygen when organic solvents are being

introduced may also have a detrimental effect on the ionisation temperature.

9.4.2 Experimental

The calculations used to calculate the ionisation temperatures have been described in Section 9.2. The desolvation of the samples was performed using the membrane drying tube (Chapter 5), to give a comparison between the ionisation temperatures obtained with and without desolvation.

9.4.3 Results and Discussion

The plasma ionisation temperatures obtained for the introduction of diethyl ether into an ICP-MS are shown in Table 9.4.1. The ionisation both with and without desolvation increase as the forward power of the plasma is increased. This follows a similar trend for aqueous samples (Section 9.3).

However, the effect of desolvation shows the opposite trend to the aqueous samples (Section 9.3). Instead of a decrease in the ionisation temperature when the organic solvent is desolvated, there is an increase. This implies that the introduction of organic solvents into an ICP has a detrimental effect on the excitation conditions and the thermal conductivity.

There are two possible explanations for this decrease in ionisation temperature. The plasma will obviously require energy for the pyrolysis of the solvent to form predominantly hydrogen and carbon ions and radicles. The effect of the carbon in the plasma may also act to decrease the ionisation temperature. By considering the conceptual model described in Section 9.3, and considering the thermal conductivities of the various elements some explanations can be made. The thermal conductivity of carbon is not only less than oxygen but also less than

TABLE 9.4.1 EFFECT ON THE IONISATION TEMPERATURE DUE TO AN INCREASE IN FORWARD POWER FOR THE INTRODUCTION OF DIETHYL ETHER INTO AN ICP-MS SOLVATED AND DESOLVATED

FORWARD POWER/ KW	DESOLVATION	IONISATION TEMPERATURE/ K
1.5	NO	5900
	YES	6400
1.6	NO	6100
	YES	6700
1.7	NO	6500
	YES	7100

FIG 9.4.1: EFFECT OF OXYGEN ON THE IONISATION TEMPERATURE FOR THE INTRODUCTION OF DIETHYL ETHER INTO AN ICP-MS

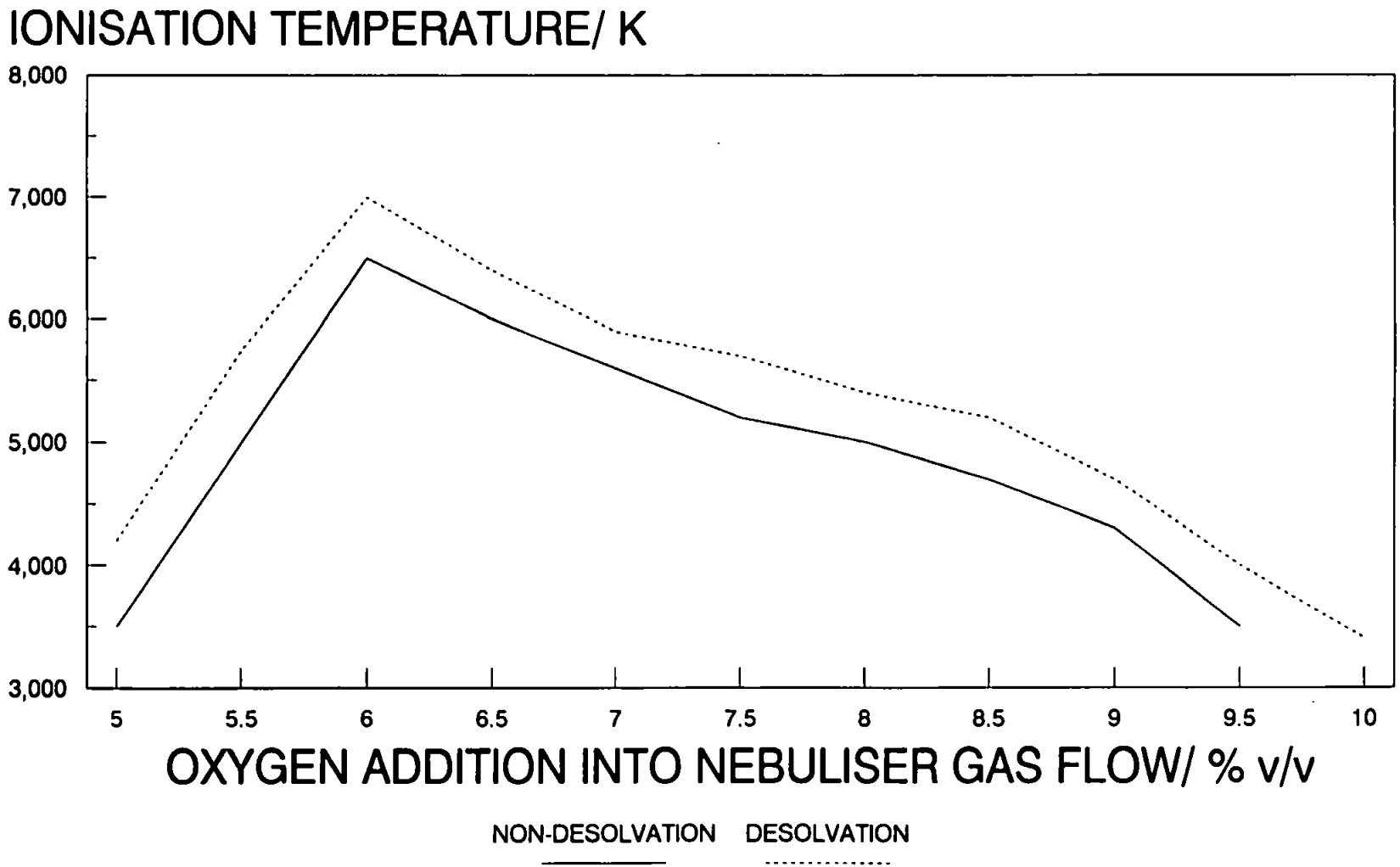

argon. Consequently the introduction of carbon into the plasma will have a detrimental effect on the ionisation temperature.

Clearly the separation of these two processes is not possible, although it seems likely that both have an effect on the decrease in the ionisation temperature. The effect of desolvation, for organics, is therefore, to decrease the amount of solvent entering the plasma and by decreasing the amount of carbon entering the plasma to increase the ionisation temperature.

The effect of introducing oxygen, into the nebuliser gas flow, has been shown to be detrimental to the plasma excitation conditions and the thermal conductivity (Section 9.3). The introduction of oxygen, into the nebuliser gas flow, is necessary for the analysis of organic solvents to prevent the build up of pyrolysis products.

The effect on the ionisation temperature caused by the introduction of oxygen is shown in Figure 9.4.1. It should be noted that the sharp decrease in the ionisation temperature below ≈ 6% v/v oxygen, is due to the effects of the products of pyrolysis being deposited on the cones. This was observed as a glowing around the tip of the sampler cone, caused by a build up of carbon, and a

decrease in the expansion pressure. Above this point no evidence of carbon deposition was observed. The effect of the oxygen on the ionisation temperature is similar for both the solvated and desolvated samples. There appears to be an optimum at the point where the cones are just being kept clear of carbon (eg ≈ 6% v/v), and any additional oxygen has a detrimental effect on the plasma, causing a decrease in the ionisation temperature.

9.5 CONCLUSION

The addition of slurries to the plasma does not have an effect on the ionisation temperature, indicating that particles have a neutral effect when introduced to the plasma. The addition of hydrogen to the nebuliser gas of the desolvated plasma acts to increase the ionisation temperature, and improve the thermal conductivity and energy transfer of the plasma. The addition of oxygen to the nebuliser gas has a marginal effect. There is a slight increase in the ionisation temperature at low levels. Above about 1% v/v there is a detrimental effect on the ionisation temperature. The effect caused by the addition of organic solvents on the ionisation temperature of an ICP is clear. There is a detrimental effect caused by the low thermal conductivity of the carbon and the energy required for pyrolysis. The use of desolvation has a beneficial effect on the plasma by lowering the amount of solvent entering the plasma. It can be concluded that whilst the introduction of oxygen is necessary when introducing organic solvents the amount introduced should be kept to a minimum, due to the effect of oxygen on the thermal conductivity of the plasma. The calculation of the ionisation temperature of the plasma provides some information on the fundamental working of the plasma.

CONCLUSION AND FURTHER WORK

This study has been successful in fulfilling many of its original objectives and in addition has provided an insight into a number of areas not identified at the onset of this work.

The use of various techniques to desolvate samples prior to analysis using an ICP have been described for use with both organic and aqueous samples. The analysis of organic samples, particularly volatile organics, is complicated by the enhanced instability of the plasma shown to be caused by the increased plasma loading. Removal of much of the solvent has been demonstrated to not only increase the plasma stability but also improve detection limits, due to an increase in the amount of analyte reaching the plasma. The novel use of flow injection has also been used to further decrease the amount of volatile solvent entering the plasma, acting to further increase the stability, and again enabling an improvement in detection limits. Flow injection also facilitates a reduction in memory effects and thereby allows increased sample throughput. The use of the desolvation techniques described can obviously be extended to other types of both volatile and non-volatile organic samples.

The use of optimisation techniques such as the variable step size simplex procedure have been used to good effect in this study to enhance the sensitivity of any technique

where the variables are interrelated. For example, the coolant gas flow effects the optimum nebuliser gas flow rate which in turn will lead to changes in the spatial effects in the plasma, changes in the electron number density and the viewing height in the plasma. The temperature of the spray chamber and the forward power will also independently affect the electron number density and the spatial effects in the plasma. These relationships have been studied with respect to the introduction of both aqueous and organic samples and reveal that, for example the viewing heights, nebuliser gas flow and forward power need to be increased and the sample uptake rate decreased, for the more volatile samples.

The use of membrane separators for desolvation has also been shown to be successful in this study for the introduction of volatile organic solvents. The use of these separators have a number of advantages over conventional desolvation devices, including robustness in routine use, ease of use and installation, and the short time required to reach stability. The use of these separators, particularly when combined with flow injection techniques, can also be extended to a large number of organic matrices, as well as for the analysis of reactive organometallics. The analysis of such organometallics species using this approach has been shown to offer a number of advantages over previously reported methods, including both an improvement in analysis time and better detection limits. In addition this approach avoids sample

pretreatment, prevents contamination, requires less material and improves safety. The use of these separators can obviously be used for other sample types to aid handling and sample introduction. The application of these separators could also be extended in future work to include the reduction in organic mobile phase reaching the plasma in directly coupled HPLC-ICP-MS metal speciation studies. The membrane tube has been shown to be of use for aqueous samples and strongly acidic samples.

The use of desolvation prior to analysis of slurry samples by ICP-MS has been shown to offer a number of advantages. The sensitivity of the technique is improved due to an increase in the transport efficiency. Particle size studies, have also shown that larger particles (8μm c.f. 5μm) may be introduced successfully. These larger particles once introduced to the plasma appear to be successfully atomised and subsequently ionised. The major disadvantage of this technique is the increased washout times (up to 3 minutes) caused by the condensation of the sample in the condenser and the added distance the sample has to travel. However, the desolvation device used in this study was designed for the introduction of organic solvents and so may need modification in further work in this area to improve its use for aqueous samples and slurries in particular. The effect of increasing the temperature of the heating stage of the desolvation system may also have a beneficial effect on the subsequent result.

The use of laser ablation for the determination of trace metals impurities in precious metals also proved successful. The use of the laser in fixed-Q mode provided the best results in terms of accuracy and precision. although the use of this technique for samples for which spatial information or depth profiling are required has been shown to be problematic. This is due to the large standard deviations obtained, particularly in Q-switch mode, resulting in degradation in the quality of the results. The choice of internal standard is also shown to be of great importance on the quality of the results, and the use of an intrinsic internal standard is recommended. The best intrinsic internal standard proved to be a minor isotope of the matrix element. The non-availibility of difficulty in producing solid standards means the use of the technique may be limited at present. However, the clear advantages in terms of sample preparation and handling is likely to encourage further work on the preparation of standards which could lead to the technique being more widely used for diverse sample types. The improvements in resolution encountered when using a dry plasma means that for some applications where the isotope of interest is not fully resolved from the matrix, the use of laser ablation provides a simple alternative method.

In addition to the above mentioned practical aspects of this study, calculation of the ionisation temperature have enabled some information about the fundamental nature of

the plasma to be obtained. The addition of hydrogen into the nebuliser gas flow of desolvated samples has been shown to increase the ionisation temperature, and improve the thermal conductivity and energy transfer in the plasma. The addition of oxygen into the nebuliser gas flow has a marginal effect at low levels, and a detrimental effect at higher concentrations. The introduction of organics consequently requires the addition of the minimum amount of oxygen required to prevent the products of pyrolysis blocking the cones. Further results from this work also show that the addition of slurries into the plasma does not appear to have an effect on the ionisation temperature. However, knowledge of the effects due to the introduction of samples into the plasma is limited and further work is needed to elucidate the fundamental processes taking place within the plasma. This is particularly true for the introduction of organic samples and molecular gases. The noted improvement in resolution caused by using a dry plasma may be a convienent starting point for such studies.

REFERENCES

1. Greenfield,S., Jones,I.L., and Berry,C.T., Analyst, 1964, 89, 713.
2. Wendt,R.H., and Fassel,V.A., Anal. Chem., 1965, 37, 920.
3. Thompson,M, and Walsh,J.N., A Handbook of Inductively Coupled Plasma Spectrometry, Blackies, London, 1983.
4. Rose,D.A., Anal. Proc., 1983, 20, 436.
5. Hutton,R.C., Bridenne,M., Coffre,E., Marot,Y., and Simondet,F., J. Anal. At. Spectrom., 1990, 5, 463.
6. Kirkbright,G.F., and Walton,S.J., Analyst, 1986, 107, 276.
7. Cope,M.J., Kirkbright,G.F., and Burr,P.M., Analyst, 1986, 107 611.
8. Wolcott,J.F., and Sohel,C.B., Appl. Spectrosc., 1978, 32, 591.
9. Wilkinson,J.R., Ebdon,L., and Jackson,K.W., Anal. Proc., 1982, 19, 305.
10. Laqua,K., Analytical Spectroscopy Using Laser Atomisers, Ed. Omenetto,N., Wiley-Interscience, New York, 1979.
11. Jansen,J.A.T., and Witmer,A.W., Spectrochim. Acta Part B 1982, 37, 483.
12. Osbourne,S.P., Applied Spectrosc., 1990, 40, 1044.
13. Gast,C.H., Kraak,J.C., Poppe,H., Maessen,F.J.M.J., J. Chromatogr., 1979, 185, 549.

14. Montaser,A., and Fassel,V.A., Anal. Chem., 1976, 48, 1490.

15. Date,A.R., and Gray,A.L., Analyst, 1981, 106, 1255.

16. Gray,A.L., and Date,A.R., in Dynamic Mass Spectrometry Vol. 6, Eds., Price,D., and Todd,T.F.J., Heyden, London, 1981.

17. Houk,R.S., Fassel,V.A., Flesch,G.D., Svec,H.J., Gray,A.L., and Taylor,C.E., Anal. Chem., 1980, 52, 2283.

18. Thompson,M., and Zao,L., Analyst, 1985 110, 229.

19. Miyazaki,A., and Bansho,K., Spectrochim. Acta Part B, 1987, 42, 227.

20. Severens,P.J.H., Klassen,E.J.M., and Maeseen,F.J.M.J., Spectrochim. Acta Part B, 1983, 38, 727.

21. Miyazaki,A., Kimura,A., and Umezaki,Y., Anal. Chim. Acta, 1981, 127, 93.

22. Fassel,V.A., Peterson,C.A., Abercrombie,F.N., and Knisely,R.N., Anal. Chim., 1976, 48, 516.

23. Algeo,J.D., Heine,D.R., Philips,H.A., Hoek,F.B.G., Schnieder,M.R., Freelin,J.M., and Denton,M.D., Spectrochim. Acta Part B, 1985, 40, 1447.

24. Jansen,E.B.M., Knipscheer,J.H., and Nagtegraal,M., J. Anal. At. Spectrom., 1992, 7, 127.

25. Brown,R.J., Spectrochim. Acta Part B, 1983, 38, 283.

26. Boorn,A.W., and Browner,R.F., Anal. Chem., 1982, 54, 1402.

27. Barrett,P., and Pruzkowska,E., Anal. Chem., 1984, 56, 1927.

28. Maessen,F.J.M.J., Seeverens,P.J.H., and Kreuning,G., Spectrochim. Acta Part B, 1984, 39, 1171.

29. Maessen,F.J.M.J., Kreuning,G., and Balke,J., Spectrochim. Acta Part B, 1986,, 41, 3.

30. Kreuning,G., and Maessen,F.J.M.J., Spectrochim. Acta Part B, 1987, 42, 677.

31. Meyer,G.A., Spoectrochim. Acta Part B, 1987, 42, 201.

32. Nygaard,D.D., and Sotera,J.J., Appl. Spectrosc., 1987, 41, 703.

33. Hauser,P.C., and Blades,M.W., Appl. Spectrosc. 1988, 42,595.

34. Xu,J., Kawaguchi,H., and Mizuike,A., Anal. Chim. Acta, 1983, 152, 133.

35. Hutton,R.C., J. Anal. At. Spectrom., 1986, 1, 259.

36. Hausler,D., Spectrochim. Part B, 1987, 42, 63.

37. Allain,P., Jaunault,L., Mauras,Y., Mermet,J.M., and Delaporte,T., Anal. Chim., 1991, 63, 1498.

38. Longerich,H.P., J. Anal. At. Spectrom., 1989, 4, 665.

39. Ebdon,L., Evans,E.H., and Barnett,N.W., J. Anal. At. Spectrom. 1989, 4, 505.

40. Dupius,R.D., Science, 1984, 226, 243.

41. Dupkus,P.D., Anal. Rev. Mater. Sci., 1982, 12, 243.

42. Comprehensive Organometallic Chemistry, Eds. Wilkinson,G., Stone,F.G.A., and Abel,E.W., Pergamon Press, Oxford, 1982.

43. Bertenyi,I., and Barnes,R.M., Anal. Chem., 1986, 58, 1734.

44. Murty,P.S., Chen,Z., and Barnes,R.M., ICP Infor. Newsl., 1989, 15, 230.

45. Murty,P.S., and Barnes,R.M., Appl. Spectrosc., 1987, 41, 851.

46. Chen,Z., Murty,P.S., and Barnes,R.M., ICP Infor. Newsl., 1989, 15, 338.

47. Jones,A.C., Jacobs,P.R., Cafferty,R., Scott,M.D., Moore,A.H., and Wright,P.J., J. Crystal Growth, 1986, 77, 47.

48. Hutton,R.C., 5th Biennial National Atomic Spectroscopy Symposium, July 1990, Loughborough, U.K.

49. Takeda,K., Minobe,M., Hoshika,T., Jinno,T., and Yaka,T., Analyst, 1990, 115, 535.

50. Novotorov,Yu.M., Novotorava,L.G.G., Zorin,A.D., and Freshenko,I.A., Zh. Anal. Khim., 1987, 42, 1969.

51. Sologanskii,Yu.M., Shushunov,N.V., Sorochkina,T.G., Gaivoranskii,P.E., Domikov,I.V., Moiseev,A.N., and Baturin,N.V., Zh. Anal. Khim., 1987, 42, 317.

52. Walters,P.E., and Barnardt,C.A., Spectrochim. Acta Part B, 1988, 43, 325.

53. Sharp,B.L., J. Anal. At. Spectrom., 1988, 3, 613.

54. Brotherton,T.J., Pfannerstill,P.E., Creed,J.T., Heitkemper,D.T., Caruso,J.A., and Pratsinis,S.E., J. Anal. At. Spectrom., 1989, 4, 341.

55. Uchida,H., Masamba,W.R., Uchida,T., Smith,B.W., and Winefordner,J.D., Appl. Spectrosc., 1989, 43, 425.

56. Tsukahara,R., and Kubota,M., Spectrochim. Acta Part B, 1990, 45, 581.

57. Gustavsson,A., Spectrochim. Acta Part B, 1988, 43, 917.

58. Backstrom,K., Gustavsson,A., Spectrochim. Acta Part B, 1989, 44, 104.

59. Weir,D.G.J., and Blades,M.W., Spectrochim. Acta Part B, 1990, 45, 615.

60. Huang,B., Yang,J., Pei,A., Zeng,X., and Boumans,P.W.J.M., Spectrochim. Acta Part B, 1991, 46, 407.

61. Wiedren,D.R., Houk,R.s, Winge, R.k., and D'Silva,A.P., Anal. Chem., 1990, 62, 1155.

62. Pan,C., Zhu,G., and Browner,R.F., J. Anal. At. Spectrom., 1990, 5, 537.

63. Gervais,L.S., and Salin,E.D., J. Anal. At. Spectrom., 1991, 6, 325.

64. Broekaert,J.A.C., Leis,F., Raeymaekers,B., and Zaray,G., Spectrochim. Acta Part B, 1988, 43, 339.

65. Fuller,C.W., Hutton,R.C., and Preston,B., Analyst, 1981, 106, 913.

66. Halicz,L., and Brenner,I.B., Spectrochim. Acta Part B, 1987, 42, 207.

67. Ebdon,L., and Collier,A.R., J. Anal. At. Spectrom., 1988, 3, 557.

68. Ebdon,L., and Collier,A.R., Spectrochim. Acta Part B, 1988, 43, 355.

69. Ebdon,L., and Wilkinson,J.R., J. Anal. At. Spectrom., 1987 2, 39.

70. Ebdon,L., and Wilkinson,J.R., J. Anal. At. Spectro., 1988, 2, 325.

71. Ambrose,A.J., Ebdon,L., Foulkes,M.E., and Jones,P., J. Anal. At. Spectrom., 1989, 4, 219.

72. Ebdon,L., Foulkes,M.E., and Hill,S.J., J. Anal. At. Spectrom. 1990, 5, 67.

73. Williams,J.G, Gray,A.L., Norman,P., and Ebdon,L., J. Anal. At. Spectrom., 1987, 2469.

74. Ebdon,L., Foulkes,M.E., Parry,H.G.M., and Tye,C.T., J. Anal. At. Spectrom., 1988, 3, 753.

75. Atkins,P.W., Physical Chemistry,3rd Edition, Oxford University Press, 1986.

76. Maiman,T.H., Nature, 1960, 187, 143.

77. Thompson,M., Goulter,J.E., and Sieper,F., Analyst, 1981, 106, 32.

78. Carr,J.M., and Horlick,G., Spectrochim. Acta Part B, 1982, 37, 1.

79. Ishizuka,T., and Unwanio,Y., Spectrochim. Acta Part B, 1983, 38, 519.

80. Gray,A.L., Analyst, 1985, 110, 551.

81. Arrowsmith,P., Anal. Chem., 1987, 59, 1437.

82. Yasuhara,H., Okano,T., and Matsumura,Y., Analyst, 1992, 117, 395.

83. Perkins,W.T., Fuge,R., and Pearce,N.J.G., J.

Anal. At. Spectrom., 1991, 6, 445.

84. Weijer,P.Van de, Vullings,P.J.M.G., Baeten,W.L.M., and Laat,W.J.M., J. Anal. At. Spectrom., 1991, 6, 609.

85. Marshall,J., Franks,J., Abell,I., and Tye,C.T., J. Anal. At. Spectrom., 1991, 6, 145.

86. Mermet,J.M., in Inductively Coupled Plasma Emission Spectroscopy, Ed. Boumans,P.W.J.M., Wiley-Interscience, New York, 1987.

87. Blades,M.W., in Inductively Coupled Plasma Emission Spectroscopy, Ed. Boumans, P.W.J.M., Wiley-Interscience, New York, 1987.

88. Moore,C.E., Atomic Energy Levels, Circular 467, Nat. Bur. Stds. I 1949, II 1952, III 1958.

89. Schram,D.C., Raeymakers,I.J.M.M., Sijde,B.Van der, Schenkelavars,H.J.M., and Boumans,P.W.J.W., Spectrochim. Acta Part B, 1983, 38, 1545.

90. Caughlin,B.L., and Blades,M.W., Spectrochim. Acta Part B, 1985, 40, 1539.

91. Caughlin,B.L., and Blades,M.W., Spectrochim. Acta Part B, 1987, 42, 353.

92. Tang,Y.Q., and Trassey,C., Spectrochim. Acta Part B, 1986, 41, 143.

93. Fister,J.C. and Olesik,J.M., Spectrochim. Acta Part B, 1991, 46, 869.

94. Alder.J.F., Bombelka,R.M., Kirkbright,G.F.,

Spectrochim. Acta Part B, 1980, 35, 163.

95. Allen,T., Particle Size Measurement, 3rd Edition, Chapman and Hall, London, 1981.

96. Skoog,D.A., and West,D.M., Fundamentals of Analytical Chemistry, 4th Edition, Holt-Saunders International Editions, London, 1982.

97. Miller,J.C., Miller,J.N., Statistics For Analytical Chemistry, Ellies Harwood Ltd., Chichester, 1984.

98. Raeymakers,I.J.M., Boumans,P.W.J.M., Sijde,B.Van der, Schram, D.C., Spectrochim. Acta Part B, 1983, 38, 697.

99. Mitcher,M., and Kruger, Partially Ionised Gases, Wiley-Interscience, New York, 1973.

100. Boumans,P.W.J.M., and Lux-Steiner,M.Ch., Spectrochim. Acta Part B, 1982, 37, 7.

101. Boorn,A.W., Cresser,M.S., and Browner,R.F., Spectrochim. Acta Part B, 1982, 35, 823.

102. Seymour,J., Physical Electronics, Pitman Publishing, London, 1972.

103. Goodall,P., CNAA, Polytechnic South West, Plymouth, PhD Thesis, 1991.

104. Lot,P., Periodic Table, Elsevier Science Publisher B.V., New York, 1987.

105. Ebdon,L., Foulkes,M.E., and Hill,S.J., Microchem. J., 1989, 40, 30.

MEETINGS ATTENDED

i) Atomic Spectroscopy Group jointly with Atomic Spectrometry Updates, meeting on "Lasers in Atomic Spectroscopy" Guildford, 30th March 1990

ii) Analytical Division of the RSC, meeting on "Research and Development Topics in Analytical Chemistry" Runcorn, 16-17th July, 1990

iii) Atomic Spectroscopy Group of the RSC with the Spectroscopy Group of the Institute of Physics, "Fifth Biennial National Atomic Spectroscopy Symposium", Loughborough, 18-20th July 1990

iv) "2nd International Conference on Plasma Source Mass Spectrometry" Durham, 24-28th September 1990

v) Analytical Division of the RSC, meeting on "Research and Development Topics in Analytical Chemistry" Aberdeen, 9-10th July 1991

vi) "Fourth Surrey Conference on Plasma Source Mass Spectrometry" Guildford, 14-19 July 1991

vii) "1992 Winter Conference on Plasma Spectrochemistry", San Diego, U.S.A. 6-11th January 1992

viii) Analytical Division of the RSC, meeting on "Research and Development Topics in Analytical Chemistry" Birmingham, 7-8th July 1992

ix) Atomic Spectroscopy Group of the RSC jointly with the Spectroscopy Group of the Institute of Physics, " Sixth Biennial National Atomic Spectroscopy Symposium" Plymouth, 22-24th July 1992

PRESENTATIONS

i) "Applications of ICP Spectroscopy to the Determination of Trace Metals in Reactive and Volatile Samples", Poster presented at "Research and Development Topics in Analytical Chemistry" Runcorn 16-17th July 1990

ii) "Effects of Volatile and Reactive Solvents in ICP Spectrometry", Poster presented at "Fifth Biennial Atomic Spectroscopy Symposium", Loughborough 18-20th July 1990

iii) "The Investigation of Trace Metals in Diethyl Ether by ICP-MS", Poster presented at " 2nd International Conference on Plasma Source Mass Spectrometry", Durham 24-28th September 1990

iv) "Analysis of Trimethylgallium Etherate by Flow Injection Inductively Coupled Plasma Mass Spectrometry", Poster presented at "Research and Development Topics in Analytical Chemistry", Aberdeen, 9-10th July 1991

v) "The Analysis of Reactive Organometallic Species using Flow Injection-Inductively Coupled Plasma-Mass Spectrometry", Poster presented "Fourth Surrey Conference on Plasma Source Mass Spectrometry", Guildford, 14-19th July 1991

vi) "A Novel Desolvation System for the Analysis of Organic Solvents by Flow Injection-Inductively Coupled Plasma-Mass Spectrometry", Presented "1992 Winter Conference on Plasma Spectrochemistry", San Diego, U.S.A. 6-11th January 1992

vii) "The Analysis of Desolvated Slurries by Inductively Coupled Plasma-Mass Spectrometry", Poster presented "Research and Development Topics in Analytical Chemistry", Birmingham, 7-8th July 1992

viii) "The Analysis of Precious Group Metals (PGMs) by Slurry Atomisation-Inductively Coupled Plasma-Mass Spectrometry", Poster presented "Sixth Biennial National Atomic Spectroscopy Symposium", Plymouth 22-24th July 1992

ix) "The Analysis of Solid Samples by Slurry Atomisation-Inductively Coupled Plasma-Mass Spectrometry Using Desolvated Slurries", Presented " Sixth Biennial Atomic National Spectroscopy Symposium", 22-24th July 1992

LECTURES AND ASSOCIATED STUDIES

i) RSC Lecture, 21st November 1989, Polytechnic South West, Dr S.K.Scott, "Clocks, oscillations and chaoes in chemistry"

ii) RSC Lecture, 26th January 1990, Polytechnic South West, Dr J.P.Leaky, "Studies in the environmental fate of a new pesticide"

iii) RSC Lecture, 19thOctober 1990, Polytechnic South West, Dr R.P. Wayne, "The origin and evolution of the atmosphere"

iv) RSC Lecture, 16th November 1990, Polytechnic South West, Dr D.H.G. Grout, "Enzymes in organic chemistry"

v) RSC Lecture, 17th, January 1991, Polytechnic South West, Dr R.J.Perriman, "Chemical Manufacturing and the Environment"

vi) Weekly Departmental Research Seminars, 1989 - 1992, Polytechnic South West/University of Plymouth

HAG YTH OF-VY DHE VLAMYA

DREFEN UNWYTH DHE SCRYFA

HENNA !